

The role of HuR in muscle development, function and muscle-related diseases

Brenda Janice Sánchez Sánchez, Department of Biochemistry, Faculty of
Medicine McGill University, Montreal

June 2021

Thesis submitted to McGill University in partial fulfillment of the requirements of
the degree of Doctor of Philosophy

©Brenda Janice Sánchez Sánchez

1. Abbreviations

GM-CSF----Macrophage-colony stimulating factor
AChR α ----Acetylcholine receptor α -subunit
AGO----Argonaute
ARE---- RNA elements enriched in adenylate and uridylylate, AU-rich elements
AS----Autophagy-lysosome system
AUF1----AU-binding factor 1
bHLH ----Basic helix–loop–helix
BMP----Bone morphogenetic proteins
Ca⁺⁺----Calcium ions
CD36----Cluster of differentiation 36/SR-B2
CDK1----Cyclin dependent kinase 1
CE----Core enhancer
CELF ----CUG-BP- and ETR-3-like factors
CHK2----Checkpoint kinase 2
CPEB ----Cytoplasmic polyadenylation protein
CREB----cAMP response element-bindingprotein
CSD----Cold shock domain
CTD ---- C terminal domain
DEAD box ----DEAD box helicase domain
DMD ----Duchenne muscular dystrophy
DRR----Distal regulatory region,
dsRBD ----Double stranded RNA-binding domain
E0.0----Embryonic day N
eIFs ----Translation initiation factors
ELAV----Embryonic lethal abnormal vision
FABP3----Fatty acid binding protein 3
FAO----Fatty acid oxidation
FFA----Free fatty acid
FMRPs ----Familial mental retardation proteins

FoxO3----Forkhead box class O
GLUT4----Enhancer factor GEF
HDAC4----Histone deacetylase 4
hnRNPD----Heterogeneous nuclear ribonucleoprotein D
HNS----Nucleocytoplasmic shuttling sequence
HuR----Human antigen R
IC ----Translation initiation complex
IRES----Internal ribosome entry sites
ITAFs ----IRES-transacting factors
KH----hnRNP K homology domain
KSRP----KH-type splicing regulatory protein
m7g----7-methyl-guanylate
MAPK----p38 mitogen-activated protein kinase
MEF----Myocyte enhancer factor
miRNA----MicroRNAs
MRF4----Myogenic factor 6
MRFs----Muscle specific transcription factors
mRNA---Messenger RNA
mTOR----Molecular target of rapamycin
muHuR-KO----Muscle-specific HuR knockout
Murf1----Muscle RING finger protein 1
Myf5----Myogenic factor 5
MyHC----Myosin heavy chain
MyoD----Myogenic differentiation antigen
Myog----Myogenin
NES----Nuclear export signals
NLS----Nuclear localization signal
NR ----Nuclear receptors
NMJ----Neuro muscular junction
NPC ----Nuclear pore complex
NPM----Nucleophosmin

NRF----Nuclear respiratory factor
p21---Cyclin-dependent kinase inhibitor 1
PABP----Poly(A)-binding protein
PARN----Poly(A)-specific ribonuclease
PARylation----Poly(ADP)-ribosylation
PAX----Paired box transcription factor
PGC-1 α ----Peroxisome proliferator-activated receptor coactivator 1 alpha
PPAR α ----Peroxisome proliferator-activated receptor alpha
PPAR β/δ ---- Peroxisome proliferator-activated receptor beta/delta
PPAR γ ---- Peroxisome proliferator-activated receptor gamma
pri-miRNA----Primary miRNA molecules
PRKCD ----Protein kinase C delta
PTB ----Polypyrimidine-tract binding protein
RBD----RNA-binding domain
RBP----RNA-binding protein
RISC----RNA-induced silencing complex
RNPC----Ribonucleoprotein complexes
RRM----RNA recognition motif
SCD----Stearoyl-CoA desaturase
SC---Satellite cells
Shh----Sonic hedgehog
Six----Sine oculis-related homeobox transcription factors
SRF----Serum response factor
ssRNAs----Single-stranded RNAs
TIA-1----T-cell intracellular antigen 1
TIAR----TIA-1-related protein
TNF----Tumor necrosis Alpha
TRBP----TAR RNA-binding protein
TRN2----Transportin 2
TSS----Transcriptional start site
TTP----Tristetraprolin TTP

UPS----Ubiquitin proteasome system

UTR----Untranslated region

Wnt----Wnt protein family

YB1----Y box binding protein 1

ZBP1----Zip binding protein 1

2. Contents

1. Abbreviations	2
2. Contents	6
2.1. List of figures	9
2.2. List of tables	11
2.3. List of Annexes.....	11
3. Abstracts	12
3.1. English	12
3.2. French	14
4. Acknowledgements	17
5. Contribution to original knowledge	18
5.1. CHAPTER I: Destabilization of Nucleophosmin mRNA by the HuR/KSRP complex is required for muscle fiber formation. Nature Communications, 2014. ...	18
5.2. CHAPTER II: Cooperativity between YB1 and HuR is necessary to regulate Myogenin mRNA stability during muscle fiber formation.	18
5.3. CHAPTER III: Depletion of HuR in murine skeletal muscle enhances exercise endurance and prevents cancer-induced muscle atrophy. Nature Communications, 2019.....	18
6. Contribution of Authors	20
6.1. CHAPTER I: Destabilization of Nucleophosmin mRNA by the HuR/KSRP complex is required for muscle fibre formation. Nature Communications, 2014. ...	20
6.2. CHAPTER II: Cooperativity between YB1 and HuR is necessary to regulate Myogenin mRNA stability during muscle fiber formation.	20
6.3. CHAPTER III: Depletion of HuR in murine skeletal muscle enhances exercise endurance and prevents cancer-induced muscle atrophy. Nature Communications, 2019.....	21

7. Introduction	22
7.1. Muscle basics.....	22
7.2. Skeletal muscle structure and contraction.....	24
7.3. Classification of skeletal muscle fiber types.	27
7.4 Skeletal muscle lineage specification and myogenesis.	31
7.4.1 <i>Specification of the muscle lineage.</i>	32
7.4.2 <i>Skeletal myogenesis during embryogenesis.</i>	35
7.4.3 <i>Skeletal myogenesis in postnatal life, regeneration.</i>	36
7.5 The gene regulatory network mediating skeletal myogenesis.	38
7.6 The role of post-transcriptional regulation in myogenesis.	41
7.6.1 <i>Cis-Regulatory elements involved in posttranscriptional regulatory mechanisms.</i>	43
7.6.2 <i>Posttranscriptional regulation through microRNAs.</i>	44
7.6.3. <i>Posttranscriptional regulation through RNA binding Proteins.</i>	47
8. Rationale and objectives of the thesis	61
9. Body of the thesis	63
9.1. CHAPTER I: Destabilization of Nucleophosmin mRNA by the HuR/KSRP complex is required for muscle fiber formation.....	63
9.1.1. <i>Abstract</i>	63
9.1.2. <i>Introduction</i>	63
9.1.3. <i>Results</i>	65
9.1.4. <i>Discussion</i>	88
9.1.5. <i>Material and Methods</i>	91
9.1.6. <i>Acknowledgements</i>	97
9.1.7. <i>References Chapter I</i>	97
9.2. CHAPTER II: Cooperativity between YB1 and HuR is necessary to regulate Myogenin mRNA stability during muscle fiber formation.	103
9.2.1. <i>Abstract</i>	103
9.2.2. <i>Introduction</i>	103
9.2.3. <i>Results</i>	105
9.2.4. <i>Discussion</i>	119

9.2.5. <i>Material and Methods</i>	122
9.2.6. <i>Acknowledgement</i>	127
9.2.7. <i>References Chapter II</i>	128
9.3. CHAPTER III: Loss of HuR in skeletal muscle promotes an oxidative fiber phenotype and prevents cancer-cachexia associated muscle atrophy.	134
9.3.1. <i>Abstract</i>	134
9.3.2. <i>Introduction</i>	134
9.3.3. <i>Results</i>	136
9.3.4. <i>Discussion</i>	155
9.3.5.- <i>Material and Methods</i>	159
9.3.6.- <i>Acknowledgement</i>	169
9.3.7.- <i>References Chapter III</i>	170
10. General Discussion	176
11. Conclusion	180
12. Bibliography	182
13. Annexes	200
13.1. Annex 1. Supplemental material for CHAPTER I	201
13.2. Annex 2. Supplemental material for CHAPTER II	216
13.3. Annex 3. Supplemental material for CHAPTER III	224

2.1. List of figures

Figure 1.1 Light micrographs of skeletal, cardiac and smooth muscle.

Figure 1.2. Schematic diagram illustrating the structural hierarchy of skeletal muscle tissues.

Figure 1.3. Labeled diagrams and electronic micrograph of sarcomeres in a relaxed and contracted configuration.

Figure 1.4. Schematic diagram illustrating the mechanism of the troponin complex.

Figure 1.5. Hierarchy of transcription factors regulating progression of the myogenic lineage.

Figure 1.6. Schematic illustrating the organization of the three germ layers during succeeding days of mouse gestation.

Figure 1.7. Signaling molecules regulating progression of the myogenic lineage.

Figure 1.8. Schematic representation of transverse sections through the embryo illustrating the process of myotome formation during succeeding days of gestation.

Figure 1.9. Stages of skeletal myogenesis from the embryo to the adult.

Figure 1.10. Modes of satellite stem cell division.

Figure 1.11. Transcription regulatory elements in the *MyoD*, *Myog* and *Myf5/Mrf4* locus.

Figure 1.12. Overall structure of eukaryotic mRNA.

Figure 1.13. Biosynthesis of miRNA.

Figure 1.14. Mechanisms of RBP-mediated regulation of gene expression.

Figure 1.15. Pathways for exonucleases access to RNAs for degradation.

Figure 1.16. RNA-binding proteins in myogenesis and their known mRNA targets.

Figure 1.17. The role of HuR in myogenesis.

Figure 1.18. Model depicting the role of HuR-regulated iNOS mRNA and thus NO secretion in changes in *MyoD* mRNA levels.

Figure 2.1. HuR regulates NPM expression in muscle cells.

Figure 2.2. Reducing NPM level is required for the commitment of muscle cells into the myogenic process.

Figure 2.3. HuR regulates the stability of the *NPM* mRNA.

Figure 2.4. HuR binds to the *NPM* mRNA via two U-rich sequences within the 3'UTR.

Figure 2.5. An intact P1-1 element is required for HuR-mediated regulation of NPM expression.

Figure 2.6. KSRP is required for the HuR-mediated destabilization of *NPM* mRNA.

Figure 2.7. HuR and KSRP form a complex and bind to the same element in the *NPM* 3'UTR.

Figure 2.8. The HuR RRM3 motif is required for the formation of KSRP/HuR complex.

Figure 2.9. The HuR/KSRP-mediated decay activity requires PARN and EXOSC5 to destabilize *NPM* mRNA and promote muscle fiber formation.

Figure 3.1. Gene ontology (GO) analysis of potential HuR protein partners in muscle cells.

Figure 3.2. YB1 is a novel HuR protein ligand and its depletion prevents muscle cell differentiation.

Figure 3.3. YB1 and HuR have common mRNA targets in muscle cells.

Figure 3.4. YB1 regulates the stability of *Myog* mRNA.

Figure 3.5. YB1 and HuR bind to a G/U rich element in the *Myog* mRNA 3'UTR.

Figure 3.6. G/URE 2 is required for the YB1/HuR mediated stabilization of the *Myog* mRNA.

Figure 3.7. G/URE 2 is required for the YB1/HuR mediated regulation of *Myog* expression.

Figure 3.8. Model depicting the molecular mechanism through which the HuR and YB1 complex regulate *Myog* mRNA stability to promote muscle fiber formation.

Figure 4.1. Generation of HuR muscle-specific knockout mice using the Cre-lox P system.

Figure 4.2. HuR muscle-specific KO mice have enhanced exercise endurance.

Figure 4.3. muHuR-KO mice show an increased oxidative capacity.

Figure 4.4. Depletion of HuR in skeletal muscle increases the proportion of type I fibers.

Figure 4.5. Increased *PGC-1 α* expression in muHuR-KO muscle.

Figure 4.6. HuR destabilizes the *PGC-1 α* mRNA in muscle cells.

Figure 4.7. KSRP collaborates with HuR to destabilize the *PGC-1 α* mRNA in muscle cells.

Figure 4.8 HuR ablation in skeletal muscle ameliorates cancer-induced muscle wasting.

2.2. List of tables

Table 1.1. Contractile characteristics and metabolic properties of muscle fiber types.

Table 1.2. Conserved sequences of ARE and GRE cis-regulatory elements.

Table 1.3. Muscle specific miRNAs and their targets in muscle.

2.3. List of Annexes

Annex 1. Supplemental material for CHAPTER I:

Annex 2. Supplemental material for CHAPTER II:

Annex 3. Supplemental material for CHAPTER III:

3. Abstracts

3.1. English

Myogenesis, the process of muscle fiber formation and regeneration, is activated during embryogenesis and in response to muscle injury to ensure normal growth and repair of injured skeletal muscle tissue. The molecular regulatory events mediating myogenesis involve the sequential activation of four basic helix–loop–helix (bHLH) muscle specific transcription factors; Myogenic differentiation antigen (MyoD), Myogenin (Myog), Myogenic factor 5 (Myf5), and myocyte enhancer factor 6 (MRF4). Collectively referred as Myogenic Regulatory Factors (MRFs)¹. The expression of MRFs is tightly regulated as ectopic expression has been shown to lead to compromised muscle function²⁻⁴. Although transcriptional mechanisms mediate the expression of these factors, recent evidence have demonstrated that transcription alone is not sufficient to maintain the high expression levels of MRFs needed during the lifespan of a myotube. Recently, the regulation of gene expression at the posttranscriptional level, including at the level of mRNA stability, localization and translation, was demonstrated to play an important role in the regulated expression of these MRFs during muscle development and maintenance⁵⁻¹¹.

The RNA binding protein (RBP) HuR (Human Antigen R) has been shown to play a prominent role in this process by stabilizing several promyogenic mRNAs including *MyoD* and *Myog*, as well as the cell cycle inhibitor *p21*^{6,11}. HuR has been previously shown to regulate its mRNA targets in several cell systems by collaborating/competing with additional trans-acting factors including RNA binding proteins (RBP) and micro RNAs (miRNAs). Although we have shown that this is also the case in muscle cells¹², the identity of the complete network of trans-acting factors, as well as the mechanisms through which they affect the pro-myogenic function, remains elusive. In this thesis I have explored the molecular mechanisms through which HuR mediates the integrity, composition and function of skeletal muscle tissue both *in vitro* and *in vivo*.

Chapter I describes how HuR, via a novel mRNA destabilizing activity, promotes the early steps of myogenesis by reducing the expression of the cell cycle promoter

Nucleophosmin (NPM). We show that HuR mediates the destabilization of the *NPM* mRNA through a collaboration with the decay factor KSRP (The KH-type splicing regulatory protein). In the early stages of myogenesis HuR forms a complex with KSRP, to recruit the exonuclease Poly(A)-specific ribonuclease (PARN) and members of the exosome to the *NPM* mRNA, leading to its degradation. Our findings, therefore, highlight the interaction of HuR with KSRP during myogenesis as being pivotal for the differentiation and integrity of muscle.

Chapter II illustrates a network of proteins ligands of HuR in muscle cells which, in addition to KSRP, may collaborate with HuR to regulate the myogenic process. We identified 20 novel protein ligands of HuR in muscle cells and provide evidence that one of these partners, the multifunctional DNA/RNA-binding protein YB1 (Y box binding protein 1), is required for the regulation of *Myog* mRNA stability and the formation of muscle fibers. We showed that during the preterminal stages of myogenesis YB1 associates to HuR. This complex regulates the stability of the *Myog* mRNA by associating with a G/U-rich element (GURE) in the 3' untranslated region (UTR). These findings demonstrate that the dual nature of HuR, functioning as a destabilizing and stabilizing RNA binding protein during myogenesis, is dependent on its interaction with different trans-acting factors.

Chapter III focuses on addressing how HuR modulates the development and physiological function of skeletal muscle tissues. We generated a HuR muscle-specific knockout mice and demonstrated, that these mice, exhibit an enrichment of type I muscle fibers, resulting in the increased oxidative metabolic capacity of the skeletal muscle. HuR mediates these effects, in part, by destabilizing the *PGC-1 α* mRNA in a KSRP-dependent manner. These results establish HuR as a powerful modulator of genetic programs implicated in energy metabolism and adaptations to endurance exercise. In addition, we demonstrate that loss of HuR specifically in skeletal muscle protects mice from cancer-induced muscle wasting in the LLC model of cancer-caquexia. muHuR-KO mice-bearing LLC tumors (LLC-muHuR-KO) demonstrated a significant protection from LLC-induced weight loss when compared to their control counterparts (LLC-Control). Given the differential sensitivity of muscle fiber types to atrophy, the HuR mediated specification of glycolytic type II fibers raise the possibility that HuR expression can be targeted

therapeutically in skeletal muscles to combat conditions such as, DMD, denervation, disuse, and cancer cachexia, where wasting of type II fiber is favored.

3.2. French

La myogénèse, processus de formation et de régénération des fibres musculaires, est activée pendant l'embryogenèse et en réponse à des lésions musculaires pour assurer une croissance normale et la réparation du tissu musculaire squelettique. Les événements régulateurs de la myogénèse impliquent l'activation séquentielle de quatre facteurs de transcription à domaine hélice-boucle-hélice (bHLH) étant spécifiques aux muscles. l'antigène de différenciation myogénique (MyoD), la Myogénine (Myog), le facteur myogénique 5 (Myf5) et le facteur d'amplification des myocytes 6 (MRF4). L'expression de ces facteurs de régulation myogéniques (MRF)¹ est elle aussi étroitement régulée. En effet, il a été démontré que l'expression ectopique de ceux-ci entraîne une altération de la fonction musculaire²⁻⁴. Bien que des mécanismes transcriptionnels servent de médiateurs pour l'expression de ces facteurs, des preuves récentes ont démontré que la transcription seule n'est pas suffisante pour maintenir les niveaux élevés d'expression des MRF nécessaires pendant la durée de vie d'un myotube. Récemment, il a été démontré que la régulation de l'expression génique au niveau post-transcriptionnel, particulièrement au niveau de la stabilité, de la localisation et de la traduction de l'ARNm, joue un rôle important dans la régulation de l'expression de ces MRF pendant le développement et le maintien des muscles⁵⁻¹¹.

De plus, il a été démontré que la protéine de liaison à l'ARN (RBP) HuR (*Human Antigen R*) joue un rôle de premier plan dans ce processus en stabilisant plusieurs ARNm promyogéniques dont *MyoD* et *Myog* ainsi que l'inhibiteur du cycle cellulaire p21⁶⁻¹¹. Il a déjà été démontré que HuR régule ses cibles d'ARNm dans plusieurs systèmes cellulaires en collaborant ou en rivalisant avec d'autres facteurs de trans-action, notamment des protéines de liaison de l'ARN et des microARN (*miRNA*). Bien que nous ayons montré que c'est également le cas dans les cellules musculaires, l'identité du réseau complet de protéines ainsi que les mécanismes par lesquels elles affectent la fonction pro-myogénique de HuR restent méconnues. Dans cette thèse, j'ai exploré les

mécanismes moléculaires par lesquels HuR médie l'intégrité, la composition et la fonction du tissu musculaire squelettique à la fois *in vitro* et *in vivo*

Le chapitre I décrit comment HuR, à travers une nouvelle activité déstabilisatrice de l'ARNm, favorise les premières étapes de la myogénèse en réduisant l'expression de la NPM. Nous montrons que HuR facilite la dégradation de l'ARNm de la NPM par une collaboration avec le facteur de désintégration KSRP (la protéine régulatrice d'épissage de type KH). Dans les premiers stades de la myogénèse, HuR forme un complexe avec KSRP, pour recruter l'exonucléase Poly(A)-spécifique ribonucléase (PARN) et l'exosome à l'ARNm de la NPM, conduisant à sa dégradation. Nos résultats mettent donc en évidence l'interaction essentielle de HuR avec KSRP pour la différenciation et l'intégrité du muscle au cours de la myogénèse.

Le chapitre II illustre le réseau complet de protéines, en plus de KSRP, qui peuvent collaborer avec HuR pour réguler le processus myogénique. Nous avons identifié 20 nouveaux ligands protéiques de HuR dans les cellules musculaires et fournissons la preuve que l'un de ces partenaires, la protéine multifonctionnelle de liaison à l'ADN/ARN nommée YB1 (Y box binding protein 1), est nécessaire pour la régulation de la stabilité de l'ARNm de Myog et la formation des fibres musculaires. Nous avons montré que pendant les stades préterminaux de la myogénèse, YB1 s'associe à HuR. Ce complexe régule la stabilité de l'ARNm de Myog en s'associant à un élément riche en G/U (GURE) dans la région 3' non traduite (UTR). Ces résultats montrent donc que la double nature de HuR, en tant que protéine de liaison ARN à fonction déstabilisante ou stabilisante pendant la myogénèse, et que ceux-ci dépendent de son interaction avec différents facteurs de trans-action.

Le chapitre III se concentre sur la manière dont HuR module le développement et la fonction physiologique des tissus musculaires squelettiques *in vivo*. Nous avons généré une souris HuR "*knockout*" spécifique au muscle et démontré, que ces souris, présentent un enrichissement des fibres musculaires de type I, entraînant une médie augmentation de la capacité métabolique oxydative du muscle squelettique. HuR agit en partie ces effets en déstabilisant de manière dépendante de la KSRP l'ARNm du coactivateur-1 α de PPAR γ (*PGC-1 α*). Ces résultats établissent HuR comme un puissant

modulateur des programmes génétiques impliqués dans le métabolisme énergétique et les adaptations à l'exercice d'endurance. En outre, nous démontrons que la perte de HuR spécifiquement dans les muscles squelettiques protège les souris contre l'atrophie musculaire induite par le modèle LLC de cancer-cachexie. Les souris muHuR-KO porteuses de tumeurs LLC (LLC-muHuR-KO) ont démontré une protection significative contre la perte de poids induite par les tumeurs LLC par rapport à leurs homologues de contrôle (LLC-Contrôle). Étant donné la sensibilité différentielle des types de fibres musculaires à l'atrophie, la spécification des fibres glycolytiques de type II par la médiation de HuR soulève la possibilité que l'expression de HuR puisse être ciblée thérapeutiquement dans les muscles squelettiques afin de combattre des conditions où l'amyotrophie des fibres de type II est favorisée telles que la dystrophie musculaire de Duchenne (DMD), la dénervation, la désuétude et la cachexie induite par le cancer.

4. Acknowledgements

I would like to thank three groups of people, without whom this thesis would not have been possible: To my family; First and foremost, to my husband Yossef for your love, encouragement and understanding, you have cherished with me every great moment and supported me thorough all the challenges, my love for you is like the ocean in storm. To my parents Eduardo y Elena, thank you for always encouraging me to meet my challenges and instilling in me that hard work does not disappoint anyone. To my siblings Celia, Shamir and Omhar, for the strength that comes from knowing that I have their unconditional support.

To my lab-mates, I could never imagine I would find such a special group of friends; to Derek and Jennifer; I'm extremely grateful for all the pep-talks, cups of coffee, game nights, therapeutic complains, hugs (specially to Derek for enduring them), scientific discussions and insightful comments. I already miss you guys!!! Thank you to Kholoud and Anne-Marie with whom I shared my work burden and were always willing to bring our work a step further. To Souad who's unmistakable "Good morning everyone!!" was always a warm welcome to the working day. To Amr and Jason whose jokes and cultural references I rarely got but would always make me smile. To Xian whose magic hands would troubleshoot all experimental problems and to Devang of course who will "maybe" read this thesis and remember those years with us.

To my coaches, without whom I wouldn't be the independent researcher I am today; a special acknowledgement goes to Sergio Di Marco and Erzsebet Kovacs whom were instrumental in my training as a scientist and whose professional expertise gave me the skills without which I would not have been able to conduct this research. To Dr, Maxime Bouchard, Dr. Michele Tremblay and Dr. Kenneth Hasting for the questions that incented me to widen my research scope and analyze my data from various perspectives. Last but certainly not least, I would like to express my deep gratitude to my advisor Dr. Imed Gallouzi for his fundamental role in my doctoral work. Thank you for helping me realize the power of critical reasoning and for providing me with the continuous guidance, assistance, and motivation that I needed through my years in the Ph.D. program. Your advice has always been invaluable in the academic as in personal life, I could not have imagined having a better mentor.

5. Contribution to original knowledge

This thesis includes the text and figures from 2 published research articles and 1 manuscript. The work has been re-formatted to fit the overall style of the thesis.

5.1. CHAPTER I: Destabilization of Nucleophosmin mRNA by the HuR/KSRP complex is required for muscle fiber formation. *Nature Communications*, 2014.

We show that HuR, via a novel mRNA destabilizing activity, promotes the early steps of myogenesis by reducing the expression of the cell cycle promoter NPM.

HuR mediated destabilization of *NPM* mRNA involves the association of HuR with the decay factor KSRP as well as the ribonuclease PARN and the exosome.

5.2. CHAPTER II: Cooperativity between YB1 and HuR is necessary to regulate Myogenin mRNA stability during muscle fiber formation.

We show that YB1 and HuR cooperate to promote the stability of *Myog* mRNA during the preterminal stage of myogenesis and that this interaction is necessary to sustain the integrity of skeletal muscle fibers.

The cooperativity between YB1 and HuR provides further precedence indicating that a general mechanism through which HuR differentially modulates the expression of its mRNA targets during muscle fiber formation is by collaborating or competing with other trans-acting factors.

5.3. CHAPTER III: Depletion of HuR in murine skeletal muscle enhances exercise endurance and prevents cancer-induced muscle atrophy. *Nature Communications*, 2019.

We show that under normal conditions HuR modulates muscle fiber type specification by promoting the formation of glycolytic type II fibers. HuR mediates these effects by collaborating with the mRNA decay factor KSRP to destabilize the *PGC-1 α* mRNA.

Muscle-specific HuR knockout (muHuR-KO) mice exhibit a significant increase in the proportion of oxidative type I fibers in skeletal muscles, leading to a high exercise endurance which in turn is associated with enhanced oxygen consumption and carbon dioxide production. The type I fiber-enriched phenotype of muHuR-KO mice protects against cancer cachexia-induced muscle loss.

6. Contribution of Authors

This thesis includes the text and figures from 2 published research article and 1 manuscript. The work has been re-formatted to fit the overall style of the thesis.

6.1. CHAPTER I: Destabilization of Nucleophosmin mRNA by the HuR/KSRP complex is required for muscle fibre formation. *Nature Communications*, 2014.

*Anne Cammas, **Brenda Janice Sanchez**, Xian Jin Lian, Virginie Dormoy-Raclet, Kate van der Giessen, Isabel López de Silanes, Jennifer Ma, Carol Wilusz, John Richardson, Myriam Gorospe, Stefania Millevoi, Matteo Giovarelli, Roberto Gherzi, Sergio Di Marco & Imed-Eddine Gallouzi.*

B.J.S. performed 40% of the work reported in this study. Under the guidance of Dr. Anne Cammas, postdoctoral fellow in the lab at that time, I was involved in performing the majority of the western blots, immunoprecipitation, qRT-PCR, immunofluorescence experiments. I also helped in generating the various constructs used in the study and contributed to the writing of the paper by commenting on the first drafts that was written by Dr. Cammas and Dr. Imed Gallouzi, and helped in interpreting many of the experiments.

6.2. CHAPTER II: Cooperativity between YB1 and HuR is necessary to regulate Myogenin mRNA stability during muscle fiber formation.

***Brenda Janice Sánchez**, Kholoud Ashour, Jason Sadek, Derek T. Hall, Xian Jin Lian, Sergio Di Marco, and Imed-Eddine Gallouzi.*

B.J.S. performed, analyzed and interpreted the majority of the experiments in the manuscript. K.A. assisted with sample preparation as well as acquisition of data. J.S. designed and carried out the HuR IP-coupled to MS experiment for the initial identification of HuR protein partners. D.T.H. helped edit the manuscript, X.J.L. assisted in sample preparation and data acquisition of the polysome fractionation, GFP-reporter experiments and Rluc-reporter experiments described in Figs. 6-7. S.D assisted with the conceptualization and data analysis, reviewed and helped edit the manuscript. I-E.G.

conceptualized, established, and directed the execution of research goals, interpreted the data, reviewed, and edited the manuscript.

6.3. CHAPTER III: Depletion of HuR in murine skeletal muscle enhances exercise endurance and prevents cancer-induced muscle atrophy. *Nature Communications*, 2019.

Brenda Janice Sánchez, Anne-Marie Tremblay, Jean-Philippe Leduc-Gaudet, Derek Hall, Erzsebet Kovacs, Jennifer F. Ma, Souad Mubaid, Patricia L. Hallauer, Brittany L. Phillips, Katherine E. Vest, Anita H. Corbett, Dimitris Kontoyiannis, Sabah N. A. Hussain, Kenneth E. M. Hastings Sergio Di Marco and Imed-Eddine Gallouzi.

B.J.S. performed, analyzed and helped in the interpretation of all the experiments in the manuscript and wrote the original draft. A.K.T. assisted with sample preparation as well as acquisition and analysis of data in the majority of the *in vivo* and *in vitro* experiments. D.T.H. contributed to the investigations and validations of the cachectic experiments and helped edit the manuscript. P.L.H. provided technical expertise and help in sample preparation and data acquisition for Fig. 4 and Supplementary Figs. 3 and 4. S.M., J.M. and B.L.P. assisted in sample preparation and data acquisition of the mRNA stability experiments. S.D. also assisted with the conceptualization, data analysis, and helped edit and review the manuscript. E.K and D.K assisted in the generation of muHuR-KO mice. J.P.L.G. and S.N.A.H. designed and performed the *in-situ* analysis experiments and helped in interpreting and describing the data. A.H.C. and K.H. helped in the interpretation of the data and helped review/edit the manuscript. I.-E.G. conceptualized, established, and directed the execution of research goals, interpreted the data, reviewed, and edited the manuscript.

7. Introduction

In the following section I will provide a comprehensive overview of muscle tissue with special emphasis in skeletal muscle. I will begin with a description of the structural characteristic and functional complexity that make skeletal muscle an important anatomical and metabolic tissue. Then, I will describe in details the process of muscle fiber formation, from its earliest developmental origin in the paraxial mesoderm to the formation of mature myofibers and its regeneration in postnatal life. In the last section of the introduction, I will provide a detailed review of our current understanding of the molecular mechanism mediating myogenesis, emphasising on the key posttranscriptional regulatory events involved in this process.

7.1. Muscle basics.

Muscle is a heterogeneous tissue serving a multitude of functions in the organism. At rest muscle tissue is responsible for approximately 20% of whole-body energy consumption. However, during vigorous exercise, this rate of energy consumption may go up 50 times or more. In vertebrates, there are three types of muscle tissue: Skeletal, Smooth and Cardiac (**Fig 1.1**). These muscle types are defined by two major characteristics: their mechanism of motor control (voluntary or involuntary), and the structure of their contractile units (striated or non-striated)¹³.

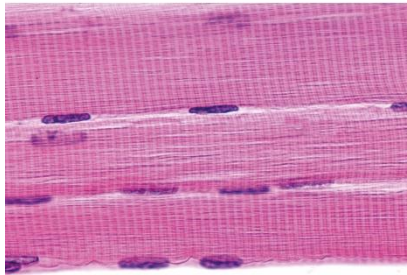
Skeletal muscle is innervated by the somatic nervous system; hence its action is under conscious control (voluntary). Skeletal muscle is composed of long, cylindrical fibers, named myofibers, that contain multiple nuclei distributed along their periphery (**Fig 1.1.A**). Each myofiber is made of repeated contractile units known as sarcomeres, arranged in regular, parallel bundles. Sarcomeres, in turn, contain two types of myofilaments: thick filaments (composed primarily of myosin) and thin filaments (composed primarily of actin). This structural arrangement gives skeletal muscle its characteristic striate appearance and categorize them as such. In response to increased levels of calcium, the thick and thin filaments interact in a sliding motion causing

sarcomere shortening. Simultaneous shortening of multiple sarcomeres results in muscle contraction, which in turn is responsible for the motion and support of the skeleton.¹³⁻¹⁵

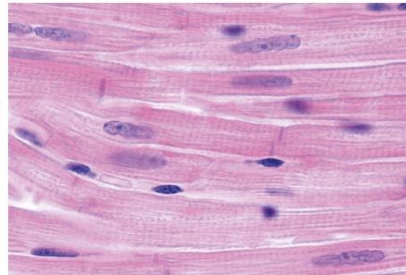
Cardiac muscle is only present in the heart and its contraction leads to the pumping of blood throughout the circulatory system. The cells of cardiac muscle, the cardiomyocytes, are single mononucleated cells attached to one another by specialized cell junctions known as “intercalated discs” (**Fig 1.1B**). Since cardiomyocytes are composed of sarcomeres, cardiac muscle is also categorized as a striated muscle. However, unlike skeletal muscle, cardiac muscle sarcomeres connect at branching, irregular angles and its contraction (heartbeats) is not the result of a single simultaneous shortening of all its sarcomeres. Due to its interconnected configuration, cardiac muscle contraction occurs in a wave-like pattern. This synchronized contraction initiates in specialized cardiac muscle cells called “pacemaker cells” that can generate electrical impulses spontaneously. The native rate of these electrical impulses can increase or decrease in response to signals from the autonomic nervous system and cannot be consciously controlled.^{13,15,16}

Smooth muscle can be found lining the walls of hollow organs, such as the intestines and blood vessels, where its contraction facilitates bodily functions, peristaltic movement and vasoconstriction respectively in the above examples. The contraction of smooth muscle is mainly under the control of the autonomous nervous system, occurring in an involuntary manner. Structurally, smooth muscle tissue is composed of single spindle-shaped cells with a single central nucleus (**Fig 1.1C**). Smooth muscle cells also contain thick and thin myofilaments, but, contrary to skeletal and cardiac muscles, they are not arranged in sarcomeres, therefore they are considered as non-striated muscle. Although their contraction involves the same sliding filament model used by striated muscle, the myofilaments in smooth muscle are anchored to unique structures that are spread throughout the cell named “focal adhesions” and “dense bodies”. When the sliding motion interaction of thick and thin filaments is initiated, focal adhesions are drawn towards dense bodies, effectively squeezing the cell into a smaller conformation. The power of smooth muscle contractions is relatively low when compared to that of striated muscle but it can be sustained over a much greater range of time.^{13,15,17}

A) Skeletal muscle



B) Cardiac muscle



C) Smooth muscle

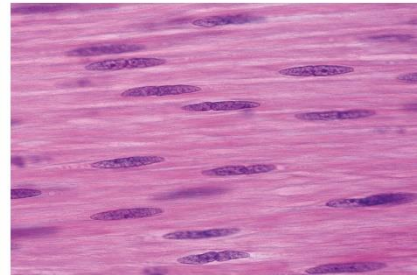


Figure 1.1 Light micrographs of skeletal, cardiac and smooth muscle. A) Transverse histological section of skeletal muscle myocytes showing large, elongated, multinucleated fibers with peripheral nuclei. B) Transverse histological section of cardiomyocytes showing irregular branched myofibrils with central, single or double, nuclei. C) Transverse histological section of smooth muscle showing elongated fusiform shape myocytes with central nuclei. Sections were stained with H&E. (300x magnification). Images used under license from Shutterstock.

7.2. Skeletal muscle structure and contraction.

The skeletal musculature of any given organism is composed of several highly organized discrete organs (muscles), each constituted by blood vessels, connective tissue, muscle fibers and nerves. An individual skeletal muscle is made up of hundreds to thousands of multinucleated muscle fibers, bundled together by an irregular layer of connective tissue known as “epimysium”, which provides protection from friction against bone and other muscles (**Fig 1.2**). The epimysium also projects inward, producing a second layer of connective tissue, the perimysium, which divides the muscle into compartments that contain clusters of muscle fibers, the fascicles. Fascicles can vary in size, from 50 to up to 300 muscle fibers per bundle. A third layer of connective tissue, the endomysium, separates individual muscle fibers within the fascicles, each one resulting from the fusion of many precursor muscle cells (myoblasts), that come together in a process known as “myogenesis” (**Fig 1.2**). The interconnection of the three connective tissue layers (epimysium, perimysium and endomysium) is continuous throughout the muscle and with the tendons allowing an effective and efficient transmission of the contraction force to the bones, thus allowing skeletal movement. In addition, this network of connective tissue also provides a strong structural framework for the blood vessels and nerves. Generally, an artery and at least one vein accompanies each motor neuron that

penetrates the epimysium of a skeletal muscle. Branches of the nerve and blood vessels will then extend along the perimysium and endomysium to transport nutrients and electrical impulses.^{13,15,16}

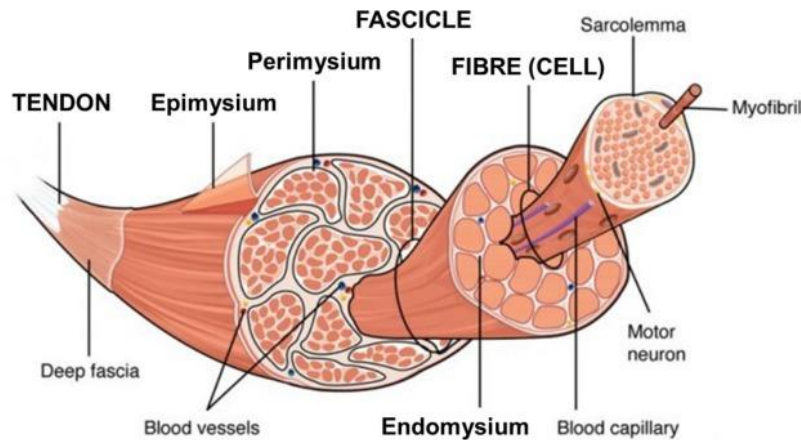


Figure 1.2. Schematic diagram illustrating the structural hierarchy of skeletal muscle tissue. Each skeletal muscle is enclosed within a thick layer of connective tissue called the epimysium, which is continuous with the fascia and the tendon, binding muscle to bone. Large muscles contain several fascicles, each wrapped in a second layer of connective tissue called the perimysium. Within fascicles, individual muscle fibers are surrounded by a third layer of connective tissue, the endomysium. Image used under license from ¹⁸

As mentioned previously, muscle fibers are mainly composed of actin (thin) and myosin (thick) myofilaments which make up more than 50% of total protein in the muscle cell¹⁴. Myofilaments are organized into sarcomeres which can be observed microscopically as structural entities (**Fig. 1.3**). The banding pattern in the sarcomeres is termed according to their appearance under polarized light. Each sarcomere is delimited by two dark colored bands called Z-lines, which define the lateral boundaries of the sarcomere and serve as anchors for thin filaments. The area between the Z-lines is further divided into two lighter colored bands at either end, the I-bands which correspond to thin

filaments, and a darker grayish band in the middle, the A band, which correspond to thick filaments (**Fig. 1.3**).

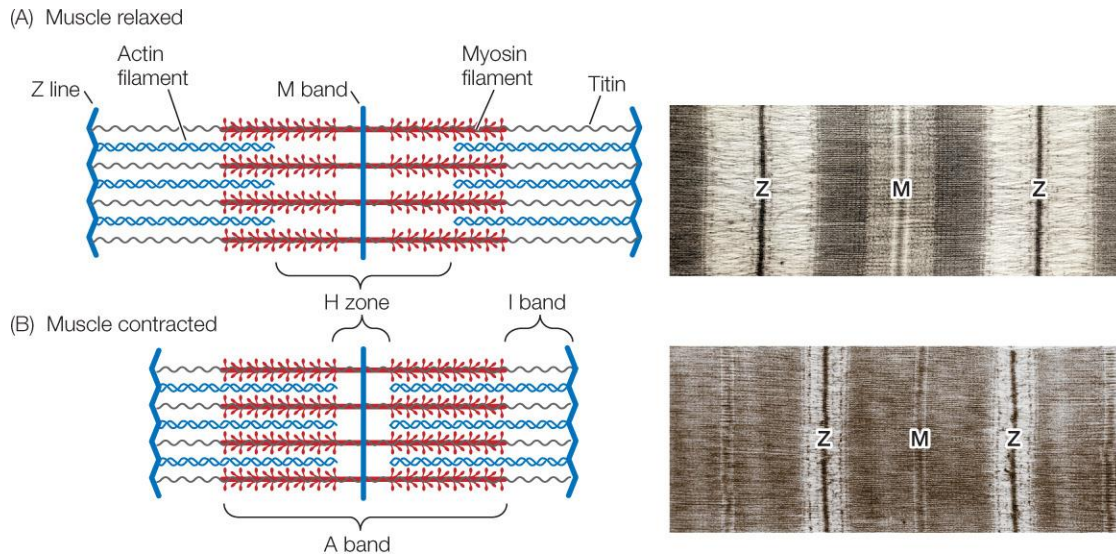


Figure 1.3. Labeled diagrams and electronic micrograph of sarcomeres in a relaxed and contracted configuration. A) Schematic diagram and electronic micrograph of a sarcomere in a relaxed configuration showing its main components. B) Schematic diagram and electronic micrograph of a sarcomere in a contracted configuration showing its main components. The A-band is composed of myosin filaments (Thick) crosslinked at the centre by the M-band assembly. Actin filaments (Thin) are tethered at their barbed end at the Z-disc and interdigitate with the thick filaments in the A-band. Mouse skeletal muscle sections were fixed with glutaraldehyde and embedded in Epoxy resin. Sections were cut with a diamond knife, stained with uranium and lead, and examined with FEI Tecnai-T12 microscope. Image modified from¹⁹.

Each individual muscle fiber is innervated by a single branch of a motor neuron which, through a neuro muscular junction (NMJ), transfers information from the nervous system to the muscle cell. A single motor neuron exclusively innervates a limited number of myofibers which can vary between as little as 3 (in extraocular muscles) to 1000-2000 fibers (in gastrocnemius muscle)^{20,21}. The combination of a motor neuron and the group of fibers that it innervates, constitutes a motor unit, which is considered as the smallest unit of force that can be activated to produce movement. When a motor unit is stimulated, the neuron releases a neurotransmitter (acetylcholine) into the cytoplasm of muscle cells triggering a series of events that lead to the release of large quantities of Calcium ions (Ca^{++}) and activation of the troponin complex. The troponin complex is composed of three regulatory proteins: troponin C (calcium binding), troponin T (tropomyosin binding), and

troponin I (inhibitory) (**Fig. 1.4**). At low intracellular calcium concentrations, the tropomyosin protein sterically blocks the interaction of actin and myosin. As the calcium concentrations increase, tropomyosin no longer blocks this interaction, resulting in the exposure of actin-binding sites and enabling the attachment of myosin to actin (cross-bridge) (**Fig. 1.4**). Following cross-bridge formation, ATP hydrolysis releases the energy required for myosin to pull the actin filament towards the centre of the A band, producing a sliding motion that causes the shortening of the thin filaments. Because actin is tethered to structures located at the Z bands, any reduction on the length of thin filaments results in the shortening of the sarcomere and thus the contraction of the muscle²². While the size, shape, and arrangement of muscle fibers of any given muscle will determine their unique mechanical function, it is the number of sarcomeres that operate together that dictates the amount of force produced by the muscle when it contracts.

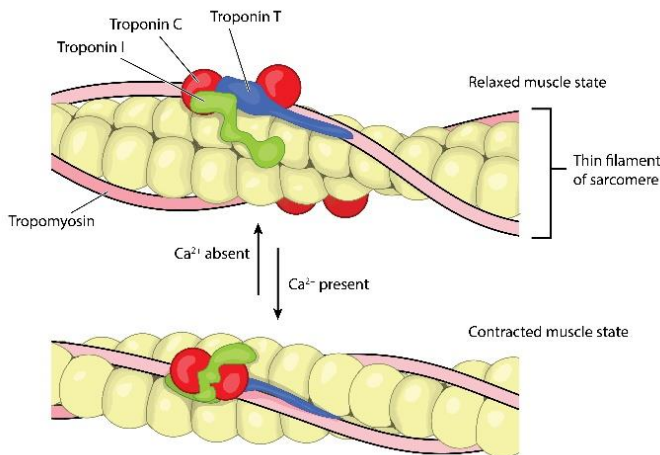


Figure 1.4. Schematic diagram illustrating the mechanism of the troponin complex. The troponin complex is composed of three subunits: TnT, which attaches to tropomyosin; TnC, which binds Ca^{2+} ; and TnI, which regulates the actin-myosin interaction. Troponin complexes attach at specific sites regularly spaced along each tropomyosin molecule. Image used under license from Shutterstock.

7.3. Classification of skeletal muscle fiber types.

In general, muscle motor tasks can be categorized in three types: 1) postural/joint stabilization, such as standing or sitting, 2) long-lasting and repetitive activities like respiration or walking, and 3) fast and powerful actions, such as jumping or running. In order to respond to these needs, muscle fibers have a broad spectrum of physiological characteristics that makes them better suited to each kind of task. The major muscle fibers in mammalian skeletal muscles can be roughly classified into four types; type I, IIA,

IIX, and IIB²³. Muscle fiber types are categorized mainly by the particular isoform of myosin heavy chain (MyHC) they express, although many other components contribute to their specific physiological profile (**Table 1.1**). Type I fibers are slow-contracting, dense with capillaries and rich in mitochondria and oxidative enzymes which allows them to carry more oxygen and sustain aerobic activity using fats or carbohydrates as fuel. Their motor units have a high amount of impulse activity (300,000–500,000 over 24 hrs) with long-lasting trains (300–500 seg) and relatively low frequency of firing (~20 Hz). As such, this fiber type is better suited for postural/joint stabilization. Type II fibers, which are further subdivided into IIA, IIX and IIB, are all consider fast-contracting and are the ones that contribute most to muscle strength. When compared to type I fibers, type II fibers have a lower mitochondrial content, and a much higher level of glycolytic enzymes, although the amount in each subgroup varies (**Table 1.1**). Type IIB produce the fastest, strongest contraction but their motor units have a modest amount of activity per day (3,000–10,000 impulses over 24 hrs), with high discharge frequency (70–90 Hz), and short duration of the trains (<3 seg). Consequently, these fibers are better suited for powerful actions. The motor units for types IIA and IIX do not exhibit major changes in their discharge frequency (50–80 Hz) when compared to type IIB, but they have the ability to sustain much greater activity per day (90,000–250,000 impulses) and relatively long train duration (60–140 seg), coinciding with the requirements for long-lasting and repetitive activities²³⁻²⁵.

Muscle Fiber Type	Gene	MyHC Type	Fiber size and motor unit	Mitochondria and Capillaries	Myoglobin Content	ATP source	Contractile speed	Fatigue resistance	Fuel storage
Type I	MyHC 7	I	Small	High	High	Oxidative phosphorylation	Slow	High	Triglycerides
Type IIA	MyHC 2	IIA	Intermediate	High	High	Oxidative phosphorylation	Intermediate	Moderate/High	Triglycerides
Type IIX	MyHC 1	IIX	Intermediate	Low	Low	Anaerobic Glycolysis	Fast	Moderate/Low	Glycogen
Type IIB	MyHC 4	IIB	Large	Low	Low	Anaerobic Glycolysis	Fast	Low	Glycogen

Table 1.1. Contractile characteristics and metabolic properties of muscle fiber types.
The profile of myosin heavy chains is consistent with speed and endurance.

Each muscle is composed of a mixture of these fiber types, which is mainly determined by genetic factors early in life^{23,26,27}. However, changes in the metabolic environment within different fiber types can lead to the activation of transcriptional programs and signaling pathways that stimulate phenotypic changes to support muscle adaptation, a process known as fiber type switching. While fiber type switching is more likely to occur in developing and regenerating muscle, adult muscle fibers are also susceptible to this fiber type conversion²⁸⁻³⁰. Depending on the stimuli, a switch in fiber type can occur in a bidirectional prearranged pattern (I \rightleftharpoons IIA \rightleftharpoons IIX \rightleftharpoons IIB)^{31,32}. Endurance training has been shown to induce a modestly increased proportion of type I fibers leading to an enhanced oxidative capacity^{33,34}. Conversely, disease states such as obesity, metabolic syndrome and type 2 diabetes have been associated with a switch towards type IIB fibers and decreases oxidative capacity³⁵⁻³⁸.

Due to the energy requirements of each type of fiber, a switch from oxidative phosphorylation (Type I) to aerobic glycolysis (Type II), which is less efficient in generating ATP, can profoundly impact whole body energy consumption. Regulatory pathways that control the metabolic flexibility of skeletal muscle fibers are frequently associated with the activity of two key metabolic regulators: peroxisome proliferator-activated receptor alpha (PPAR α) and peroxisome proliferator-activated receptor coactivator 1 alpha (PGC-1 α)³⁹⁻⁴¹. PPAR α is one of three ligand-activated transcription factors belonging to the peroxisome proliferator-activated receptor (PPARs) subfamily of Nuclear Receptors (NR)⁴². Along with the other two members, PPAR β/δ and PPAR γ , they influence lipid metabolism, inflammation and glucose homeostasis^{41,43,44}. While all three PPARs are expressed in skeletal muscle, they display distinct tissue distribution patterns, enabling them to perform distinct, although overlapping functions. PPAR α is mainly expressed in tissues with high metabolic rates such as liver, heart, muscle, and kidney and it has a central role in fatty acid oxidation and lipoprotein metabolism^{45,46}. On the other hand, PPAR γ is enriched in adipose tissue and is essential for adipocyte differentiation, lipid storage, and glucose metabolism⁴⁶⁻⁴⁹. PPAR β/δ although ubiquitously expressed, is the most abundant PPAR subtype in skeletal muscle^{44,50}. Is an essential regulator of mitochondria biogenesis and fatty acid oxidation (FAO), and its activation triggers a transcriptional program that leads to a drastic increase in the utilization of fatty

acids as fuel⁵¹⁻⁵³. Both PPAR α and PPAR β/δ have been shown to drive the up-regulation of genes involved in Free Fatty Acid (FFA) uptake (such as cluster of differentiation 36/SR-B2 (CD36) and LPL^{52,54,55}), FFA intracellular transport (such as fatty acid binding protein 3 (FABP3)⁵⁶) and fatty acid oxidation (such as CPT1)^{57,58}. In addition, their expression has been associated to skeletal muscles metabolic adaptation through fiber type transformation^{31,53,54,59-63}. Muscle-specific overexpression of an active form of the PPAR β/δ was shown to increase the percentage of type I myofibers causing a lean phenotype, mimicking exercise training⁶⁰. A correlation between the expression of PPAR α and the proportion of type I fibers has been found in human skeletal muscle^{62,64}. The transcriptional activation of PPAR-regulated genes is facilitated by transcriptional coactivators such as PGC-1 α ⁶⁵. PGC-1 α has been established as a master regulator in the maintenance of mitochondrial function, thermogenesis and energy homeostasis⁶⁶⁻⁷⁰. Similar to PPAR β/δ , overexpression of PGC-1 α in skeletal muscle causes a switch from fast to slow muscle fiber type, accompanied by resistance to fatigue⁷¹. Conversely, PGC-1 α skeletal muscle knockout mice show a shift from type I and type IIA, to type IIX and IIB fibers⁷². A decrease in exercise capacity and an enrichment of type II fibers is also evident in conditions, such as insulin resistance and type II diabetes, that result in the decreased expression of PGC-1 α .^{73,74}

Indeed, the metabolic contribution to skeletal muscle fiber type composition is an important consideration in health and disease. It has long been known that another key aspect of fiber type is their differential susceptibility to catabolic signals. While fasting, cancer cachexia, sepsis or exposure of muscles to glucocorticoids triggers the wasting of type IIX and IIB muscle fibers, types I and IIA fibers are known to be sensitive to inactivity, microgravity, and denervation⁷⁵⁻⁷⁸. The underlying cause of this sensitivity to specific atrophy signals has been suggested to be directly associated to the levels of PGC-1 α in these fiber types. PGC-1 α was shown to partially prevent denervation and fasting induced muscle atrophy by reducing the FoxO3 (Fork head box class O 3) dependent upregulation of the ubiquitin ligases Atrogin-1 and MuRF1⁷⁹, two key components of the Ubiquitin Proteasome System (UPS) that control protein turnover in skeletal muscle^{2,75,77,80}. These findings indicate that manipulation of muscle fiber type composition hold promise for treatment of muscle related diseases. However, in order to elicit an integrated

physiological response, the associated changes in neural innervation, motor neuron function, and peripheral metabolic adaptation must be considered.

7.4 Skeletal muscle lineage specification and myogenesis.

During embryonic development the formation of skeletal muscle tissue can be described in two districts but overlapping process: the specification of the myogenic lineage (formation of precursor muscles cells) and the differentiation of precursor muscles cells into muscle fibers. A broad spectrum of regulatory factors and signaling molecules direct these processes; while the specification to the muscle lineage depends on the combined action of the Sine Oculis–Related Homeobox Transcription Factors (Six), the Wnt protein family (Wnt), the bone morphogenetic proteins (BMP) and the Sonic hedgehog (Shh) signalling molecule^{1,81-83}, the progression of precursor muscle cells towards mature myofibers is mainly controlled by a core network of four muscle specific transcription factors; Myf5, MyoD, Myog and MRF4 (**Fig 1.5**)^{8,84}. The expression of these molecules follows a tight spatial and temporal regulation which is crucial for the development of functional skeletal muscle tissue.

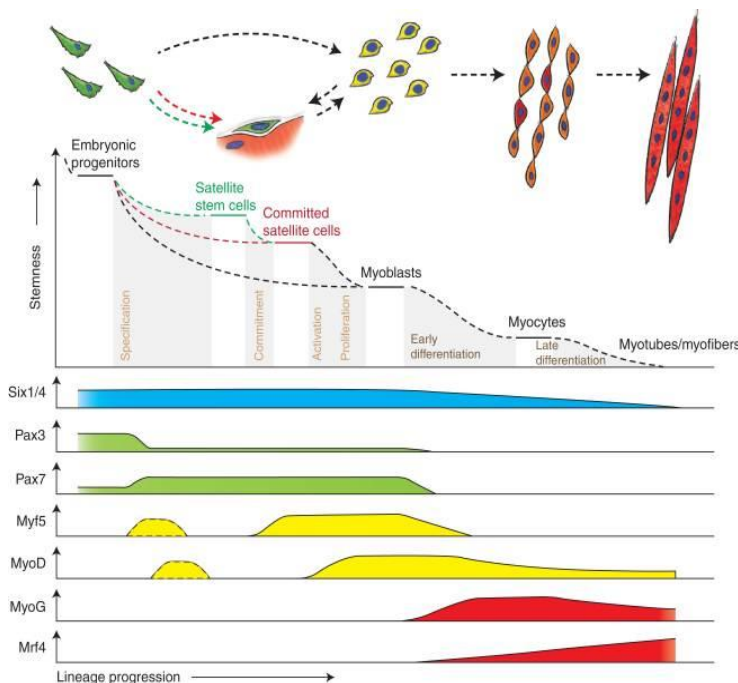


Figure 1.5. Hierarchy of transcription factors regulating progression through the myogenic lineage.

Six1/4 and Pax3/7 are master regulators of early lineage specification, whereas Myf5 and MyoD commit cells to the myogenic program. Expression of the terminal differentiation genes, required for the fusion of myocytes and the formation of myotubes, are performed by both Myog and MRF4. Muscle progenitors that are involved in embryonic muscle differentiation skip the quiescent satellite cell stage and directly become myoblasts. Image modified from ¹

7.4.1 Specification of the muscle lineage.

In mammals, the positions and identities of cells that will form the three germ layers; ectoderm, mesoderm, and endoderm, are determined early in gestation. These three layers give rise to every organ in the body; from muscle and hair, to blood vessels and brain (**Fig. 1.6**)⁸⁵. During the course of development, the middle layer, named the mesoderm, is anatomically separated into the paraxial, intermediate, and lateral mesoderm. Differential gene expression and morphogen gradients along the axis of the embryo induce pairwise condensations of paraxial mesoderm into somites. Somites are the first metameric structures in mammalian embryos, they develop progressively into distinct dorso–ventral compartments. Skeletal muscles of the body, with the exception of some head muscles, are derived from cells from the most dorsal portion of the somites, referred as dermomyotome (**Fig 1.7**)^{86,87}.

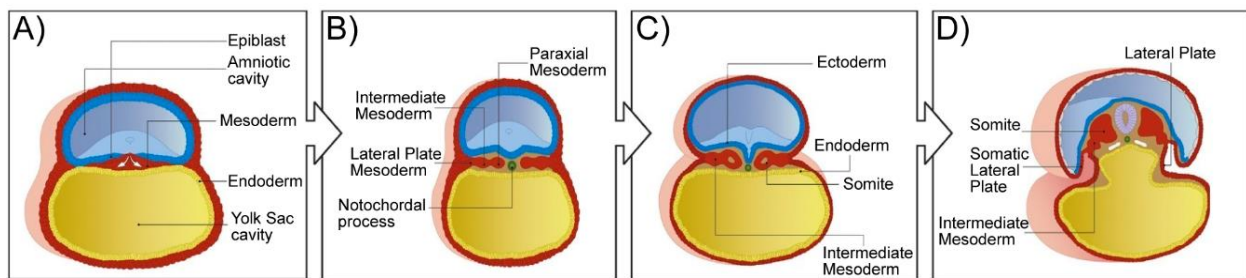


Figure 1.6. Schematic illustrating the organization of the three germ layers during succeeding days of mouse gestation. A) At E6.5 of mouse development, the three germ layers, Ectoderm, Mesoderm and Endoderm, are clearly visible in the trilaminar embryo. B) As development proceeds, the mesoderm will have organized into 3 areas: the paraxial mesoderm, adjacent to the notochord; the lateral plate mesoderm at the periphery; and the intermediate mesoderm, localized between the two. C) At E8.0, the paraxial mesoderm has increased in size and has organized itself into a somite. D) By E10.5 the somite has enlarged, and neural tube formation has concluded. Image modified from⁸⁸.

The molecular signals that direct progenitor cells from the dermomyotome towards the myogenic lineage do not act in a strictly linear manner. They are rather organized in complex feedback and feed-forward networks. Still, the expression of the transcription factors *Six1* and *Six4* at embryonic day 8 (E8.0) is currently considered as the highpoint in the genetic regulatory cascade that mediates specification of the myogenic lineage⁸⁹. Disruption of the *Six1* gene was shown to lead to neonatal lethality due to the absence of

diaphragm muscle and severe hypoplasia⁹⁰. By binding to the MEF3 sites in the promoters of its target genes *Six1*, in collaboration with its co-activators *Eya1/2*, regulate the expression of several promyogenic genes. Upregulation of one of these genes, the paired box transcription factor 3 (*Pax3*), is crucial for promoting the commitment of embryonic stem cells to the myogenic lineage^{28,91}. Although neither *Pax3* nor its paralogue *Pax7* are skeletal muscle specific, their expression in stem cells from the dermomyotome marks the acquisition of the identity as a muscle progenitor cells. *Pax3* and *Pax7* are expressed in partially overlapping domains, however, they are not functionally equivalent; while *Pax3* is required for the efficient delamination and migration of progenitor muscle cells from the dermomyotome, *Pax7* plays an important role in regulating the onset of muscle fiber formation in pre and postnatal myogenesis⁹².

Downstream of *Six1/4*, the early progenitors muscle cells delaminating from the dermomyotome continue to progress towards the myogenic lineage due to the combinatory action of *Bmp4*, *Wnt* and *Shh* signaling molecules⁹³. Activation of *Shh* signaling in both the floor plate and the notochord, and *Wnt* signal (mainly *Wnt1* and *Wnt3*) from the neural tube (**Fig. 1.7**), synergistically induce the expression of *Myf5* that, together with *Pax3*, activates *MyoD* expression^{1,94,95}. Subsequently, downregulation of *Pax3* and activation of *MRF4* in these early precursor cells leads to the formation of the myotome⁹⁶, a primitive muscle structure containing the first fully differentiated muscle cells named mononucleated myocytes (**Fig 1.8C**). At around E11, the newly formed mononucleated myocytes elongate along the anterior-posterior axis of the embryo to span the entire somite length, a process controlled by *Wnt11* signaling⁹⁷. Simultaneously, *Bmp4* expression in the lateral-plate mesoderm (**Fig 1.7**) promotes expression of *Pax3* and delays upregulation of *MyoD*^{92,98}, adversely affecting the elongation of the myotome. The apparent antagonism between *Bmp4* and *Shh/Wnt* signaling is key in muscle development, as it prevents a precocious commitment of progenitor cells into the myogenic lineage. By maintaining *Pax3* expression *Bmp4* promotes an asynchronous specification patterning, allowing the influx of a sufficient pool of cells that will enter terminal specification, while at the same time maintaining a certain population of cells in a stem like state.

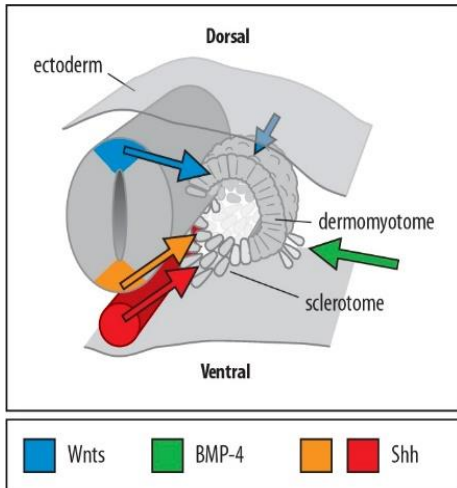


Figure 1.7. Signaling molecules regulating progression of the myogenic lineage. Several signaling molecules are secreted from various domains in the embryo to specify the maturation of the somite into the sclerotome, the dermomyotome and, subsequently, the myotome. Wnt proteins are secreted from the dorsal neural tube and the surface ectoderm while Shh is secreted from the floor plate and the notochord. The combination of Wnt and Shh signaling activities are required to induce the expression of *Myf5*. This contrasts with the function of BMP4, secreted from the lateral mesoderm plate. A balance between these dorsal and ventral signals is key to promoting local identity of precursor muscle cells. Image modified from ⁹⁹.

Myotomal myocytes transition from a mononucleated to a multinucleated state occurs rapidly during embryogenesis (**Fig. 1.9**) and is hallmarked by the formation of embryonic myoblast. Myoblasts are mitotically competent cells derived from the dermomyotome, which show a *Pax3*⁺, *MyoD*⁺, *Myf5*⁺ expression profile. These cells are considered as the final stage in the specification of the myogenic lineage. Once formed, embryonic myoblast will progressively translocate to the myotome and continue to proliferate within it. Upon myotome colonization, they will exit the cell cycle and begin fusing to form muscle fibers, a process referred as myogenesis.

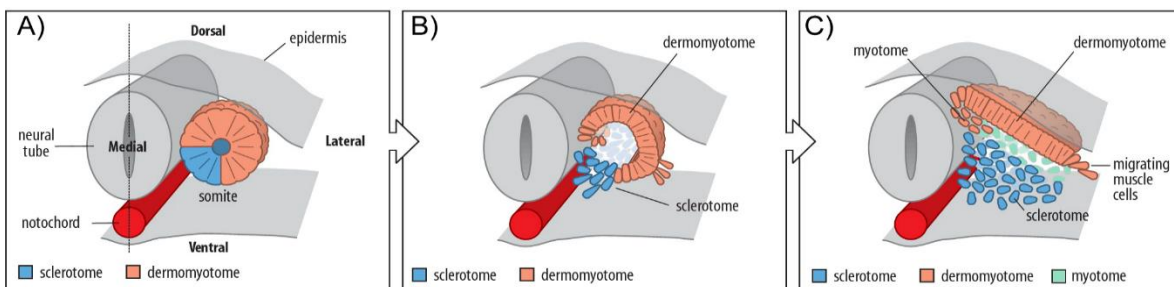


Figure 1.8. Schematic representation of transverse sections through the embryo illustrating the process of myotome formation during succeeding days of gestation. A) Upon undergoing mesenchymal-epithelial transition (MET), the newly matured somites develop into an outer epithelial region (outer pink layer), organized around a mesenchymal core (blue). B) As development proceeds, the outer epithelial cells will differentiate to form the dermomyotome while the mesenchymal cells will differentiate to form the sclerotome. C) By E11.0 of mouse embryo, muscle progenitor cells have migrated from the dermomyotome to form the myotome (green), composed of mononucleated myocytes. Image modified from ⁹⁹.

7.4.2 Skeletal myogenesis during embryogenesis.

The presence of embryonic myoblast in the myotome initiates the second phase of muscle development; Myogenesis^{84,93,100}. During embryogenesis myogenesis occurs in two distinct phases: an early embryonic or primary phase (E10.5-E12.5 in mouse,) and a later fetal or secondary phase (E14.5-17.5 in mouse)^{101,102}. During primary myogenesis, embryonic myoblasts residing in the myotome fuse to form primary (nascent) myotubes which contain few nuclei^{1,98}. Whether myotomal cells are incorporated into primary myotubes or undergo programmed death upon the formation of primary fibers is still a subject of debate. However, it is clear that these myotomal cells provide the scaffold that supports the differentiation of proliferative myoblasts into muscle fibers^{103,104}. As myoblast begin fusing, *Pax3*⁺ cells from the dermomyotome will infiltrate the myotome and align with nascent myotubes. Some of these myogenic progenitors will begin downregulating *Pax3* and start expressing *Pax7*. A subset of *Pax7*⁺ cells will then proliferate and replenish the progenitor pool, while others will withdraw from cell cycle and recapitulate the molecular regulatory pathways that lead to their differentiation into myoblast (*Pax3*⁺, *MyoD*⁺, *Myf5*⁺ expression profile). Formation of myoblast derived from these *Pax7*⁺ progenitor pool (fetal myoblast) marks the completion of primary myogenesis (**Fig. 1.9**)^{1,82,105,106}.

Secondary myogenesis is identified by the incorporation of fetal myoblasts to pre-existing primary fibers and their de novo fusion to form secondary fibers. Further maturation of the multinucleated fibers will lead to innervation and expression of muscle structural proteins such as myosin and actin and the assembly of functional myofibers¹⁰⁵. During this phase, *Pax7*⁺ progenitor cells will position beneath the basal lamina that surrounds each muscle fibre to give rise to the first satellite cells (SC). As development proceeds some of the newly formed satellite cells will enter quiescence and henceforth reside within the muscles, providing the myogenic precursors involved in myofiber growth, and repair in postnatal life (**Fig. 1.9**)^{81,107-109}.

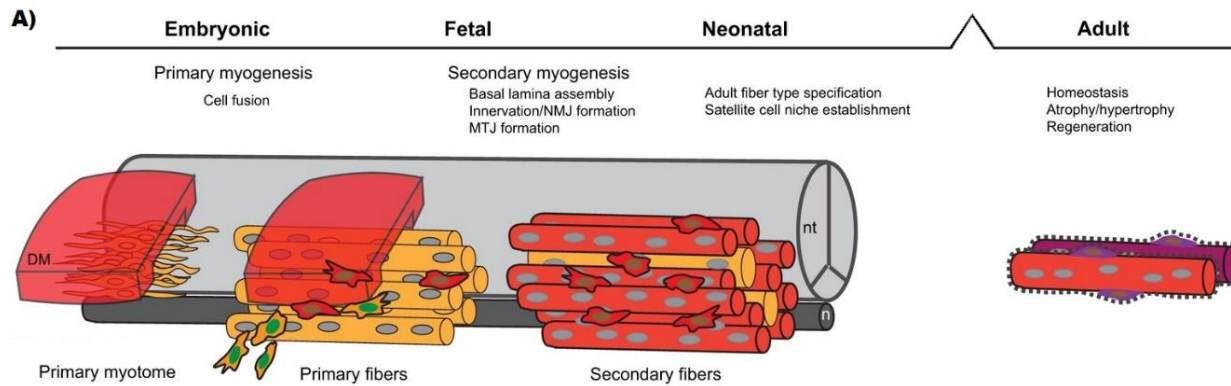


Figure 1.9. Stages of skeletal myogenesis from the embryo to the adult. A) The early myotome (left, yellow) is composed of mononucleated myocytes which are aligned along the anteroposterior axis and span each somitic compartment. During primary myogenesis (Embryonic stage), Pax3⁺ progenitors (yellow cytoplasm, green nuclei) delaminate from the dorsal side of the dermomyotome and contribute to the formation of large primary myofibers (yellow). During secondary myogenesis (Fetal stage), Pax7⁺ myogenic progenitors (red cytoplasm, brown nuclei) contribute to secondary (red) fiber formation, using the primary fibers as a scaffold and contributing to the growth of fetal muscles. During this phase, satellite cell precursors (purple cytoplasm, brown nuclei) localize under the basal lamina (dotted line) of the fibers where they can be found in adult muscles. Key processes associated with each stage are listed above. DM, Dermomyotome; nt, neural tube; n, notochord. Image modified from ¹¹⁰

7.4.3 Skeletal myogenesis in postnatal life, regeneration.

Muscle fiber formation in postnatal life, recapitulates many aspects of embryonic myogenesis however one key difference is the inability of adult tissue to generate de novo myofibers¹¹¹. In higher vertebrates, the total number of muscle fibers present in each muscle is fixed at the time of birth and while growth, injury or other subtle stresses, such as exercise-induced muscle damage, can stimulate the proliferation and fusion of myoblast to pre-existing fibers, this process slows as the animal grows so that little or no myoblast proliferation or fusion occurs in the adult¹. Similar to embryonic myogenesis, postnatal myogenesis requires the recruitment of an undifferentiated progenitor cells to the site of injury and its differentiation into myoblasts, marked by the irreversible expression of *Myf5*, and *MyoD*, this function is provided by the SC. Unless activated by muscle injury or other stimuli, adult SCs exist in a quiescent, non-proliferative state¹¹². Once activated, they will follow either self-renew or differentiate into myoblast. If self-

renewed, SC will either follow an asymmetric division in an apical–basal orientation, give rise to a stem cell that is identical to the original stem cell (Pax7⁺/Myf5⁻ expression profile) and a committed daughter cell (Pax7⁺/Myf5⁺ expression profile) or a planar symmetric division leading to the expansion of SC stem cell population (**Fig. 1.10**).

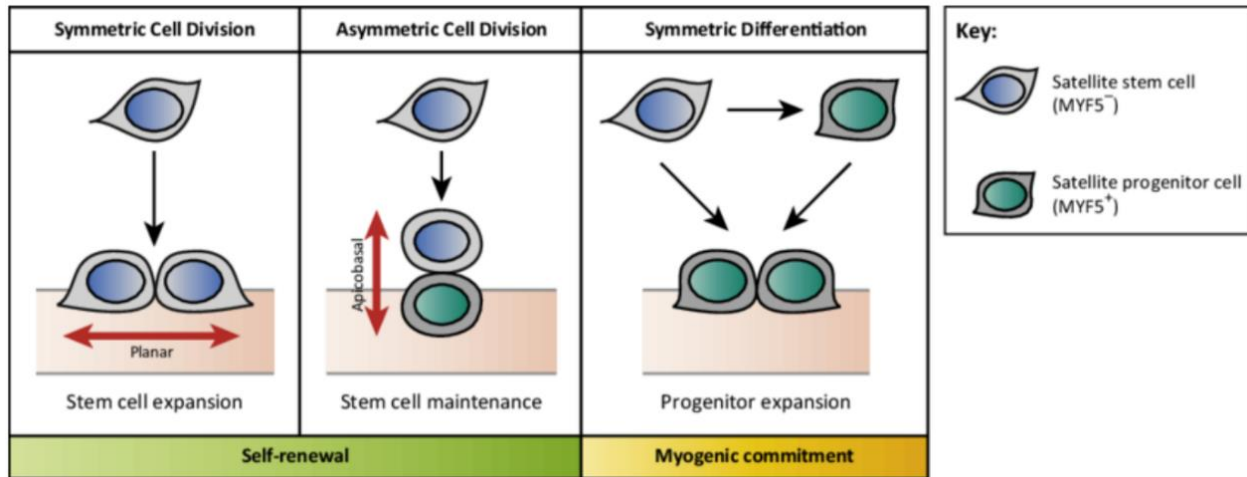


Figure 1.10. Modes of satellite stem cell division. Satellite stem cells can self-renew via symmetric or asymmetric cell divisions. A symmetric cell division along the planar axis (with respect to the myofiber) generates two stem cell daughters. Asymmetric cell divisions along the apicobasal axis give rise to a stem cell and a committed myogenic progenitor cell. Alternatively, satellite stem cells can directly express myogenic commitment factors (such as Myf5) to commit to the myogenic lineage and expand the progenitor population that will participate in muscle repair. Image from ¹¹³.

Wnt and Notch signaling are both involved in the cell fate regulation of SC. Wnt7a, released from regenerating muscle fibers, signals through the planar cell polarity pathway to expand satellite stem cell population through symmetric divisions¹¹⁴, leading to a dramatic enhancement of the regenerative capacity of injured muscle¹¹⁵. Interestingly, the timing of Wnt activation has been shown to be critical to determine the SC fate. A transition from Notch signaling, which functions to expand the progenitor pool of adult skeletal muscle upon injury, toward Wnt3a signaling has been reported to be required for efficient myoblast differentiation and muscle regeneration which is maintained in the active state by Notch signaling and inactivated by Wnt signaling¹¹⁵. The balance between self-renewal and differentiation is crucial for stem cell maintenance and tissue homeostasis. Dysfunction leading to decreased self-renewal would eventually lead to

depletion of the stem cell population, while uncontrolled self-renewal would result in overproduction of stem cells and potentially tumorigenesis.

7.5 The gene regulatory network mediating skeletal myogenesis.

As mentioned previously, myogenesis is controlled by a core network of transcription factors, the MRFs; *Myf5*, *MyoD*, *Myog* and *MRF4*, that induce or repress the expression of muscle-specific genes in response to various signals^{7,8,34,82,83,107,109,116-118}. MRF genes are expressed exclusively in myogenic cells. The transcriptional activity of the MRFs is mediated by a bHLH domain which binds to E box sequences (CANNTG) in the promoter of many pro-myogenic genes¹¹⁹. Expression of the MRFs is under strict spatial and temporal activation; while high levels of *Myf5* and *MyoD* are observed in the early stages of myogenesis, coinciding with the formation and expansion of the mononucleated myoblast population¹²⁰, *Myog* and *MRF4* levels increase only at a later stage when myoblasts fuse (a process referred to as myoblast differentiation)^{7,8,34,82,107,109,116-118,121}.

First detected at E8.5, *Myf5* mRNA reaches a maximal level between E9.5 and E10.5¹²², after this peak of expression, *Myf5* level declines rapidly beginning in the rostral part of the embryo and proceeding in caudal direction^{8,123}. *MyoD* expression begins at E10.5 and in contrast with *Myf5*, its expression is continuous and persistent throughout prenatal development. *MyoD* transcripts accumulate mostly in the hypaxial myotome, where it drives the differentiation of the limb, tongue and diaphragm muscles^{8,117,124}. *Myog* and *MRF4* act later in the myogenic process and are considered as “differentiation MRFs”. Accumulation of *Myog* mRNA is first detectable in rostral somites at the time of myotome formation. *Myog* plays a critical role in the terminal differentiation of myoblasts but is dispensable for the generation of the myogenic lineage as evidenced by the fact that mice lacking *Myog* have poorly developed skeletal muscle tissue even though myoblasts are present^{8,34,103,125,126}. Through the activation of p21, *Myog* promotes an irreversible cell cycle withdrawal, an event that also triggers the expression of muscle structural proteins such as myosin and actin^{105,127}. *MRF4* expression is first detected in somites about 12 hr after *Myog*. Similar to *Myf5*, its expression is only transient as *MRF4* transcripts can only be detected, by *in situ* hybridization, for about 2 days and its presence is restricted to the

myotome sand¹²⁸. As development proceeds, the expression of *MRF4* transcripts reoccurs from E16 onwards in fully formed skeletal muscle^{129,130}. This biphasic expression is unique to *MRF4* and is suggested to be necessary for myotome formation¹³¹. However, given that *MRF4* null mice are viable and do not show compromised muscle function¹³², the specific role and importance of *MRF4* remains unclear.

Numerous studies have been directed to uncover the transcriptional regulation of the genes encoding the MRFs. The undertaking of these studies has led to the characterization of several transcription regulatory elements in the *MyoD*, *Myog* and *Myf5/MRF4* locus (**Fig. 1.11**). In the case of *MyoD*, its expression is regulated by the concerted effects of two elements located upstream of the *MyoD* Transcriptional Start Site (TSS); the core enhancer (CE) that directs early embryonic expression, and the distal regulatory region (DRR) involved in its expression in differentiating muscles (**Fig. 1.11A**)¹³³⁻¹³⁵. Expression of *Myog* is delineated by 6 well characterized binding sequences within the 143 bp immediately upstream of the *Myog* TSS. These include a TATA Box, MEF2, MEF3, PBX, and an E-Box (**Fig. 1.11B**)^{136,137}. In addition, three elements with enhancer-like characteristics have been detected in the *Myog* locus; an early enhancer at -4.5 kb upstream of the TSS which is active within the first 24 hr of the onset of myoblast fusion and two late enhancers, at -5.5 kb, and -6.5 kb, which drive *Myog* expression 60 hr after the onset of myoblast differentiation¹³⁷.

The regulation of the *Myf5/MRF4* loci is a bit more complex, given the proximity of the *Myf5* and *MRF4* genes (8.8kb)^{138,139}. Multiple enhancer regions have been identified in the 140 kb region upstream of *Myf5*'s TSS. At least 4 different enhancer cassette control distinct expression patterns of *Myf5* in dorsal dermomyotome, ventral dermomyotome, branchial arches and limb & myotome (**Fig. 1.11C**)^{138,140,141}; *MRF4* biphasic expression (embryonic and foetal/adult) requires at least four enhancer regions that overlap with those of *Myf5*. While three elements specifically drive the embryonic phase in central thoracic myotome, ventral and dorsal myotome, and the somatic bud, a single enhancer has been implicated in its expression in multinucleated fibers (**Fig. 1.11C**)¹³⁹. Studies of the activities of MRFs enhancers in muscle progenitor lineages of wild-type and mutant embryos have provided insights into the tremendous diversity of

developmental signaling ligands and signal transduction effectors molecules that interactively and independently control MRFs activation^{90,95,133}. In addition to this network of transcriptional activation/repression, auto-regulation and cross-regulation exists among the myogenic bHLH proteins; MyoD and Myog have been long known to regulate each other while at the same time modulating their own level of expression and MRF4 has been shown to negatively regulate the level of Myog while being subject to trans-activation by all other MRFs itself^{120,132,142}.

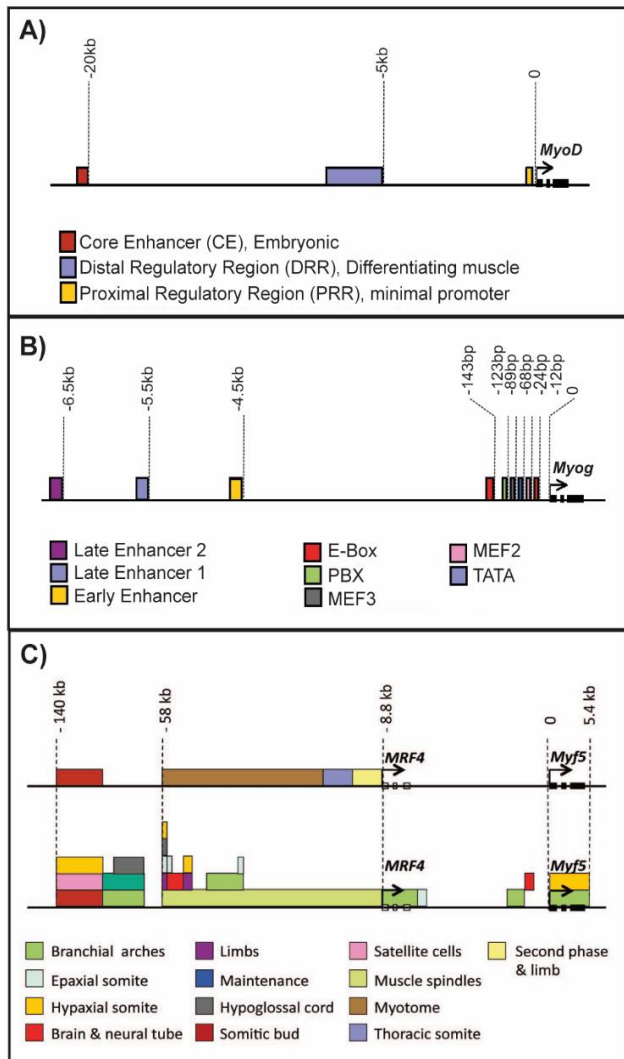


Figure 1.11. Transcription regulatory elements in the *MyoD*, *Myog* and *Myf5/Mrf4* locus. A) Enhancer regions controlling *MyoD* expression B) Conserved DNA binding elements within the *Myog* promoter. Modified from¹⁴³ C) *Myf5* and *MRF4* genes are both located on chromosome 10, about 8.8 kb apart. Elements regulating *MRF4* expression, located upstream of *MRF4* TSS are shown on the top part. *Myf5* enhancers spanning 140 kb upstream of the *Myf5* start site and the intragenic region of *Myf5* are shown on the bottom part. Image modified from¹²³.

7.6 The role of post-transcriptional regulation in myogenesis.

Gene expression studies have demonstrated that a tight and coordinated regulation of the expression levels of MRFs is required for myogenesis to occur^{1,8} and that the onset and progression various skeletal muscle disorders share a deregulation of these timely series of events^{13,14}. MRFs levels can be dynamically regulated by either restricting the abundance of mRNA, achieved by modulation of the transcriptional activity, or by restricting the abundance of the protein product through post-transcriptional regulation. While transcription plays a prominent role in the regulation of myogenesis, we now know that transcription alone is not sufficient to maintain the high levels of MRFs needed during the life span of a myotube. Over the past two decades, numerous studies have demonstrated that post-transcriptional regulatory events play prominent role in regulating the spatial/temporal abundance of MRFs during myogenesis.

When a eukaryotic gene is transcribed, the nascent RNA produced isn't immediately considered a messenger RNA (mRNA). Instead, it is present as an "immature" molecule called a pre-mRNA. The maturation of an mRNA involves an extensive series of posttranscriptional modifications which include the removal of introns, the addition of a 7-methyl-guanylate (m7G) cap structure at the 5' end and the addition of a stretch of 100-250 adenine residues at the 3' end of the mRNA (the poly(A) tail). The resultant mature mRNA has a tri-domain structure consisting of a 5' untranslated region (5'UTR), a coding region made up of triplet codons, each encoding an amino acid, and a 3'UTR (**Fig. 1.12**). UTRs are known to play crucial roles in the posttranscriptional regulation of gene expression by controlling, among other things, the nuclear export, subcellular localization, stability, and/or translation of mRNA molecules. Each one of these posttranscriptional regulatory events can potentially be speed up, slowed down, or altered allowing us to achieve a highly refined modulation of gene expression.

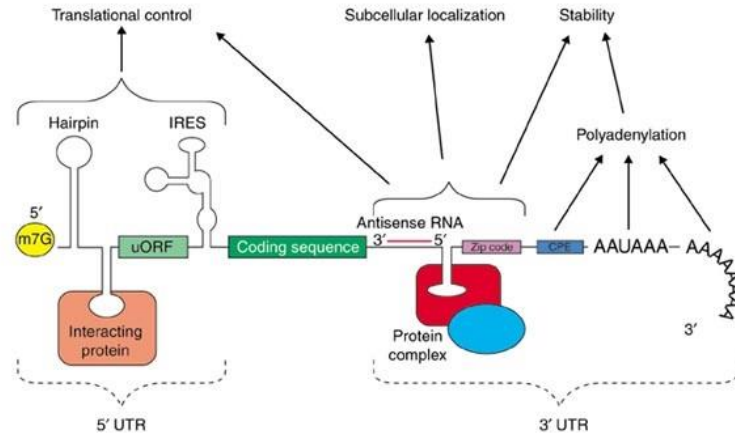


Figure 1.12. Overall structure of eukaryotic mRNA. The generic structure of a eukaryotic mRNA containing the 5' and 3'UTRs as well as the coding region. Also illustrated are some post-transcriptional regulatory elements that affect gene expression. UTR, untranslated region; m7G, 7-methyl-guanosine cap; hairpin, hairpin-like secondary structures; uORF, upstream open reading frame; IRES, internal ribosome entry site; CPE, cytoplasmic polyadenylation element; AAUAAA, polyadenylation signal. Image from¹⁴⁴.

Multiple, distinct mechanisms are involved in mediating posttranscriptional regulatory events, and nearly all of them involve the association of trans-acting factors, such as miRNAs and RBPs, to *cis*-regulatory sequence elements located in the 5' and/or 3'UTR region of the corresponding RNAs. The 5' region, which includes the 5'cap structure and the *cis*-elements in the 5'UTR, are best known for their role in regulating cap-dependent as well as cap-independent (via Internal Ribosome Entry Sites: IRES) translation¹⁴⁵. The 3' UTR is best known for its role in regulating the half-life and decay of a message due to the presence of *cis*-elements, such as the adenylate-uridylylate-rich element (ARE), that confer instability¹⁴⁶.

Individual mRNAs can harbor multiple discrete *cis*-elements for binding to multiple RBPs or miRNAs, allowing for a transcript-specific regulation that integrate multiple signals. In a complementary concept, nearly all trans-acting factors bind to a multitude of mRNAs that frequently encode functionally related proteins¹⁴⁷. Hence, the organization and active interplay between RBPs, miRNAs, and a given mRNA allows for a dynamic regulation of gene expression, which is critical in tissues like skeletal muscle, which has an inherent ability to fine tune its expression profile in response to environmental and physiological changes, including but not limited to exercise, diet, disuse, and disease.

7.6.1 Cis-Regulatory elements involved in posttranscriptional regulatory mechanisms.

While advances in high-throughput assays and genomic studies has expanded the genomic mapping of *cis*-regulatory elements, determining which sites are biologically functional remains a major challenge. Among these sequences, the ARE represent the most conserved and well-studied group of RNA *cis*-elements known to regulate a distinct subset of transcripts. This group of sequences is very heterogeneous and includes AUUUA pentamers and AT-rich stretches that can be found clustered in different combinations (**Table 1.2**). The functional role of the ARE was first established *in vitro* by subcloning the ARE-containing sequence from the 3'UTR of granulocyte macrophage-colony stimulating factor (GM-CSF) mRNA in a reporter gene construct. The inclusion of the GM-CSF mRNA ARE in the 3'UTR of the reporter construct decreased the stability of the chimeric reporter mRNA¹⁴⁸. Recently, genome-wide analyses of mRNA transcript half-lives showed that transcripts containing conserved AREs in their 3' UTRs have short half-lives¹⁴⁹ and that the combination of multiple clusters of AREs in any given transcript has an additive effect on mRNA decay and deadenylation processes¹⁵⁰. In addition to mRNA turnover, AREs also participate in regulating the translation of messages¹⁵¹. However, the specific interrelationship between the ARE-mediated control of mRNA turnover and translation is yet to be fully uncovered.

Trans-acting factors	Functional categories	ARE sequences	Cluster	GRE sequences	Functional categories	Trans-acting factors
ELAVL1	Cytokines,	AUUUUAUUUAUUUAUUUAUUUA	I	GUUUGUUUGUUUGUUUGUUUG	Transcription factors;	CELF1
ELAVL2	Chemokines				Cell cycle;	CELF2
ZFP36	Growth factors;	AUUUAUUUAUUUAUUUA	II	GUUUGUUUGUUUGUUUG	Cell metabolism; Cell-cell communication	ELAVL4
KSRP	Cell signaling;	WAUUUAUUUAUUUA	III	GUKUGUUUGUKUG	regulators	RBM38
TIA1, TIAL1	Apoptosis	WWAUUUUAUUUA	IV	KKGUUUGUUUGKK		TARDBP
HNRNPC1 HNRNPD GAPDH		WWWWAUUUA	V	KKKU/GUKUG/UKKK		FUS

Table 1.2. Conserved sequences of ARE and GRE post-transcriptional cis-regulatory elements.

Another closely related cis-element recognized as essential regulators of mRNA splicing, stability, and translation in mammalian cells is the GU-rich element (GRE) which differs from AREs by 2 nt (GUUUG) (**Table 1.2**)¹⁵². GRE-containing RNAs represent approximately 8% of transcripts of the human transcriptome and are mainly involved in controlling mRNA turnover¹⁵³. Several RBPs, mostly those containing RNA Recognition Motive (RRM) domains^{152,154-156}, have been reported to bind with higher affinity to GRE repeats, RBPs belonging to the CELF family are the preferential regulators of GRE containing transcripts, mediating their degradation. The mechanism through which GREs and AREs control of mRNA turnover rely on the formation of RNP complexes, that involves the binding of RBPs to these elements. Upon binding, these factors can either accelerate or slow down deadenylation-dependent mRNA decay by influencing multiple steps of the decay process, including the accessibility of the RNA transcripts to specific mRNA degrading machinery¹⁵⁷⁻¹⁶⁰. Both the CELF and ELAVL families of RBPs have been shown to bind strongly to the ARE and GRE elements^{155,156,161-165}. These two families share over 80% of sequence conservation within RRMs but cause opposite outcomes. While the CELF family binding to GRE leads to mRNA degradation¹⁶⁵, the ELAVL family function as stabilizers of mRNAs containing AREs in their 3'UTR^{156,159,166-170}. ARE-mediated regulatory mechanisms play a critical role in the process of muscle cell differentiation, the genes encoding for the MRFs MyoD and Myog, contain AREs/GREs in their 3'UTRs^{6,11}, and their stability has been shown to increased upon the induction of muscle differentiation^{6,7,11}. However, the mechanisms through which AREs mediate the expression of these promyogenic targets is yet to be elucidated.

7.6.2 Posttranscriptional regulation through microRNAs.

miRNAs are evolutionarily conserved, small non-coding single-stranded RNAs (ssRNAs) of ~22 nt in length that can promote translational repression or induce the decay of their targeted mRNAs. miRNAs are first transcribed as primary miRNA molecules (pri-miRNA), which base pair with themselves and fold over, creating a hairpin. Next, the hairpin is processed by the microprocessor complex Drosha/DGCR8 to generate a small double-stranded fragment of about ~70 bp (pre-miRNA) which is then exported to the

cytoplasm by the Exportin5 protein¹⁷¹. In the cytoplasm, pre-miRNAs are further processed by the RNase III Dicer to yield ~22 nt pre-miRNA duplex. Later, with the help of two closely related proteins, the TAR RNA-binding protein (TRBP /TARBP2) and PACT (PRKRA), the newly formed pre-miRNA duplex is loaded onto Argonaute (AGO) proteins to generate the RNA-induced silencing complex (RISC). One strand of the ~22-nt RNA duplex will be degraded while the other one will remain in the Ago protein as a mature miRNA (**Fig. 1.13**)¹⁷¹.

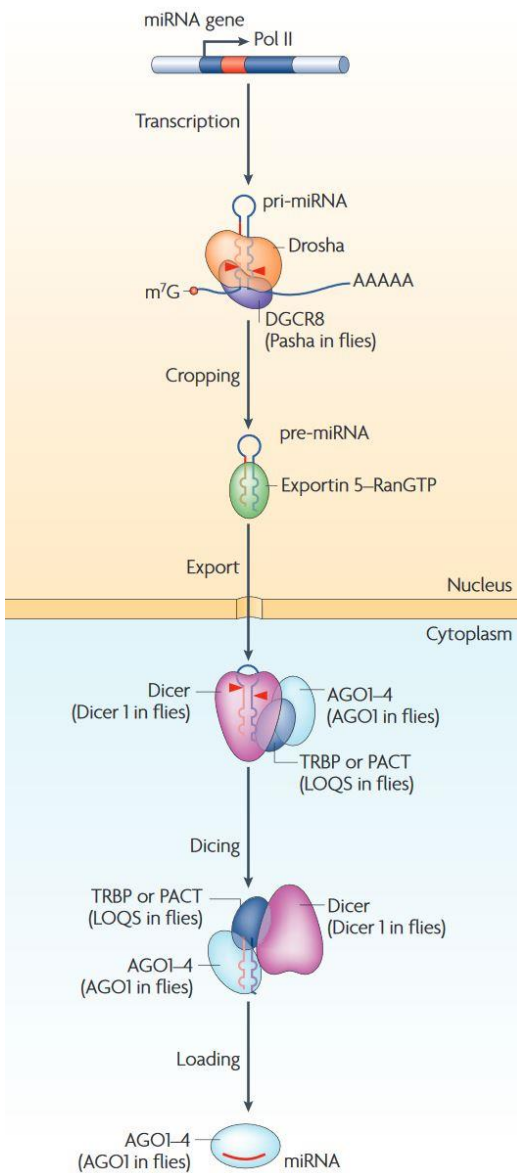


Figure 1.13. Biosynthesis of miRNA. microRNA genes are transcribed by RNA polymerase II (Pol II) to generate the primary transcripts (pri-miRNAs). The initiation step (cropping) is mediated by the Drosha–DiGeorge syndrome critical region gene 8 (DGCR8; Pasha in *Drosophila melanogaster* and *Caenorhabditis elegans*) complex (also known as the Microprocessor complex) that generates ~65 nucleotide (nt) pre-miRNAs. Pre-miRNA has a short stem plus a ~2-nt 3' overhang, which is recognized by the nuclear export factor exportin 5 (EXP5). Once exported from the nucleus, the cytoplasmic RNase III Dicer catalyses the second processing (dicing) step to produce miRNA duplexes. Dicer, TRBP (TAR RNA-binding protein; also known as TARBP2) or PACT (also known as PRKRA), and Argonaute (AGO)1–4 (also known as EIF2C1–4) mediate the processing of pre-miRNA and the assembly of the RISC complex (RNA-induced silencing complex) in humans. One strand of the duplex remains on the Ago protein as the mature miRNA, whereas the other strand is degraded. Ago is thought to be associated with Dicer in the dicing step as well as in the RISC assembly step. In *D. melanogaster*, Image from ¹⁷¹

To control their biological function, miRNAs act on their mRNA target through complete or near-complete sequence complementarity¹⁷². The interaction between miRNAs and their RNA targets is mediated through a seed element in the 3'UTR of the mRNA, which is composed of 8 nt that are complementary to nucleotides 2–9 of the 5' end of the miRNA. Canonical binding sites are characterized by a complete base pairing between the miRNA seed sequence and the mRNA target, while noncanonical sites are based on the imperfect base pairing at the seed sequence¹⁷³.

The precise molecular mechanisms that underlie the function of miRNAs remain largely unknown. However, several studies suggest that the extent of complementarity between the miRNA and its target transcript is determinant for the mechanism of silencing. For example, with the exception of miR-172, which acts as a translational repressor, all characterized plant miRNAs anneal to their targets with nearly complete complementarity at a single site, either in the coding region or in the UTRs, resulting in the degradation of these messages¹⁷⁴. Conversely, when miRNAs pair with their targets imperfectly, such as in the case of most miRNAs from mammalian, worms and flies^{175,176}, they trigger translational repression rather than mRNA cleavage. RBPs can dampen miRNA-mediated decay of mRNAs by binding directly to miRNA precursors or, indirectly, by competing for binding motifs present in the 3'UTR of their mRNA targets. Physical interaction of the RBP ZFP36 with AGO2 has been shown to enhance miRNA-dependent mRNA degradation¹⁷⁷. On the contrary, the RBP HuR has been shown to compete with miRNAs for binding to RNA regulatory motifs present in the 3'UTR of target mRNAs, enhancing their stability^{178,179} or translation¹².

7.6.2.1 miRNA in myogenesis, myomiRs.

Several miRNAs have been shown to be specifically expressed in striated muscles including miR-1, miR-206 and the miR-133 family. As such, these miRNAs are referred as “myomiRs” (**Table 1.3**). MyomiRs expression is under the control of transcription factors including MyoD, MEF2 and serum response factor (SRF)¹⁸⁰⁻¹⁸². In C2C12 skeletal muscle cells, miR-1 was shown to promote myogenesis by targeting histone deacetylase

4 (HDAC4), a repressor of the MEF2 transcription factor¹⁸³. Thus, the repression of HDAC4 by miR-1 establishes a positive feed-forward loop in which the up-regulation of miR-1 by MEF2 causes further repression of HDAC4 and increased activity of MEF2, which in turn drives myocyte differentiation. By contrast, miR-133 enhances myoblast proliferation by repressing the transcription factor SR which, in turn, suppresses proliferation by repressing cyclin D2 expression in a negative feedback loop¹⁸⁴. miR-206A differs from miR-1 by 4 nucleotides and was shown to be upregulated by MyoD and to target *Pax3* and *Pax7* mRNAs leading to their degradation. The expression of mirR-206 has also been examined *in vivo* and was shown to be upregulated in the skeletal muscle of mdx mice (a mouse model of Duchenne muscular dystrophy) injected with cardiotoxin, a potent inducer of muscle regeneration¹⁸⁵.

miR	Target Gene(s)	Function
miR-1	Hdac4	Myoblast Differentiation
	Irx5, Connexin 43, Kcnj2, Hcn2, Hcn4	Cardiac Conduction System
	Hand2	Cardiac Proliferation
	Dll1	Cardiac Mesoderm Differentiation
	Mef2	Neuromuscular Synapse Function
miR-133	Srf	Myoblast Proliferation, Smooth Muscle Gene Expression
	Cyclin D2	Cardiac Proliferation
	Rhoa, Cdc42, Whsc2	Cardiac Hypertrophy
	Ether-a-go-go, Hcn2	Cardiac Conduction System
miR-206	Pola1, Connexin 43, Fst1, Utrn	Myoblast Differentiation

Table 1.3. Muscle specific miRNAs and their mRNA targets in muscle

7.6.3. Posttranscriptional regulation through RNA binding Proteins

RBPs are a diverse group of proteins that form ribonucleoprotein complexes (RNP) by binding to either specific sequence motifs or to structural patterns predominantly located in the UTRs of their target mRNAs. RBPs regulate all aspects of RNA metabolism, including splicing and processing of mRNA-precursors (pre-mRNAs) in the nucleus, the export and localization of mRNAs to distinct subcellular regions in the cytoplasm, as well as mRNA translation and degradation¹⁸⁶ (**Fig. 1.14**). The importance of RBPs as regulators of these and other processes is underscored by the myriad of disease states and syndromes linked to disruption of RBP expression or function¹⁸⁷. RBPs are

characterized by the presence of one or more well-structured RNA-binding domains (RBD), such as the RNA recognition motif (RRM), hnRNP K-homology domain (KH), cold shock domain (CSD), zinc fingers (ZF) domain, double stranded RNA-binding domain (dsRBD) and DEAD box helicase domain¹⁸⁸. Many RBPs, such as those belonging to the ELAV family, contain multiple RNA binding domains which typically leads to an increased affinity and/or specificity for RNA, and it has been suggested to enhance the recruitment of interacting protein partners^{189,190}. Post-transcriptionally regulatory events can be broadly categorized into two subcategories: those occurring in the nuclear fraction (including capping, splicing or polyadenylation) and those occurring in the cytoplasmic fraction (including nuclear export, localization, translation or turnover (stability and decay)). For the purposes of this thesis, I will focus on regulatory events occurring in the cytoplasm.

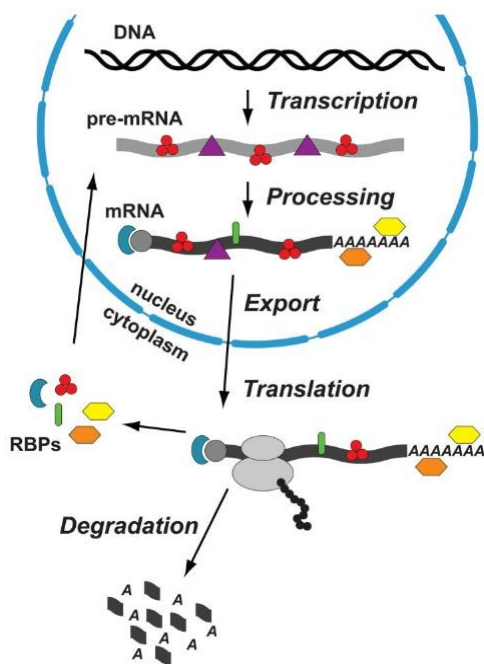


Figure 1.14. Mechanisms of RBP-mediated regulation of gene expression.

Gene expression is regulated at several levels after transcription and addition of the 5' cap and poly(A) tail. Prior to export, pre-mRNAs are spliced to remove introns forming mature mRNA. Next, mature mRNA is exported into the cytoplasm and can be further localized to a specific compartment where its translation is regulated. Localization of mRNA to specific compartments can also lead to its decay. The translation of mRNA can be either cap-dependent or cap-independent, and also subject to regulation. These processes are regulated by the dynamic association of RNA-binding proteins (RBPs, showed in colored shapes) with mRNA, which define a transcript's lifetime, cellular localization, editing, polyadenylation and rates of translation and decay, ultimately determining the levels of protein produced. Image from ¹⁹¹

7.6.3.1. Control of mRNA nuclear export

Following maturation of the mRNA, the efficient and proper transport of mRNA from the nucleus to cytoplasm occurs through the nuclear pore complex (NPC), an assembly of nucleoporins integrated within the nuclear envelope. Proteins and their RNA cargos translocate through the NPC through two major export pathways; the first one via the family of karyopherin- β nuclear export factors, which is dependant on the differential

RanGTP gradient in the nucleus and cytoplasm and the second via the non-karyopherin heterodimer Nxf1/Nxt1, which is independent of the RanGTP gradient¹⁹². The majority of poly-A transcripts are exported via the Nxf1/Nxt1 heterodimer. The NXF1 receptor is itself an RBP that harbors a RRM domain through which it can efficiently bind mRNA. However, since it does so in a non-specifically manner, additional factors are needed to mediate their attachment to specific mRNAs^{192,193}.

The karyopherin- β family contains both import and export receptors (importins and exportins respectively). Karyopherin- β proteins are not themselves RBPs. Instead, they recognize nuclear localization signals (NLSs) or nuclear export signals (NESs) in proteins which themselves have mRNA binding activity¹⁹⁴. The most extensively studied members of the karyopherin- β family are importin β 1 and importin β 2 (transportin 1 and 2 respectively) as well as Exportin 1 (Chromosomal Maintenance 1/CRM1)¹⁹⁵. Several mRNA binding proteins, such as HuR and Nmd3, have been shown to exit the nucleus by interacting with these receptors¹⁹⁶⁻¹⁹⁸. HuR, for example, has also been shown to mediate its own shuttling out of the nucleus by interacting with transportin 2¹⁰ and has also been shown to alternatively interact with CRM1 through two protein ligands, pp32 and APRIL in response to heat shock^{196,197 199}, suggesting that HuR works as an export adapter for many mRNAs¹⁹⁶.

7.6.3.2. Regulation of mRNA subcellular localization.

RNA localization generally refers to the transport or enrichment of subsets of mRNAs to specific subcellular regions. RNA localization can be achieved 'passively' by local protection from degradation or through the trapping/anchoring at specific cellular locations. Asymmetric distribution of RNA has been shown to be crucial for cell differentiation and development. To date, more than 100 mRNAs are known to undergo active mRNA transport in diverse organisms²⁰⁰. In *Drosophila* eggs, the mislocalization of *nanos* mRNAs has been shown to lead to the production of a second abdomen instead of the head and thorax²⁰¹. In yeast, approximately half of the transcripts coding for mitochondrial proteins preferentially localize to the organelle surface²⁰². Subcellular localization of mRNA is mediated by *cis*-acting elements mostly located in the 5' and 3'

UTRs generally referred to as zipcode sequences (**Fig. 1.12**) which interact with zip-code-binding proteins such as the zip binding protein 1 (ZBP1), cytoplasmic polyadenylation protein (CPEB) and members of the familial mental retardation proteins (FMRPs)²⁰³⁻²⁰⁵. The best characterized mechanism involving zip code sequences is the regulation of the local translation of *β-actin* mRNA by ZBP1²⁰⁶. ZBP1 associates with *β-actin* mRNA in the perinuclear space and mediates its transport in a translationally repressed form to the cell edge, once at the cell edge, ZBP1 is phosphorylated by Src in response to an extracellular signal, and the mRNA is released and translated²⁰⁶.

Subcellular localization can also be established by the “active” transport of RNAs via RBP-motor protein complexes. Many RBPs have been shown to shuttle from the nucleus to the cytoplasm, which is fundamental for most of their described functions on their target mRNAs²⁰⁷. In addition, their intracellular trafficking to specific cytoplasmic localization, such as the translation apparatus, the exosomes or processing (P)-bodies is an important determinant for the destiny of their bound target mRNAs. In most cell types, the shuttling of these RBPs is not a constitutive process, it is rather transiently induced by activation of different signals^{194,208}. Indeed, it has also been shown that HuR^{209,210} and its neuronal relative HuD²¹¹, members of the ELAV family of RBPs, when in the cytoplasm can utilize either the actin- or microtubule-dependent cytoskeleton for transport of mRNA cargo. Mechanistically, the interaction between Hu proteins and microtubules is thought to be indirect and mediated by Microtubule Associate Proteins (MAPs).

7.6.3.3. Control of translation efficiency

The overall process of translation of mRNAs can be divided into three steps: initiation, elongation and termination. This process is regulated in a spatial-temporal manner to modulate the abundance of the corresponding protein product. Regulation of mRNA translation can occur in two ways; global regulation, where translation regulation occurs in a non-specific manner and affects general protein biosynthesis, and mRNA-specific regulation, where only the translation of a defined group of mRNAs or a single mRNA is modulated. Global regulation is achieved by controlling the rate of initiation through targeting of translation initiation factors (eIFs), the proteins responsible for the

first step in the initiation process. eIF4E mediates the recruitment of the mRNA to the small ribosomal subunit by binding to the cap structure at the 5' end of the mRNA and promoting its interaction with eIF4G which, in turn, binds to the poly(A)-binding protein (PABP) to form the initiation complex (IC). The IC then scans the mRNA in 5' to 3' direction until the initiation codon (AUG) is reached leading to the merging of the large ribosomal subunit to the IC and the formation of active ribosomes. The rate of the initiation stage can be enhanced or inhibited by altering either the phosphorylation state of eIF4E or by targeting its binding to eIF4G. Key RBPs have been shown to repress global translation by preventing the binding of eIF4E to eIF4G; 4E-binding proteins one, two and three (4E-BP1, 4E-BP2, and 4E-BP3)^{212,213}. When 4E-BPs are hypophosphorylated, they can sequester eIF4E and prevent the interaction with eIF4G and inhibit the translation. When they are hyperphosphorylated, they cannot bind to eIF4E, which is then released to participate in the protein translation initiation²¹³⁻²¹⁵. These 4E-BPs are phosphorylated in response to growth factors, amino acids, or hormones such as insulin which activates the mTOR pathway (molecular target of rapamycin).

Several conditions such as cachexia, sarcopenia, and disuse muscle atrophy are characterized by the impairment of general protein synthesis. While the basis of this inhibition in translation is likely to be multifactorial (pro-inflammatory cytokine expression, malnutrition, insulin resistance and/or physical inactivity) it is accompanied by increased phosphorylation of 4E-BP1²¹⁶, evidencing the key role of RBPs in the onset of muscle wasting. Indeed, enhanced 4E-BP1 activity in mouse skeletal muscle was demonstrated to lead to an increased oxidative metabolism and to protect mice from diet- and age-induced insulin resistance and metabolic rate decline. 4E-BP1 mediated this metabolic protection directly through increased translation of PGC-1 α and enhanced respiratory function²¹⁷.

The second mode of translational regulation concerns mRNA-specific control, where translation of defined groups of mRNAs or an individual transcript is modulated without affecting general protein biosynthesis. This can be carried out by specific RNA-binding proteins, which often bind to sequence or structural elements in the UTRs of target transcripts. A prime example for such regulation is the Internal Ribosome Entry Site (IRES) dependent translation. IRES elements are long, highly structured RNA

sequences that function to recruit ribosomes to an mRNA in a CAP independent manner (**Fig. 1.12**). While some IRES elements are capable of recruiting the ribosomal subunits on their own, others require at least a subset of eIFs as well as certain RBPs to facilitate IRES-mediated translation (IRES-transacting factors/ ITAFs)²¹⁸. A number of these regulatory proteins enhancing or repressing IRES activity have been characterized, such as, polypyrimidine-tract binding protein (PTB), the caspase-cleaved form of DAP5/ p97 (p86), hnRNP-A1 and HuR²¹⁹⁻²²². Among these proteins, HuR is recognized as the only negative regulator of IRES function. HuR was shown to inhibit *p27* mRNA translation by binding to a *cis*-elements in the 5'UTR and locking the mRNA into a conformation which is not permissive for IRES-mediated translation initiation²¹⁹.

7.6.3.4. Regulation of mRNA Stability

RNA degradation plays a major role in regulating the quantity of gene expression in the cell, the abundance of an RNA transcript is a reflection of both its rate of synthesis and degradation. Degradation rate of an mRNA molecule is highly variable, in mammals, once transcripts are exported from the nucleus, the half-life can range from as little as 15 minutes to more than 10 hours²²³. Three main components have been linked to the rapid degradation of a transcript: the length of the poly(A) tail, the integrity of the 5' cap structure and the presence of destabilizing *cis*-elements, such as AREs and GREs motives (**Fig. 1.2**).

Deadenylation of mRNA, which involves the shortening of the poly (A) tail, is considered to be the rate-limiting step of the exonucleolytic decay pathway. Deadenylases are recruited to RNA substrates by a variety of RBPs and complexes. The poly (A)-specific ribonuclease PARN, the most extensively studied deadenylase, has been shown to interact with the 5' cap of the mRNA substrate to enhance its enzymatic activity/processivity^{224,225}. Following deadenylation, decapping is the next step in the decay of many mRNAs as the presence of the m7G-cap on mRNAs makes the mRNAs intrinsically resistant to degradation by 5' to 3' exonucleases present in both the nucleus and cytoplasm of eukaryotic cells²²⁶. Once an mRNA has been decapped and/or deadenylated, it can be targeted by cytoplasmic exonuclease at the 3' or 5' ends of the

mRNA for degradation. 3' to 5' decay in the cytoplasm is performed primarily by a multiunit complex called the exosome and requires an accessible 3' hydroxyl^{227,228} (**Fig. 1.15**). On the other hand 5' to 3' decay is mainly orchestrated by the exonuclease XRN1, the primary cytoplasmic exonuclease, which preferentially degrades RNAs with a 5' monophosphate end, precisely corresponding to the 5' termini following mRNA decapping²²⁹.

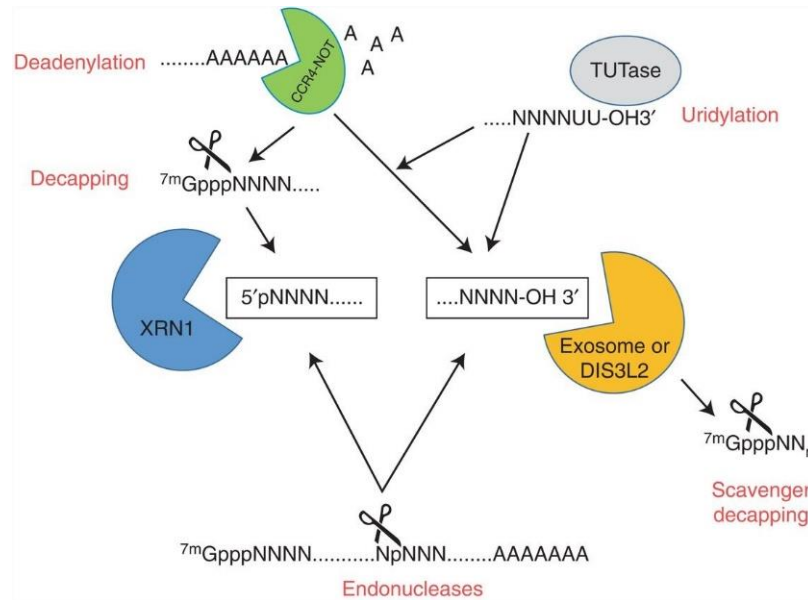


Figure 1.15. Pathways for exonucleases access to RNAs for degradation. 5'-3' exoribonucleases (XRN1) require a 5' monophosphate, whereas 3'-5' exoribonucleases (exosome and DIS3L2) require an accessible 3' hydroxyl. A 5' monophosphate can be generated in a regulated fashion by the process of decapping. Processing of the decapped mRNA can then occur in a deadenylation (poly(A) tail shortening) dependent or deadenylation independent fashion. Deadenylation itself generates an accessible 3' hydroxyl for exoribonucleases. Poly(U) polymerases (also called TUTases) can uridylate the 3' end of RNA targets to increase DIS3L2 exonuclease accessibility. In the 3'-5' exonuclease pathway, the scavenger decapping enzyme DCPS acts on short-capped oligonucleotides to promote full degradation. Finally, rather than remodeling the natural 5' and 3' ends of the target mRNA, endoribonucleases, including the RNA-induced silencing complex (RISC) complex of the RNA interference (RNAi) pathway, can cleave a transcript internally and generate fragments with 5' monophosphate and 3' hydroxyl ends for exonucleolytic decay. Image from ²²⁷.

As describe in section 7.6.1 the presence of AREs and GREs *cis*-elements has a big impact on determining the longevity of the mRNA. These sequences facilitate the binding of destabilizing/stabilizing factors, mainly RBPs, which affect the rate of decapping/deadenylation by preventing the recruitment of the degradation machinery or

facilitate their degradation by physically recruiting nucleases to their target transcripts. Many mRNA binding proteins have been discovered to date, which either stabilize (e.g. HuR/HuA, HuB, HuC, HuD, YB1, PAIP2) or destabilize (e.g. AUF1, CUGBP1, KSRP) their target transcripts.

7.6.3.5. RBPs-mediated stability in myogenesis

The role of mRNA stability in mediating changes in skeletal muscle gene expression is readily observed in studies that showed that the stability of specific mitochondrial regulators have an inverse relationship with the oxidative capacity of specific muscles^{230,231}. Such findings are attributed, in part, to the differential abundance of RBPs across the range of striated muscle fiber types²³². The rate of degradation of specific transcript, such as the utrophin A mRNA was also shown to be decrease in the presence of extracts made from soleus muscle (SOL) (predominantly slow-twitch), versus the extensor digitorum longus (EDL) (predominantly fast-twitch) muscles²³³. Furthermore, *in vivo* analysis using reporter constructs containing full and truncated lengths of the *utrophin* 3'UTR revealed a region containing elements capable of suppressing mRNA levels in EDL muscles, which were not targeted in Soleus muscle²³⁴. Suggesting that muscle fiber types distinguish themselves phenotypically using divergent rates of mRNA degradation which is itself directly related to the nonuniform distribution of selected RBPs across different fiber types²³².

In addition, in the last decade, the contribution of RBPs in directly controlling the expression of MRFs during myogenesis has taken a major role^{7,9,11,235-242} (**Fig. 1.16**). To date, KSRP and HuR are the only ARE-RBPs shown to directly modulate the expression of certain MRFs. However, CUGBP1, AUF1 and YB1 have been identified to bind GREs and AREs of promyogenic targets and to be implicated in regulating their half life^{146,230,243,244}, which makes these proteins of particular interest in the study of muscle-specific gene regulation.

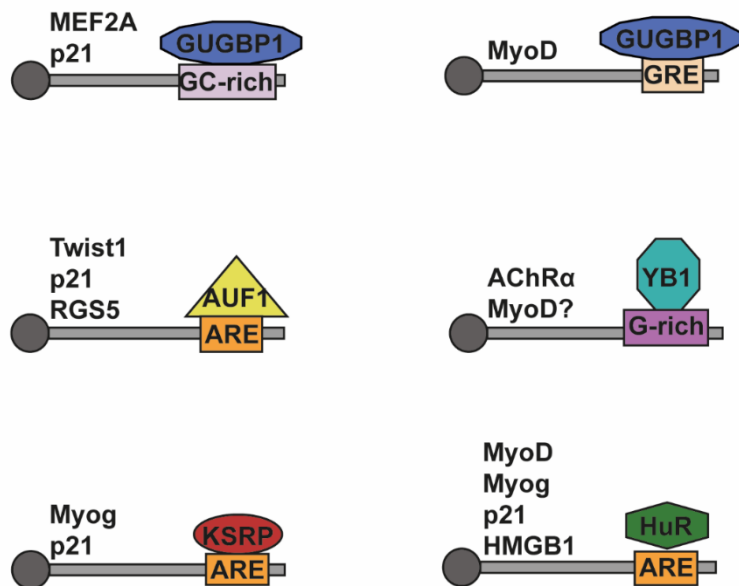


Figure 1.16. RNA-binding proteins in myogenesis and their known mRNA targets. Schematic representation illustrating the mRNA targets and binding selectivity of known RBPs involved in myogenesis. Image modified from ¹⁹¹.

7.6.3.5.1. CUG triplet repeat, RNA binding protein 1 (CUGBP1).

CUGBP1 is a member of the CELF family of RBPs, it binds to a variety of mRNA *cis*-elements including GREs, and AREs, via three RRM domains. CUGBP1 has been shown to regulate alternative splicing as well as the stability and translation of its mRNA targets⁵ (**Fig. 1.16**). CUGBP1 mediates muscle cell differentiation by regulating the translation of mRNAs encoding the promyogenic factors p21²⁴⁵. Analysis of CUGBP1 expression during myogenesis revealed a dramatic increase in its mRNA and protein levels upon induction of muscle differentiation resulting in the increase levels of CUGBP1 in the cytoplasm²⁴⁶, an essential event required for myogenesis as preventing the accumulation of CUGBP1 in the cytoplasm has been shown to lead to muscular dystrophy and myotonia due to decrease expression of p21, Myog and MEF2A.^{245,247}

7.6.3.5.2. AU-rich binding factor 1 (AUF1)

AUF1 primarily functions as a ARE-mRNA decay factor^{170,248}, it consists of four related protein isoforms named for their molecular weights (p37, p40, p42, p45), derived by differential exon splicing of a common pre-mRNA²⁴⁹. While the molecular mechanism by which AUF1 regulate its target messages is not fully understood, it involves the

interaction of the different isoforms in a variety of homo- and hetero-complexes²⁴⁸. All four isoforms of AUF1 share some common structural elements, including two tandem, non-identical RRM domains containing canonical RNP-1 and RNP-2 sequence motifs, as well as an 8-amino acid glutamine-rich sequence located C-terminal to RRM2²⁴⁹. Recently it has been demonstrated that AUF1 is involved in major stages of muscle development and regeneration, from control of the muscle stem cell (satellite cell) differentiation to development of mature muscle fibers²⁵⁰. AUF1 complete these functions by selectively targeting development checkpoint mRNAs, such as *Twist1*, *p21*, and *RGS5* for rapid degradation²⁵⁰(**Fig. 1.16**). Furthermore, AUF1 null mice showed that, while healthy skeletal muscle can develop in the absence of functional AUF1, the satellite cell population is clearly altered and once activated is quickly depleted leading to age-related and post-injury myopathy²⁵¹.

[7.6.3.5.3. Y box binding protein 1 \(YB1\)](#)

YB1, is a highly conserved member of the cold shock domain (CSD) family of proteins. The Y-box binding protein contain three main domains: the A/P domain (enriched of Alanine and Proline), the C- terminal domain (CTD) and the CSD. The CSD contains two highly conserved RNA recognition motifs, RNP-1 and RNP-2, which play a key role in mediating YB1 interaction with nucleic acids. Originally identified as a transcription factor binding to the promoter of major histocompatibility complex class II genes in the conserved Y-box motif (CCAAT)²⁵², YB1 has been shown to bind to a variety of sequences in DNA and RNA molecules^{253,254}, including mRNAs with a high GC content²⁵⁵. Having the ability to shuttle between the nucleus and the cytoplasm, YB1's functions have been linked to its localization in cells and its ability to form distinct complexes with different protein partners^{254,256,257}. YB1 is predominantly localized in the cytoplasm but has been shown to move into the nucleus in response to environmental signals such as DNA damage^{258,259}. In the nucleus, it primary functions as a transcription factor, regulating the expression of genes involved in cell proliferation and differentiation. In the cytoplasm, however, YB1 plays a key role in regulating the stability and translation of its target mRNAs^{254,256}. In skeletal muscle, YB1 was shown to regulate the maturation of the NMJ by binding to acetylcholine receptor α -subunit (AChR α) mRNA and inhibiting

its translation leading to NMJ maturation^{243,260} (**Fig. 1.17**). Additionally, nuclear localization of YB1 is thought to be preceded by its cleavage which generates a truncated isoform, YB1/P32, that displays a distinct nuclear localization. Accumulation of this truncated isoform in the nucleus was shown to inhibit C2C12 myoblast differentiation by preventing the expression of MyoD via binding to the CER of the *MyoD* promoter^{258,259}.

7.6.3.5.4. KH-type splicing regulatory protein (KSRP).

KSRP is involved in a variety of cellular processes, including nuclear RNA splicing and mRNA localization in the cytoplasm²⁶¹. KSRP contains four RNA binding KH domains, which in addition to recognizing AREs in its mRNA targets, are responsible for binding to both the exosome and PARN, therefore promoting the rapid decay of ARE-containing mRNAs¹⁵⁹. Indeed, in proliferating myoblasts, KSRP is known to associate with AREs present in the 3'UTR of the *Myog* and *p21* mRNAs leading to their rapid decay²⁶²(**Fig. 1.16**). By doing so, KSRP participates in ensuring the proliferation of myoblasts and prevents their premature commitment to the myogenic process. KSRP association to its promyogenic mRNA targets, during muscle cell differentiation, is mediated by its phosphorylation (on Thr 692) by the p38 mitogen-activated protein kinase (MAPK). p38 MAPK induced phosphorylation of KSRP leads to a loss in binding to the *p21* and *Myog* mRNAs, resulting in a failure to promote their rapid decay despite being able to bind to the mRNA degradation machinery²⁶². In addition, KSRP has been shown to regulate the biogenesis of the miR-1, miR-133a, and miR-206 miRNAs by binding to G-rich stretches in the terminal loop of their pri-miRNA molecules, as such, KSRP knockdown impairs myogenic miRNA maturation, increases the expression of some of their targets and inhibits C2C12 myoblasts differentiation²⁶³.

7.6.3.5.5. Human Antigen R (HuR) ELAVL1

Of the posttranscriptional regulator involved in myogenesis, HuR has been the most well studied. HuR is a ubiquitously expressed protein, a member of the ELAV protein family (HuR, HuB, HuC, HuD)²⁶⁴. It's main function is as an mRNA stabilizer and translational activator and has also been shown to act as adaptor protein for the nuclear

export of their target messages^{170,196,265-268}. To date, HuR protein is among the few RBPs shown to activate the expression of mRNAs that contain AU-rich sequences, as most other ARE-binding proteins function in their degradation. However, depending on the mRNA target of interest, HuR can also promote or inhibit mRNA translation without detectable changes in the turnover of the mRNA target^{170,269,270}. HuR contains three RRM domains through which it can bind directly to several classes of ARE elements (tandem repeats of AUUUA; A+U regions with interspersed AUUUA and U-rich sequence with no AUUUA pentamers)²⁷¹. While RRM1 and RRM2 are mostly required for binding to ARE/GREs^{272,273}, RRM3 has been suggested to have a predominant role in mediating protein-protein interactions, poly(A) binding and stabilization of ribonucleoprotein complexes (RNPC)^{168,199,274,275}. A hinge region, located between RRMs 2 and 3, contains a nucleocytoplasmic shuttling sequence (HNS) which regulates nuclear import/export of HuR²⁷² (**Fig. 1.17A**).

HuR has a critical function during skeletal myogenesis, which is linked to its coordinated regulation of several promyogenic targets at different posttranscriptional levels^{6,11}. In myoblasts, HuR predominantly localizes to the nucleus; however, its cytoplasmic fraction increases on the onset of differentiation becoming nearly exclusively cytoplasmic in fully mature fibers (**Fig. 1.17B**). Studies focused on HuR cytoplasmic export in muscle cells showed that during the transition phase from myoblasts to myotubes, a fraction of HuR is cleaved at its 226th residue, an Asp (D), generating two cleavage products HuR-CP1 and HuR-CP2¹⁰. HuR-CP1 binds to TRN2 and interferes with the TRN2-mediated nuclear import of HuR leading to the cytoplasmic accumulation of the remaining noncleaved HuR (**Fig. 1.17C**). HuR cleavage was shown to be essential for myoblast differentiation, as a non-cleavable isoform of HuR (HuRD226A) was unable to re-establish muscle cell differentiation in HuR-depleted myoblasts^{197,276}.

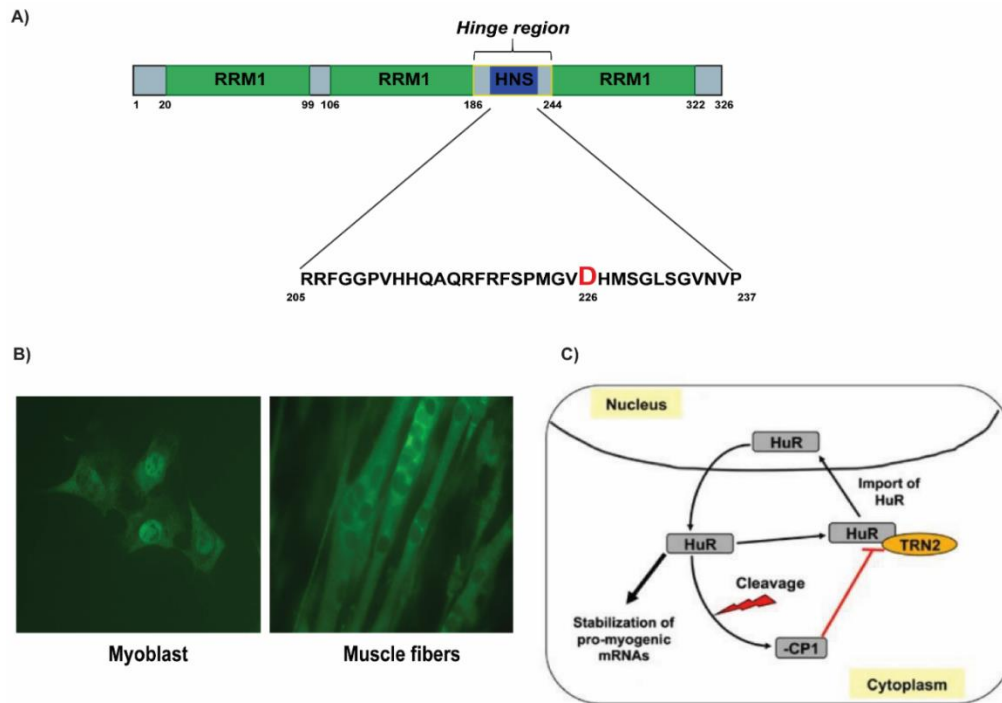


Figure 1.17. The role of HuR in myogenesis. A) Schematic of HuR RNA binding domains organization, HuR has three RNA Recognition Motifs (RRM, yellow) and a hinge region (blue). The HuR Nucleocytoplasmic Shuttling Sequence (HNS) within the Hinge region is represented in stripes. Enlargement depicts the site of HuR cleavage during muscle fiber formation. B) Localization of HuR protein in C2C12 cells grown to confluency (myoblast) or differentiated muscle fibers. Cells were fixed and used for immunofluorescence, using the monoclonal anti-HuR antibody C) Model depicting how HuR cleavage participates in the promyogenic function of HuR. During the early steps of myogenesis, the nuclear import of HuR is ensured by the import factor TRN2.10 During fusion, in which myoblasts form myotubes, HuR is needed in the cytoplasm. At this stage, HuR is cleaved by caspases generating HuR-CP1, which in turn blocks the TRN2-mediated import of HuR. HuR-CP1 competes with HuR and forms a stable complex with TRN2. HuR then accumulates in the cytoplasm. Nuclear-cytoplasmic shuttling of HuR is directly linked to its ability to bind to its mRNA targets. Image from ¹⁰

In muscle cells HuR regulates the early and pre-terminal phases of the myogenic process by associating with AREs in the mRNAs of several classic and newly identified modulators of myogenesis^{10-12,197,267}. During the early stages of myogenesis, HuR promotes the expression of HMGB1 by preventing miR-1192-mediated translation inhibition of the [the high mobility group box 1 (HMGB1) mRNA¹². Later, during the pre-terminal stage, when myoblasts begin their fusion to form myotubes, HuR associates with and stabilizes *MyoD*, *Myog*, and *p21* mRNAs leading to an increase of the corresponding protein and the promotion of muscle fiber formation^{10,11,197} (**Fig. 1.16**).

In addition to its promyogenic functions, HuR has also been implicated in muscle wasting by post transcriptionally regulating the messages encoding the pro-cachectic factors; inducible Nitric Oxide Synthase (iNOS) and Signal Transducer and Activator of Transcription 3 (STAT3)^{4,236,239}. Exposure of skeletal muscle tissue to proinflammatory cytokines was shown to increase HuR association to the ARE in the 3'UTR of the *iNOS* mRNA leading to its stabilization and increase expression, consequently activating the pro-cachectic iNOS/NO pathway (**Fig. 1.18**). Similarly, under cytokine-induced muscle wasting conditions, HuR increases the translation of the *STAT3* mRNA by preventing the binding of miR-330 to its 3'UTR leading to the onset of STAT3-induced muscle wasting

277.

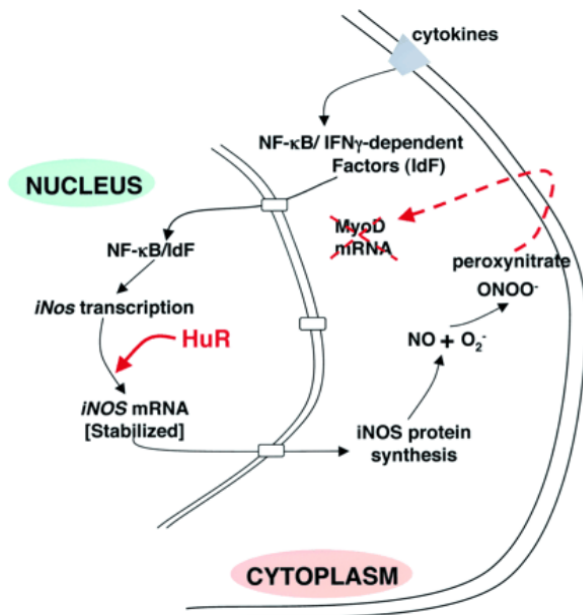


Figure 1.18. Model depicting the role of HuR-regulated iNOS mRNA and thus NO secretion in changes in *MyoD* mRNA levels. In muscle cells TNF-α and IFN-γ stimulate, respectively, the transcription factor NF-κB as well as IFN-γ-dependent transcription factors (such as STAT1), which in conjunction induce the mRNA expression of the *iNos* gene. The RNA-binding protein HuR, which is localized in the nucleus, associates with the *iNOS* mRNA through its ARE mediating its stability and probably its export to the cytoplasm. iNOS enzyme will likely induce NO conjugation with the superoxide (O₂⁻) to form peroxynitrite. The release of OONO⁻ either inside the cytoplasm or outside the cell will activate the down regulation process of *MyoD* mRNA. The exact mechanism leading to NO-dependent *MyoD* loss is still unclear and could be due to destabilization and decay of the message in the cytoplasm or to transcription inhibition of *Myod* gene in the nucleus. Image from ²³⁶

8. Rationale and objectives of the thesis.

It is clear that the integrity of skeletal muscle tissue is vital for the survival of an organism and its quality of life. Myogenesis is a tightly coordinated regulatory process^{107,121,278} whose importance is accentuated by the fact that the inability of muscle to regenerate or adapt to metabolic changes leads to the development or progression of various skeletal muscle disorders^{4,80,238,239,279-288}. Our previous work demonstrates that HuR is a key player involved in muscle fiber formation. We have shown that HuR's promyogenic function is mediated by its ability to differentially regulate the expression of key promyogenic mRNAs targets, such as *MyoD*, *Myog*, *p21* and *HMGB1*. HuR mediates these effects by competing with the miRNA miR1192 for binding to the *HMGB1* mRNA thereby increasing its translation while, alternatively, binding to AREs in the 3'UTR of *MyoD*, *Myog*, and *p21* and regulating their stability through a yet unknown mechanism.

Recent findings from our laboratory show that depletion of endogenous HuR from undifferentiated C2C12 myoblast increases the steady-state levels of the cell cycle modulator NPM. Our observations indicate that during the initiation stages of myogenesis HuR, in addition to regulating the *HMGB1* mRNA, destabilizes the *NPM* transcript, a function not previously described for HuR. The possibility of HuR downregulating the expression of its mRNA targets is unexpected as HuR is a well-known stabilizer of mRNAs^{7,264,269}. However, since HuR was shown to affect the expression of *NPM* mRNA in intestinal epithelial cells, we reasoned that this could also be the case in muscle cells. Our previous work also demonstrated that HuR differentially regulates its mRNA targets during the different stages of the myogenic process. While the HuR-mediated regulation of the *HMGB1* mRNA is restricted to the early stages of myogenesis, when HuR is predominantly localized in the nucleus²⁴², the stabilization of *MyoD*, *Myog* and *p21* mRNAs occurs at later stages when myoblast begin to fuse and HuR translocate to the cytoplasm¹¹. Taken together these observations support the established notion that the pleiotropic function of HuR is directly associated to the nature of its protein ligands^{7,197,238-242,265,268,276,289,290}. Therefore, the function of HuR during the different stages of myogenesis is likely linked to its collaboration/competition with other protein partners which help establish the specificity with which it binds to its mRNA targets during this

process. To identify these protein ligands, we performed an immunoprecipitation (IP) experiment using muscle cell extracts followed by mass spectrometry. From this analysis, we identified KSRP and YB1 as potential ligands of HuR, two well-characterized RBPs that have been previously linked to myogenesis^{243,259,260,262,291}. Together these observations provide strong evidence in support of the hypothesis put forth in this thesis that the differential promyogenic functions of HuR during the different stages of myogenesis involves its collaboration/competition with various protein ligands such as KSRP and YB1.

In addition, despite these advances, little is known about the physiological relevancy of HuR in this process. One of the main drawbacks in addressing the *in vivo* importance of HuR in muscle formation/function is that HuR-null mice are embryonically lethal at embryonic day 7.5 (E7.5) due to problems in placental branching morphogenesis²⁹². Therefore, in this thesis we will establish the molecular mechanisms that regulate HuR function during myogenesis and, furthermore, assess the *in vivo* importance of HuR in muscle formation/function by addressing the following questions: (1) Is HuR destabilizing activity of the *NPM* mRNA part of its promyogenic function? Is KSRP involved in the HuR-mediated destabilization of *NPM*? (2) What are the molecular mechanisms through which HuR regulates the stability of its promyogenic mRNAs such as *Myog*? Do these HuR-mediated effects involve YB1 as part of the regulatory mechanism (3) Does HuR play an important role in regulating muscle development, formation and function *in vivo*?

By determining the HuR-mediated regulatory events required for myogenesis and elucidating the distinct molecular mechanisms through which HuR regulates the expression of its target mRNAs, this work will provide new insights into the importance of post-transcriptional regulatory events in a key physiological process and provide candidate targets to modulate muscle fiber formation under normal and disease conditions.

9. Body of the thesis

9.1. CHAPTER I: Destabilization of Nucleophosmin mRNA by the HuR/KSRP complex is required for muscle fiber formation.

9.1.1. Abstract

HuR promotes myogenesis by stabilizing the *MyoD*, *Myog* and *p21* mRNAs during the fusion of muscle cells to form myotubes. Here we show that HuR, *via* a novel mRNA destabilizing activity, promotes the early steps of myogenesis by reducing the expression of the cell cycle promoter Nucleophosmin (NPM). Depletion of HuR stabilizes the *NPM* mRNA, increases NPM protein levels and inhibits myogenesis, while its overexpression elicits the opposite effects. *NPM* mRNA destabilization involves the association of HuR with the decay factor KSRP, as well as the ribonuclease PARN and the exosome. The C-terminus of HuR mediates the formation of the HuR-KSRP complex and is sufficient for maintaining a low level of the *NPM* mRNA as well as promoting the commitment of muscle cells to myogenesis. We therefore propose a model whereby the downregulation of the *NPM* mRNA, mediated by HuR, KSRP and its associated ribonucleases, is required for proper myogenesis.

9.1.2. Introduction

Muscle differentiation, also known as myogenesis, represents a vital process that is activated during embryogenesis and in response to injury to promote the formation of muscle fibers^{1,2}. Myogenesis requires the activation of muscle-specific promyogenic factors that are expressed at specific steps of the myogenic process and act in a sequential manner. We and others have demonstrated that the expression of genes encoding some of these promyogenic factors such as *MyoD*, *Myog* and the cyclin-dependent kinase *p21*, are not only regulated at the transcriptional level but are also modulated posttranscriptionally³⁻⁸. Indeed, modulating the half-lives of these mRNAs plays an important role in their expression. The RNA-binding protein HuR, *via* its ability

to bind specific AU-rich elements (AREs) in the 3'untranslated regions (3'UTRs) of these mRNAs, protects them from the AU-rich-mediated decay (AMD) machinery^{4,5,7-9}. This HuR-mediated stabilization represents a key regulatory step that is required for the expression of these promyogenic factors and proper myogenesis.

HuR, a member of the ELAV family of RNA binding proteins, specifically binds to AREs located in the 3'UTRs of its target transcripts⁸⁻¹² leading to their stability, which in turn enhances the expression of the encoded proteins^{5,7}. In addition to mRNA stability, HuR modulates the nucleocytoplasmic movement and the translation of target transcripts¹³⁻¹⁶. Our previous data have indicated that HuR associates with *MyoD*, *Myog* and *p21* transcripts only during the fusion step of myoblasts to form myotubes⁵. This finding led to the conclusion that HuR promotes myogenesis by stabilizing these mRNAs specifically at this step. In the same study however, we showed that depleting HuR from proliferating myoblasts prevented their initial commitment to the differentiation process. These observations indicated that HuR promotes muscle fiber formation by also regulating the expression of target mRNAs during the early steps of myogenesis.

Recently, we discovered that HuR promotes myogenesis through a novel regulatory mechanism involving its caspase-mediated cleavage⁴. As muscle cells are engaged in the myogenic process a progressive accumulation of HuR in the cytosol is triggered. In the cytoplasm, HuR is cleaved by caspase-3 at its 226th residue, an Asp (D), generating two cleavage products (HuR-CPs: -CP1, 24kDa and -CP2, 8kDa). These HuR-CPs, generated from ~50% of cytoplasmic HuR, are required for muscle fiber formation^{4,8}. Indeed, while wt HuR can rescue myogenesis in cells depleted of endogenous HuR, the non-cleavable HuRD226A mutant failed to do so^{4,8}. Additionally, HuR-CP1, by associating with import factor Transportin 2 (TRN2), prevents HuR nuclear import promoting its cytoplasmic accumulation. While these data clearly establish that HuR-CP1 modulates the cellular movement of HuR during myogenesis, the role of HuR-CP2 remains unclear.

HuR is not the only RNA binding protein involved in the posttranscriptional regulation of promyogenic factors. The KH-type splicing regulatory protein (KSRP) is

known to associate, in proliferating myoblasts, with the AREs of the *Myog* and *p21* mRNAs leading to their rapid decay³. By doing so, KSRP participates in ensuring the proliferation of myoblasts and prevents their premature commitment to the myogenic process. KSRP promotes mRNA decay in muscle cells by recruiting ribonucleases such as PARN and members of the exosome complex (e.g. EXOSC5) to ARE-containing mRNAs such as *Myog* and *p21*^{3,17}. It was also suggested that when myoblasts become competent for differentiation, KSRP releases *Myog* and *p21* mRNAs leading to their stabilization. As a consequence, myoblasts enter myogenesis and fuse to form myotubes³. Since at this same step HuR associates with and stabilizes these ARE-bearing mRNAs^{5,7}, we concluded that the induction of myogenesis involve both KSRP and HuR that modulate the expression of the same mRNAs in an opposite way but at different myogenic steps.

Surprisingly, however, here we report that in undifferentiated muscle cells HuR and KSRP do not compete but rather collaborate to downregulate the expression of a common target, the *Nucleophosmin* (NPM, also known as B23) mRNA. HuR forms a complex with KSRP that is recruited to a U-rich element in the 3'UTR of *NPM* mRNA. The HuR/KSRP complex, in collaboration with PARN and the exosome, then destabilizes the *NPM* mRNA leading to a significant reduction in NPM protein levels. Our data also provide evidence supporting the idea that the HuR/KSRP-mediated decrease of NPM expression represents one of the main events that helps myoblasts commit to the myogenic process.

9.1.3. Results

9.1.3.1. NPM is a HuR-mRNA target in undifferentiated muscle cells.

We first identified the mRNAs that depend on HuR for their expression in undifferentiated, C2C12 cells. Endogenous HuR was depleted (siHuR) or not (siCtr) from these cells and total RNA was then prepared and hybridized to mouse arrays containing 17,000 probe sets of known and unknown expressed sequence tags. Consistent with the fact that HuR acts as a stabilizer for many of its mRNA targets^{10,12} we observed a significant decrease in the steady-state levels of 18 mRNAs in siHuR-treated cells. Surprisingly, however, we found that 12 mRNAs are significantly upregulated in these cells (**Annex 1**. Supplementary Table 1). While many of these transcripts do not have

typical AREs and are not known to modulate myogenesis, these observations suggested that in muscle cells HuR, in addition to stabilizing some of its target mRNAs, could also be involved in the destabilization of other transcripts. Therefore, we investigated further this unexpected possibility and assessed whether this HuR destabilizing activity is part of its promyogenic function. To this end we chose to study, among these upregulated HuR mRNA targets, the *NPM* mRNA. *NPM* was identified as a target of HuR in other cell systems¹⁸ and its downregulation has been shown to be required for the differentiation of other cell models^{19,20}. Hence, moderating NPM expression in muscle cells could be one of the early events through which HuR promotes myogenesis.

First, we validated the results of our microarray data using Northern blot analysis. The knockdown of HuR in C2C12 cells increased the level of *NPM* mRNA by two-fold while, as previously described⁵, it decreased the level of *MyoD* mRNA by >50% (**Fig. 2.1a**). Knocking down HuR in these cells also increased NPM protein levels, while Myog protein levels were reduced (**Fig. 2.1b**). Conversely, overexpressing GFP-HuR protein in C2C12 cells significantly decreased the levels of both *NPM* mRNA and protein, compared to cells transfected with GFP only (**Annex 1. Supplementary Fig. 1**). Together these observations establish that in undifferentiated muscle cells HuR prevents the overexpression of *NPM* mRNA and protein.

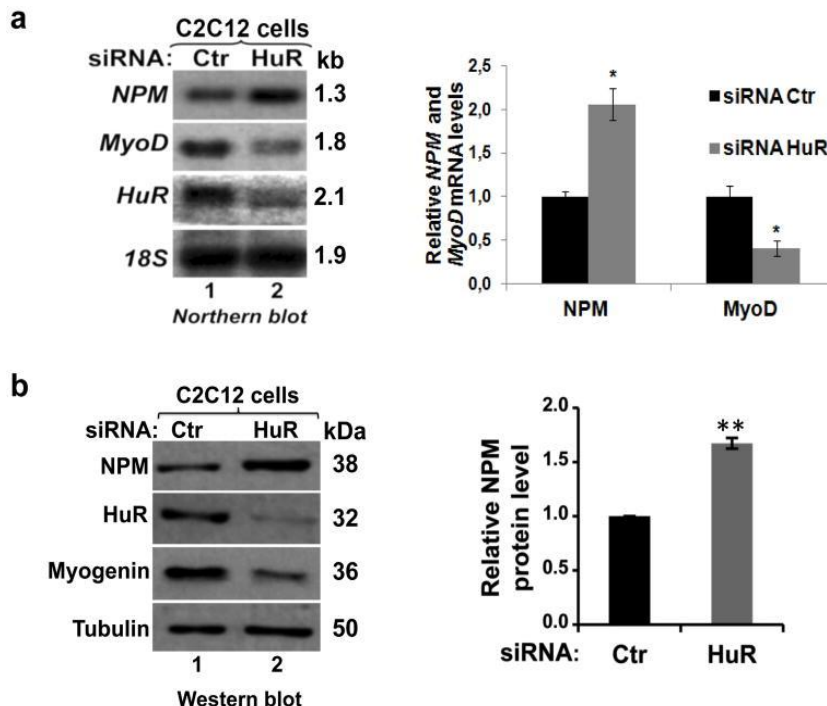


Figure 2.1 HuR regulates NPM expression in muscle cells. Exponentially growing C2C12 myoblasts were transfected with the HuR or Control (Ctr) siRNAs. **(a)** RNA was prepared 48h after transfection with HuR or Ctr siRNAs. Northern blotting was performed using radiolabeled probes against *NPM*, *MyoD*, *HuR* mRNAs and *18S* (loading control). The band intensities of *NPM*, *MyoD* mRNAs and *18S* were determined using ImageQuant Software. The *NPM* and *MyoD* mRNA levels were normalized on *18S* rRNA level. **(b)** Forty-eight h after transfection with HuR or Ctr siRNAs whole-cell extracts were prepared and Western blotting was performed using antibodies against NPM, HuR, myogenin and α -tubulin (loading control). ImageQuant was used to determine the NPM level, normalized on α -tubulin level. In the histograms, the siRNA HuR condition was plotted relative to the siRNA Ctr condition +/- the standard error of the mean (S.E.M.) of three independent experiments * $P < 0.01$, ** $P < 0.001$ (t test).

9.1.3.2. HuR-mediated *NPM* mRNA destabilization promotes myogenesis.

If downregulating NPM levels represent an important event during the early steps of myogenesis, decreasing its expression levels in C2C12 cells should promote their ability to enter this process. To investigate this possibility, we assessed *NPM* mRNA and protein levels during muscle cell differentiation. We observed that although, as expected²¹, *MyoD* mRNA levels increased during this process, the abundance of the *NPM* mRNA and protein significantly decreased as soon as myogenesis was initiated (**Fig. 2.2a–c**). To determine whether decreasing NPM expression is required for the initiation of myogenesis, we tested the impact that NPM knockdown (**Fig. 2.2d**) could have on the ability of C2C12 cells, expressing or not HuR, to enter this process. We observed that the depletion of endogenous NPM by siRNA not only triggered the formation of more and larger muscle fibers when compared to siCtr-treated cells, but also re-established myogenesis in HuR-knockdown C2C12 cells (**Fig. 2.2d–h** and **Annex 1**. Supplementary Fig 2). These observations, together with the fact that overexpressing GFP-NPM prevented myogenesis (**Annex 1**. Supplementary Fig. 3), clearly demonstrate that one way by which HuR promotes the early steps of muscle fibers formation is by downregulating NPM expression.

We have previously shown that HuR is cleaved during muscle cell differentiation into two cleavage products HuR-CP1 (24 kDa) and HuR-CP2 (8 kDa). Our data also indicated that HuR cleavage is a key regulatory event required for proper muscle fiber

formation⁴. Since our data (**Fig. 2.2c**) have shown that the cleavage of HuR during myogenesis correlates with a decrease in NPM expression, we decided to investigate the effect of HuR-CPs on NPM expression in muscle cells. As expected, we observed that in muscle cells depleted of endogenous HuR, the wild type (wt-HuR) but not the non-cleavable isoform of HuR (HuRD226A) was able to re-establish myogenesis as well as the downregulation of the steady state level of the *NPM* mRNA. Surprisingly however, HuR-CP2 but not HuR-CP1 was also able to re-establish, in these cells, the downregulation of *NPM* mRNA levels and myogenesis similarly to wt-HuR (**Fig. 2.2i-l**). While these results suggest a correlation between HuR cleavage and the HuR-mediated down regulation of the *NPM* transcript, they clearly indicate that the C-terminus of HuR could play an important role in this effect.

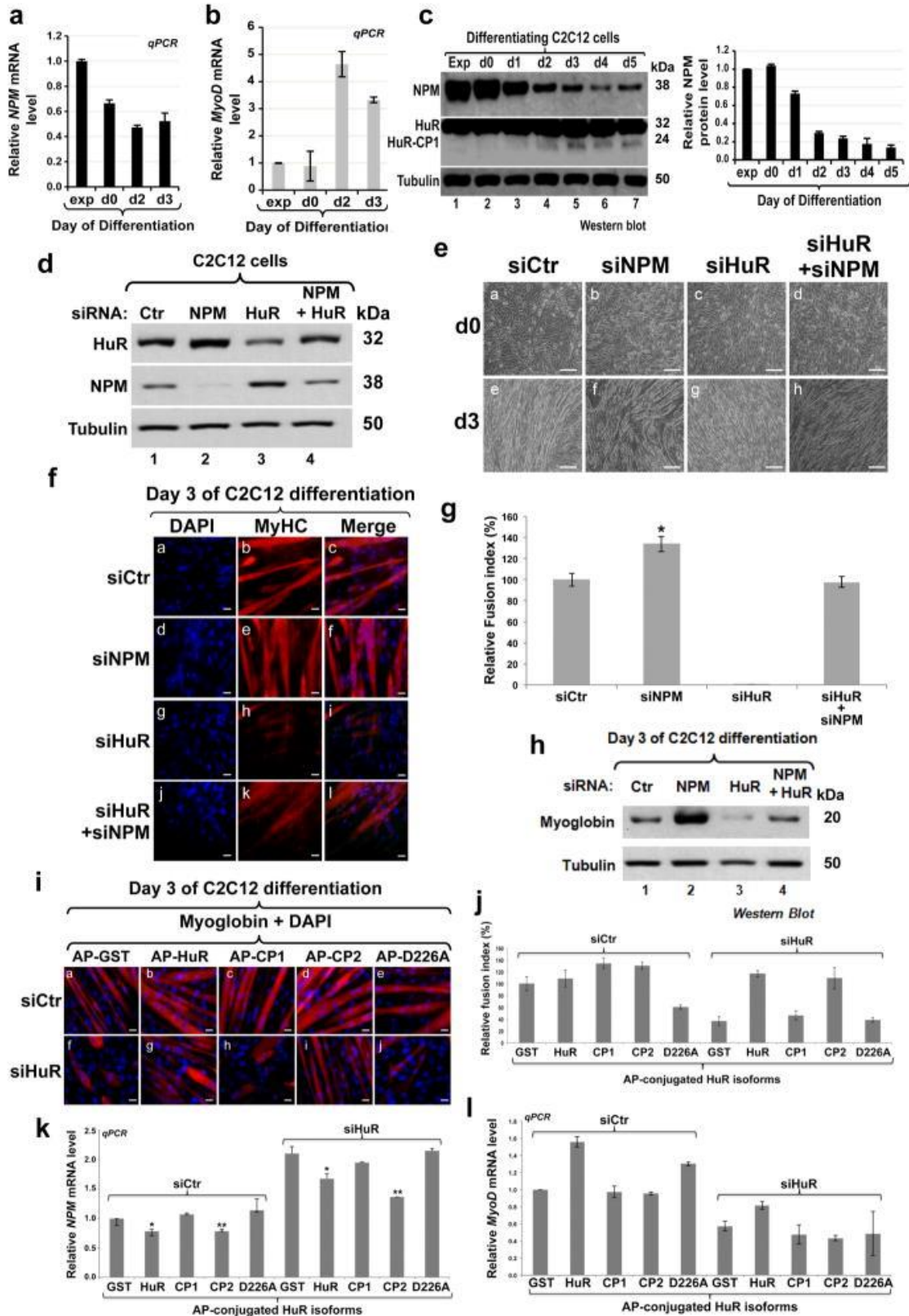


Figure 2.2 Reducing NPM level is required for the commitment of muscle cells into the myogenic process (a–b) Total RNA was isolated from exponentially growing (exp) or

confluent C2C12 myoblasts (day 0) and during the differentiation process (days 1 to 3). (a) *NPM* and (b) *MyoD* mRNA levels, determined by RT-qPCR, were standardized against *GAPDH* mRNA and expressed relative to the exponential condition. Values were plotted \pm the S.E.M. of three independent experiments. (c) Total cell extracts were prepared from growing (exp) as well as differentiating C2C12 myoblasts (days 1 to 5) and used for Western blotting with antibodies against NPM, HuR or α -tubulin (loading control). The NPM protein level was determined using the ImageQuant software, standardized against tubulin levels and plotted relative to the exponential condition \pm the S.E.M. of three independent experiments. **(d–h)** Knockdown of HuR, NPM and NPM+HuR was performed in C2C12 cells and differentiation was induced 48 hours post treatment with siRNAs. (d) Total cell lysates were prepared 48 hours post-transfection and used for Western blotting with antibodies against NPM, HuR, and α -tubulin. (e) Phase contrast pictures showing the differentiation status at d0 and d3. Bars, 50 μ m. (f) Immunofluorescence (IF) experiments were performed using the anti-MyHC antibody and DAPI staining. Images of a single representative field were shown. Bars, 10 μ m. (g) The fusion index (calculated from three independent experiments) was determined for muscle fibers shown in (f). (h) Total cell extracts were prepared from the cells described above and used for Western blotting analysis using antibodies against myoglobin and α -tubulin. **(i–l)** C2C12 cells depleted or not of HuR were treated twice (see Methods) with 50nM AP-GST, -HuR-GST, -CP1-GST, -CP2-GST or -HuRD226A-GST and 24h after the second treatment with these chimeras they were induced for differentiation. (i) Immunofluorescent images and (j) fusion index of fibers fixed on day 3 of differentiation process. Bars, 10 μ m. (k–l) *NPM* (k) and *MyoD* (l) mRNA levels in confluent myoblasts treated as described above. mRNA levels were plotted relative to the GST-and siCtr-treated conditions \pm the S.E.M. of three independent experiments. For histograms in Figures 2g,k * P <0.01, ** P <0.001 (t test).

In order to identify the mechanisms responsible for the decreased expression of *NPM* mRNA during myogenesis (**Fig. 2.2a**), we first performed a nuclear run-on assay²² to assess whether this decrease is due to a change in transcription. Since we did not observe any change in the transcription rate during myogenesis (**Annex 1. Supplementary Fig. 4**), we concluded that the HuR-mediated downregulation of *NPM* mRNA expression is likely to occur at the level of mRNA stability. Indeed, a pulse-chase experiment²³ using the RNA polymerase II inhibitor Actinomycin D (ActD), showed that depleting HuR in C2C12 cells significantly increased, from ~5h to >9 h, the half-life of the *NPM* mRNA (**Fig. 2.3a–b**). Of note, treatment of cells with ActD did not affect their viability (**Annex 1. Supplementary Fig. 5**). These results, together with the fact that HuR does not affect the localization or the translation of the *NPM* mRNA (**Fig. 2.3c–d**), indicates that HuR promotes the formation of muscle fibers by destabilizing the *NPM* mRNA.

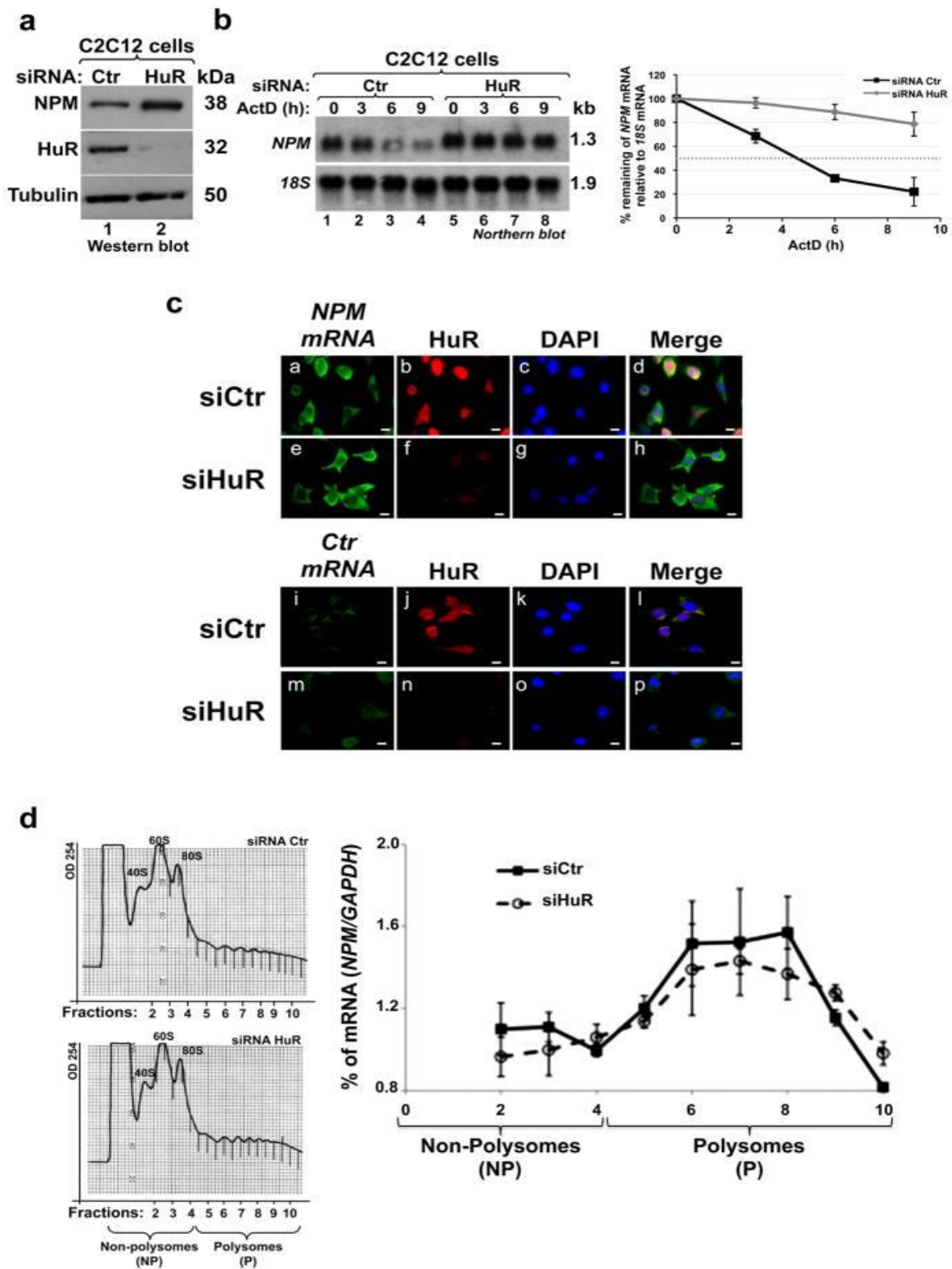


Figure 2.3 HuR regulates the stability of the *NPM* mRNA (a) Total extracts from C2C12 myoblasts treated with siRNA HuR or siRNA Ctr were used for western blot analysis to detect

NPM, HuR, and α -tubulin (loading control). Representative gel of three independent experiments. **(b)** RNA was prepared from C2C12 transfected with HuR or Ctr siRNAs (for 48h), and then treated with ActD for 0, 3, 6 or 9 hours. Northern blot analysis was performed using radiolabeled probes against *NPM* mRNA and *18S* rRNA (loading control). *NPM* and *18S* band intensities were measured using ImageQuant and the stability of *NPM* mRNA was determined relative to the *18S* for each time point. *NPM* signal in each one of these time points was compared to *NPM* level at 0h of ActD treatment, which is considered 100%. These percentages were then plotted \pm S.E.M of three independent experiments. **(c)** C2C12 cells transfected with siRNA HuR or siRNA Ctr were fixed, permeabilized, and incubated with digoxigenin-labeled *in vitro* transcribed antisense probe to detect *NPM* mRNA (panels a, e) and with sense RNA probe (panels i, m) as a control (*Ctr* probe). IF staining with anti-HuR antibody (panels b, f, j and n) and with DAPI was performed. A single representative field for each cell treatment is shown. Bars, 10 μ m. **(d)** 48h post-transfection of exponentially growing C2C12 cells with siRNA HuR or Ctr, polysomes were fractionated through sucrose gradients (15–50% sucrose). Absorbance at wavelength 254 nm was measured in order to determine the profile of polysome distribution. 10 fractions were collected and divided in two groups to non-polysome (NP, fractions 1–4) and polysome (P, fractions 5–10, contain mRNAs engaged in translation) (left panel). RT-qPCR was performed on each fraction using specific primers for *NPM* and *GAPDH* mRNAs (right panel). *NPM* mRNA level was standardized against *GAPDH* mRNA in each fraction and plotted \pm S.E.M of three independent experiments.

9.1.3.3. HuR destabilizes the *NPM* mRNA via U-rich elements.

HuR is known to regulate its mRNAs targets by interacting with AU-/U-rich elements in their 3'UTRs^{9,24}. Therefore, to define the molecular mechanism by which HuR destabilizes the *NPM* mRNA, we first assessed whether HuR and *NPM* mRNA associate in muscle cells. Immunoprecipitation (IP) (**Fig. 2.4a**) followed by RT-PCR (upper panel) or RT-qPCR (lower panel) analyses^{23,25} showed that HuR and the *NPM* mRNA coexist in the same complex in muscle cells. In order to determine whether this association is direct or indirect, we performed RNA electromobility shift assays (REMSAs)²³ using recombinant GST or GST-HuR proteins and radiolabeled RNA probes corresponding to the entire 5' or 3' UTRs of *NPM* mRNA (**Fig. 2.4b**). We observed that GST-HuR forms a complex only with the 3' but not the 5' UTR of *NPM* mRNA (**Fig. 2.4c**). To further define the binding site(s) of HuR, we divided the *NPM* 3'UTR into 2 probes, P1 and P2 (**Fig. 2.4b**) and observed a strong association of GST-HuR with only the P1 probe (**Fig. 2.4d**).

Using surface plasmon resonance (SPR) analysis, we confirmed these associations and showed that GST-HuR bound to the *NPM*-3'UTR and P1 probe with higher affinity (dissociation constants (KD) of 86×10^{-9} M and 132×10^{-9} M respectively) than the P2 probe (KD = 324×10^{-9} M) (**Fig. 2.4e**). In addition, further subdivision of P1 and 2 probes into three smaller regions, P1/2-1, -2 and -3, showed that HuR only binds to the P1-1 region of *NPM*-3'UTR (**Fig. 2.4f** and **Annex 1. Supplementary Fig.6a–b**). Analysis of the secondary structure of the P1-1 region, using the mfold prediction software for mRNA folding²⁶ indicated the existence of two U-rich elements (E1 and E2) similar to HuR *cis*-binding motifs previously identified in other mRNA targets^{11,23,26} (**Annex 1. Supplementary Fig. 6c**). To determine whether E1 and/or E2 elements mediate the binding of HuR to the *NPM* 3'UTR, we mutated each one of their uracils (Us; shown as Ts) as well as those of the element separating E1 and E2 to cytosine (C) (**Fig. 2.4g**) and performed REMSA experiments as described above. Since mutating each site separately (P1-1-mut-1 or -mut-2) but not those of the hinge element (P1-1-mut-3), equally disrupted the P1-1/HuR complex (**Fig. 2.4h–i**), we concluded that the E1 and E2 elements together constitute the minimum U-rich-element required for the direct binding of HuR to the *NPM*-3'UTR.

Next, we tested whether these U-rich elements are involved in the HuR-mediated destabilization of the *NPM* mRNA in muscle cells. We generated reporter cDNA plasmids expressing the Renilla Luciferase (Rluc) in which we inserted, at the 3'end, either the wild type *NPM* 3'UTR (Rluc-*NPM*-3') or the *NPM* 3'UTR mutant 1 (Rluc-*NPM*-3'-mut1, deficient in its ability to bind HuR) (**Fig. 2. 4h** and **2.5a**). An IP/RT-qPCR experiment showed that the association between HuR and the *Rluc-NPM-3'* mRNA is significantly higher than its association with the control reporters *Rluc* or *Rluc-NPM-3'-mut1* (**Fig. 2.5b–c**). We next assessed the impact of depleting endogenous HuR on the expression of the *Rluc-NPM-3'* mRNA. siCtr- or siHuR-treated C2C12 cells were transfected with the Rluc, Rluc-*NPM*-3' or Rluc-*NPM*-3'-mut1 plasmids (**Annex 1. Supplementary Fig. 7a**) and the steady state levels of these mRNAs were determined by RT-qPCR analysis. While we observed a 3.5-fold increase in the level of the *Rluc-NPM-3'* mRNA in cells depleted of HuR but not in those treated with siCtr, the levels of *Rluc-NPM-3'-mut1* remained high in both cell types (**Fig. 2.5d**).

on total cell lysates (TE) from C2C12 cells. RNA was isolated from the immunoprecipitate, and RT-PCR or RT-qPCR was performed using primers specific for *NPM* and *RPL32* mRNAs. The agarose gel (Upper panel) shown is representative of three independent experiments. For RT-qPCR (lower panel), *NPM* mRNA levels were standardized against *RPL32* mRNA levels. The normalized *NPM* mRNA levels were plotted relatively to the IgG IP condition +/- S.E.M. of three independent experiments ** $P < 0.001$ (t test). **(b)** Schematic representation of the *NPM* mRNA sequence. The probes covering the *NPM* 3'UTR (P1, P2, P1-1 to P1-3) used to generate radiolabeled RNA probes for RNA electrophoretic mobility shift assays are indicated (black lanes). **(c–d, f and h–i)** Gel-shift binding assays were performed by incubating 500 ng of purified GST or GST-HuR protein with the radiolabeled cRNA (c) 3'UTR and 5'UTR, (d) P1 and P2, (f) P1-1 to P1-3, (h) P1-1, P1-1-mut1 and P1-1-mut2, (i) P1-1 and P1-1-mut3 probes. These gels are representative of three independent experiments. **(e)** BIACORE, a surface plasmon resonance (SPR)-based biosensor technology, was used for a kinetic binding study between GST-HuR and *NPM* 3'UTR, P1 or P2 probes. GST-HuR was captured on a Series S CM5 chip and increased concentrations of *NPM* cRNA probes, as indicated, were injected over the surface. Injections were performed for 150s, to measure association, followed by a 400s flow of running buffer to assess dissociation. The association/dissociation ratio of GST-HuR to *NPM* 3'UTR is shown in the sensorgram (top left panel). The binding affinity (KD) of GST-HuR to *NPM* 3'UTR (top right panel), P1 or P2 (bottom panels) cRNA probes is also shown. **(g)** Nucleotide sequence of probe P1-1 showing the thymidine (T) residues that were mutated to cytidine (C) residues (identified by asterisks) to generate the P1-1-mut1, P1-1-mut2 and P1-1-mut3. The sequences highlighted by the dashed boxes as E1 and E2 are the single-strand AU-rich sequences identified using mfold software. * shown in panels 4c, f and h indicate the location of shifted complex.

On the other hand, overexpressing GFP-HuR in C2C12 cells decreased the level of the *Rluc-NPM-3'* mRNA by >65% but had no significant effect on the levels of *Rluc* or *Rluc-NPM-3'-mut1* mRNAs (**Fig. 2.5e, Annex 1. Supplementary Fig. 7c**). The effect of knocking down or overexpressing HuR on luciferase activity (which is proportional to *Rluc* protein levels) was similar to those seen for the mRNA levels (**Annex 1. Supplementary Fig. 7b,d**). Next, we investigated the functional relevance of these HuR binding sites on *NPM* mRNA stability. We performed ActD pulse-chase experiments on C2C12 cells expressing the various *Rluc* reporters described above and treated or not with 50nM of recombinant HuR conjugated to the cell-permeable peptide Antennapedia (AP)¹⁴ (**Fig. 2.5f**). We observed that the half-life of the *Rluc-NPM-3'* mRNA was significantly reduced (<2h) only in cells treated with AP-HuR-GST but not in those treated with AP-GST (>6h). However, the *Rluc-NPM-3'-mut1* mRNA remained stable under all treatments (half-life >6h). While these results clearly demonstrate that an intact HuR binding sites is required for HuR-induced destabilization of the *NPM* mRNA, it does not provide any indication on

their relevance during myogenesis. To address this question, we generated GFP-conjugated full-length wild type (GFP-NPM-3') or mutated (GFP-NPM-3'-mut1) isoforms of NPM (**Fig. 2.5g**). These NPM isoforms were then overexpressed in C2C12 cells and 48h later these cells were induced for differentiation for 3 days. Our experiments showed that overexpressing GFP-NPM-3' reduced the efficiency of muscle fiber formation by ~50% when compared to GFP alone (**Fig. 2.5h-j**). Interestingly, the overexpression of the GFP-NPM-3'-mut1 isoform, that does not bind HuR, provided a much higher inhibition of myogenesis efficiency than GFP-NPM-3' (>70%). Together these results show that the recruitment of HuR to the E1 and E2 U-rich elements of *NPM* 3'UTR is required for NPM downregulation and the promotion of myogenesis.

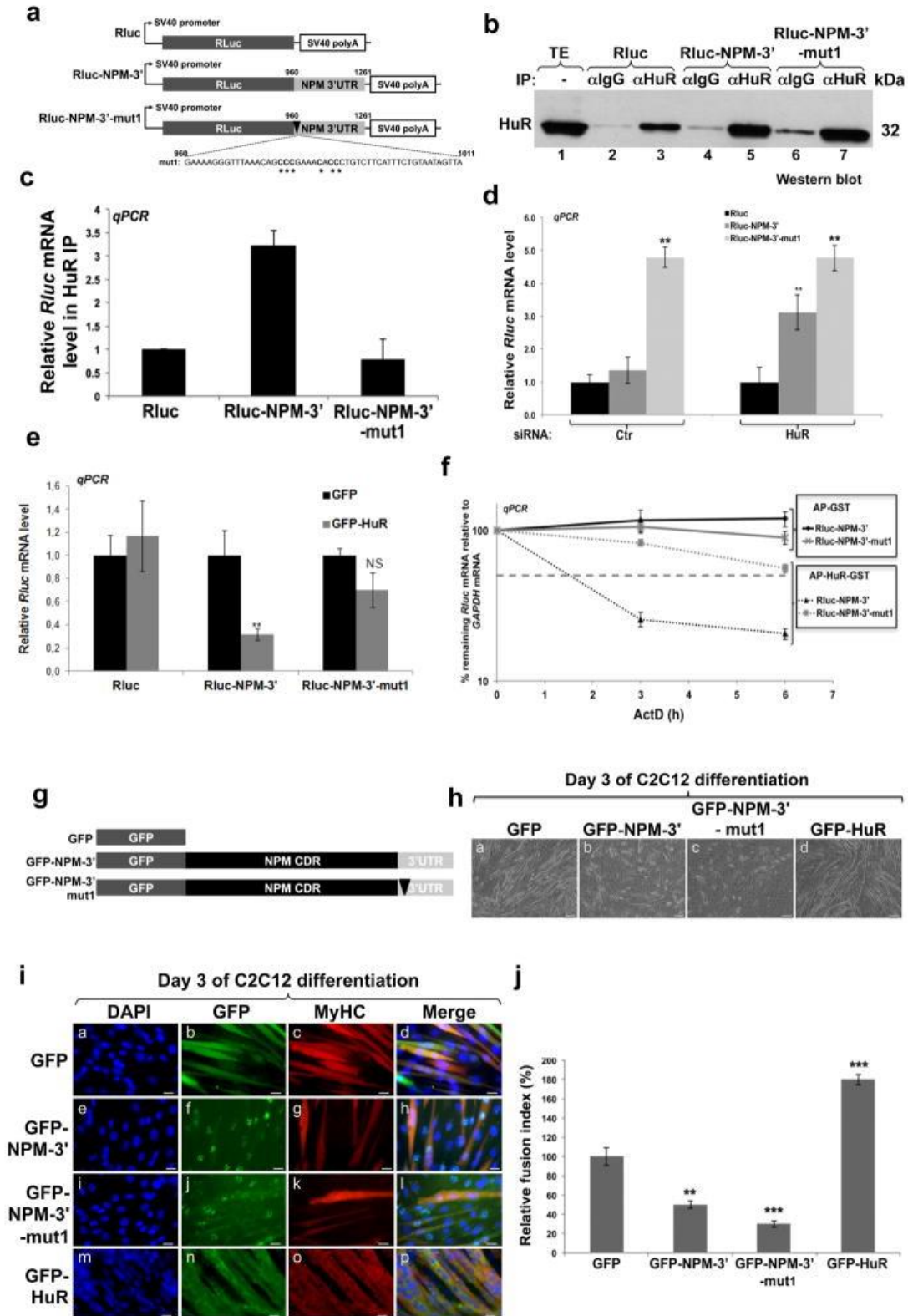


Figure 2.5 An intact P1-1 element is required for HuR-mediated regulation of NPM expression (a) Schematic diagram of the renilla luciferase reporters used in the experiments described in Figs.5a–f. (b–c) Exponentially growing C2C12 cells were transfected with

plasmids expressing *Rluc*, *Rluc-NPM-3'* or *Rluc-NPM-3'-mut1*. Total extracts from these cells were prepared 24 h after transfection and used for IP using the anti-HuR antibody (3A2) or IgG as a control. (b) Western blotting analysis with the anti-HuR antibody was performed using these IP samples. (c) *Rluc* mRNA associated with the immunoprecipitated HuR was determined by RT-qPCR. The relative *Rluc* RNA levels from *Rluc-NPM-3'* and *Rluc-NPM-3'-mut1* were plotted relatively to the *Rluc* RNA reporter \pm S.E.M. of three independent experiments. (d–e) The expression levels of these *Rluc* RNA reporters were also determined by RT-qPCR in C2C12 cells depleted or not of HuR (d) or overexpressing GFP or GFP-HuR (e). The expression levels of the *Rluc* mRNAs were normalized over total *Rluc* DNA transfected as described⁵⁹ and then standardized against *GAPDH* mRNA level \pm S.E.M. of three independent experiments * P <0.01, ** P <0.001, NS: Nonsignificant (t test). (f) C2C12 cells were transfected with the *Rluc* reporter RNA described above in the presence of AP-GST or AP-HuR-GST proteins. The stability of these reporter *Rluc* mRNAs was determined by AcD pulse-chase experiments. The percentages shown were plotted \pm S.E.M of three independent experiments. (g) Schematic diagram of GFP or the GFP-conjugated full-length NPM isoforms: WT NPM (GFP-NPM-3') and the NPM 3'UTR with the first AU rich sequence mutated (GFP-NPM-3'-mut1). The coding region of NPM is shown as NPM CDR. (h–j) C2C12 cells expressing these isoforms or the GFP-HuR protein were fixed on day 3 of muscle cell differentiation. (h) Phase contrast images of the myotubes described above. (i) IF (using the anti-My-HC antibody) images of these myotubes were used to calculate the fusion index \pm S.E.M. (j) of three independent experiments ** P <0.001, *** P <0.0001, (t test). Images of a single representative field are shown. Bars, 50 μ m for (h) and 10 μ m for (i).

9.1.3.4. HuR destabilizes the *NPM* mRNA in a KSRP dependent manner.

It has been shown that during myogenesis transcripts such as *Myog* and *p21* but not *MyoD* are destabilized by KSRP in proliferating myoblasts³. However, at later stages (fusion step) these mRNAs are stabilized by HuR, leading to an increase in their expression levels and to the promotion of myotube formation^{5,7}. Therefore, since KSRP and HuR target common transcripts in muscle cells^{3,5,7} and our observation showed that depleting the expression of either of these two proteins in C2C12 cells equally prevented myogenesis (**Annex 1**. Supplementary Fig. 8), we tested whether KSRP could be implicated in the HuR-mediated destabilization of the *NPM* mRNA in proliferating C2C12 cells. We first determined the effect KSRP depletion could have on the expression level of the *NPM* mRNA and protein. We showed that, similarly to HuR depletion, the knockdown of KSRP significantly increased the expression levels of *NPM* mRNA (>2 fold) and protein (>1.5 fold) (**Fig. 2.6a–b**). Additionally, ActD pulse chase experiments indicated that the knocking down KSRP increased the half-life of *NPM* mRNA to a similar extent than HuR (compare **Fig. 2.3b to 2.6c**). However, as expected³, KSRP knockdown

had no effect on the stability of the *MyoD* mRNA, while it increased the half-life of *p21* mRNA from ~3.6h to >6h (**Fig. 2.6c**). Altogether, these data show that both HuR and KSRP decrease the expression level of the NPM protein by shortening the half-life of the *NPM* mRNA. Surprisingly we additionally observed that overexpressing KSRP alone in C2C12 cells, unlike HuR, does not affect *NPM* mRNA or protein levels (**Fig. 2.6d–e**) despite promoting the decreased expression of p21. Since knocking down KSRP by >90% prevented the HuR-mediated decrease of the *NPM* mRNA and protein (**Fig. 2.6f–h**), we concluded that although KSRP alone is not able to destabilize *NPM* mRNA, KSRP is required for the HuR-mediated down-regulation of NPM level in muscle cells.

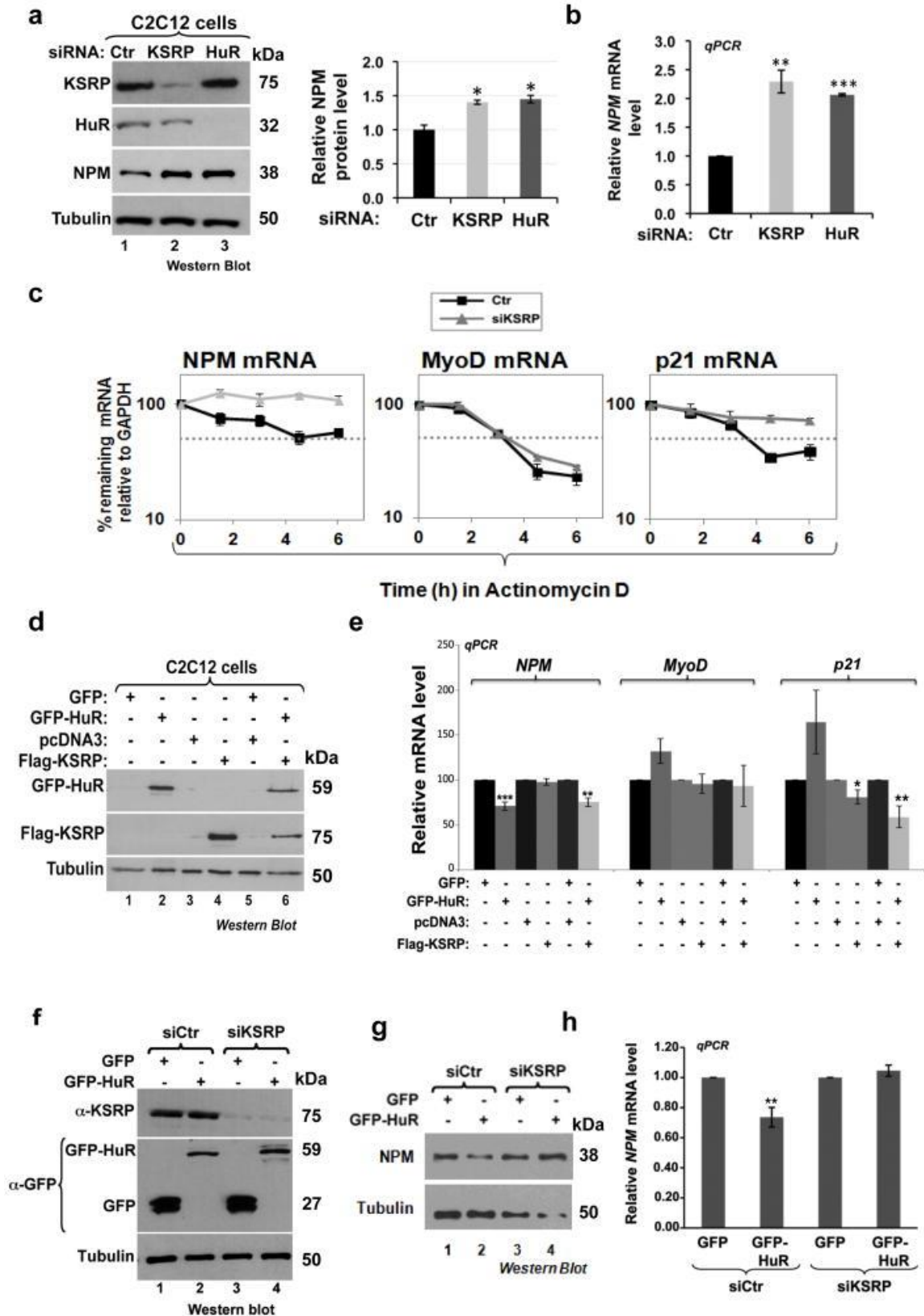


Figure 2.6 KSRP is required for the HuR-mediated destabilization of *NPM* mRNA. (a-b) Exponentially growing C2C12 cells were treated with siRNA Ctr or siRNA against HuR or KSRP.

Total cell (a) or RNA (b) extracts from these cells were prepared 48 hours after transfection. (a) Western blotting analysis was performed using antibodies to detect KSRP, NPM, HuR and α -tubulin (loading control). (b) RT-qPCR analysis was performed to assess *NPM* mRNA levels which were standardized against *GAPDH* mRNA. The levels of NPM protein (a) or mRNA (b) in cells depleted of HuR or KSRP were plotted relative to the siRNA Ctr condition +/- the S.E.M. of three independent experiments. (c) The stability of the *NPM*, *MyoD* and *p21* mRNA in C2C12 depleted or not of KSRP was determined by AcD pulse-chase experiments. RT-qPCR analysis was performed using specific primers for these three mRNAs. mRNA levels were then standardized against *GAPDH* mRNA and plotted +/- S.E.M of three independent experiments. (d–e) Exponentially growing C2C12 cells were transfected with the pcDNA3, pcDNA-Flag-KSRP, GFP and GFP-HuR. (d) Total cell extracts or (e) RNA extracts from these cells were prepared 24h post-transfection. (d) Western blotting was performed using antibodies against Flag, HuR, or α -tubulin (loading control). (e) RT-qPCR analysis was performed as described above in 6c and mRNA levels were plotted relative to their levels in control cells +/- the S.E.M. of three independent experiments. (f–h) GFP and GFP-HuR plasmids were transfected in C2C12 cells depleted or not of KSRP. 24 h later total protein extracts and RNA were prepared. (f–g) Western blotting analysis was performed with antibodies against (f) KSRP, GFP and (g) NPM. α -tubulin levels were assessed as a loading control in both (f) and (g). (h) RT-qPCR analysis was performed as described above. *NPM* mRNA levels were standardized against *GAPDH* mRNA level. In each condition the level of *NPM* mRNA in siKSRP treated cells was plotted relative to its levels in siRNA Ctr-treated and GFP-transfected cells +/- the S.E.M. of three independent experiments. In the histograms presented in Figures 6 a,b,e,h * P <0.01, ** P <0.001, *** P <0.0001 (t test).

To gain insight into the molecular mechanisms by which HuR and KSRP affect the fate of *NPM* mRNA in muscle cells, we first determined whether KSRP also associates with this transcript. IP experiments using the anti-KSRP antibody¹⁷ followed by RT-PCR and -qPCR analyses showed that KSRP binds to the *NPM* mRNA similarly to HuR (**Fig. 2.7a** and **2.4a**). REMSA using total extracts prepared from C2C12 cells that were incubated with radiolabeled *NPM*-3'UTR or the P1 or P2 probes (**Fig. 2.4b**) and with the anti-KSRP antibody showed that, similarly to HuR (**Fig. 2.4**), KSRP associates with the 3'UTR of *NPM* through the P1 but not the P2 region (**Fig. 2.7b**). To determine the KSRP binding site(s) in the *NPM* 3'UTR, we incubated the recombinant KSRP with intact or mutated radiolabeled P1 probes and performed the same REMSA experiments described in Figure 2.4. KSRP formed complexes with P1-1 and P1-1-mut2 but not with P1-1-mut1 (mut-E1) probes (**Fig. 2.7c**). In addition, IP experiments with anti-KSRP antibody were performed on cells expressing the *Rluc*-reporters described in Fig. 2.5a. We observed that while KSRP associated with the *Rluc-NPM-3'* mRNA and *Rluc-NPM-3'-mut2*, it failed to interact with the *Rluc-NPM-3'-mut1* message (**Fig. 2.7d–e** and **Annex 1. Supplementary Fig. 9**). Therefore, together these results show that KSRP directly

associates with the *NPM* mRNA through the E1 element that is also one of the sites that mediates HuR binding.

Next we investigated whether HuR and KSRP can form a complex. IP experiments on cell extracts treated or not with 100µg/ml RNase A indicated that HuR and KSRP associate in C2C12 cells in an RNA-independent manner (**Fig. 2.7f–g**). However, this RNA independent interaction between HuR and KSRP was not seen using a lower dose of RNase A (12.5µg/ml). Moreover, GST-pulldown experiments, using recombinant His-KSRP and GST-HuR, further confirmed this direct interaction (**Fig. 2.7h**). We then assessed whether the association between the *NPM* mRNA and HuR or KSRP requires an intact HuR/KSRP complex. IP/RT-qPCR experiments showed that depleting HuR from C2C12 cells significantly decreased (>40%) the amount of *NPM* mRNA that binds to KSRP (**Fig. 2.7i**). Similarly, although knocking down KSRP in C2C12 cells did not affect the binding of HuR to the *Myog* and *p21* mRNAs (**Annex 1. Supplementary Fig. 10**), it decreased its association with the *NPM* mRNA (**Fig. 2.7j**). Taken together, these data suggest that in muscle cells the HuR/KSRP complex assembles in an RNA-independent manner and is recruited to the P1-1 element thus promoting the rapid destabilization of the *NPM* mRNA.

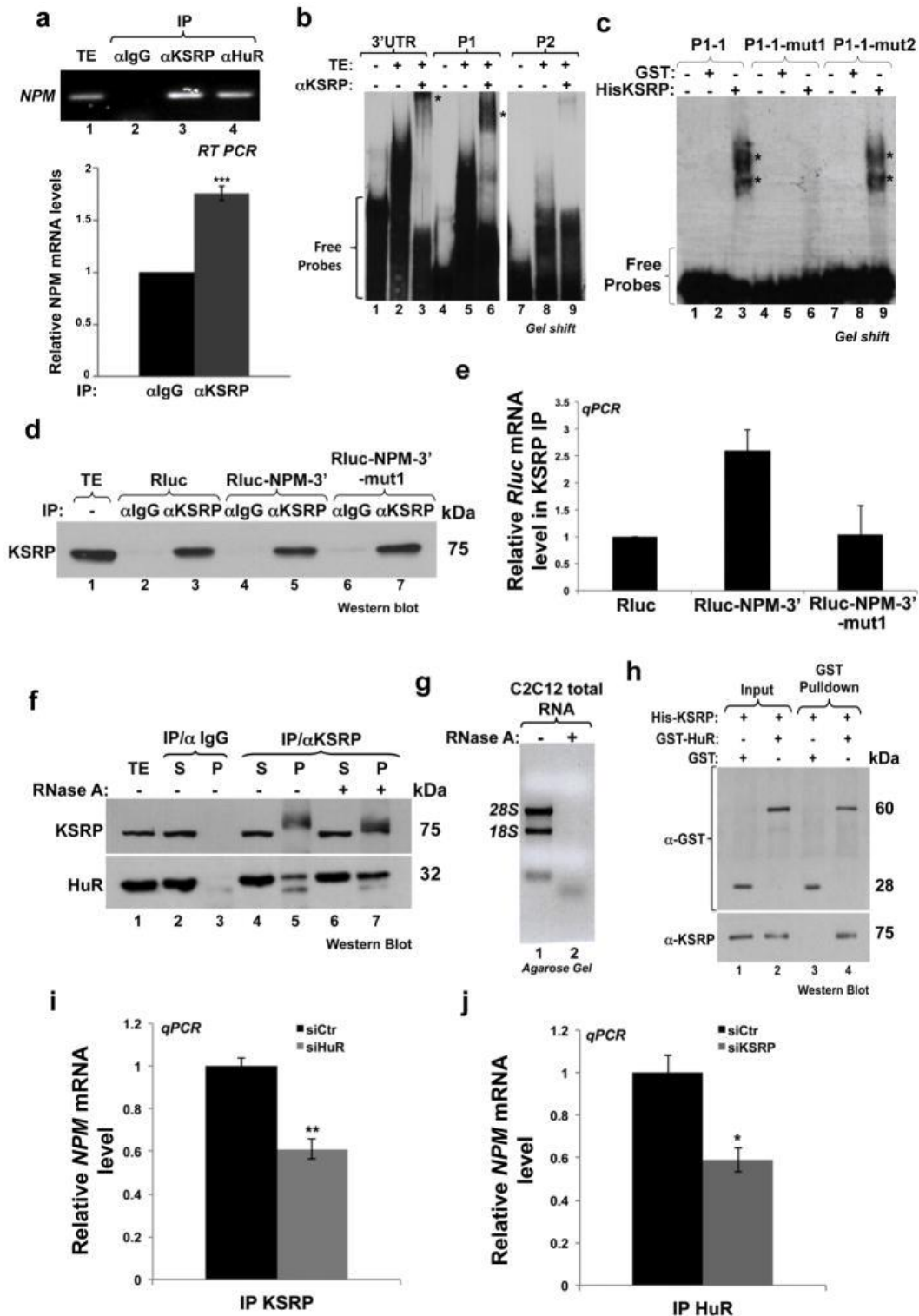


Figure 2.7. HuR and KSRP form a complex and bind to the same element in the *NPM* 3'UTR. (a) IP coupled to RT-PCR (upper panel) or RT-qPCR (lower panel) experiments were performed to determine the association of KSRP and HuR with the *NPM* mRNA in C2C12 cells. For RT-qPCR, *NPM* mRNA levels are shown +/- S.E.M. of three independent experiments *** $P < 0.0001$ (t test). (b) Supershift binding assay was performed to demonstrate that the radiolabelled *NPM* 3'UTR as well as the P1 cRNA probe, unlike the P2 probe, can

associate to a complex containing KSRP (indicated by an asterisk (*)). **(c)** Gel-shift binding assay was performed with 500 ng of purified GST or His-KSRP proteins and the indicated radiolabeled cRNA probes. **(d–e)** IP experiments were performed on C2C12 cells expressing Rluc, Rluc-NPM-3' and Rluc-NPM-3'-mut1 using the KSRP or IgG antibody. Immunoprecipitation of KSRP (d) and association with reporter RNAs (e) were determined as described in Figure 2.5b–c. **(f)** C2C12 extracts treated or not with RNase A were used for IP experiments with the anti-KSRP or -IgG antibodies. The binding of HuR to KSRP was then assessed by western blot. For unknown reasons, we observed a shift in the molecular weight of KSRP that we believe could be due to the immunoprecipitation of a post-translationally modified KSRP isoform. **(g)** Agarose gel demonstrating effectiveness of RNase treatment. **(h)** *In vitro* GST pull-down assay demonstrating that HuR directly interacts with KSRP. Input lanes account for 10% of the reaction performed in the assay. **(i–j)** IP coupled to RT-qPCR experiments were performed using anti-KSRP (i) or HuR (3A2) (j) antibodies on total extract (TE) from C2C12 cells treated with siHuR (i) or siKSRP (j). *NPM* mRNA levels in the immunoprecipitates were standardized (as described in the Methods) and normalized to the corresponding IgG and input sample. The *NPM* mRNA levels in siHuR or siKSRP conditions were plotted relative to siCtr conditions \pm S.E.M. of three independent experiments, * $P < 0.01$, ** $P < 0.001$ (t test). All gels/blots shown in the figure are representative of three independent experiments (except for the gel shown in 2.7b which is representative of two). * shown on gel indicates the location of shifted complexes.

To gain insight into the mechanism by which HuR executes these functions, we first determined the HuR domain responsible for this activity. We generated plasmids expressing GFP-tagged wild-type HuR or various deletion mutants of HuR (**Fig. 2.8a**). Each one of these isoforms was then expressed in C2C12 cells that were subsequently used for IP experiments with the anti-KSRP antibody. Western blotting analysis with the anti-GFP antibody has shown that similarly to wt HuR, polypeptides harboring the RRM3 motif (GFP-HNS-RRM3 and GFP-RRM3), but not those harboring RRM1-2 or HNS alone, were able to associate with KSRP (**Fig. 2.8b**) and promote a significant decrease in *NPM* mRNA level (**Fig. 2.8c**). In addition, an IP/RT-qPCR experiment on cells expressing GFP-HuR, -RRM1-2 or -RRM3 indicated that while RRM1-2 did not show a strong association with the *NPM* mRNA, RRM3 associated with more *NPM* message than wt-HuR (**Fig. 2.8d–e**). Since, during myogenesis cytoplasmic HuR undergoes caspase-mediated cleavage generating HuR-CP1 (24 kDa, RRM1-RRM2- Δ HNS₁) and HuR-CP2 (8 kDa, Δ HNS₂-RRM3)⁴ (**Fig. 2.2c** and **Annex 1**. Supplemental Fig. 12a), we next verified the effect of these CPs on *NPM* expression. Our data confirmed that HuR-CP2, which harbors the RRM3 motif, but not HuR-CP1, associated with KSRP and the *NPM* mRNA and was also able to form a complex with the HuR/KSRP binding element in the *NPM* 3'UTR (the P-1-1 probe) (**Annex 1**. Supplementary Fig.11b–g). In addition, similarly to GFP-RRM3

(Fig. 2.8c), we observed that the overexpression of HuR-CP2 promoted a significant decrease in *NPM* mRNA the steady-state level and that this effect is KSRP-mediated (Annex 1. Supplementary Fig.11h-i). Together, these results strongly indicate that the RRM3 motif of HuR plays a key role in mediating the formation of the HuR/KSRP in differentiating muscle cells.

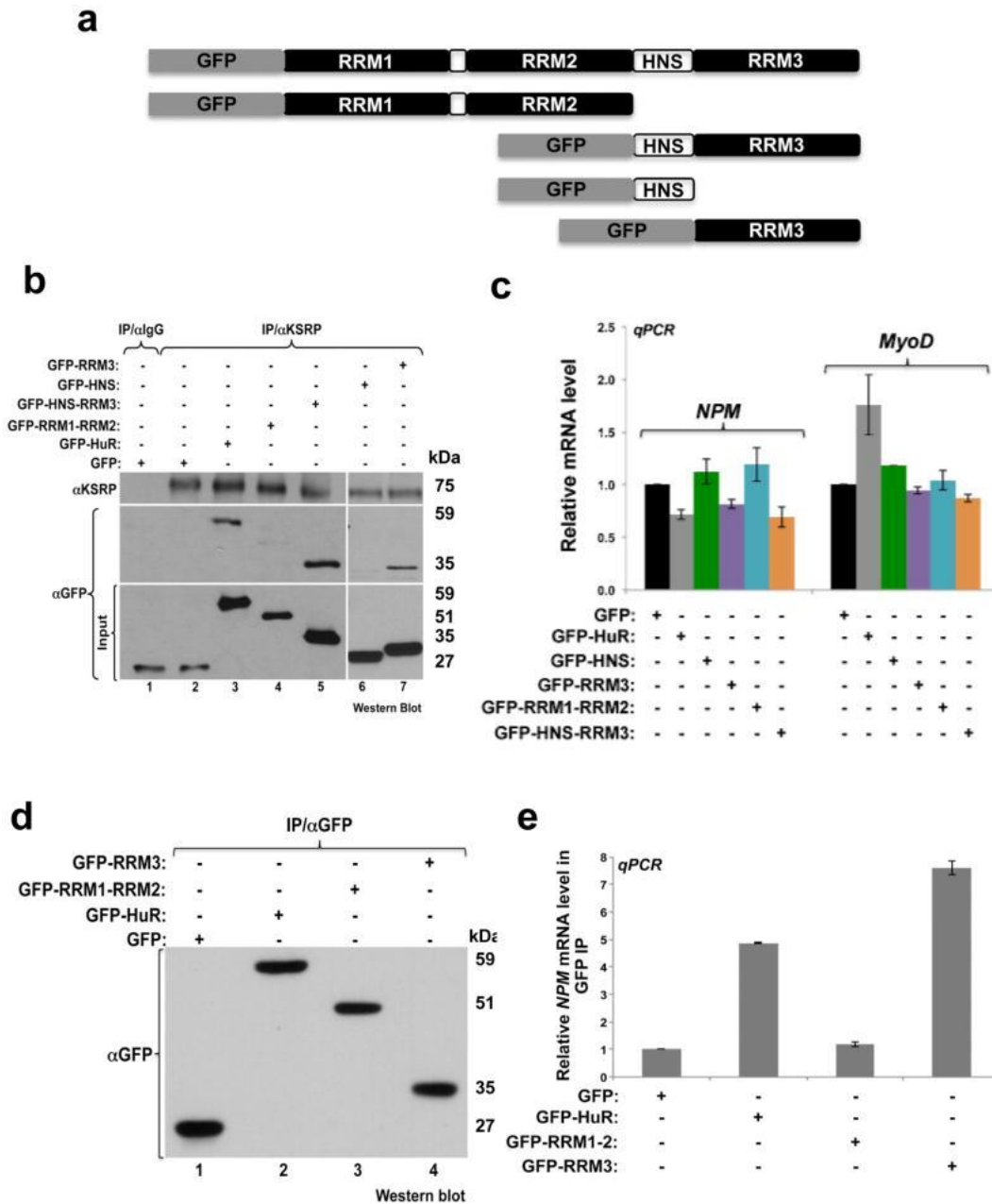


Figure 2.8 The HuR RRM3 motif is required for the formation of KSRP/HuR complex. (a) Schematic diagram depicting the primary structure of HuR protein shows the three RNA

binding domains (RRM1-3) and the HuR Nucleocytoplasmic Shuttling domain (HNS). Also shown are the different HuR isoforms conjugated to the GFP tag. **(b–e)** Exponentially growing C2C12 muscle cells were transfected with GFP, GFP-HuR, GFP-RRM1-RRM2, GFP-HNS-RRM3, GFP-HNS or GFP-RRM3 plasmids. Total cell extracts (b and d) or total RNA (c and e) were prepared from these cells 24 hours post-transfection. (b) IP experiments on these cell extracts were performed using the KSRP antibody or IgG as a control. The input (10% of the total extract) and the immunoprecipitate were analyzed by western blot using antibodies against GFP. (c) RT-qPCR analysis on total RNA prepared from these cells was performed using specific primers for *NPM*, *MyoD* and *GAPDH* mRNAs. *NPM* and *MyoD* mRNA levels were standardized against *GAPDH* mRNA and plotted relative to the GFP control condition +/- the S.E.M. of three independent experiments. (d) IP experiments were performed using the GFP antibody on extracts from the C2C12 cells expressing GFP, GFP-HuR, GFP-RRM1-RRM2 or GFP-RRM3 and analyzed by western blot using the GFP antibody. (e) RNA was isolated from the IP described in (d) and RT-qPCR were performed using primers specific for *NPM* and *RPL32* mRNAs. *NPM* mRNA levels were standardized against *RPL32* mRNA levels. For each IP sample, *NPM* mRNA levels were normalized as described in Figure 5 and plotted relative to the GFP IP +/- S.E.M. of three independent experiments.

Since KSRP has been shown to promote mRNA decay by recruiting the ribonuclease PARN and components of the exosome such as EXOSC5^{3,17} we investigated whether these enzymes could play a role in the HuR/KSRP-mediated destabilization of *NPM* mRNA. Our IP experiments showed that HuR associates with both PARN and EXOSC5 in an RNA independent manner (**Fig. 2.9a** and **Annex 1. Supplementary Fig. 12**). Interestingly, although both PARN and EXOSC5 interact with the *NPM* mRNA in C2C12 cells, this association is lost in HuR or KSRP depleted cells (**Fig. 2.9b**). To assess whether PARN and/or EXOSC5 play a role in the HuR/KSRP-mediated effect on *NPM* expression, we expressed GFP-HuR or GFP-HuR-CP2 in C2C12 cells depleted or not of these two ribonucleases (**Fig. 2.9c**) and the expression level of the *NPM* mRNA was determined using RT-qPCR. Our data showed that while knocking down PARN (**Fig. 2.9d**) or EXOSC5 (**Fig. 2.9e**) in C2C12 cells increased the expression of the *NPM* mRNA, the absence of these ribonucleases prevented the HuR- or HuR-CP2-mediated *NPM* mRNA decay (**Fig. 2.9f**). The fact that the depletion of XRN1 (a 5'-3' exoribonuclease component of the decapping complex)²⁷ did not have a major effect on *NPM* mRNA expression (**Annex 1. Supplementary Fig. 13**) suggests that only ribonucleases that are recruited by KSRP such as PARN and EXOSC5 take part in this destabilization activity. Interestingly, we also demonstrate that knocking down PARN and EXOSC5 totally prevented C2C12 cells from entering the differentiation process (**Fig.**

2.9g–i) and the depletion of NPM in these cells partially re-established their myogenic potential (**Annex 1. Supplementary Fig. 14**). Of note, the weak rescue of myogenesis in cells depleted of both EXOSC5 and NPM suggests that EXOSC5 targets other messages in muscle cells. Together, our data indicate that during early myogenesis the formation of the HuR/KSRP complex leads to the recruitment of ribonucleases such as PARN and EXOSC5 which in turn destabilize the *NPM* mRNA thus promoting muscle fiber formation.

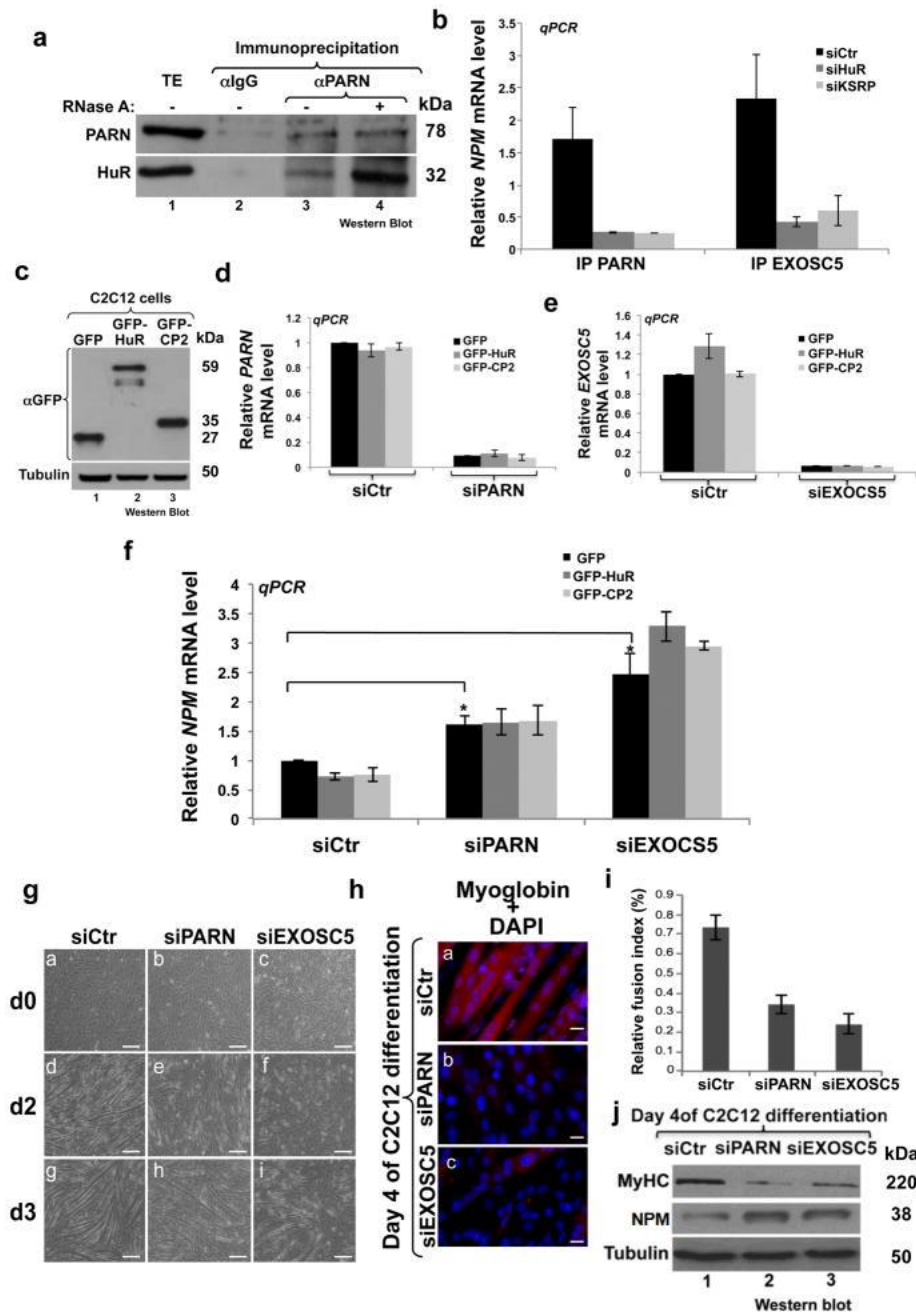


Figure 2.9 The HuR/KSRP-mediated decay activity requires PARN and EXOSC5 to destabilize *NPM* mRNA and promote muscle fiber formation. (a) IP experiments using the

anti-PARN antibody were performed on total cell extracts prepared from proliferating C2C12 cells treated or not with RNase A. The precipitates were used for Western blotting analysis with anti-PARN and –HuR antibodies. The blots shown are representative of two independent experiments. **(b)** IP coupled to RT-qPCR experiments were performed using the PARN or the EXOSC5 antibodies on total extract (TE) from C2C12 cells treated with siHuR or siKSRP. The *NPM* mRNA in the immunoprecipitate was standardized and normalized as described in Figs.2.7i,j. The PARN- or EXOSC5- associated *NPM* mRNA levels in siHuR or siKSRP treated C2C12 cells were plotted relative to siCtr conditions +/- S.E.M. of three independent experiments * $P < 0.01$ (t test). **(c–f)** GFP, -HuR and -CP2 proteins were expressed in C2C12 cells treated or not with siRNA-PARN or -EXOSC5. 24h later protein extracts and total RNA were prepared. (c) Western blotting analysis was performed using antibodies against GFP and α -tubulin (loading control). (d–f) RT-qPCR analysis was performed using primers specific for *GAPDH* as well as *PARN* (d), *EXOSC5* (e), *NPM* (f) mRNAs. The levels of *PARN*, *EXOSC5* and *NPM* mRNAs were normalized against *GAPDH* mRNA level and were plotted relatively to the siRNA Ctr-treated and GFP-transfected cells +/- the S.E.M. of three independent experiments * $P < 0.01$ (t test). **(g–j)** Confluent C2C12 depleted of PARN or EXOSC5 were induced for differentiation for up to 4 days. (g) Phase contrast pictures showing the differentiation status of these cells at day (d) d0 (panels a–c), d2 (panels d–f), and d3 (panels g–i). Bars, 50 μ m. (h) These cells, on day 4 of muscle cell differentiation, were also fixed and used for IF with anti-Myoglobin antibody and DAPI staining. Images of a single representative field were shown. Bars, 10 μ m. (i) The fusion index was determined as described in Methods. (j) Total extracts from these cells were prepared and used for western blotting analysis with antibodies against My-HC, NPM and α -tubulin (loading control).

9.1.4. Discussion

In this work we delineate the molecular mechanisms by which muscle cells down regulate NPM expression and show that this event represents a key regulatory step required for their commitment to myogenesis. Though previous studies have indicated that lowering the expression of NPM is required for the differentiation of a variety of cells such as HL60 and K562^{19,20}, the molecular mechanism and the players behind this reduction remained elusive. Here we show that the decrease in NPM expression involves the destabilization of its mRNA via a mechanism mediated by the RNA-binding protein HuR. This observation was unexpected since HuR has been previously shown to stabilize the *NPM* mRNA in intestinal cells undergoing stress¹⁸. In undifferentiated muscle cells the depletion of endogenous HuR results in the stabilization of the *NPM* mRNA and its increased expression, while HuR overexpression elicits the opposite effects. This mRNA destabilization activity of HuR involves its association, via the HuR-RRM3 motif, with KSRP and the ribonucleases PARN and EXOSC5¹⁷. Together, our data support a model whereby in response to a myogenic signal HuR forms a complex with KSRP, PARN and

the exosome, which in turn is recruited to a U-rich element in the 3'UTR leading to the destabilization of the *NPM* mRNA and the promotion of the early steps of myogenesis.

Although a NPM overexpression was previously linked to the inhibition of the differentiation of human promyelocytic leukemia HL60 cells and megakaryocytic K562 cells^{19,20}, our work provides the first demonstration that NPM is implicated in muscle fiber formation. NPM is highly expressed in a variety of cell lines and tissues and has been involved in many cellular processes such as cell proliferation and stress response^{28,29}. In fact, manipulating the abundance of NPM has a dramatic effect on cell fate and on embryogenesis. *Npm*^{-/-} mice do not complete their embryonic development and die between embryonic days E11.5 and E16.5 due to a severe anemia caused by a defect in primitive hematopoiesis³⁰. On the other hand, a high expression level of NPM is involved in cell transformation and tumour progression^{29,31–33}. NPM levels significantly decrease in response to a variety of stimuli, among them those known to trigger cell cycle arrest and cell differentiation^{19,20,29}. These data and the fact that NPM and HuR are both essential for the development of numerous cell lines and tissues^{12,28,29,34–36}, highlight the importance of delineating the mechanism(s) by which HuR down regulates NPM expression.

Previously, other and we have demonstrated that HuR plays a prominent role during muscle cell differentiation by increasing the stability of promyogenic mRNAs at the later stages of this process^{5,7}. Here we show that HuR is also involved in the early stages of myogenesis by degrading the *NPM* mRNA in a KSRP dependent manner. Since previous reports have indicated that during myogenesis HuR and KSRP affect the half-lives of the same promyogenic transcripts, but in opposite ways, their collaboration to degrade a common target mRNA in undifferentiated muscle cells was unexpected. Indeed, it has been shown that KSRP plays a key role in maintaining low levels of *p21* and *Myog* mRNAs in undifferentiated muscle cells by promoting their rapid decay³. The fact that HuR does not associate with these mRNAs in these cells⁵ could explain why these transcripts became available to KSRP and the KSRP-associated decay machinery. However, during the step where muscle cells fuse to form myotubes, p38^{MAPK} phosphorylates KSRP leading to the release of *p21* and *Myog* mRNAs from this decay machinery³. These findings, together with the data outlined in this manuscript, confirm the

importance of HuR during muscle fiber formation and indicate that the functional consequences and the binding specificity of HuR to its target mRNA could change from one myogenic step to another depending on the nature of its protein ligand.

It is not surprising that HuR exerts different/opposite functions on its target transcripts. Numerous reports have indicated that depending on extra- or intracellular signals and/or the *trans*- or the *cis*-binding partners, HuR either activates or represses the turnover or translation of its mRNA targets^{10,16,37,38}. Indeed, the Steitz laboratory has shown that HuR mediates the decay of the viral small nuclear RNA (snRNA) Herpesvirus saimiri U RNA 1 (HSUR 1) in an ARE-dependent manner^{39,40}. Recently, HuR has been associated with the destabilization of the *p16* mRNA both in HeLa and in IDH4 cells³⁸. HuR participates in the decay of this message by forming a complex with AUF1 and Argonaute, two well-known mRNA decay factors^{38,41–43}. Our data uncover a novel mechanism by which HuR mediate the decay of its mRNA target leading to muscle fiber formation. This mRNA decay-promoting activity of HuR depends on its association with KSRP, a factor known to promote the decay of AU-rich containing mRNAs^{17,44}. Interestingly, besides a difference in the way they form, the HuR/AUF1 and HuR/KSRP complexes also show a difference in their functional outcome. While in muscle cells HuR/KSRP assemble in an RNA-independent manner prior to their recruitment to the same U-rich element in the *NPM* 3'UTR, the formation of the HuR/AUF1 complex in HeLa cells is RNA-dependent and occurs via the binding of each one of these two proteins with a different element in the *p16* 3'UTR³⁸. Likewise, unlike the HuR/AUF1 complex that promotes the proliferation of HeLa and IDH4 cells³⁸, the HuR/KSRP complex triggers the differentiation of muscle cells, an event linked to a cell cycle withdrawal²¹.

Besides the association with different protein ligands, we still do not know whether other processes such as posttranslational modifications are also involved in the functional switch of HuR during myogenesis. It has been shown that phosphorylation on various serine residues could impact the association of HuR with some of its target mRNAs such as *p21*^{45–47}. While the implication of phosphorylation in HuR-mediated effects in muscle cells is still elusive, we recently showed that caspase-mediated cleavage plays a key role in modulating the promyogenic function of HuR^{4,8}. Although our data indicated that HuR-CP1 promotes the cytoplasmic accumulation of HuR during the myoblast-to-myotube

fusion⁴, the function of HuR-CP2 remained unclear. Here, we demonstrate that HuR-CP2 associates with KSRP and is sufficient to downregulate the expression of *NPM* mRNA in muscle cells (**Annex 1**. Supplementary Fig. 11). Interestingly we also show that, unlike the non-cleavable isoform of HuR (HuRD226A), HuR-CP2 can re-establish the myogenic potential of C2C12 cells depleted of endogenous HuR (**Fig. 2.2i–l**). While additional experiments are needed to confirm the role of this cleavage product in the promyogenic function of HuR, these observations raise the possibility of its implication in maintaining a low expression of levels of NPM during myogenesis. While these and likely other modifications modulate HuR function in muscle cells, the data described above establish that HuR, through its ability to promote the decay of target mRNAs, acquires more flexibility to use different ways to impact important processes such as muscle fiber formation. Therefore, since a change in HuR function and associated partners has been linked to chronic and deadly diseases such as cancer and muscle wasting^{48–50}, delineating the molecular mechanisms behind the HuR-mediated mRNA decay activity could identify novel targets that help design effective strategies to treat these patients.

9.1.5. Material and Methods

Plasmid construction

The pYX-Asc plasmid containing the full-length mouse NPM cDNA (Accession Number: BC054755) was purchased from Open Biosystems (Catalogue Number: MMM1013-9497870). To generate the GFP-NPM plasmid, full-length mouse NPM was amplified by PCR using the pYX-Asc plasmid as template and the following primers: forward 5'GGC AAG CTT CGT CTG TTC TGT GGA ACA GGA-3' and reverse 5'-CGG GATC CGG GAA AGT TCT CAC TTT GCA TT-3'. The pAcGFP1-C1 (Clontech) and the PCR products were digested by HindIII and BamHI restriction enzymes (NE Biolabs). To generate the pRL-SV40-NPM plasmid, the full-length 3'UTR of mouse NPM was amplified by PCR using the pYX-Asc plasmid as template and the following primers: forward 5'-GCT CTA GAG AAA AGG GTT TAA ACA GTT TGA-3' and reverse 5'-CCG GCG GCC GCA CTT TAT TAA AAT ACT GAG TTT ATT-3'. The pRL-SV40 vector (Promega) and the PCR products were digested by XbaI and NotI restriction enzymes (NE Biolabs). PCR

inserts were ligated into the plasmids using the T4 DNA ligase (NE Biolabs) according to the manufacturer's instructions. pRL-SV40-NPMmut1 and mut2 plasmid was generated by Norclone Biotech Laboratories, Kingston, ON, Canada (as described in text). The GFP and GFP-HuR plasmids were generated and used as described in ⁵¹.

Cell culture and transfection

C2C12 muscle cells (ATCC, Manassas, VA, USA) were grown in media containing 20% fetal bovine serum (FBS, Invitrogen) in DMEM (Dulbecco's modified eagle medium from Invitrogen). In order to induce muscle cell differentiation, cells were switched to a media containing DMEM, 2% horse serum, penicillin/streptomycin antibiotics (Invitrogen), and 50mM HEPES, pH 7.4 (Invitrogen) when their confluency reached 100%^{5,6}.

For the generation of stable cell lines, C2C12 cells were transfected with GFP, GFP-HuR and GFP-NPM plasmids, and 24 hours post-transfection G418 (1 mg/ml; Sigma-Aldrich) was added to the media. The stable cell lines were selected with G418 for 2 weeks and then sorted by flow cytometry (FACS) to select clones with equal expression levels. Transfections with siRNAs specific for HuR were performed using jetPEI (Polyplus Transfection) according to the manufacturer's instructions. For DNA plasmid transfections, C2C12 cells at 70% confluency were transfected in 6-well plates with 1.5 µg of plasmid DNA using Lipofectamine and Plus reagents (Invitrogen) according to the manufacturer's instructions. Cells were subsequently incubated at 37°C for 24 hours before harvesting and analysis.

siRNA

siRNA oligonucleotides against HuR (5'-AAG CCU GUU CAG CAG CAU UGG-3'⁵), NPM (5'-CAU CAA CAC CGA GAU CAA A dT dT -3') (Dharmacon, USA), KSRP (5'-GGA CAG UUU CAC GAC AAC G dT dT-3'³), and the siRNA Ctr (5'-AAG CCA AUU CAU CAG CAA UGG-3'⁵), were synthesized by Dharmacon, USA. siRNA PARN (5'-GGA UGU CAU GCA UAC GAU Utt- 3'), EXOSC5 (5'-UCU UCA AGG UGA UAC CUC Utt- 3') and XRN1 (5'-GAG GUG UUG UUU CGA AUU Att- 3') were acquired from Ambion USA.

Preparation of cell extracts and immunoblotting

Total cell extracts were prepared⁵² and western blotting was performed using antibodies against HuR (3A2, 1:10,000)⁵³, NPM (anti-B23 clone FC82291, Sigma-Aldrich, 1:30000), MyHC (Developmental studies Hybridoma⁵, 1:1000), Myoglobin (DAKO, 1:500), α -tubulin (Developmental studies Hybridoma Bank, 1:1000), GFP (Clontech, Mountain View, CA, USA, 1:1000), and KSRP (affinity-purified rabbit serum¹⁷, 1:3000), anti-Myog (F5D, obtained from Developmental Studies Hybridoma Bank, 1:250) and caspase 3 cleavage product (Cell Signaling Technology, 1:1000).

Immunofluorescence

Immunofluorescence was performed to detect GFP expression as well as to visualize myotubes using antibodies against MyHC (1:1000) and Myoglobin (1:500). Staining with 4',6-diamidino-2-phenylindole (DAPI) was employed to visualize nuclei.

Fusion Index

The fusion index⁵ indicating the efficiency of C2C12 differentiation was determined by calculating the number of nuclei in each microscopic field in relation to the number of nuclei in myotubes in the same field.

Northern blot analysis and actinomycin D pulse-chase experiments

The extraction of total RNA from C2C12 cells was performed using Trizol reagent (Invitrogen) according to the manufacturer's instructions. Northern blot analysis²³ was performed using probes specific for MyoD, HuR, 18S⁴⁸, and NPM (**Annex 1**, Supplementary Table 2). These probe RNAs were generated using the PCR Purification Kit (GE Healthcare) and radiolabeled with $\alpha^{32}\text{P}$ dCTP using Ready-to-Go DNA labelling beads (GE Healthcare) according to the manufacturer's instructions. The stability of NPM mRNA was assessed by the addition of the transcriptional inhibitor actinomycin D (5 $\mu\text{g/ml}$; Sigma-Aldrich)⁴⁸ for the indicated periods of time.

RT-qPCR

1 µg of total RNA was reverse transcribed using the M-MuLV RT system. A 1/80 dilution of cDNA was used to detect the mRNAs using SsoFast™ EvaGreen® Supermix (Bio-Rad). Expression of *NPM*, *MyoD*, *p21*, *Myog* and *RLuc* was standardized using *GAPDH* as a reference and relative levels of expression were quantified by calculating $2^{-\Delta\Delta CT}$, where $\Delta\Delta CT$ is the difference in CT (cycle number at which the amount of amplified target reaches a fixed threshold) between target and reference.

Genomic DNA extracts and analysis with RT-qPCR

Cell pellets are resuspended in the digestion buffer (100 mM NaCl; 10 mM Tris-HCl, pH 8; 25 mM EDTA, pH 8; 0.5% SDS; 0.1 mg/ml proteinase K) and incubated at 50°C overnight. gDNA is extracted with phenol chloroform (invitrogen) according to the manufacturer's instructions. RT-qPCR experiment was performed as described above starting from 16 pg of extracted gDNA.

Immunoprecipitation

Cell extracts were prepared in the lysis buffer (50mM Tris, pH 8; 0.5% Triton X-100; 150mM NaCl; complete protease inhibitor (Roche)). When indicated, cell extracts were digested for 30 min at 37°C with RNase A (100 µg/ml). Two µl of the anti-KSRP serum (affinity purified rabbit serum¹⁷) was incubated with 50µl of protein A-Sepharose slurry beads (washed and equilibrated in cell lysis buffer) for 1h at 4°C. Beads were washed three times with cell lysis buffer and incubate with 300µg of cell extracts overnight at 4°C. Beads were washed three times with cell lysis buffer and co-immunoprecipitated proteins were analyzed by western blotting. HuR, PARN and EXOSC5 immunoprecipitation were performed^{3,5,54} using antibodies against HuR (3A2), PARN (Cell Signaling, USA), EXOSC5 (Abcam, USA) and IgG (Jackson Immunoresearch Laboratories, USA).

Preparation of mRNA (mRNP) complexes and analysis with RT-PCR

Purified RNA from mRNP complexes^{5,54} was resuspended in 10 µl of water and 4 µl was reverse transcribed using the M-MuLV RT system (NE Biolabs) according to the manufacturer's protocol. Subsequently, 2 µl of cDNA was amplified by PCR or qPCR using NPM specific primers (Supplementary Table 2). When analysed by qPCR, a 1/20 dilution of cDNA was used to detect the mRNAs using SybrGreen (SsoFast™ EvaGreen® Supermix). The mRNA levels associated with these mRNP complexes were then standardized against *RPL32* mRNA levels (used as a reference) and compared to mRNA levels in the IgG control. In experiments transfected with Rluc reporter constructs, the *Rluc* mRNA associated with immunoprecipitated HuR was determined by RT-qPCR, standardized against *RPL32* mRNA levels and then the steady-state levels for each treatment. These standardized Rluc mRNA levels were then compared to *Rluc* mRNA levels in the IgG IP.

cDNA array analysis

Microarray experiments were performed using mouse array, which contain probe sets of characterized and unknown mouse ESTs from 17,000 genes⁵⁵. RNAs from siHuR- and siCtr-treated C2C12 cells extracts were prepared⁵⁶, processed and hybridized on the cDNA arrays. The data were processed using the Array Pro software (Media Cybernetics, Inc.), then normalized by Z-score transformation⁵⁵ and used to calculate differences in signal intensities. Significant values were tested using a two-tailed Z-test and a P of ≤0.01. The data were calculated from two independent experiments.

Fluorescence *in situ* hybridization

The fluorescence *in situ* hybridization experiments were performed⁵⁷ using a DNA fragment of ~500 bp corresponding to the coding region of mouse NPM. The fragment was amplified by PCR using the following primers fused to either a T7 or T3 minimal promoter sequence: NPM forward, 5'-TAA TAC GAC TCA CTA TAG GGA CGG TTG AAG TGT GGT TCA G -3', and NPM reverse, 5'-AAT TAA CCC TCA CTA AAG GAA CTT

GGC TTC CAC TTT GG -3'. The PCR product was used as the template for *in vitro* transcription of the *NPM* probe needed for fluorescence *in situ* hybridization. The antisense (T3) and sense (T7) probes were prepared using digoxigenin-RNA labeling mix (Roche Diagnostics). The RNA probes were quantified, denatured, and incubated with permeabilized cells⁵⁷. After the hybridization, the cells were used for immunofluorescence to detect HuR⁵⁷.

Polysome fractionation

4x10⁷ myoblasts were grown and treated with siRNAs as described above. Briefly, the cytoplasmic extracts obtained from lysed myoblast cells were centrifuged at 130,000 x g for 2 h on a sucrose gradient (10–50% w/v)⁵⁸. RNA was extracted using Trizol LS (Invitrogen), and was then analyzed on an agarose gel. The levels of *NPM* and *GAPDH* mRNAs were determined using RT-qPCR.

RNA electrophoretic mobility shift assays

The *NPM* cRNA probes were produced by *in vitro* transcription⁵⁹. The accession number in the NCBI database of the *NPM* mRNA sequence used to generate these probes is NM_008722. The *NPM* probes 5'UTR, 3'UTR, P1, and P2 were generated by PCR amplification using a forward primer fused to the T7 promoter (**Annex 1. Supplementary Table 2**) as well as pYX-Asc-*NPM* expression vector as the template. For smaller probes (P1-1 to P2-3, P1-1-mut1, P1-1-mut2, P1-1-mut1-2), oligonucleotide sense and anti-sense were directly annealed and used for *in vitro* transcription. The RNA binding assays²³ were performed using 500 ng purified recombinant protein (GST or GST-HuR) incubated with 50 000 cpm of ³²P-labelled cRNAs. Supershift experiments were also performed with 10 µg total C2C12 cell extract (TE) incubated with 50 000 cpm of ³²P-labelled cRNAs. An anti-KSRP antibody was then added to the reaction to supershift the RNP/cRNA complex containing KSRP.

Luciferase activity

The activity of Renilla luciferase was measured using a Renilla luciferase assay system (Promega) with a luminometer following the manufacturer's instructions.

In vitro pull-down experiments

GST pull-down assay⁴ were performed using GST-HuR and recombinant His-KSRP. The interaction of the His-KSRP with the pulled-down GST-HuR was analyzed by western blotting using the GST and KSRP antibodies.

9.1.6. Acknowledgements

We thank Dr C. von Roretz for critical review of this manuscript and insightful discussion. We are grateful to Veronique Sauve and Dr Kalle Gehring for their help with the BIACORE experiments. A.C. is a recipient of the Canderel scholarship for PDFs(2010–2011) as well as the Peter Quinlan Fellowship in Oncology (2011–2012). V.D.-R. Isa Research Fellow of the Terry Fox foundation through an award from the Canadian Cancer Society (former National Cancer Institute of Canada). This work was supported by a CIHR (MOP-89798) operating grant to I.-E.G. M.G. is supported by the NIA-IRP,NIH. R.G. is supported by grants from AIRC (IG 2010–2012) and AICR (No. 10-0527).I.-E.G. is a recipient of a TierII Canada Research Chair.

9.1.7. References Chapter I

1. Tallquist, M. D., Weismann, K. E., Hellstrom, M. & Soriano, P. Early myotome specification regulates PDGFA expression and axial skeleton development. *Development* 127, 5059–5070 (2000).
2. Jun, J. I. & Lau, L. F. The matricellular protein CCN1 induces fibroblast senescence and restricts fibrosis in cutaneous wound healing. *Nat. Cell Biol.* 12, 676–685 (2010).
3. Briata, P. *et al.* p38-dependent phosphorylation of the mRNA decay-promoting factor ksrp controls the stability of select myogenic transcripts. *Mol. Cell* 20, 891–903 (2005).

4. Beauchamp, P. *et al.* The cleavage of HuR interferes with its transportin-2- mediated nuclear import and promotes muscle fiber formation. *Cell Death Differ.* 17, 1588–1599 (2010).
5. van der Giessen, K., Di-Marco, S., Clair, E. & Gallouzi, I. E. RNAi-mediated HuR depletion leads to the inhibition of muscle cell differentiation. *J. Biol. Chem.* 278, 47119–47128 (2003).
6. van der Giessen, K. & Gallouzi, I. E. Involvement of transportin 2-mediated HuR import in muscle cell differentiation. *Mol. Biol. Cell* 18, 2619–2629 (2007).
7. Figueroa, A. *et al.* Role of HuR in skeletal myogenesis through coordinate regulation of muscle differentiation genes. *Mol. Cell. Biol.* 23, 4991–5004 (2003).
8. von Roretz, C., Beauchamp, P., Di Marco, S. & Gallouzi, I. E. HuR and myogenesis: being in the right place at the right time. *Biochim. Biophys. Acta* 1813, 1663–1667 (2011).
9. von Roretz, C. & Gallouzi, I. E. Decoding ARE-mediated decay: is microRNA part of the equation? *J. Cell Biol.* 181, 189–194 (2008).
10. Abdelmohsen, K., Kuwano, Y., Kim, H. H. & Gorospe, M. Posttranscriptional gene regulation by RNA-binding proteins during oxidative stress: implications for cellular senescence. *Biol. Chem.* 389, 243–255 (2008).
11. Lopez de Silanes, I., Zhan, M., Lal, A., Yang, X. & Gorospe, M. Identification of a target RNA motif for RNA-binding protein HuR. *Proc. Natl Acad. Sci. USA* 101, 2987–2992 (2004).
12. Brennan, C. M. & Steitz, J. A. HuR and mRNA stability. *Cell. Mol. Life Sci.* 58, 266–277 (2001).
13. Gallouzi, I. E., Brennan, C. M. & Steitz, J. A. Protein ligands mediate the CRM1-dependent export of HuR in response to heat shock. *RNA* 7, 1348–1361 (2001).
14. Gallouzi, I. E. & Steitz, J. A. Delineation of mRNA export pathways by the use of cell-permeable peptides. *Science* 294, 1895–1901 (2001).
15. Abdelmohsen, K., Srikantan, S., Kuwano, Y. & Gorospe, M. miR-519 reduces cell proliferation by lowering RNA-binding protein HuR levels. *Proc. Natl Acad. Sci. USA* 105, 20297–20302 (2008).

16. Kim, H. H. *et al.* HuR recruits let-7/RISC to repress c-Myc expression. *Genes Dev.* 23, 1743–1748 (2009).
17. Gherzi, R. *et al.* A KH domain RNA binding protein, KSRP, promotes ARE-directed mRNA turnover by recruiting the degradation machinery. *Mol. Cell* 14, 571–583 (2004).
18. Zou, T. *et al.* Polyamine depletion increases cytoplasmic levels of RNA-binding protein HuR leading to stabilization of nucleophosmin and p53 mRNAs. *J. Biol. Chem.* 281, 19387–19394 (2006).
19. Hsu, C. Y. & Yung, B. Y. Over-expression of nucleophosmin/B23 decreases the susceptibility of human leukemia HL-60 cells to retinoic acid-induced differentiation and apoptosis. *Int. J. Cancer* 88, 392–400 (2000).
20. Hsu, C. Y. & Yung, B. Y. Involvement of nucleophosmin/B23 in TPA-induced megakaryocytic differentiation of K562 cells. *Br. J. Cancer* 89, 1320–1326 (2003).
21. Charge, S. B. & Rudnicki, M. A. Cellular and molecular regulation of muscle regeneration. *Physiol. Rev.* 84, 209–238 (2004).
22. Garcia-Martinez, J., Aranda, A. & Perez-Ortin, J. E. Genomic run-on evaluates transcription rates for all yeast genes and identifies gene regulatory mechanisms. *Mol. Cell* 15, 303–313 (2004).
23. Dormoy-Raclet, V. *et al.* The RNA-binding protein HuR promotes cell migration and cell invasion by stabilizing the beta-actin mRNA in a U-rich-element-dependent manner. *Mol. Cell. Biol.* 27, 5365–5380 (2007).
24. Barreau, C., Paillard, L. & Osborne, H. B. AU-rich elements and associated factors: are there unifying principles? *Nucleic Acids Res.* 33, 7138–7150 (2005).
25. Sanduja, S., Kaza, V. & Dixon, D. A. The mRNA decay factor tristetraprolin (TTP) induces senescence in human papillomavirus-transformed cervical cancer cells by targeting E6-AP ubiquitin ligase. *Aging (Albany NY)* 1, 803–817 (2009).
26. Drury, G. L., Di Marco, S., Dormoy-Raclet, V., Desbarats, J. & Gallouzi, I. E. FasL expression in activated T lymphocytes involves HuR-mediated stabilization. *J. Biol. Chem.* 285, 31130–31138 (2010).
27. Long, R. M. & McNally, M. T. mRNA decay: x (XRN1) marks the spot. *Mol. Cell* 11, 1126–1128 (2003).

28. Frehlick, L. J., Eirin-Lopez, J. M. & Ausio, J. New insights into the nucleophosmin/nucleoplasmin family of nuclear chaperones. *Bioessays* 29, 49–59 (2007).
29. Grisendi, S., Mecucci, C., Falini, B. & Pandolfi, P. P. Nucleophosmin and cancer. *Nat. Rev. Cancer* 6, 493–505 (2006).
30. Grisendi, S. *et al.* Role of nucleophosmin in embryonic development and tumorigenesis. *Nature* 437, 147–153 (2005).
31. Gubin, A. N., Njoroge, J. M., Bouffard, G. G. & Miller, J. L. Gene expression in proliferating human erythroid cells. *Genomics* 59, 168–177 (1999).
32. Feuerstein, N. & Randazzo, P. A. In vivo and in vitro phosphorylation studies of numatrin, a cell cycle regulated nuclear protein, in insulin-stimulated NIH 3T3 HIR cells. *Exp. Cell Res.* 194, 289–296 (1991).
33. Dergunova, N. N. *et al.* A major nucleolar protein B23 as a marker of proliferation activity of human peripheral lymphocytes. *Immunol. Lett.* 83, 67–72 (2002).
34. Katsanou, V. *et al.* The RNA-binding protein Elavl1/HuR is essential for placental branching morphogenesis and embryonic development. *Mol. Cell. Biol.* 29, 2762–2776 (2009).
35. Katsanou, V. *et al.* HuR as a negative posttranscriptional modulator in inflammation. *Mol. Cell* 19, 777–789 (2005).
36. Papadaki, O. *et al.* Control of thymic T cell maturation, deletion and egress by the RNA-binding protein HuR. *J. Immunol.* 182, 6779–6788 (2009).
37. Bhattacharyya, S. N., Habermacher, R., Martine, U., Closs, E. I. & Filipowicz, W. Relief of microRNA-mediated translational repression in human cells subjected to stress. *Cell* 125, 1111–1124 (2006).
38. Chang, N. *et al.* HuR uses AUF1 as a cofactor to promote p16INK4 mRNA decay. *Mol. Cell. Biol.* 30, 3875–3886 (2010).
39. Fan, X. C., Myer, V. E. & Steitz, J. A. AU-rich elements target small nuclear RNAs as well as mRNAs for rapid degradation. *Genes Dev.* 11, 2557–2568 (1997).
40. Myer, V. E., Fan, X. C. & Steitz, J. A. Identification of HuR as a protein implicated in AUUUA-mediated mRNA decay. *EMBO J.* 16, 2130–2139 (1997).

41. DeMaria, C. T. & Brewer, G. AUF1 binding affinity to A U-rich element correlates with rapid mRNA degradation. *J. Biol. Chem.* 271, 12179–12184 (1996).
42. Thomas, M., Lieberman, J. & Lal, A. Desperately seeking microRNA targets. *Nat. Struct. Mol. Biol.* 17, 1169–1174 (2011).
43. Parker, R. & Sheth, U. P bodies and the control of mRNA translation and degradation. *Mol. Cell* 25, 635–646 (2007).
44. Gherzi, R. *et al.* The RNA-binding protein KSRP promotes decay of beta-catenin mRNA and is inactivated by PI3K-AKT signaling. *PLoS Biol.* 5, e5 (2006).
45. Masuda, K. *et al.* Global dissociation of HuR-mRNA complexes promotes cell survival after ionizing radiation. *EMBO J.* 30, 1040–1053 (2011).
46. Abdelmohsen, K., Lal, A., Kim, H. H. & Gorospe, M. Posttranscriptional orchestration of an anti-apoptotic program by HuR. *Cell Cycle* 6, 1288–1292 (2007).
47. Lafarga, V. *et al.* p38 Mitogen-activated protein kinase- and HuR-dependent stabilization of p21(Cip1) mRNA mediates the G(1)/S checkpoint. *Mol. Cell. Biol.* 29, 4341–4351 (2009).
48. Di Marco, S. *et al.* NF-(kappa)B-mediated MyoD decay during muscle wasting requires nitric oxide synthase mRNA stabilization, HuR protein, and nitric oxide release. *Mol. Cell. Biol.* 25, 6533–6545 (2005).
49. Lopez de Silanes, I. *et al.* Global analysis of HuR-regulated gene expression in colon cancer systems of reducing complexity. *Gene Expr.* 12, 49–59 (2004).
50. Lopez de Silanes, I., Lal, A. & Gorospe, M. HuR: post-transcriptional paths to malignancy. *RNA Biol.* 2, 11–13 (2005).
51. Mazroui, R. *et al.* Caspase-mediated cleavage of HuR in the cytoplasm contributes to pp32/PHAP-I regulation of apoptosis. *J. Cell Biol.* 180, 113–127 (2008).
52. von Roretz, C. & Gallouzi, I. E. Protein kinase RNA/FADD/caspase-8 pathway mediates the proapoptotic activity of the RNA-binding protein human antigen R (HuR). *J. Biol. Chem.* 285, 16806–16813 (2010).
53. Gallouzi, I. E. *et al.* HuR binding to cytoplasmic mRNA is perturbed by heat shock. *Proc. Natl Acad. Sci. USA* 97, 3073–3078 (2000).

54. Tenenbaum, S. A., Lager, P. J., Carson, C. C. & Keene, J. D. Ribonomics: identifying mRNA subsets in mRNP complexes using antibodies to RNA-binding proteins and genomic arrays. *Methods* 26, 191–198 (2002).
55. Cheadle, C., Vawter, M. P., Freed, W. J. & Becker, K. G. Analysis of microarray data using Z score transformation. *J. Mol. Diagn.* 5, 73–81 (2003).
56. Lopez de Silanes, I. *et al.* Identification and functional outcome of mRNAs associated with RNA-binding protein TIA-1. *Mol. Cell. Biol.* 25, 9520–9531 (2005).
57. Lian, X. J. & Gallouzi, I. E. Oxidative stress increases the number of stress granules in senescent cells and triggers a rapid decrease in p21waf1/cip1 translation. *J. Biol. Chem.* 284, 8877–8887 (2009).
58. Cammas, A. *et al.* Cytoplasmic relocalization of heterogeneous nuclear ribonucleoprotein A1 controls translation initiation of specific mRNAs. *Mol. Biol. Cell* 18, 5048–5059 (2007).
59. Gallouzi, I. E. *et al.* A novel phosphorylation-dependent RNase activity of GAP-SH3 binding protein: a potential link between signal transduction and RNA stability. *Mol. Cell. Biol.* 18, 3956–3965 (1998).

9.2. CHAPTER II: Cooperativity between YB1 and HuR is necessary to regulate Myogenin mRNA stability during muscle fiber formation.

9.2.1. Abstract

The ubiquitously expressed protein HuR plays a key role in the posttranscriptional regulation of gene expression during myogenesis. HuR has been shown to upregulate the expression of pro-myogenic genes while suppressing the expression of anti-myogenic genes. However, the mechanisms and the complete network of trans-acting factors by which HuR manages this differential regulation is still elusive. By performing an immunoprecipitation-coupled to mass spectrometry experiment we identified 41 novel protein partners of HuR in muscle cells and provide evidence that one of these partners, the multifunctional DNA/RNA-binding protein YB1, forms a complex with HuR in an RNA independent manner. We also identify a list of shared mRNA binding targets between HuR and YB1 and demonstrate that the HuR/YB1 complex promotes myogenesis by regulating the expression of the *Myog* mRNA. We show that depletion of YB1, similarly to HuR, destabilizes the *Myog* mRNA, decreases *Myog* protein levels, and inhibits myogenesis. HuR and YB1 stabilizes the *Myog* mRNA by associating with a G/U-rich element (G/URE) in the *Myog* mRNA 3'UTR. This regulatory event requires an intact HuR/YB1 complex, as depletion of either one compromises the binding of the other to the *Myog* mRNA. Taken together, our study delineates a novel mechanism for HuR-mediated posttranscriptional regulation of myogenesis, one that requires its association to YB1, and provides new insights into the central role of posttranscriptional regulatory networks in modulating many vital cellular processes.

9.2.2. Introduction

Mammalian adult skeletal muscle tissue is composed of bundles of fibers derived from the fusion of several mononucleated precursor muscle cells (myoblasts)^{1,2}. The integrity of muscle tissue is vital for an organism to ensure its basic functions, such as locomotor activity, postural behavior, and breathing. Therefore, it is not surprising that myogenesis (the process of muscle formation and regeneration) is tightly regulated and

highly conserved in all mammals^{1,2}. Myogenesis is activated during embryogenesis, leading to the formation of skeletal muscle tissue, as well as in response to injury, to allow the regeneration of damaged muscle fibers^{1,3-9}. The myogenic process involves the sequential activation of a specific set of genes encoding key proteins known as Myogenic Regulatory Factors (MRFs), which activate muscle cell differentiation through induction of a muscle-specific transcriptional program⁹⁻¹¹. These MRFs consist of Myogenic differentiation antigen (MyoD), Myogenin (Myog), Myogenic factor 5 (Myf5), and Myogenic factor 6 (MRF4). It has been shown that high levels of these MRFs must be maintained throughout the differentiation process in order to ensure muscle development and integrity^{1,2,11-13}. While it is well-accepted that transcriptional induction of MRF genes represents a critical regulatory step^{2,11-13}, work from several groups including ours has established that transcription alone is not sufficient to maintain the high expression levels of MRFs during the lifespan of a muscle cell^{1,14-16}.

Over the past two decades, it has become clear that regulation of gene expression at the posttranscriptional level plays a critical role in modulating muscle fiber formation¹⁴⁻¹⁷. This dynamic level of regulation involves many steps in the maturation of mRNA, including splicing, stability of the mRNA transcript, cellular movement, and translation into protein as well as posttranslational modifications of key players in these processes^{1,18-20}. It is well-established that the processing and expression of mRNAs is mediated by the combined interactions of several RNA-binding factors^{1,4,14,16,21,22}, been RNA-binding proteins (RBPs) one of the key posttranscriptional regulatory trans-acting factors that target mRNAs in various cells including muscle^{1,18-20}. We and others have shown that the RBP HuR, a well characterized posttranscriptional regulator, play a key role in promoting myogenesis, by modulating muscle function and integrity^{1,4,14-16,22,23}. Interestingly, the mechanisms by which HuR performs its promyogenic function are unique and sometimes opposing. Indeed, during the initial stages of myogenesis, HuR promotes the translation of the mRNA encoding the alarmin HMGB1 by negating the translational inhibitory effects of the microRNA miR-1192²³. Simultaneously, HuR also destabilizes the mRNA encoding the cell cycle modulator Nucleophosmin (NPM) through its interaction with the decay factor KSRP²². Later, during the pre-terminal stages of the differentiation process, HuR binds to and stabilizes the mRNAs encoding for the cyclin-dependent kinase inhibitor P21

as well as the MRFs MyoD and Myog^{3,15,24,25}. Hence, the mechanisms by which HuR modulates myogenesis are both diverse and complex and, importantly, require its interaction with other RNA-binding factors. However, the characterization of the complete network of RBPs that interact with HuR during myogenesis and, furthermore, how their interplay dictates the expression of pro- and anti-myogenic mRNAs has yet to be fully explored.

In order to gain a more complete understanding of the HuR-network of protein partners during myogenesis we used a combination of protein purification techniques and mass spectroscopy analysis to identify novel HuR protein ligands. We identified the multifunctional DNA/RNA-binding protein YB1^{26,27} as a novel HuR binding partner during myogenesis. We demonstrate that depletion of YB1 resulted in decreased expression of Myog protein which, consequently, prevented the commitment of myoblast cells into the differentiation process. We show that similarly to HuR, YB1 associates to a G/URE in the *Myog* mRNA 3'untranslated region, regulating its stability. Importantly, the function of HuR and YB1 in the regulation of the *Myog* mRNA during myogenesis is dependent on the cooperative interplay between these two proteins. Our findings, therefore, clearly establish the cooperation between HuR and YB1 as a novel regulatory mechanism required for the formation of muscle fibers.

9.2.3. Results

9.2.3.1. YB1 is a novel HuR protein ligand required for muscle fiber formation.

HuR has previously been shown to modulate the expression of pro-myogenic genes by collaborating or competing with other RNA binding factors during the early steps of muscle cell differentiation^{23,2812,293}. To identify novel protein ligands that collaborate with HuR at the pre-terminal stage of myotube formation we immunoprecipitated (IP) HuR from C2C12 cell extracts collected at day 2 of the differentiation process (**Fig. 3.1a**) and performed mass spectrometry analysis of the HuR-bound proteins. We identified 41 putative protein ligands of HuR in these cells (**Annex 2. Supp. Table 1**). Gene Ontology (GO) classification of these proteins based on molecular functions (**Fig. 3.1b**) and cellular

compartments (**Annex 2. Supp. Fig. 1**) revealed that HuR protein ligands are most commonly RNA binding proteins (RBP) localized in ribonucleoprotein complexes. To further understand the relationship between HuR and its putative protein ligands we used geneMANIA²⁹ to generate a protein-protein interaction (PPI) network which includes the RBPs identified above (**Fig. 3.1b right**) as well as additional proteins that are predicted by geneMANIA to mediate the function of these RBPs (**Fig. 3.1c**, and **Annex 2. Supp. Table 2**). The co-localization analysis showed two clusters of proteins, with YB1 (*Ybx1*) and NCL (*Ncl*) as center nodes. Since the molecular function of YB1 resembles that of HuR (*Elavl1*) our data therefore highlights YB1 as a potentially important protein partner of HuR during muscle fiber formation (**Fig. 3.1c**).

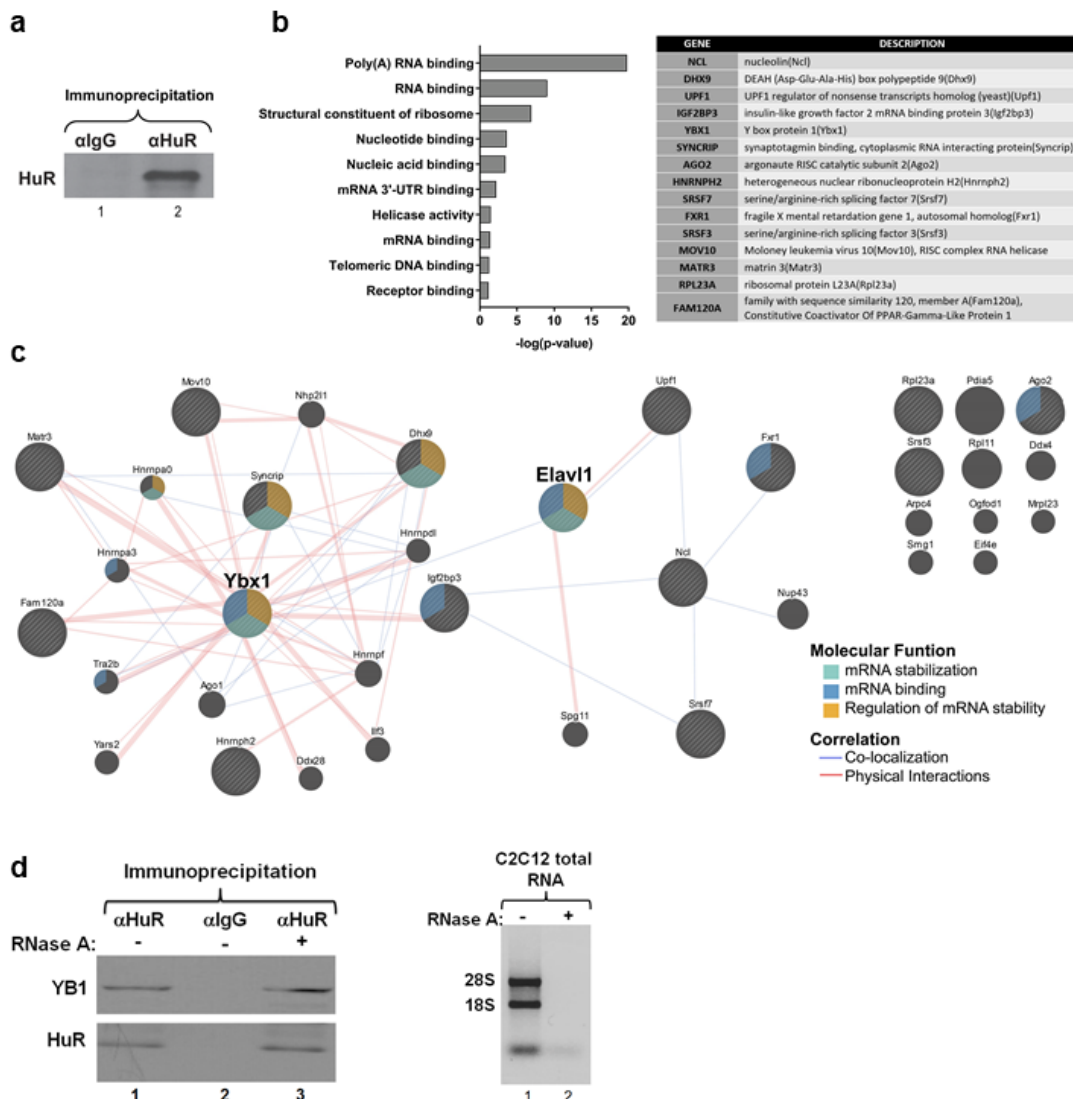
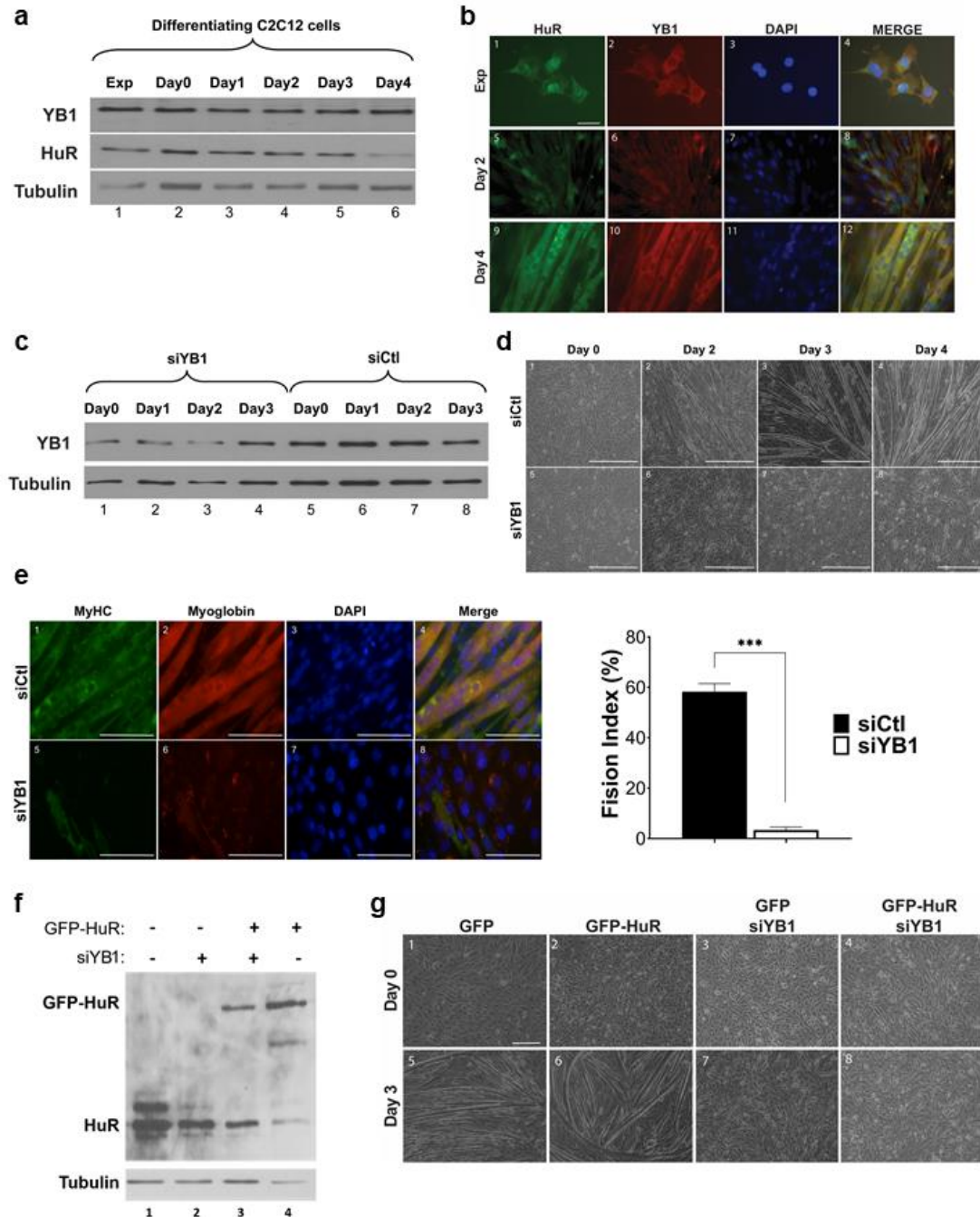


Figure 3.1. Gene ontology (GO) analysis of potential HuR protein partners in muscle cells. Immunoprecipitation experiments were performed on C2C12 cell lysates using a monoclonal HuR antibody (3A2) or IgG as a control. **a)** IP samples were analyzed by western blot using an anti-HuR antibody. **b)** Gene Ontology (GO) analysis was conducted using DAVID v6.8[®] to classify HuR putative protein partners based on molecular functions. **Left;** top 10 GO-terms enriched as analyzed by DAVID v6.8[®]. **Right;** List of RBP identified by GO analysis. **c)** GeneMANIA interaction network of HuR putative protein ligand in muscle. Physical interaction analysis is displayed as pink lines, co-localization analysis as violet lines. Line thickness represents interaction strength. Stripe nodes represent the queried genes and non-stripe nodes represent mediated protein for interactions (predicted by GeneMANIA). Molecular functions are shown by color triangles inside each node. Proteins are identified by their gene name. A total of 36 proteins were analyzed. **d)** Immunoprecipitation (IP) experiments were performed on C2C12 cell lysates treated or not with RNase A using a monoclonal HuR antibody (3A2) or IgG as a control; **Left;** IP samples were analyzed by western blot using anti-YB1 or -HuR antibodies. **Right;** Agarose gel demonstrating the efficiency of RNA degradation in cell extracts digested for 30 min at 37°C with RNase A (100 µg/ml).

It has been suggested that the pleiotropic functions of YB1 are the result of its ability to form distinct complexes with different protein partners, allowing it to carry out specific functions in a variety of regulatory events³⁰⁻³². To investigate the role of YB1 in the HuR-mediated regulation of myogenesis we first validated our mass spectrometry results. We performed IP experiments on C2C12 cell extracts collected at day 2 of the differentiation process, treated with or without 100 µg/ml RNase A, using anti-YB1 and anti-HuR antibodies. Our results demonstrated that YB1 and HuR associate during muscle differentiation and that their association occurs in an RNA-independent manner in muscle cells (**Fig. 3.1d**). Since the association of YB1 and HuR occurs during the pre-terminal stage of muscle fiber formation, we assessed whether this interaction resulted from an increased expression of YB1 protein during muscle fiber formation. Western blot experiments using total cell extracts from differentiating myoblasts demonstrated that neither HuR nor YB1 expression is altered during the myoblast to myotube transition (**Fig. 3.2a**). It is well established that HuR cytoplasmic accumulation during muscle cell differentiation directly correlates with its function in regulating the expression of its pro-myogenic targets^{3,2}. The fact that, similarly to HuR, YB1 is known to shuttle between the nucleus and the cytoplasm^{27,33,34} raises the possibility of a direct relation between YB1 localization in muscle cells and its association to HuR. To investigate this possibility, we

visualized the cellular localization of HuR and YB1 during muscle fiber formation. Contrary to HuR, which is localized in the nucleus in myoblasts and translocate to the cytoplasm during differentiation (**Fig. 3.2b panel 1, 5, 9**), our immunofluorescence experiments revealed that YB1 is primary found in the cytoplasm of myoblasts and that there is no change in its localization during myogenesis (**Fig. 3.2b panel 2, 6, 10**). Our data therefore indicate that HuR and YB1 interact with each other during the pre-terminal stage when HuR and YB1 are both localized to the cytoplasm of myotubes.

We next assessed whether YB1, similarly to HuR, plays an important role in regulating the myogenic process. To address this question, we first knocked down YB1 in myoblasts using an siRNA that specifically targets the *Ybx1* gene (siYB1) (**Fig. 3.2c**). We demonstrated that knocking down YB1 in C2C12 cells significantly reduced the efficiency of muscle cell differentiation as determined by visualizing the morphology of C2C12 cells by phase contrast (**Fig. 3.2d**) and the expression of two known markers of muscle fiber formation, myoglobin and myosin heavy chain (MyHC), by immunofluorescence (IF) (**Fig. 3.2e**). Interestingly, overexpression of HuR in C2C12 cells (**Fig. 3.2g**), which on its own enhances muscle fiber formation^{28,35}, was not sufficient to rescue the myogenic capacity of siYB1 treated cells (**Fig. 3.2f**). These observations, therefore, demonstrate that HuR collaborates with YB1 to promote muscle fiber formation and suggest that their interaction affects the outcome of their regulatory actions on pro-myogenic targets.



over the different days of C2C12 muscle cell differentiation. Blots were probed with antibodies against YB1 and α -tubulin (loading control). **d)** Phase contrast pictures showing the differentiation status of these cells from day 0 to day 4 of the differentiation process. Bars 500 μ m. Images of a single representative field are shown **e)** Myogenic capacity was assessed on C2C12 cells depleted (siYB1) or not (siCtl) of YB1 **Left**; IF pictures showing the differentiation status of siCtl and siYB1 treated cells at day 3 of the myogenic process using an anti-MyHC and anti-Myoglobin antibodies and stained with DAPI. Images of a single representative field are shown. Bars 100 μ m. **Right**, Fusion index indicating the efficiency of C2C12 differentiation. Data are presented +/- the s.e.m. of three independent experiments *** $P < 0.0005$ (t test). **f-g)** C2C12 cells expressing GFP or GFP-HuR were depleted (siYB1) or not (siCtl) of YB1 and induced for differentiation for 3 days. **f)** Cell extracts from these cells were used for western blot analysis with antibodies against HuR, Myog or α -tubulin (loading control). **g)** Phase contrast pictures showing the differentiation status of these cells from Day 0 to Day 3. Bars 500 μ m. Images of a single representative field are shown.

9.2.3.2. HuR and YB1 bind to Myog mRNA during muscle fiber formation.

In order to investigate if HuR and YB1 cooperate together during myogenesis to affect the expression of common pro-myogenic mRNA targets, we performed RNA immunoprecipitation (RIP) experiments (using anti-HuR and anti-YB1 antibodies) coupled to RNA sequencing analysis (RIP-seq) on C2C12 cell extracts collected at day 2 of differentiation. We determined that in these cells HuR and YB1 associate with 1513 and 1103 mRNA transcripts, respectively. Comparison of both RIP-seq datasets identify 409 common mRNA targets for HuR and YB1 (**Fig. 3.3a-b, Annex 2, Supp. Table 3**). GO enrichment analysis based on biological processes revealed that of the 409 common targets, 4 of these, *Myog*, *MyoD*, *Gata4* and *Myc*, encoded for proteins involved in skeletal muscle cell differentiation (**Fig. 3.3c**).

Given that our RIP-Seq experiments demonstrated that HuR and YB1 bound most strongly to the *Myog* mRNA we decided, as a proof-of-principle, to investigate if HuR collaborates with YB1 to post transcriptionally regulate the *Myog* mRNA during muscle fiber formation. We began by performing RNA-IP experiments coupled with RT-qPCR to validate the binding of YB1 and HuR to the *Myog* mRNA. We showed that both HuR and YB1 strongly associate to *Myog* mRNA during the pre-terminal stage of muscle fiber formation (**Fig. 3.3d-e, Annex 2, Supp. Fig. 2**) when an elevated level of Myog is necessary to promote the fusion of myoblasts into myotubes¹¹. We then assessed whether YB1 and HuR associate, in a cooperative manner, to the *Myog* mRNA. We

demonstrated that although the knockdown of HuR did not alter the cellular localization of YB1 in myotubes, it did inhibit, by more than 45%, YB1's association to the *Myog* mRNA (Fig. 3.3f and Annex 2. Supp. Fig. 3). Likewise, the association of HuR to *Myog* mRNA also decreased by more than 60% due to the depletion of YB1, without affecting the cellular localization of HuR. (Fig. 3.3g and Annex 2. Supp. Fig. 3) Together these results suggest that one way by which HuR promotes myogenesis is by collaborating with YB1 to modulate *Myog* expression.

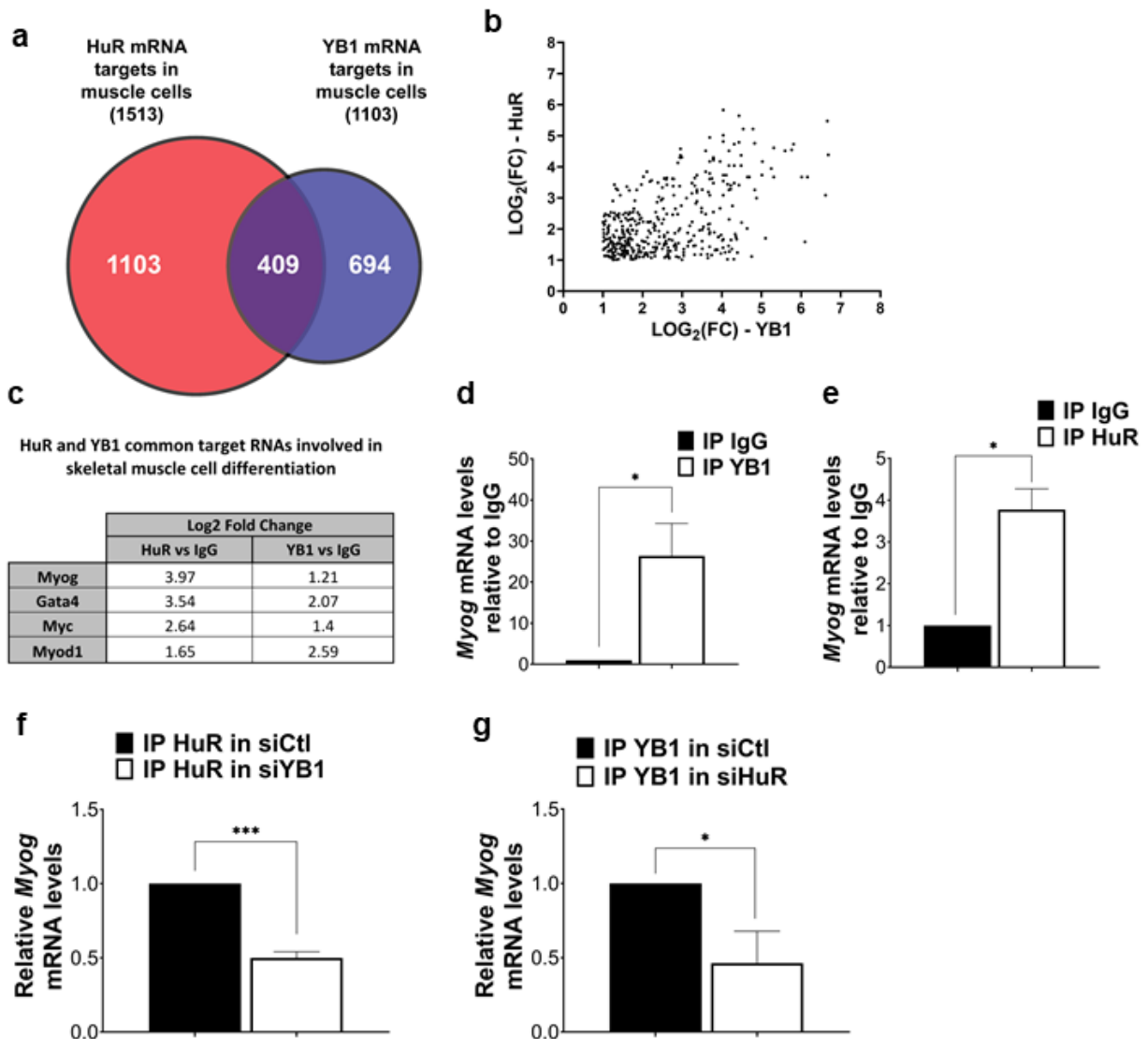


Figure 3.3. YB1 and HuR have common mRNA targets in muscle cells. YB1 and HuR mRNA targets in C2C12 cells were identified by performing RIP-seq experiments using anti-HuR and anti-YB1 antibodies. **a)** Venn diagram of significantly enriched common HuR and

YB1 mRNA targets identified by RIP-seq **b)** Scatterplot comparing the log₂ fold enrichments of common mRNA targets of YB1 and HuR in muscle cells. **c)** Gene Ontology (GO) analysis was conducted using DAVID v6.8[®] to classify common mRNA targets of YB1 and HuR based on Biological Processes. **Left;** top 10 GO-terms enriched as analyzed by DAVID v6.8[®]. **Right;** Comparison of log₂ fold change values of mRNA transcripts involved in skeletal muscle cell differentiation as identify by DAVID v6.8[®]. **d-e)** Validation of *Myog* mRNA association to **d)** YB1 and **e)** HuR. RNA was isolated from the IP of YB1 and HuR (IgG was used as a negative control) and RT-qPCR was performed using primers specific for *Myog* and *GAPDH* mRNAs. *Myog* mRNA levels were standardized against *GAPDH* mRNA levels. The normalized *Myog* mRNA levels were then plotted relatively to the IgG IP condition +/- s.e.m. of 4 independent experiments. **P*<0.05 (t test). **f-g)** IP experiments were performed using YB1 **(f)** or HuR **(g)** antibodies on cell lysates from C2C12 cells treated with siHuR **(f)** or siYB1 **(g)**. RNA was isolated from the IP, and RT-qPCR analysis was performed using specific primers for *Myog* mRNA. For each IP sample, relative *Myog* mRNA levels were normalized to the corresponding IP IgG and to the corresponding total mRNA input sample. The relative *Myog* mRNA level from siHuR or siYB1 conditions were then plotted relative to the siCtl condition. Data are presented +/- the s.e.m. of 4 independent experiments **P*<0.05. ****P*<0.0005 (t test).

9.2.3.3. YB1 stabilizes *Myog* mRNA via a G/U-rich element in the 3'-UTR.

Next, we determined how YB1 regulates *Myog* expression during myogenesis. Total RNA was isolated from C2C12 cells depleted of endogenous YB1 and *Myog* steady-state level was determined by RT-qPCR. We observed that the knockdown of YB1 significantly decreased *Myog* protein levels (**Fig. 3.4a**). *Myog* mRNA levels were also considerably reduced (>3-fold) in the absence on YB1 (**Fig. 3.4b**). The decrease in mRNA levels were similar to those observed when HuR was knocked down in the cells (**Fig. 3.4b**). Since the knockdown of YB1 decreases *Myog* mRNA levels, we sought to determine if this effect occurred because of a reduction in the transcription of *Myog* or due to the destabilization of its mRNA. Towards this end, we performed a nuclear run-on assay on C2C12 cells depleted of endogenous YB1. We did not observe any change in the transcription rate of *Myog* in the absence of YB1 (**Fig. 3.4c**). Next, to determine if the loss of *Myog* mRNA was due to destabilization of the transcript, we performed a pulse-chase experiment using the RNA polymerase II inhibitor actinomycin D (ActD) and found that depleting either HuR or YB1 in C2C12 cells significantly decreased the half-life of the *Myog* mRNA (**Fig. 3.4d**). Furthermore, the knockdown of YB1 decreased the level of *Myog* mRNA by more than 2-fold in the presence or absence of GFP-HuR (**Fig. 3.4e**). Likewise, *Myog* protein levels on siYB1 treated cells were not restore to normal levels upon overexpression of the GFP-HuR protein (**Fig. 3.4f**). Based on this result, we

conclude that in C2C12 cells, YB1 and HuR collaborate to promote the stabilization of *Myog* mRNA which is necessary to ensure the formation of muscle fibers.

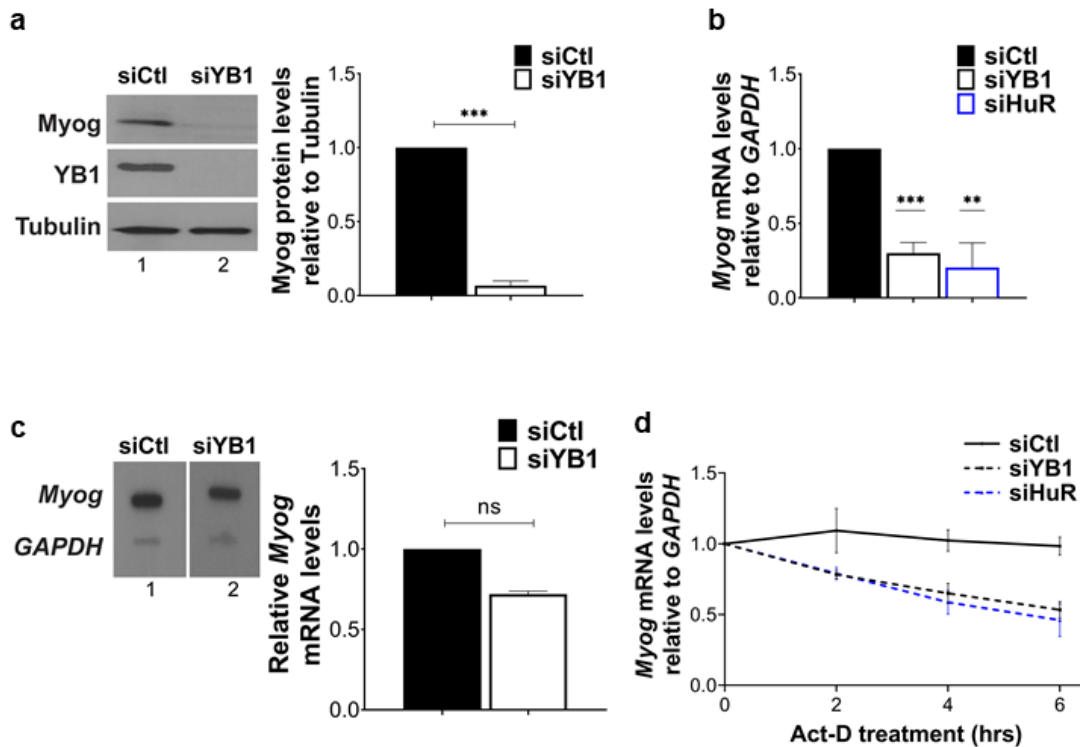


Figure 3.4. YB1 regulates the stability of *Myog* mRNA. **a-b)** Exponentially growing C2C12 depleted (siYB1) or not (siCtl) of YB1 were used to assess *Myog* mRNA and protein levels. **a)** WB demonstrating the efficiency of YB1 knockdown and *Myog* protein levels on C2C12 extracts collected at day 2 of the differentiation process. Blots were probed with antibodies against *Myog*, YB1 and α -tubulin (loading control). **b)** *Myog* mRNA levels were assessed by RT-qPCR using specific primers for *Myog* and *GAPDH* mRNAs. *Myog* mRNA levels were standardized against *GAPDH* mRNA levels. The normalized *Myog* mRNA levels were plotted relatively to the siCtl condition. **c)** C2C12 cells depleted (siYB1) or not (siCtl) of YB1 were collected at 100% confluency and used for nuclear run-on analysis. **Right;** the band intensities of *Myog* and *GAPDH* mRNAs were determined using ImageJ Software. **Left;** The *Myog* mRNA levels were normalized over *GAPDH*. +/- s.e.m. of 2 independent experiments. **d)** The stability of the *Myog* mRNA in C2C12 cells depleted (siYB1) or not (siCtl) of YB1 and HuR (siHuR) was determined by ActD pulse-chase experiments. Cells were treated with Actinomycin D (ActD) for 0, 2, 4 or 6h and total RNA used for RT-qPCR analysis. The expression level of the *Myog* mRNA in each time point was determined relative to *GAPDH* mRNA levels and plotted relative to the abundance of each message at 0 hrs. of ActD treatment, which is considered as 1. Data is presented +/- the s.e.m. of 3 independent experiments.

It is well established that both YB1 and HuR modulate the expression of target mRNAs by directly interacting with sequence motifs located in the 3'UTRs of their target

messages³⁶⁻³⁸. Previous experiments from our laboratory demonstrated that HuR binds to a GU-rich element (G/URE) in the 3'UTR of *Myog* mRNA²⁴. Sequence analysis of the *Myog* mRNA showed that, in addition to the previously characterized HuR binding site (G/URE-2), two additional putative binding sites for HuR and/or YB1 (G/UREs 1 and 3) were present in the 3'UTR (**Fig. 3.5a, Annex 2. Supp. Fig. 3**). To determine whether YB1 and/or HuR associated to these regions, we performed RNA electromobility shift assays (REMSAs) using recombinant GST, GST-HuR or GST-YB1 proteins and radiolabeled RNA probes corresponding to the three G/UREs found on the 3'UTR of the *Myog* mRNA. We observed that while GST-HuR forms a complex with the three regions, GST-YB1 associated only to G/URE-2 (**Fig. 3.5b**). Together these results show that HuR and YB1 directly associate to the G/URE-2 binding sites in the *Myog* mRNA 3'UTR.

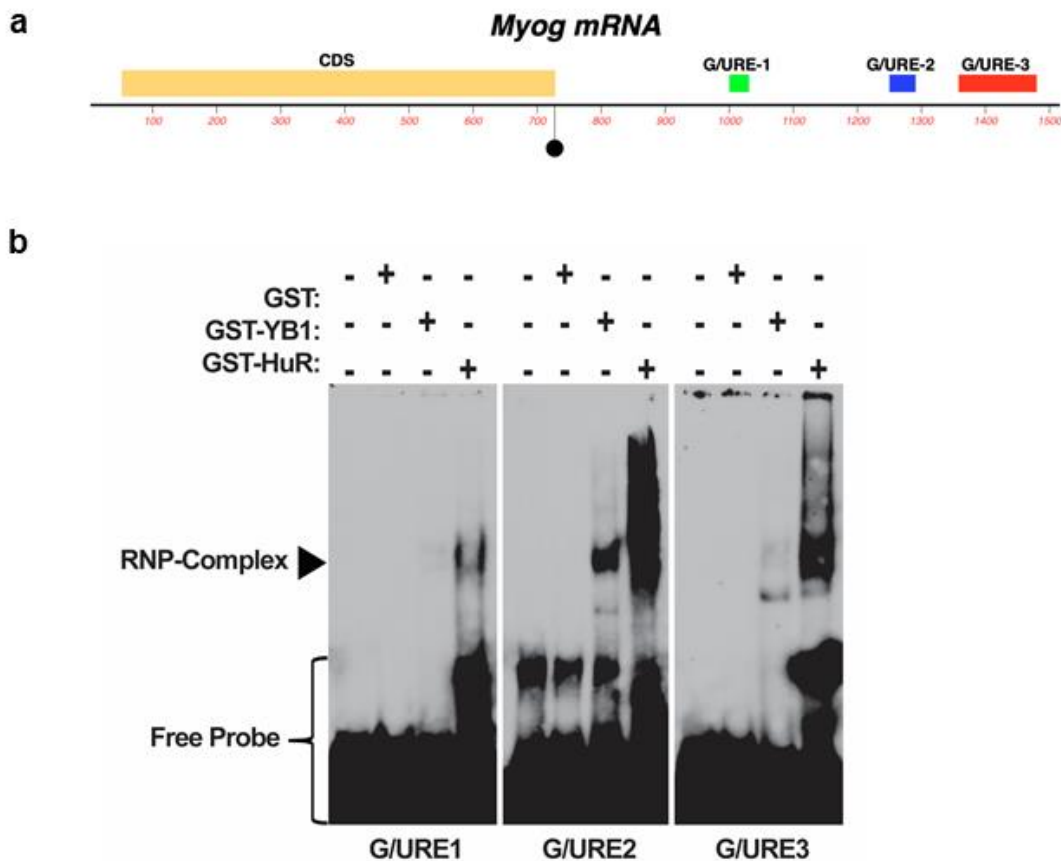


Figure 3.5. YB1 and HuR bind to a G/U rich element in the *Myog* mRNA 3'UTR. a) Schematic representation of the *Myog* mRNA sequence. *Myog* coding sequence is highlighted in yellow (Nucleotide 53-727). The initial nucleotide of the 3'UTR (nucleotide 728) is marked with a black circle. G/UREs present in the *Myog* 3'UTR are colored boxed; G/URE 1 is highlighted in green (nucleotide 1001-1030), G/URE 2 is highlighted in blue (nucleotide 1251-

1290), and G/URE 3 is highlighted in red (nucleotide 1359-1479). **b)** G/URE 1, 2 and 3 were used to generate radiolabeled RNA probes for RNA electromobility shift assays (REMSA). Assays were performed by incubating purified GST, GST-YB1 or GST-HuR protein with the radiolabeled cRNA probes. Blots are representative of 2 independent experiments.

Next we investigated the role of these binding sites on the HuR/YB1 mediated stabilization of the *Myog* mRNA in muscle cells. We generated Renilla luciferase (Rluc) reporter constructs expressing either wild-type (pRL-*Myog*-3'UTR), or a mutant *Myog* mRNA 3'UTR in which G/URE 1 (pRL-*Myog*-3'UTR-mut1), G/URE 2 (pRL-*Myog*-3'UTR-mut2) or G/URE 3 (pRL-*Myog*-3'UTR-mut3) were deleted (**Fig. 3.6a**). C2C12 cells were transfected with these Rluc-reporters and the steady-state level of the *Rluc* mRNA determined by RT-qPCR analysis. We observed that the level of pRL-*Myog*-3'UTR-mut2 mRNA, unlike the pRL-*Myog*-3'UTR-mut1 and pRL-*Myog*-3'UTR-mut3 mRNAs, were 2-fold less than those observed with the wild-type pRL-*Myog*-3'UTR (**Fig 3.6b**).

Luciferase activity assay (which is proportional to Rluc protein levels) showed that, similarly to the mRNA levels, the luciferase activity of the pRL-*Myog*-3'UTR-mut2 reporter (but not the other 2 mutants) was significantly suppressed when compared to the wild-type pRL-*Myog*-3'UTR (**Fig. 3.6c**). RIP coupled to RT-qPCR experiments demonstrated that both HuR and YB1 bind to the *Myog* mRNA 3'UTR by associating with the G/URE-2 element. Indeed, the association of YB1 and HuR to the pRL-*Myog*-3'UTR-mut2 mRNA, but not the other constructs, was significantly decreased by more than 2 folds due to the deletion of the G/URE 2 element (**Fig. 3.6d-e**). We then assessed the functional relevance of these YB1/HuR binding sites on the stability of the *Myog* mRNA by performing ActD pulse-chase experiments on C2C12 cells expressing the various Rluc-reporters described above (**Fig. 3.6a**). We observed that only the half-life of the pRL-*Myog*-3'UTR-mut2 mRNA was significantly reduced, while similarly to the wild-type pRL-*Myog*-3'UTR, that of pRL-*Myog*-3'UTR-mut1, and pRL-*Myog*-3'UTR-mut3 remained stable (**Fig. 3.6f**). These results clearly demonstrate that the YB1/HuR mediated stability of the *Myog* mRNA is due to their cooperative binding to the G/URE 2 element in the *Myog* mRNA 3'UTR.

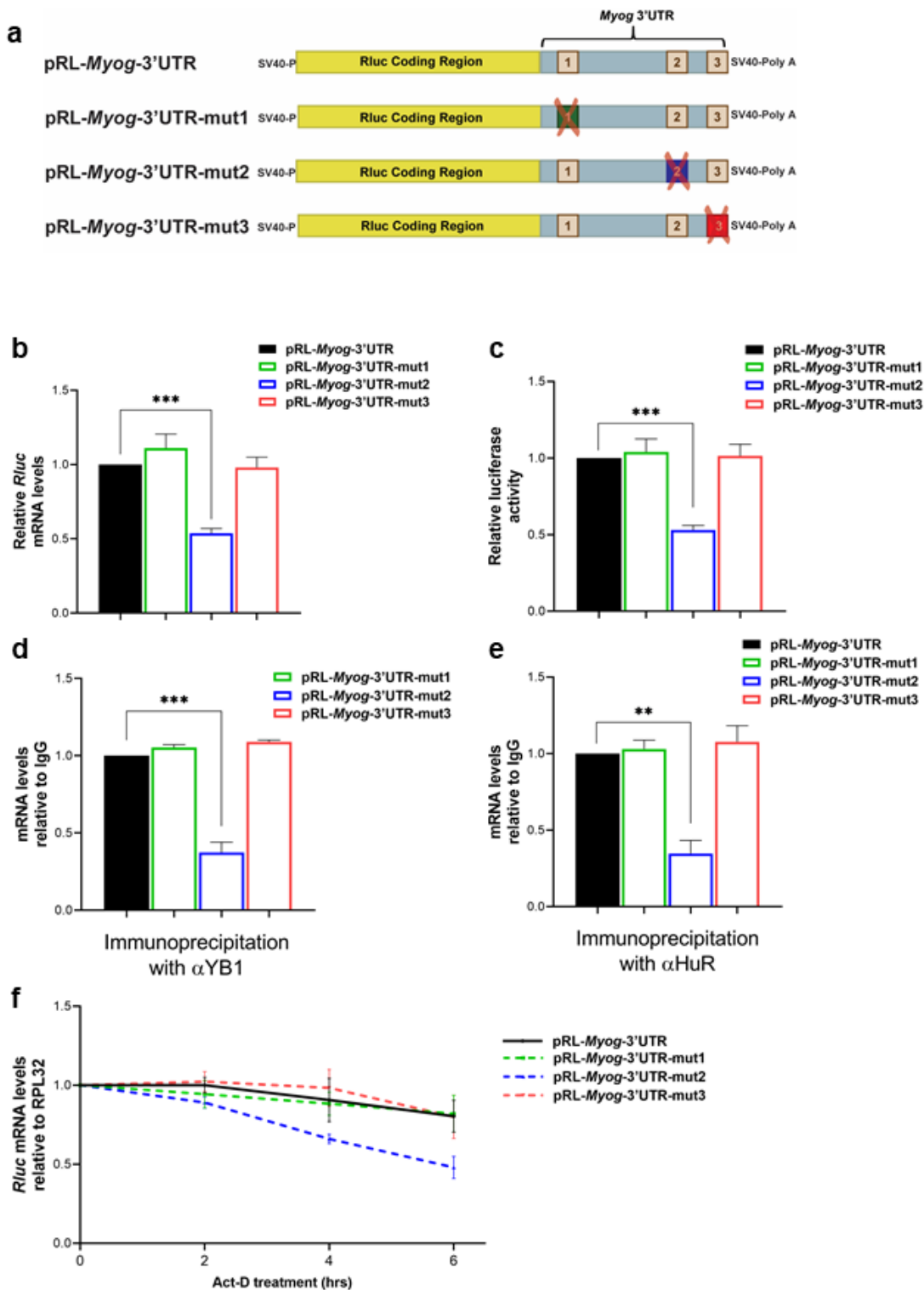


Figure 3.6. G/URE 2 is required for the YB1/HuR mediated stabilization of the *Myog* mRNA. **a)** Schematic representation of the Rluc reporter constructs containing the *Myog* mRNA 3'UTR with or without deletion of the G/URE 1, 2 or 3 (indicated by colored blocks). **b)** Exponentially growing C2C12 cells were transfected with the reporter constructs described in

a. Total RNA was isolated from these cells and the expression levels of Rluc mRNA determined by RT-qPCR. Expression levels of the Rluc reporters was standardized against *RPL32* mRNA level and plotted relative to the expression of the pRL-*Myog*-3'UTR reporter. **c)** Total cell extracts from C2C12 cells expressing the Rluc reporters were used to determine Luciferase activity. **d-e)** Lysates from cells expressing our Rluc reporters were used for RIP-coupled to RT-qPCR experiments using the anti-YB1, anti-HuR antibody (3A2). The amount of *Rluc* mRNA associated to **d)** YB1 or **e)** HuR was determined by RT-qPCR. **f)** The stability of the Rluc RNA reporters was determined by ActD pulse-chase experiments. Cells were treated with Actinomycin D (ActD) for 0, 2, 4 or 6h and total RNA used for RT-qPCR analysis. The expression level of the *Rluc* mRNA in each time point was determined relative to *RPL32* mRNA levels and plotted relative to the abundance of each message at 0 hrs. of ActD treatment, which is considered as 1. Data is presented +/- the s.e.m. of 3 independent experiments. ** $P < 0.005$; *** $P < 0.0005$. (*T*-test).

Additionally, we generated GFP-conjugated Myog plasmids expressing full-length (GFP-Myog) or mutated isoforms of the Myog protein in which G/URE1, 2 and 3 were deleted (GFP-Myog-mut1, GFP-Myog-mut2, GFP-Myog-mut3) (**Fig. 7A**). These Myog isoforms were then expressed in C2C12 cells and GFP-Myog protein levels assessed by WB and IF. We showed, by performing these experiments, that only the deletion of the G/URE 2 element decreased, by more than 2 folds, GFP-Myog protein levels (**Fig. 7B, C**). Taken together our data indicate that a HuR/YB1 complex regulates the stability of *Myog* mRNA during the pre-terminal stage of myogenesis by binding, in a cooperative manner, to a G/URE in the 3'UTR. In doing so our findings describe, for the first time, the importance of this complex in regulating the expression of Myog, consequently, promoting muscle cell differentiation.

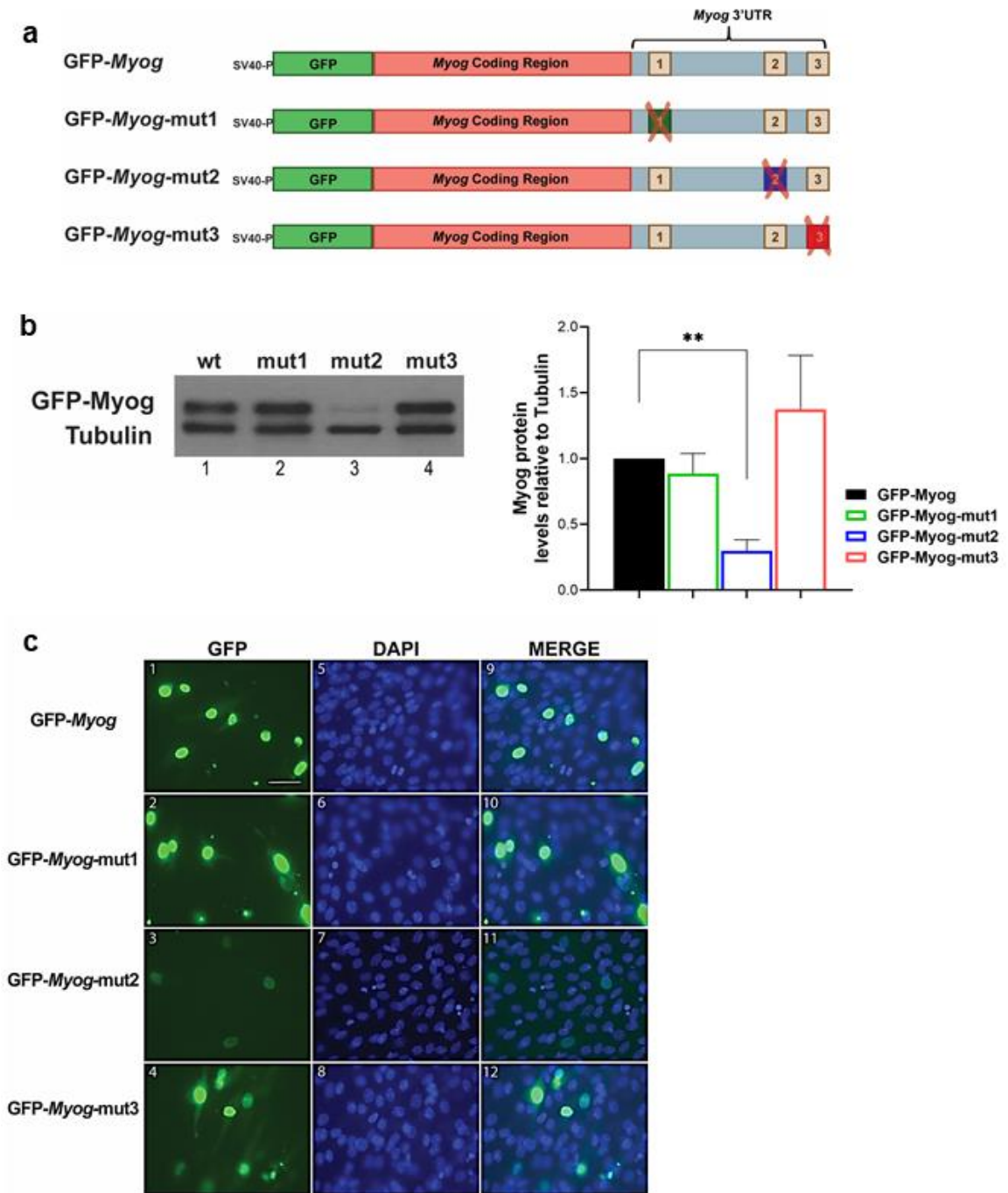


Figure 3.7. G/URE 2 is required for the YB1/HuR mediated regulation of Myog expression. **a)** Schematic representation of the GFP constructs containing the full length *Myog* mRNA with or without deletion of the G/URE 1, 2 or 3 (indicated by colored blocks). **b)** Exponentially growing C2C12 cells were transfected with the reporter constructs described in a. Lysates from these cells were then analyzed by WB using antibodies against GFP and α -tubulin (loading control) to assess GFP-Myog protein levels. **c)** IF demonstrating GFP levels in cells transfected as described in a. Cells were fixed, stained with DAPI and used for fluorescent Imaging. Images of a single representative field are shown. Bars 100 μ m.

9.2.4. Discussion

HuR-mediated regulation of myogenesis was one of the first examples of a link between a posttranscriptional regulator and muscle fiber formation^{15,24}. Previous work from our lab demonstrated that HuR associates with elements in the mRNAs of several classic (*MyoD*, *Myog*, *p21*)^{24,35,39} and newly identified modulators of myogenesis (*HMGB1*, *NPM*)^{23,28}. First described as a positive regulator of mRNA stability, we now know that HuR can have multiple and sometime opposite functions on its targeted transcripts, switching from a promoter of translation^{23,40,41} to a mRNA stabilizer^{24,37,42,43}, to a promoter of mRNA decay^{21,28}. Numerous reports have indicated that the versatility of HuR is mediated by collaboration or competition with other trans-acting factors^{15,28,35}. Thus, identifying the HuR network of trans-acting factors is paramount to our understanding of its regulatory functions in physiological processes such as myogenesis. Herein, we have identified a novel protein-protein interaction network for HuR during myogenesis. Using the *Myog* mRNA as a model to investigate the HuR interaction with YB1 in muscle cells, we validated a novel posttranscriptional mechanism by which HuR regulates its pro-myogenic targets. Together our data supports a model whereby, during the transition step from myoblast to myotubes, the stabilization activity of HuR on the *Myog* mRNA requires its direct association with the RBP YB1. Once formed, the HuR/YB1 complex is recruited to G/URE 2 in the 3'-UTR of *Myog* mRNA leading to its stabilization and the increased expression of *Myog*, resulting in the concomitant formation and maintenance of muscle fibers (**Fig. 3.8**).

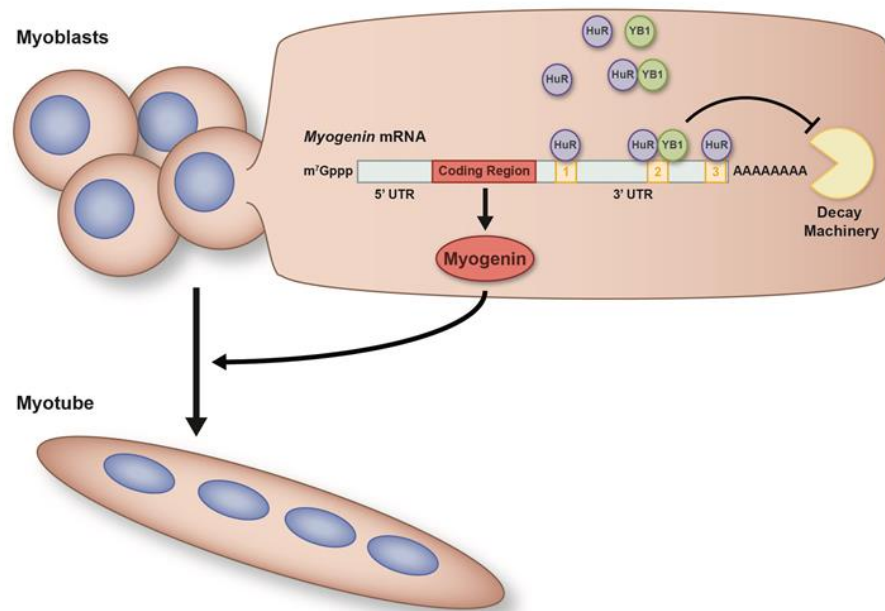


Figure 3.8. Model depicting the molecular mechanism through which the HuR/YB1 complex regulate *Myog* mRNA stability to promote muscle fiber formation.

The observation that depletion of either HuR or YB1 caused a reduced association of the other with *Myog* mRNA (**Fig. 3.3f-g**) indicates that the two proteins must first bind to each other before they can be efficiently recruited to the *Myog* transcript. This provides a potential mechanism behind our previous observation that HuR must translocate to the cytoplasm during myogenesis in order to associate to the *Myog* mRNA²⁴. Since YB1 is found primarily in the cytoplasm (**Fig. 3.2b**), the translocation of HuR, from the nucleus to the cytoplasm, is necessary to allow for their interaction and subsequent stabilization of the *Myog* mRNA. Adding to this, the observation that YB1 and HuR share a common set of target transcripts (**Fig. 3.3a**) representing about ~2% of the transcriptome⁴⁸⁻⁵⁰, suggests that the effect of the HuR/YB1 complex in muscle fiber formation is the result, of not only the stabilization of *Myog*, but of the concerted regulation of a common set of genes.

In our study we characterized the HuR network of protein partners in C2C12 muscle cells during the pre-terminal stage of myogenesis. We identified 41 protein binding partners of HuR in differentiated muscle cells (**Annex 2. Supp. Table 1**). Our analysis showed that HuR had the greatest affinity for proteins with RNA/DNA binding activity (**Fig.**

3.1b). Given the importance of HuR in the regulation of RNA metabolism, it is not surprising that its interacting protein partners share similar functions and binding activity. The fact that ~15% of proteins identified in our study localized within ribonucleoprotein complexes (**Fig. 3.1b, c and Annex 2.** Supp. Fig. 1) provides further evidence that many physiological processes, such as myogenesis, are regulated by an interplay between RBPs rather than by the individualities of single regulators.

HuR has been shown to modulate the turnover and the translation of mRNA encoding pro- and anti-myogenic factors. During the early stages of myogenesis promotes the expression of the alarmin HMGB1 by preventing miR-1192-mediated translation inhibition of its mRNA²³. At the same time, HuR also collaborates with the mRNA decay factor KSRP to reduce the expression of the Nucleophosmin (NPM) protein by destabilizing its mRNA²². Here we show that another important function of HuR in the myogenic process is stabilizing the *Myog* mRNA through a collaboration with the RBP YB1. Our results further support the growing evidence that the functional diversity of HuR-mediated regulation relies in the diversification of its trans-acting partners^{15,28,35} allowing a fine tuning of the transcriptional program during myogenesis. To understand the mechanisms behind this interplay, future studies will be needed to map not just the interactions between HuR and its trans-acting factors, but also the proximity of their binding sites on target messages. Adding to this complexity, post-translational modifications may also be involved in the functional switches of HuR during myogenesis. For example, recently, both HuR and YB1 have been shown to be polyADP-ribosylated (PARylated)^{51,52}. PARylation has been shown to promote the recruitment of protein partners to PARylated proteins⁵³⁻⁵⁵. Thus, of interest would be to investigate whether PARylation is activated during muscle fiber formation and whether it plays a role in the formation of the HuR/YB1 complex.

Together our study suggest that the complexity of post-transcriptional regulation may rival that of transcriptional regulation in several, if not all, physiological processes and shows that establishing the network of RBPs that interact with HuR as well as the mechanism through which these HuR-mediated complexes mediate posttranscriptional events during myogenesis may open a venue for the development of novel therapeutics, targeting HuR specificity for its protein ligands to prevent muscle related pathologies.

9.2.5. Material and Methods

Plasmid construction

To generate the GST-YB1 plasmid, mouse YB1 coding sequence was amplified by PCR and cloned into the pGEX-6P-1 plasmid (GE Healthcare). GFP-HuR was prepared by PCR using the GST-HuR²⁶ plasmid as a template. The PCR fragments were then cloned into the pAcGFP1-C1 vector (BD Biosciences). GFP-Myog was prepared by PCR amplification of the mouse *Myog* coding sequence which was then cloned into the pGEX-6P-1 plasmid (GE Healthcare)²⁴. To generate the pRL-*Myog*-3'UTR plasmid, the full-length 3'-UTR of mouse *Myog* was amplified by PCR and cloned into the pRL-SV40 plasmid (Promega). pRL-*Myog*-3'UTR or GFP-Myog mutants containing a deleted G/URE 1, G/URE 2, or G/URE 3 region respectively were generated by Norclone Biotech Laboratories, Kingstone, ON, Canada. Full sequence details in **Annex 2**. Supp. Table 4.

Cell culture and transfection

C2C12 cells (ATCC, Manassas, VA, USA) were grown and maintained in Dulbecco's modified eagle medium (DMEM, Invitrogen) containing 20% fetal bovine serum (Invitrogen), and 1% penicillin/streptomycin antibiotics, following the manufacturer's instructions (Invitrogen). Differentiation was induced when the cells reached 100% confluency on plates previously coated with 0.1% gelatin (Day 0). To induce differentiation, growth media was replaced with differentiation media containing DMEM, 2% horse serum, and 1% penicillin/streptomycin antibiotics. The transfection of siRNA into C2C12 cells was performed as previously described²⁴. Briefly, the transfection with siYB1, siHuR, or siCtl was performed when cells were 20-30% confluent. The transfection treatment was repeated 24 h later when cells were 50-60% confluent. 6-8 h after the second transfection, two wells (with the same siRNA treatment) were combined into one by trypsinizing the cells from one well and transferring them to the corresponding wells on the second plate. All siRNAs duplexes were used at a final concentration of 60nM. For DNA plasmid transfections, C2C12 cells at 60-70% confluency, were transfected in six-well plates with 1.5 µg of plasmid DNA. *jetPRIME*® (Polyplus)

transfection reagent was used, for all transfections following the manufacturer's instructions.

siRNA

siRNA oligonucleotides against YB1 (5'- CGA AAG GUU UUG GGA ACA GU-3'), was obtained from Ambion-Life Technologies. siHuR (5'-AAG CCU GUU CAG CAG CAU UGG-3')²⁴, and siCtl (5'- AAG CCA AUU CAU CAG CAA UGG-3')²⁴, were obtained from Dharmacon.

Preparation of cell extracts and immunoblotting

Cell extracts were prepared by incubating undifferentiated or differentiated C2C12 cells on ice for 15 min with lysis buffer (50 mM HEPES pH 7.0, 150 mM NaCl, 10% glycerol, 1% Triton, 10 mM pyrophosphate sodium, 100 mM NaF, 1 mM EGTA, 1,5 mM MgCl₂, 1X protease inhibitor (Roche)). The lysed cells were then centrifuged at 12000 rpm for 15 min at 4°C in order to collect the supernatant. The extracts were then run on an SDS-PAGE gel and transferred to nitrocellulose membranes (BioRad). Finally, the samples were analyzed by western blotting with antibodies against HuR (3A2 ²⁹⁴, 1:10000), YB1 (ab12148 abcam, 1:1000), Myog (F5D, Developmental studies Hybridoma Bank, 1:250), GFP (Cell Signaling, 1:1000) or α -tubulin (Developmental studies Hybridoma Bank, 1:1000) as loading control.

Immunofluorescence

Immunofluorescence was performed as previously describe²⁴. Briefly, cells were rinsed twice in PBS, fixed in 3% phosphate-buffered paraformaldehyde (Sigma), and permeabilized in PBS-goat serum with 0.5% Triton. After permeabilization, cells were incubated with primary antibodies against the RBPs HuR (1:1000) and YB1 (1:500) or against markers of muscle cell differentiation, Myosin Heavy Chain (MyHC) (1:1000) and Myoglobin (1:250), in 1% normal goat serum/PBS at room temperature for 1 hr. The cells were then incubated with goat anti-mouse or goat anti-rabbit secondary antibodies (Alexa

Fluor® 488, 594) and stained with DAPI (4', 6-diamidino-2-phenylindole) to visualize the nucleus. A Zeiss Axiovision 3.1 microscope was used to observe the cells using a 40x oil objective, and an Axiocam HR (Zeiss) digital camera was used for immunofluorescence photography.

Fusion index

The fusion index indicating the efficiency of C2C12 differentiation was determined by calculating the number of nuclei in each microscopic field in relation to the number of nuclei in myotubes in the same field as previously described²⁴.

RNA extraction, and actinomycin D pulse-chase experiments

mRNA stability was assessed by treating the cells with the RNA polymerase II inhibitor, actinomycin D (ActD) (5 µg/ml) for 0, 2, 4 and 6 hours. Total RNA was isolated at the indicated periods of time using Trizol reagent (Invitrogen) according to the manufacturer's instructions and analyzed by RT-qPCR.

RT-qPCR

1µg of total RNA was reverse transcribed using the M-MuLV RT system (New England BioLab). A 1:80 dilution of cDNA was then used to detect mRNA levels using SsoFast™ EvaGreen® Supermix (Bio-Rad). Expression was standardized using *GAPDH* or *RPL32* as a reference, and relative levels of expression were quantified by calculating $2^{-\Delta\Delta C_T}$, where $\Delta\Delta C_T$ is the difference in C_T (cycle number at which the amount of amplified target reaches a fixed threshold) between target and reference. In the case of immunoprecipitated samples a 1:20 dilution was used. Primer sequences can be found in **Annex 2**. Supp.Table 4.

Immunoprecipitation/RNA-IP

Fifteen μ l of the anti-YB1, -HuR or IgG antibodies were incubated with 60 μ l of protein A-Sepharose slurry beads (washed and equilibrated in cell lysis buffer) for 4h at 4°C. Beads were washed three times with cell lysis buffer and incubated with 500 μ g of cell extracts overnight at 4°C. Beads were then washed again three times with cell lysis buffer and co-immunoprecipitated proteins or RNA was then eluted and processed for analysis. When indicated, cell extracts were digested for 30 min at 37°C with RNase A (100 μ g/ml).

RNA electrophoretic mobility shift assays (REMSA)

Myog cRNA probes G/URE-1 and G/URE-2 were generated using sense and antisense oligonucleotides complementary to these regions which were directly annealed, probe G/URE-3 was generated by PCR amplification using a forward primer fused to the T7 promoter as well as the pEMSV-Myog plasmid (kindly supplied by Dr. A. Lassar, at Harvard Medical School) as template. Probes were then used for *in vitro* transcription reactions using a T7 RNA polymerase (Promega). 500 ng of purified protein (glutathione S-transferase (GST), GST-YB1 or GST-HuR was incubated with 100,000 cpm of ³²P-UTP-labeled cRNAs in a total volume of 20 μ l EBMK buffer (25 mM HEPES, pH 7.6, 1.5 mM KCl, 5 mM MgCl₂, 75 mM NaCl, 6% sucrose, and protease inhibitors) at room temperature for 15 min. Two microliters of a 50-mg/ml heparin sulfate stock solution were then added to the reaction mixture for an additional 15 min at room temperature to prevent nonspecific protein-RNA binding. Finally, samples were loaded on a non-denaturing 4% polyacrylamide gel containing 0.05% NP-40 and run for 2 h at 180 V. Gels were then fix in 7% acetic acid/10% ethanol, dried and exposed overnight at -80°C. Primer sequences can be found in **Annex 2**. Supp.Table.4.

Nuclear Run-On

Nuclei were prepared from C2C12 cells 24 h after transfection with either siCtl or siYB1 as previously described⁵⁷. C2C12 cell were then washed twice with cold PBS, centrifuged at 1500 rpm and suspended in NP-40 lysis buffer (10mM Tris-Cl (pH 7.4), 10mM NaCl, 3mM MgCl₂, 0.5% Nonidet P-40). Nuclei were pelleted at 1,000 rpm for

10min at 4°C, resuspended in nuclear freezing buffer (50mM Tris-Cl (pH 8.3), 40% glycerol, 5mM MgCl₂, 0.1mM EDTA) and frozen at -85°C until analysis. Nuclear transcription assays were carried out in run-on buffer (25mM Tris-Cl pH 8.0, 12.5mM MgCl₂, 750mM KCl, 1.25mM ATP, 1.25mM GTP, 1.25mM CTP), in the presence of 150µCi of [α -³²P] UTP (3000^{Ci}/_{mmol}) at 37°C for 15 min. Nuclear transcription activity was determined by measurement of [α -³²P] UTP incorporation in RNA transcripts elongated *in vitro*. The cDNAs for *Myog* and *GAPDH* were blotted (~10µg of cDNA per blot) onto nitrocellulose membrane (BioRad). Afterwards, these membranes were dried at 80°C for 2 h and subsequently hybridized with [α -³²P] RNA isolated from nuclear transcription experiments for 24 h at 65°C. Membranes were washed in 2x SSC at 65°C for 1 h and then exposed to Kodak XAR-2 film at -80°C.

mRNA sequencing (RNA-seq)

RNA was isolated from IP experiments performed on C2C12 total cell extract collected at day 2 of differentiation, using TRIzol reagent (Invitrogen). RNA samples were assessed for quantity and quality using a NanoDrop UV spectrophotometer (Thermo Fisher Scientific Inc), and a Bioanalyser (Agilent Technology Inc). The 3 RNA-seq libraries (IgG, YB1 and HuR) were sequenced on the Illumina NextSeq 500 platform at the Institute for Research in Immunology and Cancer (IRIC) Genomics Core Facility, University of Montreal, to produce over 37 million, 100 nucleotide paired-end reads per sample. The reads were then trimmed for sequencing adapters and aligned to the reference mouse genome version mm10 (GRCm38) using Tophat version 2.0.10. Gene quantification was performed on the mapped sequences using the htseq-count software version 0.6.1.

Mass Spectrometry

Proteins immunoprecipitated with HuR from extracts obtained on Day 2 of muscle cell differentiation using an antibody against HuR or IgG (used as a negative control) were analyzed by mass spectrometry at the centre de recherche du CHU de Québec. Proteins

that showed enrichment in the anti-HuR samples and no enrichment in the anti-IgG controls were considered for analysis.

Gene Ontology Analysis

GO analysis using DAVID 6.8 was performed on gene targets identified by mass spectrometry and RIP-seq. Gene targets were evaluated for their Biological Processes (BP), Molecular Function (MF), and Cellular Compartment (CC). The EASE Score, a modified Fisher Exact P-Value, was used for gene-enrichment analysis.

Luciferase expression/activity

Renilla luciferase mRNA steady state levels were determined by RT-qPCR using primers specific for Rluc. Primer sequences can be found in **Annex 2**. Supp.Table.4. Luciferase activity was furthermore measured using a Renilla luciferase assay system (Promega) following the manufacturer's instructions as previously described⁴.

9.2.6. Acknowledgement

We are grateful to Xian Jin Lian for technical help with some of the experiments in the manuscript and Amr Omer for reading and commenting on the manuscript. This work is funded by CIHR operating grants (MOP-142399, MOP-89798) to I.E.G. B.J.S was funded by a scholarship received from the Consejo Nacional de Ciencia y Tecnologia (CONACyT), the Fonds de recherche du Québec – Nature et technologies (FRQNT) and the Biochemistry department at McGill University. J.S. was funded by a FRQS Master's studentship. D.T.H. was funded by a scholarship received from the Canadian Institute of Health Research (CIHR) funded Chemical Biology Program at McGill University.

9.2.7. References Chapter II

- 1 von Roretz, C., Beauchamp, P., Di Marco, S. & Gallouzi, I.-E. HuR and myogenesis: Being in the right place at the right time. *Biochimica et Biophysica Acta (BBA) - Molecular Cell Research* 1813, 1663-1667, (2011).
- 2 Charge, S. B. & Rudnicki, M. A. Cellular and molecular regulation of muscle regeneration. *Physiological reviews* 84, 209-238, (2004).
- 3 Beauchamp, P. et al. The cleavage of HuR interferes with its transportin-2-mediated nuclear import and promotes muscle fiber formation. *Cell death and differentiation*, (2010).
- 4 Janice Sanchez, B. et al. Depletion of HuR in murine skeletal muscle enhances exercise endurance and prevents cancer-induced muscle atrophy. *Nat Commun* 10, 4171, (2019).
- 5 Tallquist, M. D., Weismann, K. E., Hellstrom, M. & Soriano, P. Early myotome specification regulates PDGFA expression and axial skeleton development. *Development* 127, 5059-507, (2000).
- 6 Tapscott, S. J. & Weintraub, H. MyoD and the regulation of myogenesis by helix-loop-helix proteins. *The Journal of clinical investigation* 87, 1133-1138, (1991).
- 7 Wang, Y. & Jaenisch, R. Myogenin can substitute for Myf5 in promoting myogenesis but less efficiently. *Development* 124, 2507-2513, (1997).
- 8 Bentzinger, C. F., Wang, Y. X., von Maltzahn, J. & Rudnicki, M. A. The emerging biology of muscle stem cells: Implications for cell-based therapies. *BioEssays : news and reviews in molecular, cellular and developmental biology*, (2012).
- 9 Fan, C. M., Li, L., Rozo, M. E. & Lepper, C. Making Skeletal Muscle from Progenitor and Stem Cells: Development versus Regeneration. *Wiley Interdiscip Rev Dev Biol* 1, 315-327, (2012).
- 10 Kaeser, M. D. & Emerson, B. M. Remodeling plans for cellular specialization: unique styles for every room. *Curr Opin Genet Dev* 16, 508-512 (2006).

- 11 Bentzinger, C. F., Wang, Y. X. & Rudnicki, M. A. Building muscle: molecular regulation of myogenesis. *Cold Spring Harb Perspect Biol* 4, (2012).
- 12 Rudnicki, M. A., Le Grand, F., McKinnell, I. & Kuang, S. The molecular regulation of muscle stem cell function. *Cold Spring Harb Symp Quant Biol* 73, 323-331 (2008).
- 13 Figliola, R., Busanello, A., Vaccarello, G. & Maione, R. Regulation of p57(KIP2) during muscle differentiation: role of Egr1, Sp1 and DNA hypomethylation. *J Mol Biol* 380, 265-277, (2008).
- 14 Apponi, L. H., Corbett, A. H. & Pavlath, G. K. RNA-binding proteins and gene regulation in myogenesis. *Trends Pharmacol Sci* 32, 652-658, (2011).
- 15 Figueroa, A. et al. Role of HuR in skeletal myogenesis through coordinate regulation of muscle differentiation genes. *Molecular and cellular biology* 23, 4991-5004 (2003).
- 16 Phillips, B. L. et al. Post-transcriptional regulation of Pabpn1 by the RNA binding protein HuR. *Nucleic Acids Res*, (2018).
- 17 von Roretz, C., Macri, A. M. & Gallouzi, I. E. Transportin 2 regulates apoptosis through the RNA-binding protein HuR. *The Journal of biological chemistry* 286, 25983-25991, (2011).
- 18 Schaefer, B., Sun, W., Li, Y. S., Fang, L. & Chen, W. The evolution of posttranscriptional regulation. *Wiley Interdiscip Rev RNA*, e1485, (2018).
- 19 Ji, Y. & Tulin, A. V. Post-transcriptional regulation by poly(ADP-ribosylation) of the RNA-binding proteins. *International journal of molecular sciences* 14, 16168-16183, (2013).
- 20 Abdelmohsen, K., Kuwano, Y., Kim, H. H. & Gorospe, M. Posttranscriptional gene regulation by RNA-binding proteins during oxidative stress: implications for cellular senescence. *Biol Chem* 389, 243-255, (2008).
- 21 Chang, N. et al. HuR uses AUF1 as a cofactor to promote p16INK4 mRNA decay. *Mol Cell Biol* 30, 3875-3886, (2010).
- 22 Cammas, A. et al. Destabilization of nucleophosmin mRNA by the HuR/KSRP complex is required for muscle fibre formation. *Nat Commun* 5, (2014).

- 23 Dormoy-Raclet, V. et al. HuR and miR-1192 regulate myogenesis by modulating the translation of HMGB1 mRNA. *Nat Commun* 4, 2388, (2013).
- 24 van der Giessen, K., Di-Marco, S., Clair, E. & Gallouzi, I. E. RNAi-mediated HuR depletion leads to the inhibition of muscle cell differentiation. *The Journal of biological chemistry* 278, 47119-47128, (2003).
- 25 van der Giessen, K. & Gallouzi, I. E. Involvement of transportin 2-mediated HuR import in muscle cell differentiation. *Molecular biology of the cell* 18, 2619-2629, (2007).
- 26 Song, Y. J. & Lee, H. YB1/p32, a nuclear Y-box binding protein 1, is a novel regulator of myoblast differentiation that interacts with Msx1 homeoprotein. *Exp Cell Res* 316, 517-529, (2010).
- 27 Zhang, Y. F. et al. Nuclear localization of Y-box factor YB1 requires wild-type p53. *Oncogene* 22, 2782-2794, (2003).
- 28 Cammas, A. et al. Destabilization of nucleophosmin mRNA by the HuR/KSRP complex is required for muscle fibre formation. *Nat Commun* 5, 4190, (2014).
- 29 Warde-Farley, D. et al. The GeneMANIA prediction server: biological network integration for gene prioritization and predicting gene function. *Nucleic Acids Res* 38, W214-220, (2010).
- 30 Eliseeva, I. A., Kim, E. R., Guryanov, S. G., Ovchinnikov, L. P. & Lyabin, D. N. Y-box-binding protein 1 (YB-1) and its functions. *Biochemistry. Biokhimiia* 76, 1402-1433, (2011).
- 31 Lyabin, D. N., Eliseeva, I. A. & Ovchinnikov, L. P. YB-1 protein: functions and regulation. *Wiley Interdiscip Rev RNA* 5, 95-110, (2014).
- 32 Kohno, K., Izumi, H., Uchiumi, T., Ashizuka, M. & Kuwano, M. The pleiotropic functions of the Y-box-binding protein, YB-1. *BioEssays : news and reviews in molecular, cellular and developmental biology* 25, 691-698, (2003).
- 33 Fujita, T. et al. Increased nuclear localization of transcription factor Y-box binding protein 1 accompanied by up-regulation of P-glycoprotein in breast cancer pretreated

- with paclitaxel. *Clinical cancer research: an official journal of the American Association for Cancer Research* 11, 8837-8844, (2005).
- 34 Miao, X. et al. Y-box-binding protein-1 (YB-1) promotes cell proliferation, adhesion and drug resistance in diffuse large B-cell lymphoma. *Exp Cell Res* 346, 157-166, (2016).
 - 35 von Roretz, C., Beauchamp, P., Di Marco, S. & Gallouzi, I. E. HuR and myogenesis: being in the right place at the right time. *Biochimica et biophysica acta* 1813, 1663-1667, (2011).
 - 36 Gallouzi, I. E., Brennan, C. M. & Steitz, J. A. Protein ligands mediate the CRM1-dependent export of HuR in response to heat shock. *RNA* 7, 1348-1361, (2001).
 - 37 Dormoy-Raclet, V. et al. The RNA-binding protein HuR promotes cell migration and cell invasion by stabilizing the beta-actin mRNA in a U-rich-element-dependent manner. *Molecular and cellular biology* 27, 5365-5380, (2007).
 - 38 Dong, J. et al. RNA-binding specificity of Y-box protein 1. *RNA biology* 6, 59-64, (2009).
 - 39 Sabourin, L. A. & Rudnicki, M. A. The molecular regulation of myogenesis. *Clin Genet* 57, 16-25, (2000).
 - 40 Liu, L. et al. Competition between RNA-binding proteins CELF1 and HuR modulates MYC translation and intestinal epithelium renewal. *Mol Biol Cell* 26, 1797-1810, (2015).
 - 41 Ahuja, D., Goyal, A. & Ray, P. S. Interplay between RNA-binding protein HuR and microRNA-125b regulates p53 mRNA translation in response to genotoxic stress. *RNA biology* 13, 1152-1165, (2016).
 - 42 Ishimaru, D. et al. Regulation of Bcl-2 expression by HuR in HL60 leukemia cells and A431 carcinoma cells. *Molecular cancer research : MCR* 7, 1354-1366, (2009).
 - 43 Wigington, C. P. et al. Post-transcriptional regulation of programmed cell death 4 (PDCD4) mRNA by the RNA-binding proteins human antigen R (HuR) and T-cell

- intracellular antigen 1 (TIA1). *The Journal of biological chemistry* 290, 3468-3487, (2015).
- 44 Koike, K. et al. Nuclear translocation of the Y-box binding protein by ultraviolet irradiation. *FEBS letters* 417, 390-394 (1997).
- 45 Okamoto, T. et al. Direct interaction of p53 with the Y-box binding protein, YB-1: a mechanism for regulation of human gene expression. *Oncogene* 19, 6194-6202, (2000).
- 46 Holm, P. S. et al. YB-1 relocates to the nucleus in adenovirus-infected cells and facilitates viral replication by inducing E2 gene expression through the E2 late promoter. *The Journal of biological chemistry* 277, 10427-10434, (2002).
- 47 Stein, U. et al. Hyperthermia-induced nuclear translocation of transcription factor YB-1 leads to enhanced expression of multidrug resistance-related ABC transporters. *The Journal of biological chemistry* 276, 28562-28569, (2001).
- 48 Su, A. I. et al. Large-scale analysis of the human and mouse transcriptomes. *Proc Natl Acad Sci U S A* 99, 4465-4470, (2002).
- 49 Su, A. I. et al. A gene atlas of the mouse and human protein-encoding transcriptomes. *Proc Natl Acad Sci U S A* 101, 6062-6067, (2004).
- 50 Terry, E. E. et al. Transcriptional profiling reveals extraordinary diversity among skeletal muscle tissues. *Elife* 7, (2018).
- 51 Alemasova, E. E. et al. Poly(ADP-ribosyl)ation as a new posttranslational modification of YB-1. *Biochimie* 119, 36-44, (2015).
- 52 Ke, Y. et al. PARP1 promotes gene expression at the post-transcriptional level by modulating the RNA-binding protein HuR. *Nat Commun* 8, 14632, (2017).
- 53 Meder, V. S., Boeglin, M., de Murcia, G. & Schreiber, V. PARP-1 and PARP-2 interact with nucleophosmin/B23 and accumulate in transcriptionally active nucleoli. *Journal of cell science* 118, 211-222, (2005).

- 54 Ame, J. C., Spenlehauer, C. & de Murcia, G. The PARP superfamily. *BioEssays : news and reviews in molecular, cellular and developmental biology* 26, 882-893, (2004).
- 55 Hsiao, S. J. & Smith, S. Tankyrase function at telomeres, spindle poles, and beyond. *Biochimie* 90, 83-92, (2008).
- 56 Gallouzi, I. E. et al. HuR binding to cytoplasmic mRNA is perturbed by heat shock. *Proc Natl Acad Sci U S A* 97, 3073-3078 (2000).
- 57 Garcia-Martinez, J., Aranda, A. & Perez-Ortin, J. E. Genomic run-on evaluates transcription rates for all yeast genes and identifies gene regulatory mechanisms. *Mol Cell* 15, 303-313, (2004).

9.3. CHAPTER III: Loss of HuR in skeletal muscle promotes an oxidative fiber phenotype and prevents cancer-cachexia associated muscle atrophy.

9.3.1. Abstract

The master posttranscriptional regulator HuR promotes muscle fiber formation in cultured muscle cells. However, its impact on muscle physiology and function *in vivo* is still unclear. Here, we show that muscle-specific HuR knockout (muHuR-KO) mice have high exercise endurance that is associated with enhanced oxygen consumption and carbon dioxide production. muHuR-KO mice exhibit a significant increase in the proportion of oxidative type I fibers in several skeletal muscles. HuR mediates these effects by collaborating with the mRNA decay factor KSRP to destabilize the *PGC-1 α* mRNA. The type I fiber-enriched phenotype of muHuR-KO mice protects against cancer cachexia-induced muscle loss. Therefore, our study uncovers that under normal conditions HuR modulates muscle fiber type specification by promoting the formation of glycolytic type II fibers. We also provide a proof-of-principle that HuR expression can be targeted therapeutically in skeletal muscles to combat cancer-induced muscle wasting.

9.3.2. Introduction

The importance of skeletal muscle is underscored by its requirement for locomotion, posture, and breathing and by the fact that loss of muscle function and integrity can lead to crippling and deadly consequences^{1,2}. Many cancers trigger rapid muscle wasting, a condition also known as cachexia, that in turn leads to resistance to treatment, low quality of life and death³.

Muscle fibers can be classified into two categories. Type I fibers are slow-contracting and are specialized for oxidative energy metabolism, having high levels of mitochondria and oxidative enzymes, and low levels of glycolytic enzymes which are enriched in type II fibers. Type II fibers are fast-contracting and are subdivided into three types. Type IIB are specialized for glycolytic metabolism, having high levels of glycolytic

enzymes and low mitochondrial content. Type IIA are not metabolically specialized, having higher glycolytic enzyme levels than type I and higher mitochondrial content than type IIB. Type IIA and type I generate less force but are more resistant to fatigue in comparison with IIB fibers. Type IIX are intermediate between type IIA and type IIB in metabolic and contractile properties^{1,4}. Each one of these fiber types expresses a unique isoform of the myosin heavy chain (MyHC) (Type I, IIA, IIX, and IIB respectively)^{1,4}. Each individual muscle is composed of a mixture of various fiber types⁴. This heterogeneity in fiber type enables different muscle groups to achieve a variety of functions and movements⁴. Owing to their distinctive physiological and metabolic characteristics, fiber types are also differentially sensitive to specific pathophysiologic assaults. In pre-clinical mouse models of muscle-loss diseases, such as Duchenne Muscular Dystrophy (DMD) and cancer cachexia, Type II fibers are more prone to wasting when compared to Type I fibers^{1,4,5}. Therefore, factors regulating fiber type in muscle could represent ideal drug targets for treating cachexia and other muscle wasting diseases.

It is well-established that factors such as the transcription factor peroxisome-proliferator-activated receptor gamma coactivator-1 alpha (PGC-1 α) and the deacetylase Sirtuin 1 (Sirt1), modulate the fiber-type composition of skeletal muscles. Sirt1 enhances PGC-1 α activity and together they promote the formation of oxidative (Type I) fibers^{1,4}. In response to a stimulus such as voluntary exercise, the activation of Sirt1 leads to the deacetylation of PGC-1 α , this in turn, upregulates the expression of NRFs (nuclear respiratory factors) and Tfam (mitochondria transcription factor A), which are key players in mitochondrial biogenesis and oxidative metabolism in muscles^{1,4,6,7}. On the other hand, transcription factors such as Six1 and nuclear factor of activated T-cells, cytoplasmic4 (NFATc4) modulate the expression of target genes involved in the formation of glycolytic type II or IIX fibers^{1,4}. In addition to the specific genes activated by these factors, their impact on fiber-type specification also depends on their level of expression in response to various stimuli^{1,4}. Therefore, the molecular mechanisms controlling the expression levels of these factors play a crucial role in muscle fiber-type specification under different conditions.

Although the expression of these and other factors is modulated transcriptionally^{1,4}, some observations have established that post-transcriptional regulatory mechanisms also affect their levels in response to exercise. A decrease in the half-life of *PGC-1 α* and *TFAM* messenger RNAs (mRNAs) by ~40–60% in slow-twitch oxidative muscles correlates with an increase in the expression levels of RNA-binding proteins (RBPs) such as HuR and the mRNA decay factor KSRP⁸. While a role for HuR and KSRP in the regulation of these and other mRNAs during exercise is still elusive, the involvement of HuR and KSRP in the formation of muscle fibers in cell culture is well-established^{9–13}. During the early stages of myogenesis, HuR both promotes the translation of the *HMGB1* mRNA¹¹ and collaborates with KSRP to reduce the expression of nucleophosmin (NPM) protein by destabilizing the *NPM* mRNA¹². At later steps of myogenesis, however, HuR stabilizes the mRNAs encoding promoters of muscle fiber formation such as *MyoD*, *Myog*, and *p21*, only when muscle cells begin their fusion to form fibers (myotubes)¹⁰.

To investigate the *in vivo* relevance of HuR in muscle tissues, in this study we use the Cre-LoxP system to generate a HuR muscle-specific knockout mouse (*MyoDCre⁺;Elav1^{fl/fl}*). We show that the loss of HuR leads to the enrichment of type I fibers resulting in the increased oxidative metabolic capacity of the skeletal muscle. This indicates that one of the main roles of HuR in skeletal muscles is to promote the formation and maintenance of glycolytic type II fibers. HuR mediates these effects by destabilizing the *PGC-1 α* mRNA in a KSRP-dependent manner. We also provide data demonstrating that depleting the expression of HuR in muscles protects mice against cancer-induced muscle atrophy.

9.3.3. Results

9.3.3.1. HuR depletion in muscle improves endurance and oxidative capacity.

The total knockout of the HuR gene (also known as *Elav1*) is embryonic lethal (embryos die between E10.5-E14.5)¹⁴. We therefore generated an *Elav1* muscle-specific knockout (muHuR-KO) mouse to investigate the *in vivo* role of HuR in muscle formation

and muscle physiology. Mice carrying the *Elavl1^{fl/fl}* allele¹⁴ and mice expressing Cre recombinase under the control of the *MyoD* promoter¹⁵ were bred to obtain the HuR muscle-specific knockout (**Fig. 4.1a**). The knockout of HuR is initiated in muscle progenitor cells during embryogenesis, since Cre under the *MyoD* promoter is activated in the branchial arches and limb buds as early as day E10.5¹⁵.

muHuR-KO mice are viable and do not exhibit any major change in their total body weight (**Fig. 4.1b, c**). Knockout of HuR was confirmed by genotyping with PCR primers and by western blot (WB) analysis in several hindlimb skeletal muscles, including the quadriceps, gastrocnemius, tibialis anterior (TA), soleus, peroneus, and extensor digitorum longus (EDL) (**Fig. 4.1d–f**). The fact that muHuR-KO mice are healthy with no obvious defect suggests that, *in vivo*, the role of HuR in the formation, development and function of skeletal muscles is either redundant with other RBPs (see discussion) or that HuR-mediated regulation is more relevant in post-natal muscle development during adaptation to various muscle-related functions and needs.

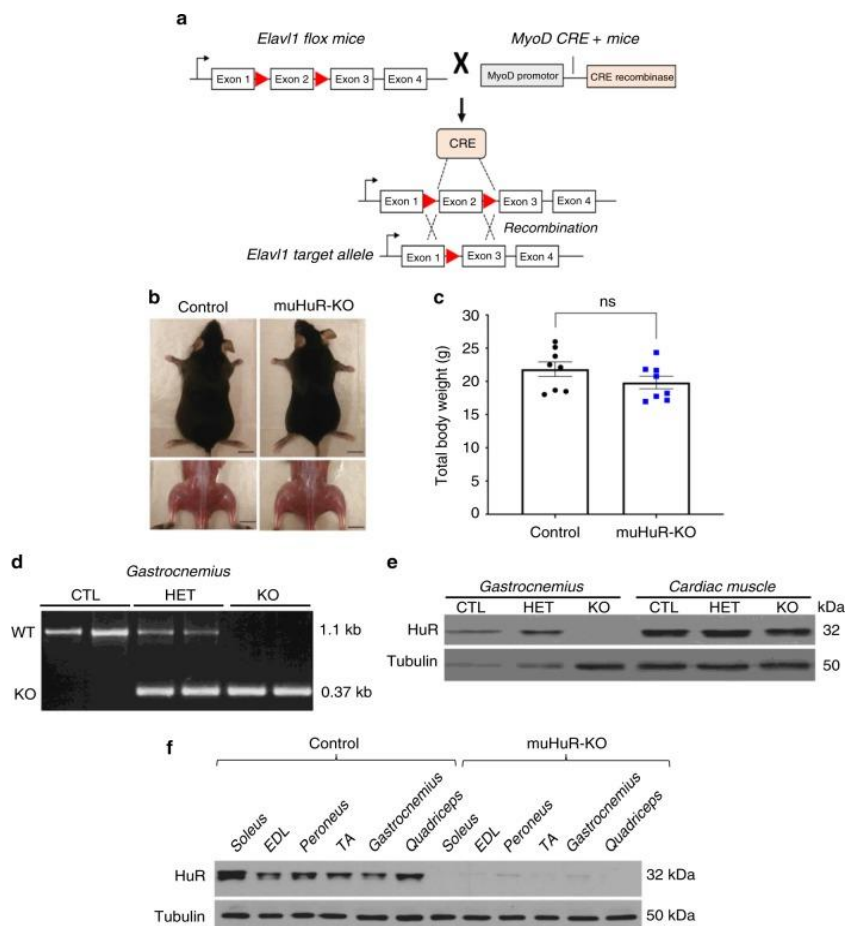


Figure 4.1. Generation of HuR muscle-specific knockout mice using the Cre-lox P system. **a)** Diagram depicting the tissue-specific knockout strategy. *Elavl1*-flox mice (Lox P sites ►) were bred with mice expressing Cre recombinase under the control of the MyoD promoter (MyoD CRE⁺) to generate muscle-specific HuR KO mice. **b)** Photographs of 2-month-old muHuR-KO and control male mice. Scale bars = 1 cm. **c)** Total body weights of 8–10-weeks-old muHuR-KO and control mice ($n=8$). The results are presented as mean \pm S.E.M, * $p < 0.05$ unpaired *t*-test. **d)** PCR amplification of the targeted region of the *Elavl1* gene in gastrocnemius muscle samples from control (CTL), heterozygote (HET), and muHuR-KO (KO) mice. Shown is a representative of agarose gel of the genotyping of all the mice used in this study ($n=30$). **e)** Representative western blot analysis, from four independent experiments of HuR expression in skeletal and cardiac muscle tissue from control CTL, HET, and KO mice using antibodies against HuR or α -tubulin. **f)** Representative western blot analysis of soleus, extensor digitorum longus (EDL), peroneus, tibialis anterior (TA), gastrocnemius, and quadriceps muscles from control and muHuR-KO mice using antibodies against HuR or α -tubulin. This blot is a representative of four independent experiments.

To investigate the above-mentioned possibilities, we assessed muscle-related functions in muHuR-KO compared to control mice. To do this, we used invasive and non-invasive *in vivo* tests: *in situ* analysis of muscle contractility, which measures force generation and fatigability^{16,17}, the treadmill exhaustion test, which estimates exercise capacity and endurance, and the limb grip strength assays, which determines muscle strength¹⁸. *In situ* analysis showed that although TAs of muHuR-KO mice exhibited a higher contraction force than those of control animals, they did not demonstrate any notable differences in the fatigability test (**Fig. 4.2a**). Additionally, a treadmill exhaustion test indicated that the time to exhaustion and the running distance covered by muHuR-KO mice was significantly longer than their control counterparts (**Fig. 4.2b, c**). In this test, muHuR-KO mice performed 20% more work than the control mice (**Fig. 4.2d**). Of note, this increase in endurance was accompanied by a slight decrease in muscle strength of the muHuR-KO mice (**Fig. 4.2e** and **Annex 3. Supplementary Fig.1**). We also confirmed increased exercise endurance in the muHuR-KO mice using the accelerating Rota-rod and the Inverted-grid platform (**Fig. 4.2f, g**).

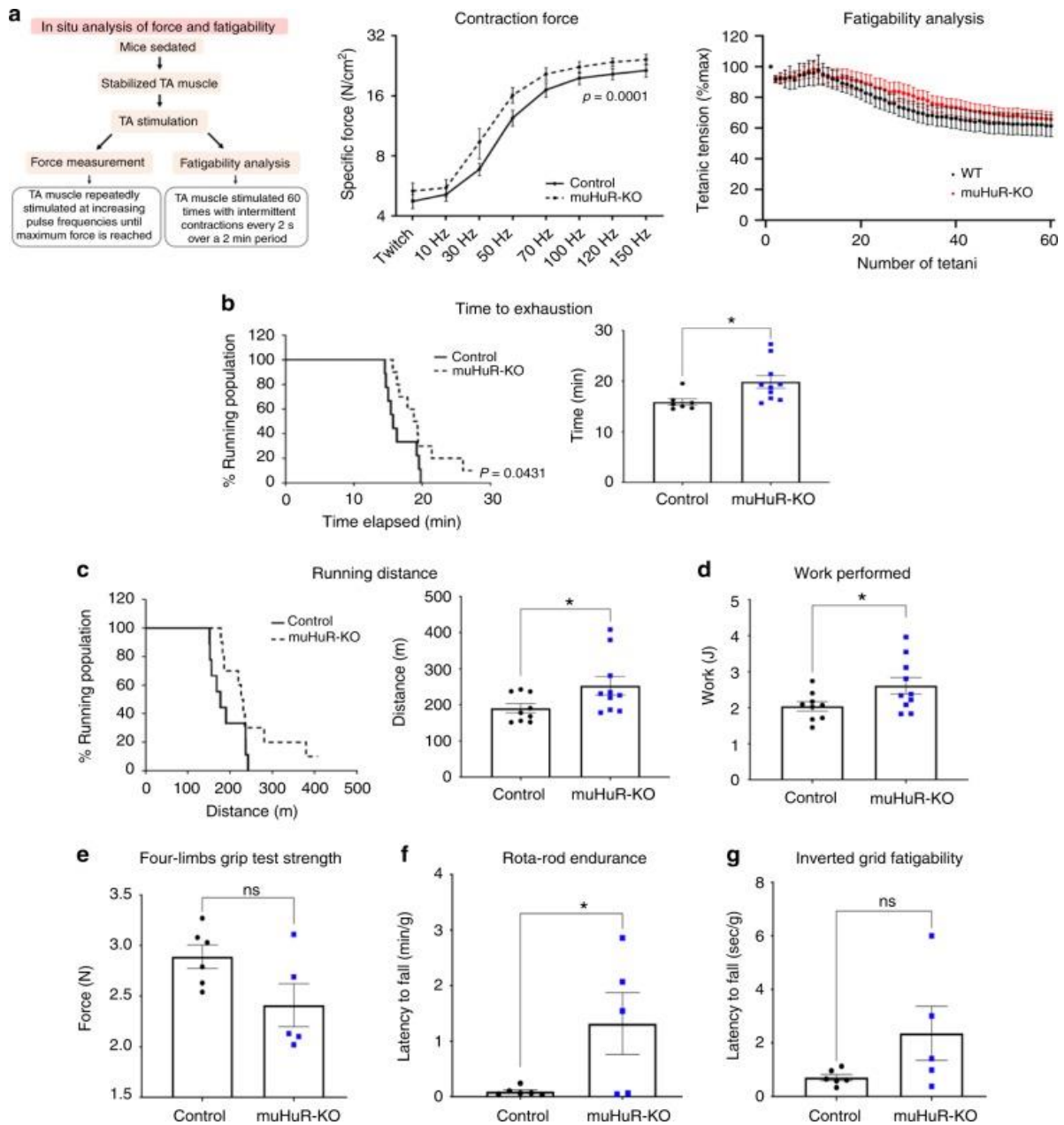


Figure 4.2. HuR muscle-specific KO mice have enhanced exercise endurance. **a)** Left panel: schematic describing the method used to determine, in situ, force measurement, and fatigability of control and muHuR-KO mice. Middle panel: contractile function of the TA muscle was assessed *in situ* at various stimulation frequencies (Control: $n = 8$, muHuR-KO: $n = 6$). Right panel: fatigability of TA muscle was assessed in situ over 60 stimulation sessions with a resting period of 2 min between stimuli. Fatigability was normalized to TA muscle weight shown in (Annex 3. Supplementary Fig.1a) (Control: $n = 8$, muHuR-KO: $n = 6$). **b–g)** Physical performance was evaluated in age-matched control and muHuR-KO mice by performing a treadmill exhaustion test. Three parameters were measured with this test: **b)** Time to exhaustion (left panel; survival plot showing the percentage of mice running at indicated time

points. Right panel; mean duration of the run). **c)** Running distance (left panel; survival plot showing the percentage of mice running at indicated distances. Right panel; mean distance ran) and **d)** Work performed during test. **b)** Control: $n = 7$, muHuR-KO: $n = 10$, **c)** control: $n = 9$, muHuR-KO: $n = 10$, **d)** control: $n = 9$, muHuR-KO: $n = 10$. **e)** Grip strength was evaluated on control and muHuR-KO mice using a digital force gauge. Mice were allowed to grip using their four limbs (forelimb and hindlimbs) and peak force was measured in triplicate during two sessions (Control: $n = 6$, muHuR-KO: $n = 5$). **f)** Endurance performance was assessed using a Rota-rod system. For each animal, the duration on the rod was measured twice with a resting period of 4 days in between. The latency to fall represents an average of the two sessions of evaluation (Control: $n = 6$, muHuR-KO: $n = 5$). **g)** Fatigability was evaluated by performing an inverted-grid test, the latency to fall represents an average of two sessions of evaluation normalized to total body weight (Control: $n = 6$, muHuR-KO: $n = 5$). Statistical analysis for *in situ* data shown in **a)** was performed using two-way ANOVA. The results are presented as mean \pm S.E.M, * $p < 0.05$ unpaired *t*-test **b–g**.

Enhanced endurance is generally associated with an increased oxidative capacity of skeletal muscle fibers^{1,4,19}. Therefore, we used the Columbus Instrument's Comprehensive Animal Monitoring System (CLAMS)[®] (**Fig. 4.3a**) to determine the rate of oxygen consumption (VO_2) and carbon dioxide production (VCO_2), two indicators widely used to measure the oxidative capacity of rodents and humans²⁰. While we did not observe any change in the voluntary movement of these animals (**Annex 3. Supplementary Fig. 2a**), muHuR-KO mice showed a higher rate of VO_2 consumption and VCO_2 production than their control littermates (**Fig. 4.3b, c**). The muHuR-KO animals exhibited a slight increase in the respiratory exchange ratio (RER), that is most evident during the peak of voluntary movement (**Fig. 4.3d**), suggesting that, at least under non-exercise conditions, the depletion of HuR favors the usage of carbohydrate as a source of energy in skeletal muscles²¹. On the other hand, several key components of the electron transport chain (ETC) complexes such as CIII and CIV, as well as the ATP synthase CV, well-established indicators of mitochondrial oxidative respiration²², show a significant increase in their expression level in muHuR-KO muscles (**Fig. 4.3e**). The fact that the absence of HuR did not have any effect on heat production levels (**Annex 3. Supplementary Fig. 2b**), suggested that the oxidative phenotype observed in muHuR-KO mice is not associated with metabolic uncoupling²³. Therefore, overall, our results indicate that the specific disruption of the *HuR* gene in muscle improves exercise endurance and oxygen consumption.

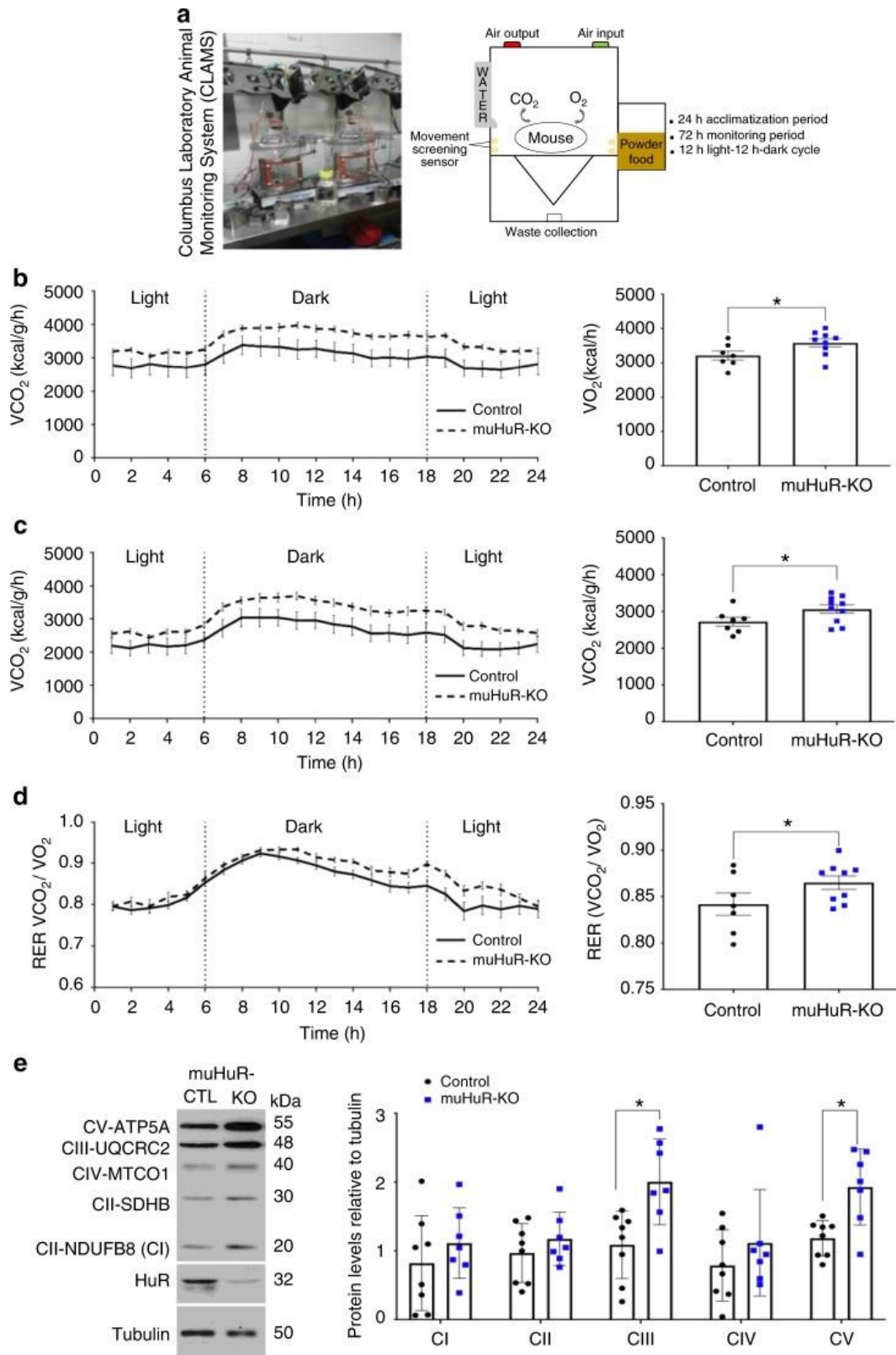


Figure 4.3. muHuR-KO mice show an increased oxidative capacity. a) Schematic illustrating the Comprehensive Animal Monitoring System (CLAMS; Columbus Instruments,

Columbus, OH) that was used to complete a 3-day indirect calorimetry study in age-matched mice under a 12 h light–12 h dark cycle. **b)** Oxygen consumption ($\dot{V}O_2$) and **c)** carbon dioxide production ($\dot{V}CO_2$) were measured over the 3 days following a 24 h acclimation period. **d)** Respiratory exchange ratio (RER) was calculated as the ration of $\dot{V}CO_2/\dot{V}O_2$. The graphs on the left depicts the average values at each time point while that on the right shows the average values over the 72 h period. **b–d)** Data obtained was analyzed using the CLAMS examination tool (CLAX; Columbus Instruments) version 2.1.0. (Control: $n=7$, muHuR-KO: $n=9$). The results are presented as mean \pm S.E.M, $*p < 0.05$ unpaired t -test. **e)** Left panel: western blot analysis of levels of OXPHOS complexes in the mitochondria of control and muHuR-KO mice. Right panel: quantifications of the levels of the complexes are presented as the mean \pm S.E.M, $*p < 0.05$ unpaired t -test (control: $n=8$, muHuR-KO: $n=7$).

9.3.3.2. Loss of HuR in muscle promotes type I oxidative fibers.

Improved endurance is, in general, associated with a noticeable increase in the proportion of type I fibers²⁴. Hence, we examined the fiber-type composition of several muscles isolated from control and muHuR-KO mice by performing metachromatic ATPase staining with specific antibodies against Myosin Heavy Chain (MyHC) I, IIA, and IIB. The soleus of muHuR-KO mice showed a ~17% enrichment of Type I fibers when compared to control animals, while Type IIA fibers decreased by ~16% (**Fig. 4.4a–c** and **Annex 3**. Supplementary Table 1). In keeping with this, the soleus of muHuR-KO mice showed an increase in the steady-state levels of mRNAs encoding some promoters of type I-fibers such as *Tnni1* and *MyHC I*, and a decrease in promoters of type II-fibers such as *Tnnt3* and *MyHC IIB* (**Fig. 4.4d**). The same effects on the proportion of fiber type I and on the expression modulators of fiber-type specification were also observed in both the peroneus and EDL of the muHuR-KO mice (**Annex 3**. Supplementary Figs. 3 and 4 and Supplementary Table 1). We also carried out a muscle fiber size analysis by measuring cross-sectional area and found that the distribution pattern of fiber size in the soleus was not affected by HuR loss (**Fig. 4.4e–g**). Thus, the observed change in fiber-type composition is not associated with a defect in muscle fiber generation or growth. Altogether these findings demonstrate the involvement of HuR in the regulation of muscle fiber-type composition *in vivo*, where the presence of HuR favors the formation of type II, while its depletion promotes the formation of type I.

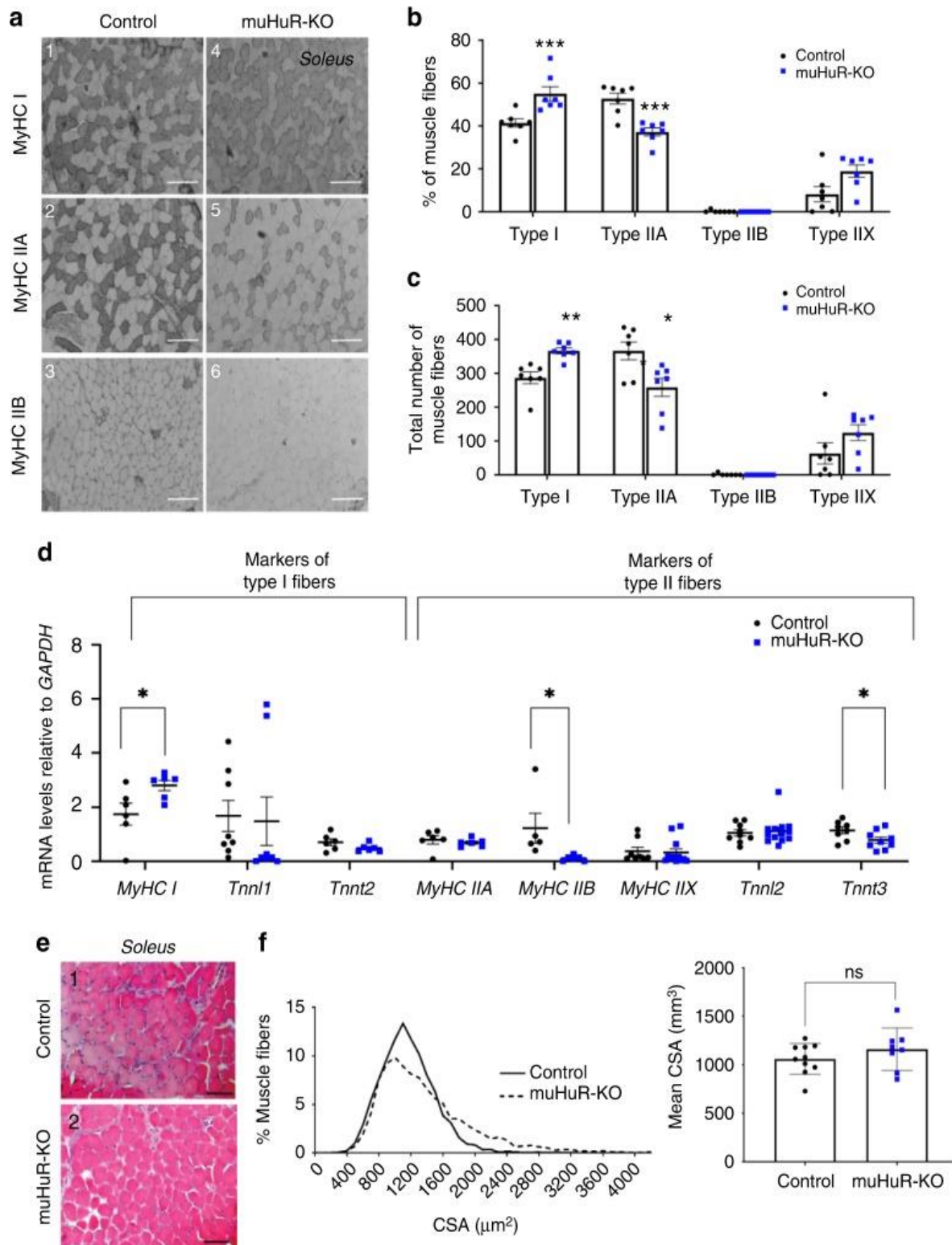


Figure 4.4. Depletion of HuR in skeletal muscle increases the proportion of type I fibers.

a) Representative photomicrographs of *soleus* muscles serial sections from control and muHuR-KO mice taken after immunostaining with anti-Myosin Heavy Chain (MyHC) antibodies type I, type IIA, and type IIB. Scale bars: 100 μm . Photomicrographs are

representative of sections prepared from seven different mice. **b)** Quantification of muscle fibers type I, type IIA, and type IIB was ascertained manually. Fibers type IIX were calculated by counting the unstained fibers. Results are graphed as a percentage of the total number of fibers per muscle. **c)** Total number of fibers per muscle is shown for the muscles analyzed in **b**. $n = 7$ mice for **b**, **c**. **d)** mRNA expression of known markers of fiber-type specificity, *MyHC I*, *Tnnt2*, and *MyHC IIA* ($n = 6$ mice), *Tnni1* ($n = 8$ mice), *MyHC IIB* (Control $n = 5$, *muHuR-KO* $n = 6$ mice), *MyHC IIX* (Control $n = 8$, *muHuR-KO* $n = 12$ mice), *Tnni2* (Control $n = 9$, *muHuR-KO* $n = 13$ mice), and *Tnnt3* (Control $n = 8$, *muHuR-KO* $n = 9$ mice) was assessed by RT-qPCR. mRNA levels were standardized against *GAPDH* and plotted relative to the expression in control mice. **e)** Representative photomicrographs of *soleus* muscles sections from control and *muHuR-KO* mice taken after H&E staining. Scale bars: 100 μm ($n = 8$ mice). **f)** Left panel: mean CSA of *soleus* muscles fibers from control and *muHuR-KO* mice were analyzed from sections stained with H&E. Right panel: frequency histogram showing the distribution of muscle fiber CSA in the *soleus* muscles from control and *muHuR-KO* mice. (control: $n = 10$, *muHuR-KO*: $n = 8$). Results are presented as mean \pm S.E.M, * $p < 0.05$, ** $p < 0.01$, *** $p < 0.001$ unpaired *t*-test.

9.3.3.3. HuR depletion in muscle activates PGC-1 α and its associated pathway.

To delineate the molecular mechanisms through which HuR modulates fiber-type specification in mice, we performed a high-throughput mRNA sequencing (RNA-seq) analysis. Total RNA was isolated from soleus muscles of *muHuR-KO* and control littermates and was used to prepare and sequence four mRNA libraries²⁵. The clear separation of the two genotypes was evident in the heatmap showing the 17,534 genes detected through RNA-seq analysis in both control and *muHuR-KO* mice (**Annex 3. Supplementary Fig. 5a**). RNAseq-data was further examined using a DESeq2 package for differential expression analysis. A volcano plot of the acquired data shows the general profile of gene expression and highlights the genes that are up (right side) or downregulated (left side) in *muHuR-KO* muscles when compared to control counterparts (**Fig. 4.5a**). Each dot represents a single gene while the horizontal and vertical dashed lines indicate the statistical significance threshold ($\log_2\text{FC} > 0.5$ or < -0.5 , $p = 0.05$). From the 1914 genes affected in the soleus muscle of HuR knockout mice (1.5-fold change or more), 86% were increased, while only 14% were decreased (**Annex 3. Supplementary Data 1**). Of note, the steady level of well-known HuR mRNA targets in muscle fibers, such as *MyoD*, *Nucleophosmin (NPM)* and *HMGB1*, were as expected, decreased (*MyoD*), increased (*NPM*) or remained unaffected (*HMGB1*) (**Fig. 4.5b**)⁹⁻¹².

The fact that the majority of the affected transcripts in the absence of HuR are increased, raises the possibility that, *in vivo*, HuR has an overall destabilizing activity on its mRNA targets in skeletal muscle.

Next, to identify the pathways affected by the loss of HuR, we performed a core analysis using the Ingenuity Pathway Analysis software (IPA: Ingenuity Systems®). Two of the top five canonical pathways identified by IPA were associated with the activity of the transcription factor, Peroxisome proliferator-activated receptor alpha (PPAR α) (**Fig. 4.5c** and **Annex 3**. Supplementary Fig. 5b). PPAR α plays a critical role in energy production and lipid and carbohydrate metabolism and also regulates the expression of genes involved in peroxisomal and mitochondrial β -oxidation⁴. A reduction in the expression levels or a complete deletion of the *PPAR α* gene are associated with an increased endurance capacity of animals. On the other hand, PPAR β/δ collaborate with PGC-1 α to promote oxidative phenotype and increase endurance capacity of skeletal muscles⁴.

To validate our IPA analysis, total RNA from soleus, peroneus and EDL muscles of both control and muHuR-KO mice was prepared and used to determine the transcript levels of genes involved in the PPAR α signaling pathway or fiber-type specification such as *PGC-1 α* , *PGC-1 β* , *Tfam*, *PPAR α* , *Six1* (Sineoculis homeobox homolog 1), *NCOA6* (Nuclear receptor coactivator 6), *Tpm1* (Tropomyosin 1), and *MyoD*^{1,4}. Consistent with the RNAseq data and the observed type I fiber enrichment phenotype, we observed a two-fold increase in the steady-state level of both *PGC-1 α* mRNA and protein in the soleus of muHuR-KO mice when compared to control littermates (**Fig. 4.5d, e**). However, although maintained, the increase in *PGC-1 α* expression level was less drastic in the peroneus and EDL of muHuR-KO mice (**Annex 3**. Supplementary Fig. 6). HuR loss, on the other hand, had a very little effect on the steady-state level of *PGC-1 β* and *Tfam* mRNAs, two factors associated with the oxidative phenotype (**Fig. 4.5d** and **Annex 3**. Supplementary Fig. 6). In addition, loss of HuR not only decreased, as expected^{9,12}, the steady-state level of *MyoD* mRNA, but also the levels of mRNAs encoding other factors involved in the glycolytic phenotype such as *PPAR α* , *Six1* and *Tpm1* (**Fig. 4.5d** and **Annex 3**. Supplementary Fig. 6)⁴.

It is well-established that the induction of an oxidative phenotype in muscles is, in general, associated with an increase in fatty acid oxidation and mitochondria biogenesis and function^{1,4}. While muHuR-KO muscle did not exhibit any change in the expression levels of genes involved in fatty acid transport and oxidation, such as *Acadv1*, *CD36*, *FAS*, *LDL*, *UCP2*, and *UCP3*^{1,4}, it did show an increase in the level of *NRF1* (nuclear respiratory factor 1) mRNA (**Annex 3. Supplementary Fig. 7b**), a known promoter of mitochondrial oxidative respiration in various tissues including muscle⁴. However, the ratio between mitochondrial (*mtDNA*) and nuclear (*nDNA*) DNA was unchanged in both muHuR-KO muscles and their control counterparts (**Annex 3. Supplementary Fig. 7c**), indicating that while the depletion of *HuR* gene in muscles does not affect mitochondrial biogenesis, it could be associated with an enhancement of mitochondrial activity. Altogether, these results show that by regulating the expression levels of key genes such as *PGC-1 α* , HuR controls energy metabolism and fiber-type specification of skeletal muscles.

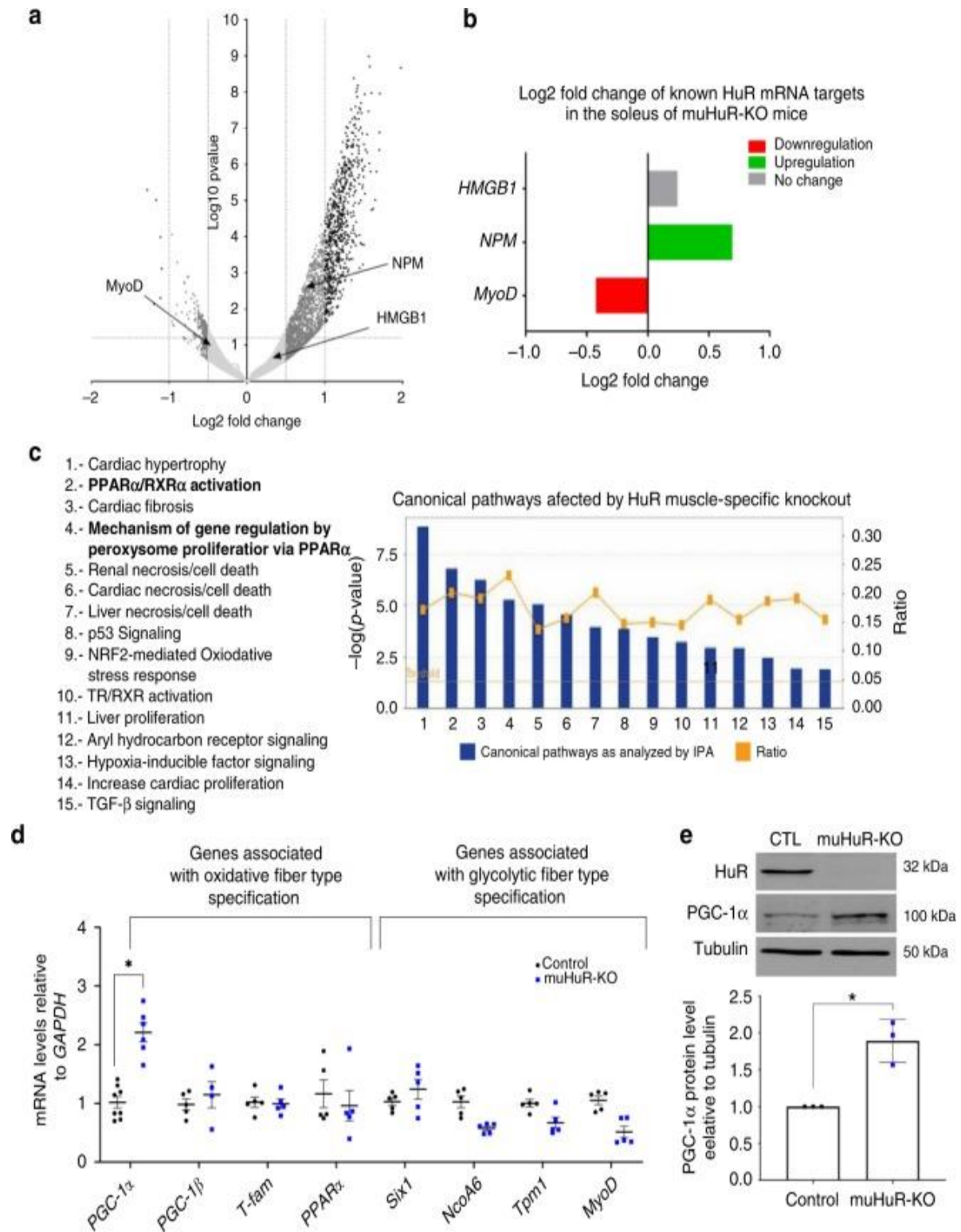


Figure 4.5. Increased PGC-1 α expression in muHuR-KO muscle. a) Volcano plot showing the log₂ fold-difference in mRNA expression in the soleus muscle of control and muHuR-KO mice as assessed by the DESeq2 analysis of the RNA-seq data. Negative values indicate

decrease in gene expression while positive values refer to upregulation of gene expression. Dash lanes indicate threshold for statistical significance ($p = 0.05$ for $\log_2FC > 0.5$, < 0.5). The location of known HuR mRNA targets, including *NPM*, *HMGB1*, and *MyoD* are shown. **b**) Comparison of \log_2 fold change score of the previously identified HuR mRNA targets *NPM*, *HMGB1*, and *MyoD* is shown. **c**) Bar graph indicating the signaling pathways affected by the knockout of HuR in *soleus* muscle as analyzed by Ingenuity Pathway Analysis software (IPA®). The x-axis represents the identified pathways. The y-axis (left) shows the $-\log_{10}$ of the p -value. The ratio (y-axis, right) represented by the orange points is calculated as follows: numbers of genes in each pathway that meet cut-off criteria, divided by total numbers of genes that are involved in that pathway. The horizontal orange line indicates the threshold above which there is statistical significance. **d**) Total RNA was isolated from soleus muscles of control and muHuR-KO mice and relative expression level of genes associated with PPAR signaling and/or fiber-type specification (*PGC-1 α* , *PGC-1 β* , *Tfam*, *PPAR α* , *Six1*, *NCOA6*, *Tpm1*, *MyoD*) was assessed by RT-qPCR. Relative mRNA levels were standardized against *GAPDH* and plotted relatively to the expression in control mice ($n = 5$ mice all the genes except for *PGC-1 α* , were control $n = 8$ and muHuR-KO $n = 6$). **e**) Western blot (top panel) and relative quantification (bottom panel) of PGC-1 α protein levels in soleus muscle from control and muHuR-KO mice using antibodies against PGC-1 α , HuR, or α -tubulin ($n = 3$). The results are presented as mean \pm S.E.M, * $p < 0.05$ unpaired t -test.

9.3.3.4. HuR collaborates with KSRP to destabilize *PGC-1 α* mRNA in muscle cells.

PGC-1 α is one of the major promoters of type I oxidative phenotype in skeletal muscle⁴. As a first step in determining the way by which HuR regulates PGC-1 α expression, we investigated whether HuR binds to the *PGC-1 α* mRNA in muscle cells. Consistent with previous observations²⁶, we were unsuccessful in immunoprecipitating HuR from skeletal muscle extracts. Therefore, we used the well-established C2C12 myoblasts, to assess, as we did before^{9,11,12,27}, the association between HuR and *PGC-1 α* mRNA. Similar to what was observed in the soleus, small- interfering ribonucleic acid (siRNA)-mediated HuR depletion in C2C12 myoblasts^{11,12} significantly increased *PGC-1 α* mRNA and protein levels (**Fig. 4.6a, b**). Immunoprecipitation of HuR from these myoblasts coupled with reverse transcription quantitative PCR (RT-qPCR) analysis revealed that HuR forms a complex with the *PGC-1 α* mRNA (**Fig. 4.6c**).

Next, we determined the post-transcriptional level through which HuR regulates *PGC-1 α* mRNA expression. To test mRNA translation, we performed polysome fractionation experiments on C2C12 myoblasts depleted or not of HuR, using siRNA control (siCtl) or against HuR (siHuR), and followed the recruitment of *PGC-1 α* mRNA to

heavy polysomes, a well-established assay used to identify actively translated messages¹². We observed no difference in the levels of *PGC-1 α* mRNA in heavy polysomes in the presence or absence of HuR (**Annex 3**. Supplementary Fig. 8). Actinomycin D pulse-chase experiment^{12,28} was used to determine if HuR regulates the stability of the *PGC-1 α* mRNA in these cells. Knocking down HuR in myoblasts increased the half-life of *PGC-1 α* mRNA from 6 to > 10 h (**Fig. 4.6d**). As expected¹², however, loss of HuR destabilized known mRNA targets of HuR such as *MyoD* (**Fig. 4.6e**) and *Myog* (**Annex 3**. Supplementary Fig. 9). On the other hand, C2C12 myoblasts overexpressing GFP-HuR exhibited a significant decrease in the expression levels of PGC-1 α protein and mRNA, as well as a ~40% reduction in the half-life of *PGC-1 α* transcript (**Fig. 4.6f–i**). We also observed that the depletion of HuR does not affect the stability of other mRNAs involved in fiber-type specification such as *TnnI1*, *TnnI2*, *Six1*, *NFATc1*, and *NCOA6* (**Annex 3**. Supplementary Fig. 9). Collectively, these results strongly suggest that HuR antagonizes the type I fiber phenotype in muscle cells by destabilizing *PGC-1 α* mRNA, leading to a decreased expression of PGC-1 α protein.

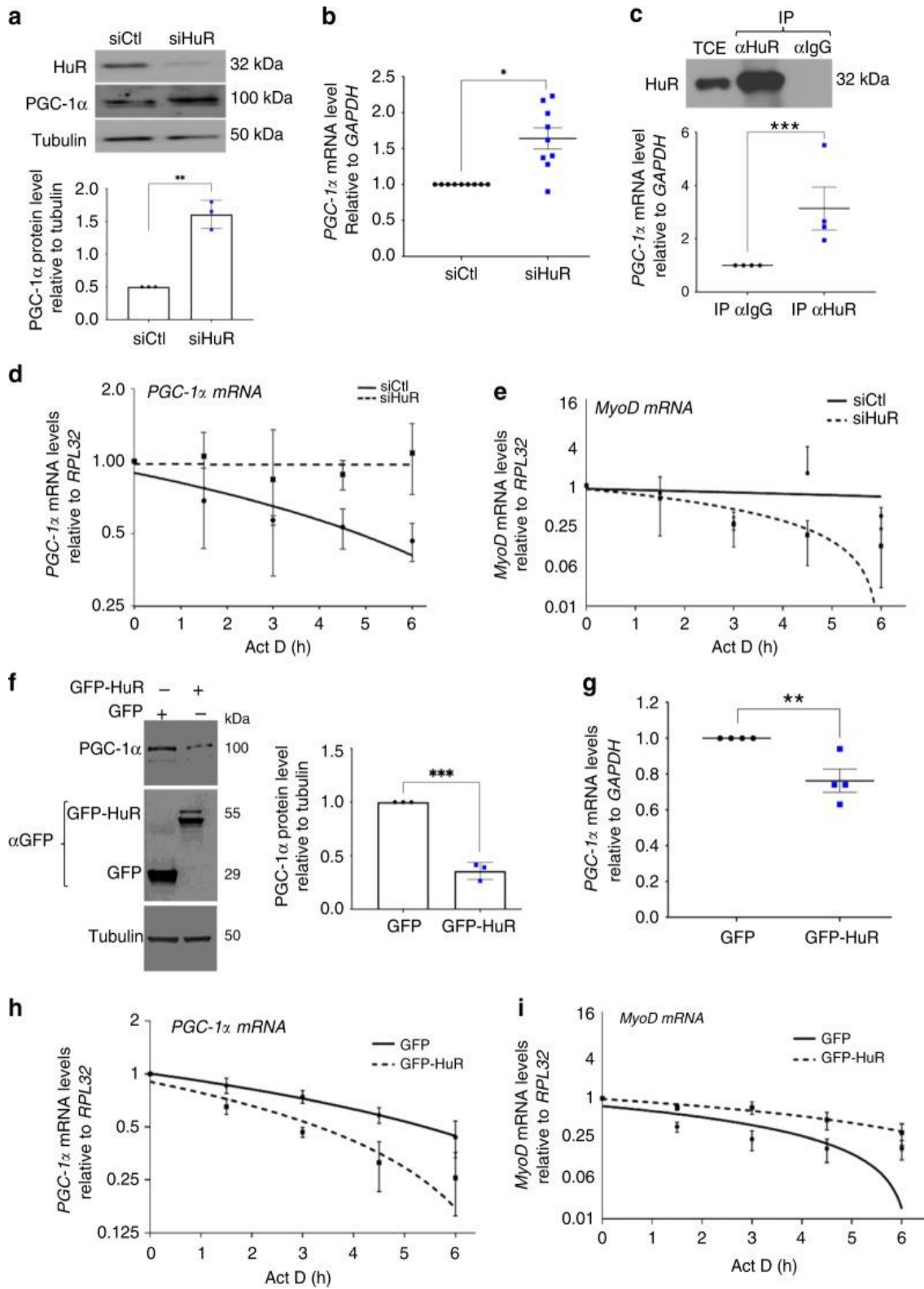


Figure 4.6. HuR destabilizes the *PGC-1 α* mRNA in muscle cells. a) Western blot (top panel) and relative quantification (bottom panel) of PGC-1 α protein levels in myoblasts treated

with or without siHuR using antibodies against PGC-1 α , HuR, or α -tubulin ($n = 3$). **b**) Total RNA was isolated from myoblasts treated as in **a** and PGC-1 α expression was assessed by RT-qPCR. PGC-1 α mRNA level were standardized against GAPDH and plotted relatively to siCtl ($n = 9$). **c** Top panel: western blot showing the immunoprecipitation (IP) of HuR using an anti-HuR antibody (3A2) or IgG as control. (Bottom panel) RT-qPCR were used to determine the association of the PGC-1 α mRNA to HuR. Normalized PGC-1 α mRNA levels were plotted relatively to the IgG control ($n = 4$). **d, e**) The stability of the PGC-1 α (**d**) and MyoD mRNAs (**e**) was determined in myoblasts depleted (siHuR) or not (siCtl) of HuR and treated with Actinomycin D (ActD) for 0, 1.5, 3, 4.5, or 6 h (**h**). mRNA levels were then standardized against RPL32 mRNA levels and plotted relative to the abundance of mRNA at time 0 of ActD treatment (which is represented as 1) ($n = 3$). The line of best fit was determined by linear regression using the data points for siCtl and siHuR. Error bars represent \pm S.E.M. **f**) Western blot (left panel) and relative quantification (right panel) of PGC-1 α protein levels in myoblasts expressing GFP or GFP-HuR using antibodies against PGC-1 α , GFP or α -tubulin ($n = 3$). **g**) Total RNA was isolated from myoblasts overexpressing or not HuR (GFP-HuR) and relative PGC-1 α expression was assessed by RT-qPCR. PGC-1 α mRNA level were standardized against GAPDH and plotted relatively to siCtl ($n = 4$). **h, i**) Myoblasts expressing GFP or GFP-HuR were used to assess the stability of the PGC-1 α (**h**) and MyoD (**i**) was determined as described in panels **d, e** ($n = 3$). For **d, e, h, i** the line of best fit was determined by linear regression using the data points for siCtl and siHuR. Error bars represent \pm S.E.M. The results in **b, c, f, g** are presented as mean \pm S.E.M, * $p < 0.05$, ** $p < 0.05$, *** $p < 0.005$ unpaired t -test.

Next, we examined the possibility that KSRP could be involved in the HuR-mediated destabilization of the PGC-1 α mRNA. Immunoprecipitation experiment coupled with RT-qPCR analysis showed that KSRP, similarly to HuR, associates with the PGC-1 α mRNA in myoblasts (**Fig. 4.7a**). Furthermore, knockdown of KSRP in these cells¹² significantly increased both the steady-state level and the half-life of PGC-1 α mRNA (**Fig. 4.7b, c**). We previously demonstrated that HuR and KSRP form a tight complex in C2C12 myoblasts and that the binding of HuR or KSRP to the NPM mRNA requires an intact HuR/KSRP complex¹². Using similar experimental approaches, we observed that this is also the case for the binding of PGC-1 α mRNA to either one of these RBPs (**Fig. 4.7d, e**). Therefore, one way by which HuR promotes the glycolytic phenotype in muscle cells and tissues is by destabilizing the PGC-1 α mRNA in a KSRP-dependent manner.

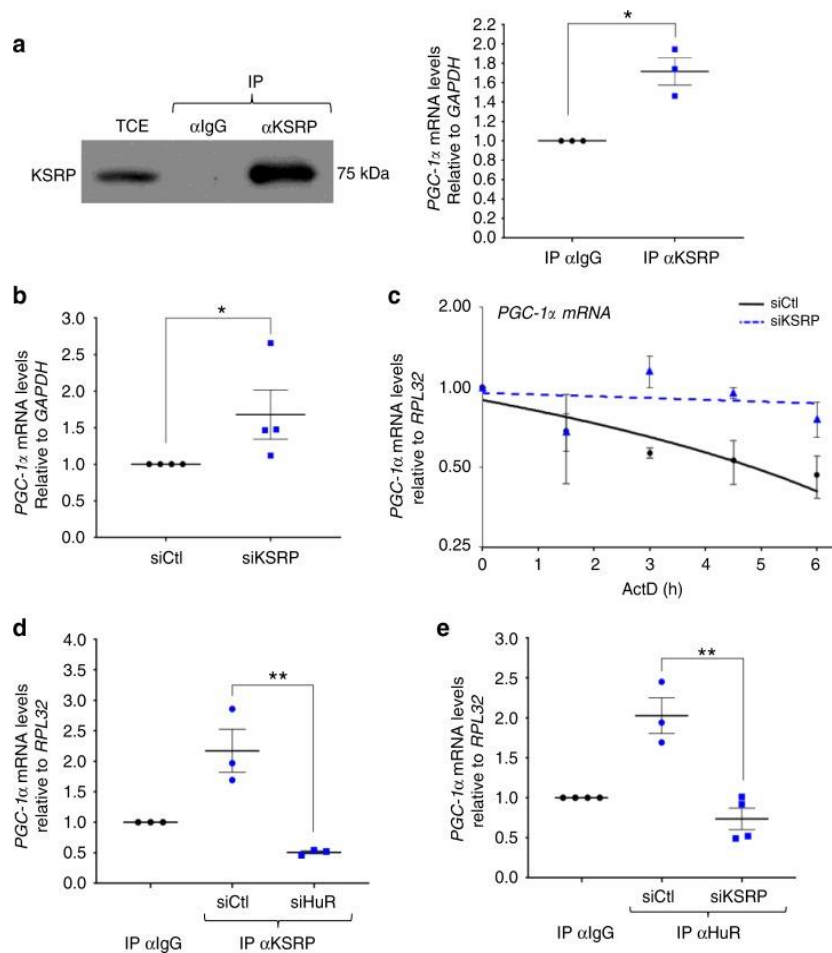


Figure 4.7. KSRP collaborates with HuR to destabilize the *PGC-1α* mRNA in muscle cells. **a)** Left panel: western blot demonstrating the immunoprecipitation (IP) of KSRP using an anti-KSRP antibody or IgG as a negative control. Right panel: RT-qPCR experiments were performed to determine the association of *PGC-1α* mRNA to immunoprecipitated KSRP. Normalized *PGC-1α* mRNA levels were plotted relative to the IgG negative control ($n = 3$). **b)** Total RNA was isolated from C2C12 myoblasts treated with or without siKSRP and relative *PGC-1α* expression was assessed by RT-qPCR. *PGC-1α* mRNA level were standardized against *GAPDH* and plotted relative to the siCtrl condition ($n = 4$). **c)** The stability of the *PGC-1α* mRNA was determined in muscle cells depleted or not of KSRP and treated with Actinomycin D (ActD) for 0, 1.5, 3, 4.5, or 6 h. mRNA levels were then standardized against *RPL32* mRNA levels and plotted relative to the abundance of mRNA at time 0 of ActD treatment (which is represented as 1) ($n = 3$). The line of best fit was determined by linear regression using the data points for siCtrl and siKSRP. Error bars represent \pm S.E.M. **d, e)** IP coupled to RT-qPCR experiments was performed using anti-KSRP (**d**) or anti-HuR (**e**) antibodies on total extract from C2C12 myoblasts treated with siHuR (**d**), or siKSRP (**e**). *PGC-1α* mRNA levels in the samples immunoprecipitated with anti-KSRP or anti-HuR were normalized to the corresponding IgG sample. The results are presented as mean \pm S.E.M, ** $p < 0.01$ unpaired *t*-test. **d** ($n = 3$), **e** ($n = 4$ for IPIgG siCtrl, IPIgG siKSRP, and IPHuR siKSRP; $n = 3$ for IPHuR siCtrl).

9.3.3.5. muHuR-KO mice are resistant to cancer-induced muscle wasting.

Several reports have suggested that at late stages, numerous cancers preferentially target type II glycolytic fibers to trigger rapid muscle loss, a deadly condition also known as cachexia-induced muscle wasting²⁹. Furthermore, the upregulation of PGC-1 α expression has been associated with not only the promotion of type I oxidative fibers but also with the prevention of muscle atrophy induced by several conditions^{30,31}. Therefore, we tested the possibility that the muHuR-KO mice could be protected from disease-induced muscle wasting.

To achieve this, we injected in control and muHuR-KO mice the Lewis Lung Carcinoma (LLC) cells, a cancer-cell model that is widely used to trigger muscle wasting in C57BL/6 mice^{32,33}. Although, both control and muHuR-KO mice-bearing LLC tumors (LLC-Control and LLC-muHuR-KO) show no change in total body weight during the four weeks of tumor growth (**Annex 3**. Supplementary 10a), upon sacrifice the carcass weight minus tumor weight of the muHuR-KO mice demonstrated a significant protection from LLC-induced weight loss when compared to their control counterparts (**Fig. 4.8a**). Of note, control and muHuR-KO mice-bearing LLC tumors show no difference in tumor growth or tumor burden and exhibit comparable levels of systemic inflammatory response, as evidenced by the enlargement of the spleen, as well as by the loss of hindlimb fat pad (**Annex 3**. Supplementary Fig. 10b-e). Importantly, the atrophy of several hindlimb muscles, including the gastrocnemius, TA, soleus and peroneus, is significantly lower in LLC-muHuR-KO mice when compared to LLC-control mice (**Fig. 4.8b**). In addition, the expression levels of *atrogen-1/MAFbx* and *MuRF-1* mRNAs, two muscle-specific ubiquitin ligases that play an essential role in promoting cancer-induced muscle loss³⁴, is strongly induced (6-fold) in the muscle of LLC-control but not in LLC-muHuR-KO mice (**Fig. 4.8c**). Moreover, the high expression levels of *PGC-1 α* observed in muHuR-KO muscle was also maintained in the presence of LLC tumors (**Fig. 4.8d**). The expression levels of *MyHC I* was significantly reduced in control mice-bearing LLC tumors, while the high expression levels of MyHC I observed in the absence of HuR was maintained in muscles from LLC-muHuR-KO mice (**Fig. 4.8e**). Furthermore, the cross-sectional area (CSA) analysis of muscle fibers in LLC-control mice is decreased when

compared to those of the LLC-muHuR-KO mice (**Fig. 4.8f**). Collectively, these results demonstrate that loss of HuR specifically in skeletal muscle protects mice from cancer-induced muscle wasting.

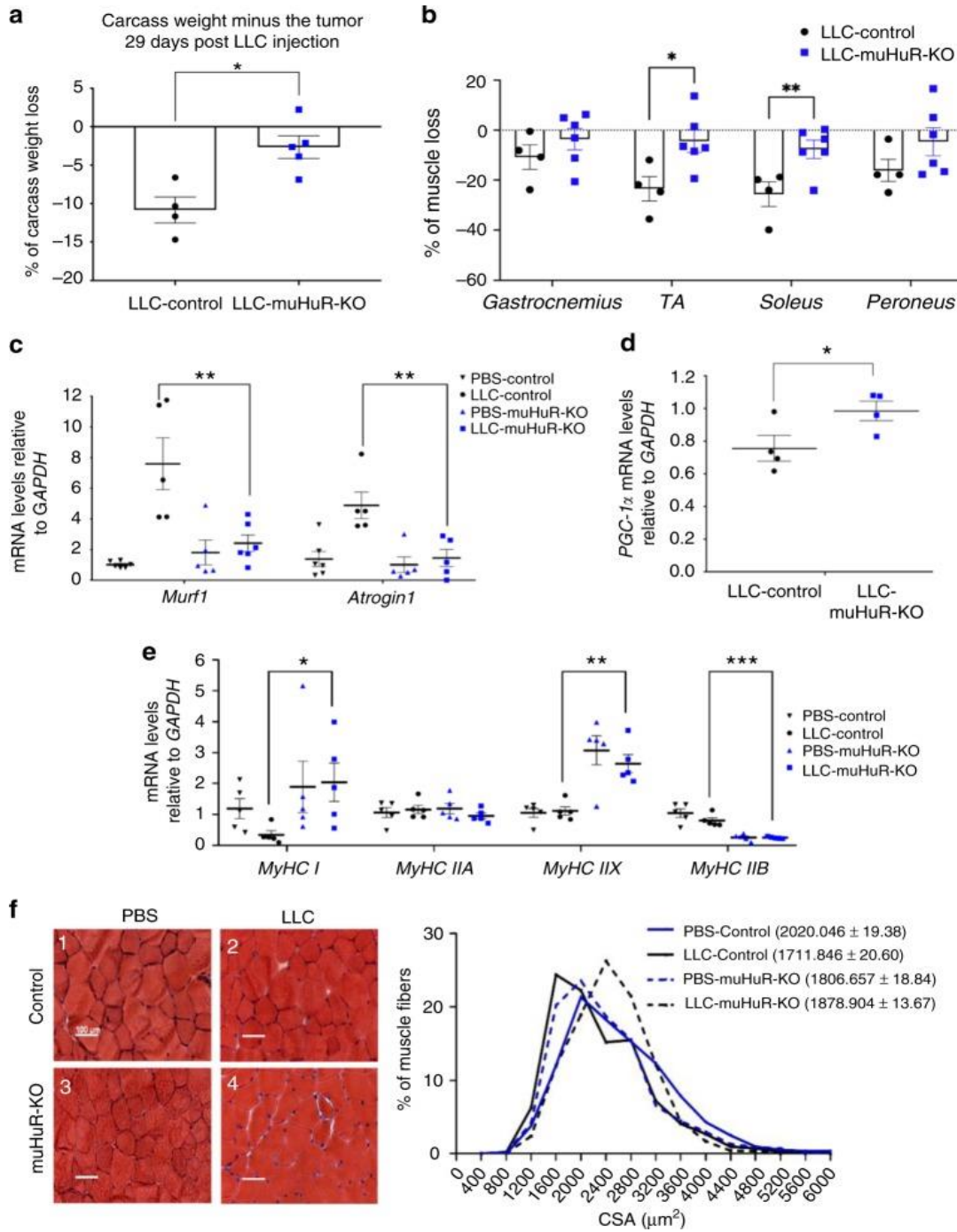


Figure 4.8 HuR ablation in skeletal muscle ameliorates cancer-induced muscle wasting. Muscle atrophy was evaluated in Ctl and muHuR-KO mice using the LLC model of cachexia.

a) Catabolic wasting was assessed post-mortem on tumor-bearing LLC-Ctl and -muHuR-KO mice by measuring total body weight minus tumor weight. The results are presented as mean \pm S.E.M * $p < 0.05$ unpaired t -test, (LLC-Control $n = 4$, LLC-muHuR-KO $n = 5$). **b)** Muscle atrophy was assessed by determining the relative loss of muscle mass in *gastrocnemius*, TA, *soleus*, and *peroneus* muscles from LLC-Control and LLC-muHuR-KO mice. Percentage (%) of muscle loss in both groups is shown relative to non-tumor PBS injected mice from each cohort (LLC-Control $n = 4$ and LLC-HuR-KO $n = 6$). **c–e)** Total RNA was isolated from the *gastrocnemius* muscle of control and muHuR-KO mice bearing or not LLC tumors. Relative mRNA expression levels of *Atrogin1* and *MuRF1* (**c**), *PGC-1 α* (**d**), *MyHC I*, *MyHC IIA*, *MyHC IIB*, and *MyHC IIX* (**e**) was assessed by RT-qPCR and mRNA expression levels was determined relative to *GAPDH* transcript. Expression levels are shown as the fold of induction relative to control-PBS treated mice. (**d**, $n = 4$), (**c**, **e**, $n = 5$). **f** Left panel: representative photomicrographs of *gastrocnemius* muscles sections from control and muHuR-KO mice taken after H&E staining. Scale bars = 100 μ m. Right panel: frequency histogram showing the distribution of muscle fiber CSA in the *gastrocnemius* muscles from control and muHuR-KO mice bearing or not LLC tumors ($n = 4$ mice per group). A total of 500 fiber per muscle were used for the CSA analysis. The results are presented as mean \pm S.E.M, * $p < 0.05$, ** $p < 0.005$, *** $p < 0.0005$ unpaired t -test.

9.3.4. Discussion

In this work, we demonstrate that, *in vivo*, the RBP HuR plays an important role in muscle physiology as well as in deciding muscle fate under disease conditions. muHuR-KO mice show a significant increase in exercise endurance, a phenotype that is explained in part by an enrichment of type I fibers. This enrichment most likely arises from an increase in PGC-1 α levels, a key regulator of energy metabolism and a promoter of type I muscle fiber formation⁴. These observations establish that, under normal conditions, HuR plays a crucial role in the formation and probably maintenance of type II fibers, and antagonizes the formation of type I fibers, by reducing the expression of PGC-1 α . Mechanistically, HuR mediates this effect by forming a complex with the mRNA decay factor KSRP¹², leading to the destabilization of the *PGC-1 α* mRNA. Additionally, HuR also participates in the debilitating outcome of cancer cachexia on muscle integrity since the muHuR-KO mice are protected from cancer-induced muscle wasting. Overall, our findings demonstrate that an important function of HuR in adult skeletal muscle is to favor the formation of type II fibers and provide a proof-of-principle that interfering with the function of HuR can prevent cancer-induced muscle loss.

Based on the fact that HuR is required for muscle fiber formation in cell culture^{9,11,12}, we anticipated that muHuR-KO mice would show strong muscle defects with debilitating consequences. The absence of an obvious and severe phenotype in these mice was, therefore, surprising and unexpected. Interestingly, previous studies have reported similar discrepancy between the *ex-vivo* (cell culture) and the *in vivo* impact on the myogenic process of important pro-myogenic factors, such as MyoD and Myf5. While the overexpression of MyoD or Myf5 triggers myogenesis in several cell types, leading to their conversion to muscle fibers³⁵, the knockout of either one of these genes in mice did not affect muscle development, leading to normal and healthy animals^{36,37}. However, the double knockout of both *MyoD* and *Myf5* genes generated mice without functional muscles that die soon after birth³⁸. Hence, it was concluded that MyoD and Myf5 proteins have an overlapping role in muscle development and formation during embryogenesis. It is, therefore, possible that this could also be the case for HuR, and functional redundancies with other RBPs could exist to ensure proper muscle fiber formation and function. Indeed, it is well-established that RBPs such as KSRP, Zfp3611, Zfp3612, and YB1 (Y-Box-binding protein 1) modulate muscle fiber formation *in vitro*^{13,39,40}. This work and previous observations¹² indicate that HuR collaborates with KSRP to execute some of its function in muscle cells. In addition, similarly to HuR, YB1 promotes muscle fiber formation *in vitro*, by stabilizing target mRNAs³⁹. Hence, it will be of high interest to investigate whether HuR could have functional redundancy with RBPs such as YB1 or others both *in vitro* and *in vivo*.

muHuR-KO mice exhibit a significant increase in their exercise endurance capacity, oxygen consumption, and CO₂ release. These observations together with high level of oxidative type I fibers in various muscles of muHuR-KO mice, was a clear indication that the depletion of HuR in skeletal muscles is associated with an oxidative phenotype. However, unexpectedly the respiratory exchange ratio (RER) (VCO₂/VO₂), which is normally used as an indicator of substrate utilization (carbohydrate or fat) by mitochondria for energy production⁴¹, was also increased in the muHuR-KO mice. These results suggest that under conditions of voluntary movement, muHuR-KO mice have an improved rate of carbohydrate oxidation when compared to control littermates. It is well-established, however, that high RER during exercise is associated with reduced

endurance in rodents⁴² and is a predictor for obesity in human populations⁴³. Therefore, the fact that muHuR-KO have a higher RER may seem contradictory to their enhanced exercise endurance. However, this discrepancy could be explained in part by the fact that our calorimetry studies were performed in the absence of imposed exercise conditions. During exercise, substrate utilization for energy production rapidly switches from carbohydrate to fat⁴². Therefore, based on the high endurance level of muHuR-KO mice, we predict that during their engagement into continued physical exercise the RER response will show an increase at the early stages that will be followed by a rapid decrease. This pattern will be consistent with a shift in substrate usage for energy metabolism from carbohydrate to fat as the exercise activity continues and intensifies⁴¹. Performing such experiments will test this possibility and will shed more light on the role of HuR in muscle function.

Our RNA-seq data indicate that the largest group of genes affected by the depletion of HuR in muscle are those involved in primary metabolic processes such as the PPAR α signaling pathway⁴⁴. Interestingly, many of the genes (such as sarcoplasmic reticulum Ca²⁺ -ATPases (SLN), Ras-related glycolysis inhibitor, and calcium channel regulator (Rrad), insulin receptor substrate 2 (irs2), and peptide transporter 2 (PEPT2) (**Annex 3. Supplementary Data 1**) are associated with metabolic imbalance and weight-related diseases^{45,46,47}. These results raise the possibility that *in vivo* HuR could be involved in metabolic plasticity, impacting muscle function and fate. Future studies will be needed to address the potential involvement of HuR in the onset of metabolic disorders or weight-related diseases.

Our data clearly establish that the enrichment of oxidative type I fibers in muHuR-KO mice is driven, at least in part, by the increased expression of PGC-1 α . This observation also indicates that in skeletal muscles HuR promotes a glycolytic type II fibers and that this effect could be mediated by its ability to down-regulate PGC-1 α expression by destabilizing PGC-1 α mRNA in a KSRP-dependent manner. This conclusion is supported by two facts, (1) our observation that in myoblasts HuR associates with KSRP and that similar to HuR knockdown, the depletion of KSRP stabilizes PGC-1 α mRNA, (2) an intact HuR/KSRP complex is required for the association of either of these RBPs with

PGC-1 α mRNA. Although, the mRNA destabilizing activity of HuR has been previously reported in several cell lines, including muscle cells^{48,12,49}; this effect of HuR was considered a rare event that is either specific to some cell types or is linked to particular growth conditions. The fact that the depletion of HuR in the soleus leads to the upregulation of > 85% of the ~1900 affected mRNAs provide a strong indication that in skeletal muscle HuR mainly acts as an mRNA destabilizer rather than a stabilizer. It is likely however, that the impact of HuR on the fate of its mRNA targets *in vivo* is tissue specific. Indeed, the knockout of HuR specifically in the pyramidal neurons of the hippocampus leads to a significant reduction in the expression levels of the *PGC-1 α* transcript⁵⁰, indicating that in the brain HuR likely acts as a stabilizer for this mRNA. One explanation of this functional dichotomy of HuR is that in different cell types and tissues, HuR associates with various protein ligands and undergoes unique post-translational modifications such as phosphorylation and methylation^{9,12,51,52}. However, we still do not know whether any of these regulatory mechanisms affect HuR function *in vivo* nor their impact on HuR functional switch from stabilizing to destabilizing the same target mRNA.

In addition to the impact of the oxidative phenotype on muscle function and exercise endurance, type I fibers are resistant to atrophy during various disease conditions such as, DMD, denervation, disuse, and cancer cachexia^{24,53–55}. In keeping with this, we show that the muHuR-KO mice are protected against cancer (LLC)-induced muscle wasting. Interestingly, despite being composed largely of type I fibers, we observed significant wasting in the soleus muscle of wild-type mice, which was prevented in muscles lacking HuR. In fact, the resistance of oxidative muscle fibers to cachectic stimuli is presently under debate, since some reports indicate that type I-rich muscles such as the soleus are resistant to cancer-induced muscle wasting, while others have shown the opposite outcome^{56,57}. However, while oxidative fibers may or may not be inherently resistant, numerous studies have demonstrated the therapeutic benefit of promoting oxidative metabolic adaptations^{24,29,53,54,58}. Since HuR plays a key role in muscle fiber formation *in vitro*^{9,10,12,59,60} and its expression pattern dramatically changes during muscle regeneration *in vivo*⁹, we speculate that HuR could also impact the commitment of satellite cells to myogenesis under cachectic conditions. Indeed, the onset of cachexia-induced muscle wasting is associated with an impairment of the regenerative

capacity of satellite cells⁶¹. Hence, it is possible that under normal conditions HuR promotes satellite cells commitment to the myogenic process, while that under cachectic conditions HuR undergoes a functional switch to become a promoter of muscle loss. Experimentally addressing this possibility would provide more insight into on how HuR could promote both muscle formation and function, as well as the deleterious outcome of cachexia. While more work is needed to understand the mechanisms underlying the atrophic resistance of muHuR-KO mice, our results clearly establish that interfering with HuR function in muscle is protective against muscle atrophy in the LLC model of cancer cachexia.

Our results highlight the possibility that HuR can be considered as a viable target in future strategies to design novel approaches to combat cancer-induced muscle atrophy. This is of particular interest given the recent development of small molecules that can inhibit HuR function^{62–64}. However, given the systemic importance of HuR, future studies using HuR inhibitors to treat muscle atrophy will need to investigate potential side effects, as well as mechanisms for specific delivery to muscle tissue. Some of these issues may be circumvented, however, by targeting HuR functions specifically in muscular tissue. As described above, one apparent unique feature of HuR in muscle is a role in destabilizing target transcripts, which is at least in some cases mediated by interactions with co-factors, such as KSRP. Thus, targeting HuR interaction with protein ligands, such as KSRP, may prove to be a more viable strategy than a direct inhibition of HuR itself.

Overall, our findings are consistent with a model whereby HuR regulates the expression of key modulator of fiber-type specification, thus inhibiting the formation of type I muscle fibers. Taken together, our data suggest HuR is a potential pharmacological target to modulate skeletal muscle metabolism, which could have implications in muscle physiology and diseases such as cancer-induced cachexia.

9.3.5.-Material and Methods

Animals

All experiments using animals were approved by the McGill University Faculty of Medicine, Animal Care Committee and comply with guidelines set by the Canadian Council of Animal Care. Mice were housed in a controlled environment and provided commercial laboratory food (Harlan #2018; 18% protein rodent diet; Madison, WI). Housing of the mice was set on a 12h light–12h dark cycle. Mice were maintained in sterile cages with corn-cob bedding and had free access to food and water. For our study we used 3 non-pathogenic mouse strains on a C57BL/6 background; mice expressing cre-recombinase under the MyoD promoter (*MyoDCre*)¹⁵, mice in which the exon 2 of the *Elavl1* gene is floxed (*Elavl1^{fl/fl}*)¹⁴, and the HuR muscle specific knockout mice (*MyoDCre⁺;Elavl1^{fl/fl}*, muHuR-KO) generated by our laboratory at McGill University using the Cre-LoxP system. The breeding strategy to maintain the muscle specific HuR knockout colony consisted in back-crossing *Elavl1^{fl/fl}* mice with *MyoDCre⁺;Elavl1^{fl/fl}* mice. Littermates not expressing Cre recombinase (*MyoDCre⁻;Elavl1^{fl/fl}*) were used as control animals in this study.

Genotyping

Mouse genomic DNA was isolated *in vivo* from tail biopsies or *ex-vivo* from muscle tissue as previously describe⁶⁵. Tail biopsies were incubated for 20min in 300µl of 0.5M NaOH at 95°C. 25 µl of 1M Tris-HCl, pH 8 were then added and 2ul of the resulting sample used as template DNA for PCR amplification of a fragment of the CRE recombinase gene and a fragment containing the LoxP sites. For isolation of genomic DNA from skeletal muscle, tissue was incubated with DNA extraction buffer (100Mm NaCl, 25Mm EDTA pH 8, 10mM Tris-Cl pH 8, 0.5% SDS, 1^{mg/ml} Proteinase K) overnight at 56°C. DNA was then isolated by phenol-chloroform extraction and mice were genotyped by assessing PCR amplification of the *Elavl1* gene (exon 2 region). PCR products were visualized by Ethidium Bromide staining on 2% Agarose gel. Primer sequences are provided in **Annex 3**. Supplementary Table 2.

Lewis Lung Carcinoma (LLC) animal model of cachexia

Subcutaneous LLC tumors were established in the right hindlimb region of male muHuR-KO mice or control littermates (8-9 weeks old) by subcutaneously injecting 1×10^6 LLC cells. During the observation phase (30-day post injection), mice were monitored for tumor size and body weight every other day. The tumor volume was calculated using the formula: $(L \times W^2)/2$, where L is the longest tumor diameter and W the perpendicular axis diameter. At the end of experiment, mice were sacrificed by cervical dislocation and muscles were carefully dissected, weighed and frozen in liquid nitrogen or in isopentane precooled in liquid nitrogen. The weight of the spleen (an indicator of an active immune response) and hindlimb fat pad was also determined. muHuR-KO mice or control littermates injected with PBS were used as control.

Energy balance measurement

Indirect calorimetry study was performed in male, age-matched (8-10 week) muHuR-KO and control mice. Housing was under 12h light–12h dark cycle, with free access to food and water. The Oxygen consumption ($\dot{V}O_2$), carbon dioxide production ($\dot{V}CO_2$), and ambulatory activity were measured using a Comprehensive Animal Monitoring System (CLAMS; Columbus Instruments, Columbus, OH) over 72h, following a 24h acclimation period. Measurements proceeded under a constant airflow rate of $1,000^{ml}/min$. The system allowed for eight individually housed mice to be monitored simultaneously. Oxygen consumption ($\dot{V}O_2$) and carbon dioxide production ($\dot{V}CO_2$) were recorded every 10 min. Respiratory exchange ratio (RER) was calculated as $\dot{V}O_2/\dot{V}CO_2$. Ambulatory activity was estimated by the number of infrared beam breaks along the x-axis of the metabolic cage. Heat production on per animal basis was calculated from the following equation: $((3.82 + 1.23 \times RER) \times \dot{V}O_2)$. Data was analyzed using CLAMS examination tool (CLAX; Columbus Instruments) version 2.1.0. Each animal was considered one experimental unit.

Treadmill exhaustion test

Male, age-matched (8-10 week) muHuR-KO mice or control littermates were exercised on a Columbus 1050-RM Exer-3/6 Treadmill. The system allowed for six individual mice

to be exercised simultaneously. Before the exhaustion test, mice were subject to an acclimation process for three consecutive days with the following program: Day 1. Static treadmill band 15min. Day 2. Walking on the treadmill for 15min (5^m/min). Day 3. Running for 10 min (10^m/min). Electric stimulus of 1hz was employed to force mice to run. Exhaustion test was conducted on 2 separate days (2 day resting period in-between) with the following program: 5^m/min for 1 min, 7^m/min for 1 min, 8^m/min for 5 min, followed by an increase of 1^m/min every minute until a maximum velocity of 21^m/min. Exhaustion was considered after 5 second permanence on the electric grid on a 1hz, 0.15mA, 163V electric stimulus. Maximum exercise capacity was estimated from each run-to-exhaustion trial using three parameters: the duration of the run (min), the distance ran (m), and the work performed (J). Work was calculated as $W = \text{body weight (kg)} \times \text{running speed (}^m\text{/min)} \times \text{running time (min)} \times \text{grade} \times 9.8 \text{ (}^J\text{/kg} \times \text{m)}$. Values from the two sessions were averaged to provide exercise capacity. Each animal was considered one experimental unit.

Rota-rod

Male, age-matched (20 weeks), muHuR-KO and control mice were tested on a rota-rod apparatus (Ugo Basile, 47600). Animals received 1 day of training prior to testing with the following program: 5 minutes on acceleration rotarod at 5 revolutions per minute (rpm). Exercise days consisted of a program of the following: 2min at 5rpm followed by an acceleration period from 5rpm to 20rpm in 2min. Tests were considered finished when mice fell off the apparatus. Exercising sessions (two in all) were completed over the period of a week with 4 days of resting in between the sessions. The latency to fall from the rod was recorded for each trial and values from both sessions were averaged to provide the rotarod latency statistic. If the mouse remained on the rod for more than 30 minutes, mice were removed from the machine and the test was considered as completed.

Inverted grid test

Fatigability of limbs was tested using the inverted-grid hanging test. Male, age-matched (20 weeks), muHuR-KO and control animals were placed on a mesh grid (10cm×10cm) mounted 60cm above a padded surface. The grid was then inverted, and

mouse was suspended upside down. Latency to fall from the grid was recorded; the maximum time allowed per trial was 6 minutes. Each mouse was tested in 2 different session consisting of 3 consecutive days each, with 4 days of resting in between sessions. Both sessions were averaged to provide the latency to fall and normalized to total body weight.

Grip Test

Muscle strength of male muHuR-KO and control mice (20 weeks) was evaluated using a DFE II Series Digital Force Gauge (Ametek DFE II 2-LBF 10-N) with an attached metal grid (10cm×10cm). Mice were allowed to grasp the metal grid with either 2 limbs (forelimbs) or 4 limbs (forelimbs and hindlimbs) and gently pulled along the axis of the grid by the tip of the tail. Maximal strength (Newtons) with which mice pulled the grid was measured in two sessions, each one consisting in triplicate trials over 3 consecutive days. 4 days of resting were allowed in-between sessions.

***In situ* assessment of muscle contractile function**

To determine contractile function, mice were anesthetized with an intraperitoneal injection of a ketamine-xylazine cocktail (ketamine: 130 mg/kg; xylazine: 20 mg/kg). Anesthesia was maintained with 0.05 ml supplementary doses as needed. The distal tendon of the left TA muscle was isolated and attached in turn with surgical 4.0 silk to the lever arm of a 305C-LR servomotor (Aurora Scientific Instruments), as done previously, with minor modifications¹⁻³. The Dynamic Muscle Control (DMC) and Analysis Software Suite (Aurora Scientific Instruments) was used for collection and data analysis. The partially exposed muscle surface of the TA was kept moist with PBS (pH 7.4) for the isometric contractile stimulation protocol and was directly stimulated with an electrode placed on the belly of the muscle. *In situ* measurement of the TA with direct stimulation was chosen over sciatic nerve stimulation, thereby removing potential negative effects such as a central contribution and, because blood delivery is intact, eliminating potential problems of isolated muscles⁴. Optimal muscle length and voltage was progressively adjusted to produce maximal tension and length was measured with a microcaliper. The

pulse duration was set to 0.2 ms for all tetanic contractions. Force-frequency relationships curves were determined at muscle optimal length at 10, 30, 50, 70, 100, 120 and 150 Hz, with 1 min intervals between stimulations to avoid fatigue. After tetanic-force measurement, the TA muscle was rested for 2 min and then subjected to 60 tetanic contraction. The fatigue resistance protocol was 60 tetanic contraction (75hz stimulation/200-ms duration) every 2 seconds for a total of 2 min. At the end of each experiment, mice were sacrificed by cervical dislocation and muscles were carefully dissected, weighed and frozen in liquid nitrogen or in isopentane precooled in liquid nitrogen. *In situ* muscle force was normalized to tissue cross-sectional area (expressed as newtons/cm²). Muscle cross-sectional area was estimated by dividing muscle mass by the product of the muscle length and muscle density (1.056 g/cm³). During experiments, the investigators were blinded to mice genotype. Statistical analyses for data related to muscle specific strength were performed using a two-way ANOVA with corrections for multiple comparisons by controlling for the false discovery rate using the two-stage method of Benjamini and Krieger and Yekutieli (with $q < 0.1$ and $P < 0.05$).

Muscle freezing and sectioning

Gastrocnemius, soleus, EDL and peroneus muscles were carefully dissected, mounted on 7% tragacanth gum and snap frozen in liquid-nitrogen-cooled isopentane for 10-20sec. Samples were stored at -80°C before cryosectioning. Sections (10 μm) were kept at room temperature for 30 min before processing.

Cross-sectional analysis

Muscle sections were routinely stained with haematoxylin and eosin (H&E) ²⁹⁵. Wide-field images were taken with a 20X objective lens on an inverted Zeiss Axioskop microscope with an AxioCam MRc color camera in the McGill University Life Sciences Complex Advanced BioImaging Facility. Cross-sectional analysis (CSA) of myofibers in muHuR-KO and control mice was determined on muscle sections. Fibers were circled manually, and area determination was calculated using the Image J software (NIH). A

minimum of five hundred fibers per muscle was used for the calculation of the cross-sectional area.

Immunostaining

Serial muscle cryosections were incubated with the following monoclonal antibodies from the Developmental Studies Hybridoma Bank: BA-D5 (MyHC-I, 1:500), SC-71 (MyHC-IIA, 1:500), and BF-F3 (MyHC-IIB, 1:500)⁶⁸. The immunohistochemical staining was performed using a goat anti-mouse secondary antibody conjugated to peroxidase-labeled complex (Dako, Glostrup, Denmark). After rinsing in PBS buffer section were incubated for 30 min at room temperature with a freshly prepared solution of 10mg of 3,3'-diaminobenzidine tetrahydrochloride (DAB; Sigma, St. Louis, MO) in 15ml of a 0.05M Tris buffer at pH 7.6, containing 1.5ml of 0.3% H₂O₂. Sections were then analyzed using a 20x objective lens on an inverted Zeiss Axioskop microscope.

Cell culture

Murine Lewis Lung carcinoma cells (LLC) were obtained from the ATCC and grown in DMEM with 10% FBS and 1% streptomycin–penicillin (Invitrogen). C2C12 myoblasts (ATCC, Manassas, VA, USA) were grown and maintained in Dulbecco's modified eagle medium (DMEM, Invitrogen) containing 20% FBS, and 1% penicillin/streptomycin antibiotics (Invitrogen). All cells were grown in a humidified incubator at 37°C, 5% CO₂.

Transfection

The transfection of siRNA into C2C12 cells was performed as previously described¹². Briefly, the transfection with siHuR, siKSRP or siCtl was performed when cells were 20–30% confluent. The transfection treatment was repeated 24 h later when cells were 50–60% confluent. All siRNAs duplexes were used at a final concentration of 120 nM. The GFP and GFP-HuR plasmids were generated and used as described in ref.

9. *jetPRIME*[®] (Polyplus) transfection reagent was used for all transfections following the manufacturer's instructions. siRNA oligonucleotides against siHuR, siKSRP as well as the control siRNA Ctl, was obtained from Dharmacon. siRNA sequences are provided in **Annex 3**. Supplementary Table 2.

Preparation of muscle/cell extracts and immunoblotting

Muscle extracts were prepared by homogenization of frozen muscle tissue in extraction buffer (1x PBS, 1% NP-40, 0.5% DOC, 0.1% SDS, 2mM SOV, 1X protease inhibitor (Roche)). Cell extracts were prepared by incubating C2C12 muscle cells with lysis buffer (50mM HEPES pH 7.0, 150mM NaCl, 10% glycerol, 1% Triton, 10mM pyrophosphate sodium, 100mM NaF, 1mM EGTA, 1,5mM MgCl₂, 1X protease inhibitor (Roche) for 15min on ice. The lysed muscle/cells were then centrifuged at 0.1 times gravity (xg) 12000rpm for 15min at 4°C in order to collect the supernatant. Western blot experiments were performed as previously described in ref. 12. Western blots were probed with antibodies against HuR (3A2, 1:10000), PGC-1 α (abcam, 1:1000), KSRP (abcam, 1:5000), Oxphos Antibody Cocktail (containing 5 mouse antibodies against the CI subunit NDUFB8, CII-30kDa, CIII-Core protein 2, CIV subunit I and CV alpha subunit (abcam, 1:1000) or α -tubulin as loading control (Developmental studies Hybridoma Bank, 1:1000).

RT-qPCR

Total RNA was isolated using TRIzol reagent (Invitrogen). 1 μ g of total RNA was reverse transcribed using the M-MuLV RT system according to the manufacturer's instructions (New England BioLab). A 1/80 dilution of cDNA was then used to assess mRNAs expression using SsoFast[™] EvaGreen[®] Supermix (Bio-Rad). Expression level of genes of interest were standardized using *GAPDH* or *RPL32* as reference, and relative levels of expression were quantified by calculating $2^{-\Delta\Delta C_T}$, where $\Delta\Delta C_T$ is the difference in C_T (cycle number at which the amount of amplified target reaches a fixed threshold) between target and reference genes. Primer sequences can be found in **Annex 3**. Supplementary Table 2.

Actinomycin D pulse-chase experiments

The stability of the mRNAs of interest was assessed by the addition of the RNA polymerase II inhibitor, actinomycin D (ActD) ($5\mu\text{g}/\text{ml}$) to GFP, GFP-HuR, siHuR, siKSRP and siCtl treated cells over a 6h period. Total RNA was isolated at the indicated time points, using TRIzol reagent (Invitrogen), and analyzed by RT-qPCR. The expression level of the different mRNAs at each time point was determined relative to *RPL32* mRNA levels and plotted relative to the abundance of each message at 0h of ActD treatment that is considered as 1.

Polysome fractionation

Polysome fractionation was performed as previously described¹². Briefly, the cytoplasmic extracts obtained from myoblasts treated with or without siHuR, collected at 100% confluency, were centrifuged at $130,000 \times g$ for 2h on a sucrose gradient (15–50% w/v). Absorbance at wavelength 254nm was measured in order to determine the profile of polysome distribution. 20 fractions were collected and divided in two groups: non-polysome (NP, fractions 1–6) and polysome (P, fractions 7–20). RNA was then extracted from each group using TRIzol LS (Invitrogen) according to the manufacturer instructions. RNA integrity was monitored on agarose gel and was then analyzed by RT-qPCR using specific primers for *PGC-1 α* and *GAPDH* mRNAs. *PGC-1 α* mRNA level was standardized against *GAPDH* mRNA in each group and plotted as a Polysome to Non-Polysome ratio.

Immunoprecipitation/RNA-IP

Immunoprecipitation/RNA-IP experiments were performed as previously described¹². Briefly, 15 μl of the anti-HuR, anti-KSRP or IgG antibodies were incubated with 60 μl of protein A-Sepharose slurry beads (washed and equilibrated in cell lysis buffer) for 4h at 4°C. Beads were washed three times with cell lysis buffer and incubated with 500 μg of cell extracts overnight at 4°C. Beads were then washed again three times

with cell lysis buffer and co-immunoprecipitated RNA was then eluted and processed for RT-qPCR analysis.

mRNA sequencing (RNA-seq)

Total RNA from soleus muscle from 2 muHuR-KO and 2 control mice was isolated using TRIzol reagent (Invitrogen). RNA samples were assessed for quantity and quality using a NanoDrop UV spectrophotometer (Thermo Fisher Scientific Inc), and a Bioanalyser (Agilent Technology Inc). The 4 RNA-seq libraries were sequenced on the Illumina NextSeq 500 platform at the Institute for Research in Immunology and Cancer (IRIC) Genomics Core Facility, University of Montreal, to produce over 60 million, 100 nucleotide paired-end reads per sample. The reads were then trimmed for sequencing adapters and aligned to the reference mouse genome version mm10 (GRCm38) using Tophat version 2.0.10. Gene quantification was performed on the mapped sequences using the htseq-count software version 0.6.1. We performed a differential expression analysis using DESeq2 package, log transformation was used to normalize raw read counts and to calculate normalized expression counts. Biological replicates were combined, and the data set visualized on a heatmap using the Morpheus software (version 4.7). (Data can be accessed in GEO database, GSE134241).

Ingenuity Pathway Analysis (IPA)

<https://www.qiagenbioinformatics.com/products/ingenuitypathway-analysis>

The RNA-seq dataset generated by DESeq analysis was subjected to a subsequent analysis using the “Ingenuity Pathways Analysis” Software 5.0 (IPA, Ingenuity Systems) to define the main biologic processes associated with the gene expression changes in the muHuR-KO mice. This analysis was performed using detectably-expressed (read number >0) genes across all samples.

Mitochondria number

Mitochondrial number was estimated by determining the mitochondrial to nuclear DNA ratio as previously described⁶⁹. Briefly, genomic DNA from skeletal muscle tissue was incubated with DNA extraction buffer (100Mm NaCl, 25Mm EDTA pH 8, 10mM Tris-

CI pH 8, 0.5% SDS, 1mg/ml Proteinase K) overnight at 56°C. DNA was then isolated by phenol-chloroform extraction. DNA was quantified and diluted to a final concentration of 10^{ng/μl} to be used for qPCR amplification. A comparison of ND1 (NADH dehydrogenase 1, mitochondrial gene) expression relative to HK2 (Hexokinase 2, nuclear gene) DNA expression was used to estimate mtDNA copy number to nDNA copy number ratio.

Statistical analyses

All values are reported as mean ± standard error of the mean (S.E.M). Significant differences between two group means were discerned by unpaired *t*-tests for normally distributed variables. Normality was determined using the D'Agostino–Pearson test where appropriate. Statistical analyses for *in situ* consisted in Two-way ANOVA with corrections for multiple comparisons by controlling for the false discovery rate using the two-stage method of Benjamini and Krieger and Yekutieli⁶⁶. *p* values of <0.05 were considered significant.

9.3.6.- Acknowledgement

We are grateful to Xian Jin Lian for technical help with some of the experiments in the manuscript and Amr Omer for reading and commenting on the manuscript. We thank Michel Tremblay and Maxime Bouchard for their ideas, suggestions, and guidance. We thank Dr. Siegfried Hekimi and Mrs. Eve Bigras for their help with the grip test experiment. This work is funded by CIHR operating grants (MOP-142399, MOP-89798), and a NSERC Discovery grant RGPIN-2014-06035 to I.E.G. B.J.S was funded by a scholarship received from the Consejo Nacional de Ciencia y Tecnologia (CONACyT), the Fonds de recherche du Québec – Nature et technologies (FRQNT) and the Biochemistry department at McGill University. D.T.H. was funded by a scholarship received from the Canadian Institute of Health Research (CIHR) funded Chemical Biology Program at McGill University. J.F.M. was supported by the CIHR/FRSQ training grant in cancer research of the McGill Integrated Cancer Research Training Program.

9.3.7.- References Chapter III

1. Bassel-Duby R, Olson EN. Signaling pathways in skeletal muscle remodeling. *Annu Rev. Biochem.*;75:19–37, (2006)
2. Charge SB, Rudnicki MA. Cellular and molecular regulation of muscle regeneration. *Physiological Rev.*; 84:209–238, (2004)
3. Baracos VE, Martin L, Korc M, Guttridge DC, Fearon KCH. Cancer-associated cachexia. *Nat. Rev. Dis. Prim.*;4:17105, (2018)
4. Schiaffino S, Reggiani C. Fiber types in mammalian skeletal muscles. *Physiol. Rev.*; 91:1447–1531, (2011)
5. Lassche S, et al. Sarcomeric dysfunction contributes to muscle weakness in facioscapulohumeral muscular dystrophy. *Neurology.*;80:733–737, (2013)
6. Chin ER. The role of calcium and calcium/calmodulin-dependent kinases in skeletal muscle plasticity and mitochondrial biogenesis. *Proc. Nutr. Soc.*; 63:279–286, (2004)
7. Lin J, et al. Transcriptional co-activator PGC-1 alpha drives the formation of slow-twitch muscle fibres. *Nature.*;418:797–801, (2002)
8. D'Souza D, Lai RY, Shuen M, Hood DA. mRNA stability as a function of striated muscle oxidative capacity. *Am. J. Physiol. Regul. Integr. Comp. Physiol.*;303: R408–R417, (2012)
9. Beauchamp P, et al. The cleavage of HuR interferes with its transportin-2-mediated nuclear import and promotes muscle fiber formation. *Cell Death Differ.*;17:1588–1599, (2010)
10. von Roretz C, Beauchamp P, Di Marco S, Gallouzi IE. HuR and myogenesis: being in the right place at the right time. *Biochimica et Biophysica Acta.*;1813:1663–1667, (2011)
11. Dormoy-Raclet V, et al. HuR and miR-1192 regulate myogenesis by modulating the translation of HMGB1 mRNA. *Nat. Commun.*;4:2388, (2013)
12. Cammas A, et al. Destabilization of nucleophosmin mRNA by the HuR/KSRP complex is required for muscle fibre formation. *Nat. Commun.*;5:4190, (2014)

13. Briata P, et al. p38-dependent phosphorylation of the mRNA decay-promoting factor KSRP controls the stability of select myogenic transcripts. *Mol. Cell.*;20:891–903, (2005)
14. Katsanou V, et al. The RNA-binding protein Elavl1/HuR is essential for placental branching morphogenesis and embryonic development. *Mol. Cell Biol.*; 29:2762–2776, (2009)
15. Chen JC, Mortimer J, Marley J, Goldhamer DJ. MyoD-cre transgenic mice: a model for conditional mutagenesis and lineage tracing of skeletal muscle. *Genesis.*;41:116–121, (2005)
16. Leduc-Gaudet JP, Reynaud O, Hussain SN, Gouspillou G. Parkin overexpression protects from ageing-related loss of muscle mass and strength. *J. Physiol.*; 597:1975–1991, (2019)
17. Gouspillou G, et al. Protective role of Parkin in skeletal muscle contractile and mitochondrial function. *J. Physiol.*; 596:2565–2579, (2018)
18. Castro B, Kuang S. Evaluation of muscle performance in mice by treadmill exhaustion test and whole-limb grip strength assay. *Bio Protoc.*;7: e2237, (2017)
19. Halling JF, Ringholm S, Olesen J, Prats C, Pilegaard H. Exercise training protects against aging-induced mitochondrial fragmentation in mouse skeletal muscle in a PGC-1alpha dependent manner. *Exp. Gerontol.*;96:1–6, (2017)
20. Picoli CC, et al. Peak velocity as an alternative method for training prescription in mice. *Front. Physiol.*; 9:42, (2018)
21. Niekamp K, et al. Systemic acid load from the diet affects maximal-exercise RER. *Med. Sci. Sports Exerc.*;44:709–715, (2012)
22. Greggio C, et al. Enhanced respiratory chain supercomplex formation in response to exercise in human skeletal muscle. *Cell Metab.*;25:301–311, (2017)
23. Busiello RA, Savarese S, Lombardi A. Mitochondrial uncoupling proteins and energy metabolism. *Front. Physiol.*; 6:36, (2015)

24. Reyes NL, et al. Fnip1 regulates skeletal muscle fiber type specification, fatigue resistance, and susceptibility to muscular dystrophy. *Proc. Natl. Acad. Sci. USA.*;112:424–429, (2015)
25. Terry EE, et al. Transcriptional profiling reveals extraordinary diversity among skeletal muscle tissues. *Elife.*;7: e34613, (2018)
26. Cutler AA, et al. Biochemical isolation of myonuclei employed to define changes to the myonuclear proteome that occur with aging. *Aging Cell.*;16:738–749, (2017)
27. Phillips BL, et al. Post-transcriptional regulation of Pabpn1 by the RNA binding protein HuR. *Nucl. Acids Res.*; 46:7643–7661, (2018)
28. Dauletbaev N, et al. Down-regulation of cytokine-induced interleukin-8 requires inhibition of p38 mitogen-activated protein kinase (MAPK) via MAPK phosphatase 1-dependent and -independent mechanisms. *J. Biol. Chem.*; 286:15998–16007, (2011)
29. Ciciliot S, Rossi AC, Dyar KA, Blaauw B, Schiaffino S. Muscle type and fiber type specificity in muscle wasting. *Int J. Biochem Cell Biol.*; 45:2191–2199, (2013)
30. Sandri M, et al. PGC-1alpha protects skeletal muscle from atrophy by suppressing FoxO3 action and atrophy-specific gene transcription. *Proc. Natl. Acad. Sci. USA.*;103:16260–16265, (2006)
31. Cannavino J, et al. The role of alterations in mitochondrial dynamics and PGC-1alpha over-expression in fast muscle atrophy following hindlimb unloading. *J. Physiol.*; 593:1981–1995, (2015)
32. Deboer MD. Animal models of anorexia and cachexia. *Expert Opin. Drug Disco.*;4:1145–1155, (2009)
33. Hall DT, et al. The AMPK agonist 5-aminoimidazole-4-carboxamide ribonucleotide (AICAR), but not metformin, prevents inflammation-associated cachectic muscle wasting. *EMBO Mol. Med.* (2018)
34. Fearon KC, Glass DJ, Guttridge DC. Cancer cachexia: mediators, signaling, and metabolic pathways. *Cell Metab.*;16:153–166, (2012)
35. Buckingham M. Making muscle in mammals. *Trends Genet.*;8:144–148, (1992)

36. Rudnicki MA, Braun T, Hinuma S, Jaenisch R. Inactivation of MyoD in mice leads to up-regulation of the myogenic HLH gene Myf-5 and results in apparently normal muscle development. *Cell.*;71:383–390, (1992)
37. Braun T, Rudnicki MA, Arnold HH, Jaenisch R. Targeted inactivation of the muscle regulatory gene Myf-5 results in abnormal rib development and perinatal death. *Cell.*;71:369–382, (1992)
38. Rudnicki MA, et al. MyoD or Myf-5 is required for the formation of skeletal muscle. *Cell.*;75:1351–1359, (1993)
39. Song YJ, Lee H. YB1/p32, a nuclear Y-box binding protein 1, is a novel regulator of myoblast differentiation that interacts with Msx1 homeoprotein. *Exp. Cell Res.*; 316:517–529, (2010)
40. Bye AJH, et al. The RNA-binding proteins Zfp36l1 and Zfp36l2 act redundantly in myogenesis. *Skelet. Muscle.*;8:37, (2018)
41. Egan B, Zierath JR. Exercise metabolism and the molecular regulation of skeletal muscle adaptation. *Cell Metab.*;17:162–184, (2013)
42. Perrino C, et al. Cardiovascular effects of treadmill exercise in physiological and pathological preclinical settings. *Am. J. Physiol. Heart Circ. Physiol.*;300:H1983–H1989, (2011)
43. Seidell JC, Muller DC, Sorkin JD, Andres R. Fasting respiratory exchange ratio and resting metabolic rate as predictors of weight gain: the Baltimore Longitudinal Study on Aging. *Int J. Obes. Relat. Metab. Disord.*;16:667–674, (1992)
44. Ehrenborg E, Krook A. Regulation of skeletal muscle physiology and metabolism by peroxisome proliferator-activated receptor delta. *Pharm. Rev.*; 61:373–393, (2009)
45. Zhang C, et al. Tumor suppressor p53 negatively regulates glycolysis stimulated by hypoxia through its target RRAD. *Oncotarget.*;5:5535–5546, (2014)
46. Derave W, Everaert I, Beeckman S, Baguet A. Muscle carnosine metabolism and beta-alanine supplementation in relation to exercise and training. *Sports Med.*; 40:247–263, (2010)

47. Mynatt Randall L., Noland Robert C., Elks Carrie M., Vandanmagsar Bolormaa, Bayless David S., Stone Allison C., Ghosh Sujoy, Ravussin Eric, Warfel Jaycob D. The RNA binding protein HuR influences skeletal muscle metabolic flexibility in rodents and humans. *Metabolism.*;97:40–49, (2019)
48. Myer VE, Fan XC, Steitz JA. Identification of HuR as a protein implicated in AUUUA-mediated mRNA decay. *Embo J.*; 16:2130–2139, (1997)
49. Fan XC, Myer VE, Steitz JA. AU-rich elements target small nuclear RNAs as well as mRNAs for rapid degradation. *Genes Dev.*; 11:2557–2568, (1997)
50. Skliris A, et al. Neuroprotection requires the functions of the RNA-binding protein HuR. *Cell Death Differ.*;22:703–718, (2015)
51. Abdelmohsen K, et al. Phosphorylation of HuR by Chk2 regulates SIRT1 expression. *Mol. Cell.*;25:543–557, (2007)
52. Li H, et al. Lipopolysaccharide-induced methylation of HuR, an mRNA-stabilizing protein, by CARM1. Coactivator-associated arginine methyltransferase. *J. Biol. Chem.*; 277:44623–44630, (2002)
53. Wang Y, Pessin JE. Mechanisms for fiber-type specificity of skeletal muscle atrophy. *Curr. Opin. Clin. Nutr. Metab. Care.*;16:243–250, (2013)
54. Penna F, Ballaro R, Beltra M, De Lucia S, Costelli P. Modulating metabolism to improve cancer-induced muscle wasting. *Oxid. Med. Cell. Longev.*;2018:7153610, (2018)
55. Webster C, Silberstein L, Hays AP, Blau HM. Fast muscle fibers are preferentially affected in Duchenne muscular dystrophy. *Cell.*;52:503–513, (1988)
56. Johns N, Stephens NA, Fearon KC. Muscle wasting in cancer. *Int J. Biochem Cell Biol.*; 45:2215–2229, (2013)
57. Diffie GM, Kalfas K, Al-Majid S, McCarthy DO. Altered expression of skeletal muscle myosin isoforms in cancer cachexia. *Am. J. Physiol. Cell Physiol.*;283:C1376–C1382, (2002)

58. Liu HW, Chang SJ. Moderate exercise suppresses NF-kappaB signaling and activates the SIRT1-AMPK-PGC1alpha axis to attenuate muscle loss in diabetic db/db mice. *Front. Physiol.*; 9:636, (2018)
59. Figueroa A, et al. Role of HuR in skeletal myogenesis through coordinate regulation of muscle differentiation genes. *Mol. Cell. Biol.*; 23:4991–5004, (2003)
60. Dormoy-Raclet V, et al. The RNA-binding protein HuR promotes cell migration and cell invasion by stabilizing the beta-actin mRNA in a U-rich-element-dependent manner. *Mol. Cell. Biol.*; 27:5365–5380, (2007)
61. He WA, et al. NF-kappaB-mediated Pax7 dysregulation in the muscle microenvironment promotes cancer cachexia. *J. Clin. Invest.*;123:4821–4835, (2013)
62. Wang Z, Bhattacharya A, Ivanov DN. Identification of small-molecule inhibitors of the HuR/RNA interaction using a fluorescence polarization screening assay followed by NMR validation. *PLoS ONE.*;10: e0138780, (2015)
63. Lal P, et al. Regulation of HuR structure and function by dihydrotanshinone-I. *Nucl. Acids Res.*; 45:9514–9527, (2017)
64. Muralidharan R, et al. HuR-targeted small molecule inhibitor exhibits cytotoxicity towards human lung cancer cells. *Sci. Rep.*; 7:9694, (2017)
65. Wu JC, et al. Genotyping of hepatitis D virus by restriction-fragment length polymorphism and relation to outcome of hepatitis D. *Lancet.*;346:939–941, (1995)
66. Benjamini Yoav, Krieger Abba M., Yekutieli Daniel. Adaptive linear step-up procedures that control the false discovery rate. *Biometrika.*;93:491–507, (2006)
67. Meinen S, Barzaghi P, Lin S, Lochmuller H, Ruegg MA. Linker molecules between laminins and dystroglycan ameliorate laminin-alpha2-deficient muscular dystrophy at all disease stages. *J. Cell Biol.*; 176:979–993, (2007)
68. Schiaffino S, et al. Three myosin heavy chain isoforms in type 2 skeletal muscle fibres. *J. Muscle Res. Cell Motil.*;10:197–205, (1989)
69. Quiros PM, Goyal A, Jha P, Auwerx J. Analysis of mtDNA/nDNA ratio in mice. *Curr. Protoc. Mouse Biol.*; 7:47–54, (2017)

10. General Discussion

The goal of this thesis was to further our understanding of the molecular mechanisms governing HuR-mediated post-transcriptional regulatory events in skeletal muscle. To this end, we have uncovered a novel HuR protein-protein interaction (PPI) network of RBPs involved in myogenesis and, furthermore, have defined mechanistically how these interactions govern the function of HuR in the myogenic process. In addition, we have also discovered the physiological importance of HuR in mediating the function of skeletal muscle *in vivo*. In Chapter I we show that HuR mediates the early stages of muscle fiber formation, when myoblasts are in a proliferative phase, by destabilizing the *NPM* mRNA. The HuR-mediated decay of the *NPM* mRNA relies on its interaction with the RBP KSRP. The association of HuR with KSRP, which occurs in an RNA independent manner, switches the function of HuR from a mediator of mRNA stability to a promoter of mRNA decay. The molecular mechanism leading to *NPM* mRNA degradation involve the recruitment of the exonucleases PARN and components of the exosome (EXOSC5). In Chapter II we show that during the pre-terminal stage of myogenesis, when myoblast begin to fuse into muscle fibers, HuR collaborates with yet another protein partner, the RBP YB1, to stabilize the *Myog* mRNA, a pivotal driver of myoblast differentiation. In order for YB1 and HuR association to occur, HuR must translocate from the nucleus to the cytoplasm. Upon its association to YB1, the HuR/YB1 complex collaboratively associated to a specific G/URE in 3'UTR of the *Myog* mRNA leading to its stabilization, increased expression and, subsequently, to the promotion of muscle cell differentiation. These findings clearly define the mechanisms through which HuR regulates, *in vitro*, the differentiation of muscle cells.

It is not surprising that HuR exerts different/opposite effects on its target transcripts during myogenesis. Our work confirms what numerous reports have suggested, that a collaboration or competition between trans-acting factors is an integral part of the HuR-mediated posttranscriptional regulation of gene expression^{7,197,238-242,265,268,276,289,290}. In addition, it clearly establishes that, through its association to different trans-acting partners, HuR manages to differentially regulate the expression of several mRNAs at different posttranscriptional levels in precise spatial and temporal patterns. Although the

mechanism(s) through which HuR differentially interacts with protein partners remains unknown, cumulative evidence from our laboratory and others indicate that post-translational modification(s) play a crucial role in determining which proteins partners HuR interacts with during the different stages of the myogenic process.

Posttranslational modifications have been previously shown to directly influence the subcellular localization of HuR as well as its RNA-binding activity. Phosphorylation of HuR by the p38 mitogen-activated protein kinase (MAPK), for example, increases its cytoplasmic accumulation resulting in the increased binding to the *p21* mRNA which, consequently, augments p21 protein expression, triggering cell cycle arrest²⁹⁶. In contrast, phosphorylation of HuR by checkpoint kinase 2 (CHK2) at S88, S100, and T118 does not affect HuR's subcellular localization but instead alters HuR's binding to its mRNA target *SIRT1*, triggering *SIRT1* mRNA decay²⁹⁷. The phosphorylation of HuR by Cyclin-Dependent Kinase 1 (CDK1) at S202, located in the hinge region was also shown to retain HuR in the nucleus²⁹⁸. Similarly, methylation at R217 located in the HNS region of HuR, by the methyltransferase CARM1, leads to cytoplasmic localization of HuR, and increased HuR-dependent stabilization of the tumor necrosis alpha (TNF α) mRNA²⁹⁹. Although these results indicate that posttranslational modification affect HuR subcellular localization and/or RNA binding activity, it does not directly link this modification to their impact on HuR binding to its protein partners²⁹⁶. Our unpublished data, suggest that HuR association to key protein partners during myogenesis is not regulated by either phosphorylation or methylation but rather by a novel posttranslational modifications of HuR, Poly(ADP)-ribosylation (PARylation), a reaction through which PARPs (Poly(ADP-ribose) polymerase) transfer the ADP-ribose moiety to acceptor amino acids in their substrates^{300,301}. It is therefore possible that the PARylation of HuR dictates its specificity for binding to protein partners, such as KSRP or YB1, during the myogenic process.

In Chapter III, we investigated the *in vivo* role of HuR in the formation, development and function of skeletal muscle. By breeding mice carrying the *Elavl1^{fl/fl}* allele³⁰² with mice expressing Cre recombinase under the control of the *MyoD* promoter³⁰³, we generated *Elavl1* muscle-specific knockout (muHuR-KO) mice. muHuR-KO mice were viable and showed no visible defect in muscle integrity and formation but exhibit an enhanced exercise endurance which is linked to an increase in the number of oxidative type I fibers

in several skeletal muscles²³⁸. While the viability of muHuR-KO mice may appear to be counterintuitive to the findings described in Chapter I and Chapter II, this is not as surprising as we may presume. Viability of muHuR-KO mice is reminiscent of findings observed in mice bearing loss-of-function mutations in the *MyoD* or *Myf5* genes. Although knocking out either one of these genes did not affect the viability of mice, nor development of muscle, the double knockout of both *MyoD* and *Myf5* genes generated mice without functional muscles that die soon after birth³⁰⁴. These results indicate that MyoD and Myf5 proteins have an overlapping role in muscle development and formation during embryogenesis. As mentioned in Chapter II, HuR and YB1 associate to ~ 400 common mRNA targets in muscle cells. It is, therefore, possible that compensatory mechanism may exist, *in vivo*, to overcome the loss of HuR on the development/formation of skeletal muscle. Functional redundancy with RBPs, such as YB1, could account for the mild phenotype observed in muHuR-KO mice. However, further studies are necessary to elucidate such possibilities and their impact *in vivo*.

The data presented in Chapter III clearly demonstrate that HuR plays a prominent role in mediating the formation and metabolism of type II fibers in skeletal muscle and prove that HuR mediates these effects, in part, by collaborating with KSRP to destabilize the *PGC-1 α* mRNA. Given that altered metabolism has been linked with numerous skeletal muscle pathologies/disorders such as sarcopenia, cachexia-induced muscle wasting and DMD, major clinical interest exists in understanding/uncovering the mechanisms involved in the diversification in physiological character and metabolic activity of fiber types and, furthermore, their repercussions in health and disease. muHuR-KO mice show a significant increase in exercise endurance, a phenotype that is explained in part by an enrichment of type I fibers. While this enrichment of oxidative fibers is strongly linked to the increase in PGC-1 α levels^{70 71}, it is likely that additional players are involved. Our RNA-seq data indicate that genes involved in the PPAR α signaling pathway are the most affected by the depletion of HuR in muscle²³⁸ (**Annex 3**. Supplemental Fig. 5 and Supplementary Data 1). Several of these genes, such as sarcoplasmic reticulum Ca²⁺ -ATPases (SLN), Ras-related glycolysis inhibitor, and calcium channel regulator (Rrad), insulin receptor substrate 2 (irs2), and peptide transporter 2 (PEPT2) are associated with metabolic imbalance and weight-related diseases³⁰⁵⁻³⁰⁸.

Moreover, it was recently demonstrated, using a skeletal muscle specific HuR knockout mouse obtained by crossing *Elavl1^{fl/fl}* mice with mice expressing Cre under the control of the myosin light chain 1f (*Mlc1f*) promoter (activated as early as E12.5), that HuR influences skeletal muscle metabolic flexibility. These mice showed mild obesity, impaired glucose tolerance and impaired fat oxidation when compared to control littermates³⁰⁹. These results further support our hypothesis that *in vivo* HuR could be involved in metabolic plasticity, and importantly denote that the timely expression of HuR strongly influences its impact on muscle function and physiology. Furthermore, preliminary evidence from our laboratory further supports this notion as knocking out HuR in muscle at earlier stages of embryonic development (using the Cre-LoxP system under the control of the *Myf5* promoter significantly reduced both the total number and size of muscle fibers. These mice, additionally, exhibited a significant delay in the regenerative capacity of tibialis anterior (TA) muscle treated with cardiotoxin (CTX), a potent inducer of muscle injury/regeneration (data not shown). These results suggest that the effect of knocking out HuR on the development and/or function of skeletal muscle is dictated by the timing of activation of the muscle specific promoters (*MyoD*, *Myf5*, *Mlc1f*) used to express CRE-recombinase during embryogenesis.

Our data also show that changes in oxidative capacity and fiber type composition, towards oxidative fibers, leads to a protection against cancer induce muscle wasting in a pre-clinical murine LLC-model of cachexia. Tumor-bearing muHuR-KO mice showed a much smaller decrease in muscle fiber diameter and a reduce induction of the ubiquitin ligases atrogen-1 and MuRF-1 when compared to control mice. These results are consistent with numerous studies demonstrating the therapeutic benefit of promoting oxidative metabolic adaptations in skeletal muscle^{31,61,79,310,311} and provide a proof-of-principle that modulating HuR levels can be targeted to prevent cancer-induced muscle loss. Given the systemic importance of HuR, a direct inhibition of HuR by small molecules such as CMLD-2³¹², DHTS³¹³ and MS-444³¹⁴, may prove to be challenging due to potential side effects, as well as their mechanisms for specific delivery to muscle tissue. Some of these issues may be circumvented, however, by limiting HuR interaction with specific protein partners which we have shown is determinant in its mRNA binding selectivity. Additionally, it could be possible to regulate HuR-mediated gene expression

by targeting nuclear/cytoplasmatic ratios during myogenesis hence preventing its interaction with specific RBPs and miRNAs. However, future studies will be needed to address this possibility.

11. Conclusion

In conclusion, the work contained in this thesis establishes a novel way through which muscle cells, via the HuR-mediated regulatory network, control gene expression and fine tune protein production. Our results indicate that networks of transacting factors, which include the RNA binding protein HuR, are involved in mediating key physiological processes such as myogenesis. While the full extent of the HuR-mediated post-transcriptional regulatory network is yet to be delineated, it is clear that our findings helped uncover the complex nature through which HuR regulates the myogenic process.

I have provided evidence that the multifunctional nature of HuR results from its ability to interact with different trans-acting factors and that these HuR-mediated interactions are spatio/temporal regulated. I have proven that the molecular mechanisms behind HuR's destabilizing function on *NPM* and *PGC-1 α* mRNAs in skeletal muscle fibers involves its collaboration with KSRP. During the course of this work, I have also identified 40 putative protein-partners (**Annex 2**. Supp. Table 1) of HuR that might be involved in the HuR-mediated regulation of myogenesis, and I have established that one of this protein partners, the RBP YB1, directly associates to HuR during the late stages of myogenesis to stabilize the *Myog* mRNA. I also provided a list of 409 common mRNA targets for YB1 and HuR in muscle cells (**Fig. 3.3a-b**) indicating that in addition to regulating the expression of *Myog*, the HuR/YB1 complex mediates the expression of several other promyogenic targets. This dynamic remodelling of RNPs that HuR is associated with throughout the myogenic process ensures that a broad range of tight and rapid post-transcriptional responses can be used to control the expression of anti- and pro-myogenic proteins in skeletal muscle.

Due to its ubiquitous expression and pleiotropic functions, it is possible that a HuR-mediated regulatory network is implicated in a variety of processes, and cellular systems.

While some of HuR functions are bound to be muscle specific, such as the stabilization of *MyoD* and *Myog* mRNAs, it would be interesting to assess, whether other of its functions are more general as in the case of the downregulation of *NPM*. Does HuR play a role in the regulation of *NPM* in other types of cellular differentiation where downregulation of *NPM* has been shown to be necessary? Similarly, Does the HuR-mediated stabilization of *PGC-1 α* exist in other metabolically active tissues, such as brain, liver or heart? What is its repercussion at a physiological level? Future studies will be necessary to examine the commonality of these regulatory networks in other processes or cellular systems.

In addition, our work has opened up the possibility of new therapeutic venues for the treatment of muscle related diseases. It is well established that in the presence of inflammatory cytokines, HuR activity changes from a promoter of muscle fiber formation to a promoter of muscle wasting due to its increased affinity for mRNA encoding mediators of muscle loss such as *iNOS*²³⁶ and *STAT3*²³⁹. Inflammatory signals have been shown to mediate posttranslational modification such as ubiquitination, phosphorylation, polyubiquitination, methylation, and acetylation³¹⁵. Hence it is possible that HuR dichotomy results from posttranslational modification that influence HuR selectivity for its physiological protein partners hence affecting its selectivity for RNA targets. This change in selectivity could also result from aberrant protein-protein interactions with novel trans-acting factor which drive HuR's function during inflammation. If this is the case... Can such interaction be targeted pharmacologically? Given that proteins often interface with their binding partners using distinct surfaces, structure-guided design can be a viable approach for targeting such associations. However, one major challenge will be to unravel the high level of complexity of PPI networks, especially when considering their multifactorial nature, where a fine modulation of one component may cause great consequences on another. The viability of muHuR-KO mice, described in Chapter III, is a clear example of such complexity. While it seems evident that some compensatory response is partially balancing the effect of HuR depletion in skeletal muscle, we still don't know who is responsible for this compensation. What is their relative contribution in the wildtype situation? And how does this factor/factors compensate for HuR depletion?

12. Bibliography

- 1 Bentzinger, C. F., Wang, Y. X. & Rudnicki, M. A. Building muscle: molecular regulation of myogenesis. *Cold Spring Harb Perspect Biol* **4** (2012).
- 2 Bonaldo, P. & Sandri, M. Cellular and molecular mechanisms of muscle atrophy. *Dis Model Mech* **6**, 25-39 (2013).
- 3 Cohen, S., Nathan, J. A. & Goldberg, A. L. Muscle wasting in disease: molecular mechanisms and promising therapies. *Nature reviews. Drug discovery* **14**, 58-74 (2015).
- 4 Ma, J. F., Hall, D. T. & Gallouzi, I. E. The impact of mRNA turnover and translation on age-related muscle loss. *Ageing Res Rev* (2012).
- 5 Apponi, L. H., Corbett, A. H. & Pavlath, G. K. RNA-binding proteins and gene regulation in myogenesis. *Trends Pharmacol Sci* **32**, 652-658 (2011).
- 6 Figueroa, A. *et al.* Role of HuR in skeletal myogenesis through coordinate regulation of muscle differentiation genes. *Molecular and cellular biology* **23**, 4991-5004 (2003).
- 7 von Roretz, C., Beauchamp, P., Di Marco, S. & Gallouzi, I. E. HuR and myogenesis: being in the right place at the right time. *Biochimica et biophysica acta* **1813**, 1663-1667 (2011).
- 8 Asfour, H. A., Allouh, M. Z. & Said, R. S. Myogenic regulatory factors: The orchestrators of myogenesis after 30 years of discovery. *Exp Biol Med (Maywood)* **243**, 118-128 (2018).
- 9 Di Marco, S. *et al.* The translation inhibitor pateamine A prevents cachexia-induced muscle wasting in mice. *Nat Commun* **3**, 896 (2012).
- 10 Beauchamp, P. *et al.* The cleavage of HuR interferes with its transportin-2-mediated nuclear import and promotes muscle fiber formation. *Cell death and differentiation* (2010).
- 11 van der Giessen, K., Di-Marco, S., Clair, E. & Gallouzi, I. E. RNAi-mediated HuR depletion leads to the inhibition of muscle cell differentiation. *The Journal of biological chemistry* **278**, 47119-47128 (2003).
- 12 Dormoy-Raclet, V. *et al.* HuR and miR-1192 regulate myogenesis by modulating the translation of HMGB1 mRNA. *Nat Commun* **4**, 2388 (2013).
- 13 Hill, J. A., Olson, E. N. & Griendling, K. K. (Academic Press, London ;, 2012).
- 14 Mukund, K. & Subramaniam, S. Skeletal muscle: A review of molecular structure and function, in health and disease. *Wiley Interdiscip Rev Syst Biol Med* **12**, e1462 (2020).
- 15 Frank, G. B., Bianchi, C. P. & Keurs, H. E. D. J. *Advances in Experimental Medicine and Biology*, 0065-2598 ; 311 (Springer US, Boston, MA, 1992).
- 16 Brozovich, F. V. *et al.* Mechanisms of Vascular Smooth Muscle Contraction and the Basis for Pharmacologic Treatment of Smooth Muscle Disorders. *Pharmacological reviews* **68**, 476-532 (2016).
- 17 E H Sonnenblick, a. & A C Stam, J. Cardiac Muscle: Activation and Contraction. *Annual Review of Physiology* **31**, 647-674 (1969).
- 18 Tsang, H. H., Tse, K. M., Chan, K. Y., Lu, G. & Lau, A. K. T. Energy absorption of muscle-inspired hierarchical structure: Experimental investigation. *Composite Structures* **226**, 111250 (2019).

- 19 Dennis, J. *Muscle Cells Develop Forces by Means of Cycles of Protein–Protein Interaction*, https://www.macmillanhighered.com/BrainHoney/Resource/6716/digital_first_content/trunk/est/hillis2e/hillis2e_ch33_2.html
- 20 Buchthal, F. & Schmalbruch, H. Motor unit of mammalian muscle. *Physiol Rev* **60**, 90-142 (1980).
- 21 Rudolf, R., Khan, M. M. & Witzemann, V. Motor Endplate-Anatomical, Functional, and Molecular Concepts in the Historical Perspective. *Cells* **8** (2019).
- 22 Squire, J. M. Muscle contraction: Sliding filament history, sarcomere dynamics and the two Huxleys. *Glob Cardiol Sci Pract* **2016**, e201611 (2016).
- 23 Schiaffino, S. & Reggiani, C. Fiber Types in Mammalian Skeletal Muscles. *Physiological Reviews* **91**, 1447-1531 (2011).
- 24 Resnicow, D. I., Deacon, J. C., Warrick, H. M., Spudich, J. A. & Leinwand, L. A. Functional diversity among a family of human skeletal muscle myosin motors. *Proc Natl Acad Sci U S A* **107**, 1053-1058 (2010).
- 25 Reiser, P. J., Moss, R. L., Giulian, G. G. & Greaser, M. L. Shortening velocity in single fibers from adult rabbit soleus muscles is correlated with myosin heavy chain composition. *The Journal of biological chemistry* **260**, 9077-9080 (1985).
- 26 Bottinelli, R. & Reggiani, C. Human skeletal muscle fibres: molecular and functional diversity. *Progress in biophysics and molecular biology* **73**, 195-262 (2000).
- 27 Richard, A. F. *et al.* Genesis of muscle fiber-type diversity during mouse embryogenesis relies on Six1 and Six4 gene expression. *Developmental biology* **359**, 303-320 (2011).
- 28 Grifone, R. *et al.* Six1 and Eya1 expression can reprogram adult muscle from the slow-twitch phenotype into the fast-twitch phenotype. *Mol Cell Biol* **24**, 6253-6267 (2004).
- 29 Schiaffino, S. & Reggiani, C. Fiber types in mammalian skeletal muscles. *Physiol Rev* **91**, 1447-1531 (2011).
- 30 Schiaffino, S., Sandri, M. & Murgia, M. Activity-dependent signaling pathways controlling muscle diversity and plasticity. *Physiology (Bethesda)* **22**, 269-278 (2007).
- 31 Yan, Z., Okutsu, M., Akhtar, Y. N. & Lira, V. A. Regulation of exercise-induced fiber type transformation, mitochondrial biogenesis, and angiogenesis in skeletal muscle. *Journal of applied physiology (Bethesda, Md. : 1985)* **110**, 264-274 (2011).
- 32 Bassel-Duby, R. & Olson, E. N. Signaling pathways in skeletal muscle remodeling. *Annu Rev Biochem* **75**, 19-37 (2006).
- 33 Kemi, O. J., Loennechen, J. P., Wisloff, U. & Ellingsen, O. Intensity-controlled treadmill running in mice: cardiac and skeletal muscle hypertrophy. *Journal of applied physiology (Bethesda, Md. : 1985)* **93**, 1301-1309 (2002).
- 34 Qaisar, R., Bhaskaran, S. & Van Remmen, H. Muscle fiber type diversification during exercise and regeneration. *Free Radic Biol Med* **98**, 56-67 (2016).
- 35 MÅrin, P., Andersson, B., Krotkiewski, M. & Björntorp, P. Muscle Fiber Composition and Capillary Density in Women and Men With NIDDM. *Diabetes Care* **17**, 382-386 (1994).
- 36 Stuart, C. A. *et al.* Slow-Twitch Fiber Proportion in Skeletal Muscle Correlates With Insulin Responsiveness. *The Journal of Clinical Endocrinology & Metabolism* **98**, 2027-2036 (2013).

- 37 Gaster, M., Staehr, P., Beck-Nielsen, H., Schrøder, H. D. & Handberg, A. GLUT4 Is Reduced in Slow Muscle Fibers of Type 2 Diabetic Patients. *Is Insulin Resistance in Type 2 Diabetes a Slow, Type 1 Fiber Disease?* **50**, 1324-1329 (2001).
- 38 Oberbach, A. *et al.* Altered Fiber Distribution and Fiber-Specific Glycolytic and Oxidative Enzyme Activity in Skeletal Muscle of Patients With Type 2 Diabetes. *Diabetes Care* **29**, 895-900 (2006).
- 39 Vega, R. B., Huss, J. M. & Kelly, D. P. The coactivator PGC-1 cooperates with peroxisome proliferator-activated receptor alpha in transcriptional control of nuclear genes encoding mitochondrial fatty acid oxidation enzymes. *Mol Cell Biol* **20**, 1868-1876 (2000).
- 40 Lefebvre, P., Chinetti, G., Fruchart, J. C. & Staels, B. Sorting out the roles of PPAR alpha in energy metabolism and vascular homeostasis. *J Clin Invest* **116**, 571-580 (2006).
- 41 Baskin, K. K., Winders, B. R. & Olson, E. N. Muscle as a "mediator" of systemic metabolism. *Cell metabolism* **21**, 237-248 (2015).
- 42 Burris, T. P. *et al.* Nuclear receptors and their selective pharmacologic modulators. *Pharmacological reviews* **65**, 710-778 (2013).
- 43 Madrazo, J. A. & Kelly, D. P. The PPAR trio: regulators of myocardial energy metabolism in health and disease. *J Mol Cell Cardiol* **44**, 968-975 (2008).
- 44 Youssef, J. A. & Badr, M. Z. in *Peroxisome Proliferator-Activated Receptors: Discovery and Recent Advances* 33-69 (Humana Press, 2013).
- 45 Ame, J. C., Spenlehauer, C. & de Murcia, G. The PARP superfamily. *BioEssays : news and reviews in molecular, cellular and developmental biology* **26**, 882-893 (2004).
- 46 Berger, J. & Moller, D. E. The mechanisms of action of PPARs. *Annual review of medicine* **53**, 409-435 (2002).
- 47 Tontonoz, P., Hu, E. & Spiegelman, B. M. Stimulation of adipogenesis in fibroblasts by PPAR gamma 2, a lipid-activated transcription factor. *Cell* **79**, 1147-1156 (1994).
- 48 Shook, R. P. *et al.* High respiratory quotient is associated with increases in body weight and fat mass in young adults. *European journal of clinical nutrition* **70**, 1197-1202 (2016).
- 49 Sfeir, Z., Ibrahimi, A., Amri, E., Grimaldi, P. & Abumrad, N. Regulation of FAT/CD36 gene expression: further evidence in support of a role of the protein in fatty acid binding/transport. *Prostaglandins Leukot Essent Fatty Acids* **57**, 17-21 (1997).
- 50 Braissant, O., Foufelle, F., Scotto, C., Dauça, M. & Wahli, W. Differential expression of peroxisome proliferator-activated receptors (PPARs): tissue distribution of PPAR-alpha, -beta, and -gamma in the adult rat. *Endocrinology* **137**, 354-366 (1996).
- 51 Muoio, D. M. *et al.* Fatty acid homeostasis and induction of lipid regulatory genes in skeletal muscles of peroxisome proliferator-activated receptor (PPAR) alpha knock-out mice. Evidence for compensatory regulation by PPAR delta. *The Journal of biological chemistry* **277**, 26089-26097 (2002).
- 52 Holst, D. *et al.* Nutritional regulation and role of peroxisome proliferator-activated receptor delta in fatty acid catabolism in skeletal muscle. *Biochim Biophys Acta* **1633**, 43-50 (2003).
- 53 Ehrenborg, E. & Krook, A. Regulation of skeletal muscle physiology and metabolism by peroxisome proliferator-activated receptor delta. *Pharmacological reviews* **61**, 373-393 (2009).

- 54 Kannisto, K. *et al.* Differential expression of peroxisomal proliferator activated receptors alpha and delta in skeletal muscle in response to changes in diet and exercise. *International journal of molecular medicine* **17**, 45-52 (2006).
- 55 Kersten, S. Peroxisome proliferator activated receptors and lipoprotein metabolism. *PPAR Res* **2008**, 132960 (2008).
- 56 Tan, N. S. *et al.* Selective cooperation between fatty acid binding proteins and peroxisome proliferator-activated receptors in regulating transcription. *Mol Cell Biol* **22**, 5114-5127 (2002).
- 57 Song, S. *et al.* Peroxisome proliferator activated receptor alpha (PPARalpha) and PPAR gamma coactivator (PGC-1alpha) induce carnitine palmitoyltransferase IA (CPT-1A) via independent gene elements. *Mol Cell Endocrinol* **325**, 54-63 (2010).
- 58 Djouadi, F., Aubey, F., Schlemmer, D. & Bastin, J. Peroxisome Proliferator Activated Receptor δ (PPAR δ) Agonist But Not PPAR α Corrects Carnitine Palmitoyl Transferase 2 Deficiency in Human Muscle Cells. *The Journal of Clinical Endocrinology & Metabolism* **90**, 1791-1797 (2005).
- 59 Schuler, M. *et al.* PGC1alpha expression is controlled in skeletal muscles by PPARbeta, whose ablation results in fiber-type switching, obesity, and type 2 diabetes. *Cell metabolism* **4**, 407-414 (2006).
- 60 Wang, Y. X. *et al.* Regulation of muscle fiber type and running endurance by PPARdelta. *PLoS Biol* **2**, e294 (2004).
- 61 Russell, A. P., Hesselink, M. K., Lo, S. K. & Schrauwen, P. Regulation of metabolic transcriptional co-activators and transcription factors with acute exercise. *Faseb J* **19**, 986-988 (2005).
- 62 Russell, A. P. *et al.* Endurance Training in Humans Leads to Fiber Type-Specific Increases in Levels of Peroxisome Proliferator-Activated Receptor- γ Coactivator-1 and Peroxisome Proliferator-Activated Receptor- α in Skeletal Muscle. *Diabetes* **52**, 2874-2881 (2003).
- 63 Krämer, D. K. *et al.* Human skeletal muscle fibre type variations correlate with PPAR α , PPAR δ and PGC-1 α mRNA. *Acta Physiologica* **188**, 207-216 (2006).
- 64 Kramer, D. K. *et al.* Human skeletal muscle fibre type variations correlate with PPAR alpha, PPAR delta and PGC-1 alpha mRNA. *Acta physiologica (Oxford, England)* **188**, 207-216 (2006).
- 65 Viswakarma, N. *et al.* Coactivators in PPAR-Regulated Gene Expression. *PPAR Research* **2010**, 250126 (2010).
- 66 Puigserver, P. & Spiegelman, B. M. Peroxisome proliferator-activated receptor-gamma coactivator 1 alpha (PGC-1 alpha): transcriptional coactivator and metabolic regulator. *Endocrine reviews* **24**, 78-90 (2003).
- 67 Kang, C. & Li Ji, L. Role of PGC-1alpha signaling in skeletal muscle health and disease. *Annals of the New York Academy of Sciences* **1271**, 110-117 (2012).
- 68 Fernandez-Marcos, P. J. & Auwerx, J. Regulation of PGC-1alpha, a nodal regulator of mitochondrial biogenesis. *Am J Clin Nutr* **93**, 884s-890 (2011).
- 69 Lin, J., Handschin, C. & Spiegelman, B. M. Metabolic control through the PGC-1 family of transcription coactivators. *Cell metabolism* **1**, 361-370 (2005).
- 70 Cheng, C. F., Ku, H. C. & Lin, H. PGC-1 α as a Pivotal Factor in Lipid and Metabolic Regulation. *International journal of molecular sciences* **19** (2018).

- 71 Lin, J. *et al.* Transcriptional co-activator PGC-1 alpha drives the formation of slow-twitch muscle fibres. *Nature* **418**, 797-801 (2002).
- 72 Handschin, C. *et al.* Skeletal muscle fiber-type switching, exercise intolerance, and myopathy in PGC-1alpha muscle-specific knock-out animals. *The Journal of biological chemistry* **282**, 30014-30021 (2007).
- 73 He, J., Watkins, S. & Kelley, D. E. Skeletal muscle lipid content and oxidative enzyme activity in relation to muscle fiber type in type 2 diabetes and obesity. *Diabetes* **50**, 817-823 (2001).
- 74 Mensink, M. *et al.* Improved skeletal muscle oxidative enzyme activity and restoration of PGC-1 alpha and PPAR beta/delta gene expression upon rosiglitazone treatment in obese patients with type 2 diabetes mellitus. *International journal of obesity (2005)* **31**, 1302-1310 (2007).
- 75 Ciciliot, S., Rossi, A. C., Dyar, K. A., Blaauw, B. & Schiaffino, S. Muscle type and fiber type specificity in muscle wasting. *The international journal of biochemistry & cell biology* **45**, 2191-2199 (2013).
- 76 Webster, C., Silberstein, L., Hays, A. P. & Blau, H. M. Fast muscle fibers are preferentially affected in Duchenne muscular dystrophy. *Cell* **52**, 503-513 (1988).
- 77 Wang, Y. & Pessin, J. E. Mechanisms for fiber-type specificity of skeletal muscle atrophy. *Current opinion in clinical nutrition and metabolic care* **16**, 243-250 (2013).
- 78 von Walden, F., Jakobsson, F., Edström, L. & Nader, G. A. Altered autophagy gene expression and persistent atrophy suggest impaired remodeling in chronic hemiplegic human skeletal muscle. *Muscle & Nerve* **46**, 785-792 (2012).
- 79 Sandri, M. *et al.* PGC-1alpha protects skeletal muscle from atrophy by suppressing FoxO3 action and atrophy-specific gene transcription. *Proc Natl Acad Sci U S A* **103**, 16260-16265 (2006).
- 80 Jagoe, R. T. & Goldberg, A. L. What do we really know about the ubiquitin-proteasome pathway in muscle atrophy? *Current opinion in clinical nutrition and metabolic care* **4**, 183-190 (2001).
- 81 Kuang, S., Gillespie, M. A. & Rudnicki, M. A. Niche regulation of muscle satellite cell self-renewal and differentiation. *Cell Stem Cell* **2**, 22-31 (2008).
- 82 Rudnicki, M. A., Le Grand, F., McKinnell, I. & Kuang, S. The molecular regulation of muscle stem cell function. *Cold Spring Harb Symp Quant Biol* **73**, 323-331 (2008).
- 83 Wang, Y. X., Bentzinger, C. F. & Rudnicki, M. A. Molecular regulation of determination in asymmetrically dividing muscle stem cells. *Cell cycle* **12** (2012).
- 84 Bismuth, K. & Relaix, F. Genetic regulation of skeletal muscle development. *Exp Cell Res* **316**, 3081-3086 (2010).
- 85 Arnold, S. J. & Robertson, E. J. Making a commitment: cell lineage allocation and axis patterning in the early mouse embryo. *Nat Rev Mol Cell Biol* **10**, 91-103 (2009).
- 86 Aulehla, A. & Pourquié, O. On periodicity and directionality of somitogenesis. *Anat Embryol (Berl)* **211 Suppl 1**, 3-8 (2006).
- 87 Musumeci, G. *et al.* Somitogenesis: From somite to skeletal muscle. *Acta Histochem* **117**, 313-328 (2015).
- 88 DeSesso, J. M. Vascular ontogeny within selected thoracoabdominal organs and the limbs. *Reproductive Toxicology* **70**, 3-20 (2017).

- 89 Wu, W. *et al.* The Role of *Six1* in the Genesis of Muscle Cell and Skeletal Muscle Development. *International Journal of Biological Sciences* **10**, 983-989 (2014).
- 90 Laclef, C. *et al.* Altered myogenesis in *Six1*-deficient mice. *Development* **130**, 2239-2252 (2003).
- 91 Grifone, R. *et al.* *Six1* and *Six4* homeoproteins are required for *Pax3* and *Mrf* expression during myogenesis in the mouse embryo. *Development* **132**, 2235-2249 (2005).
- 92 Lagha, M. *et al.* Regulation of skeletal muscle stem cell behavior by *Pax3* and *Pax7*. *Cold Spring Harb Symp Quant Biol* **73**, 307-315 (2008).
- 93 Marcelle, C., Stark, M. R. & Bronner-Fraser, M. Coordinate actions of BMPs, Wnts, Shh and noggin mediate patterning of the dorsal somite. *Development* **124**, 3955-3963 (1997).
- 94 Rudnicki, M. A. & Williams, B. O. Wnt signaling in bone and muscle. *Bone* **80**, 60-66 (2015).
- 95 Tickle, C. & Towers, M. Sonic Hedgehog Signaling in Limb Development. *Front Cell Dev Biol* **5**, 14 (2017).
- 96 Hollway, G. & Currie, P. Vertebrate myotome development. *Birth Defects Res C Embryo Today* **75**, 172-179 (2005).
- 97 Deries, M., Schweitzer, R. & Duxson, M. J. Developmental fate of the mammalian myotome. *Dev Dyn* **239**, 2898-2910 (2010).
- 98 Buckingham, M. & Rigby, Peter W. J. Gene Regulatory Networks and Transcriptional Mechanisms that Control Myogenesis. *Developmental Cell* **28**, 225-238 (2014).
- 99 Staveley, D. B. E. in *Molecular & Developmental Biology (BIOL3530)* (Department of Biology Memorial University of Newfoundland).
- 100 Sato, T., Rocancourt, D., Marques, L., Thorsteinsdóttir, S. & Buckingham, M. A *Pax3/Dmrt2/Myf5* regulatory cascade functions at the onset of myogenesis. *PLoS Genet* **6**, e1000897 (2010).
- 101 Biressi, S., Molinaro, M. & Cossu, G. Cellular heterogeneity during vertebrate skeletal muscle development. *Developmental biology* **308**, 281-293 (2007).
- 102 Murphy, M. & Kardon, G. Origin of vertebrate limb muscle: the role of progenitor and myoblast populations. *Curr Top Dev Biol* **96**, 1-32 (2011).
- 103 Hasty, P. *et al.* Muscle deficiency and neonatal death in mice with a targeted mutation in the myogenin gene. *Nature* **364**, 501-506 (1993).
- 104 Nabeshima, Y. *et al.* Myogenin gene disruption results in perinatal lethality because of severe muscle defect. *Nature* **364**, 532-535 (1993).
- 105 Molkenin, J. D. & Olson, E. N. Defining the regulatory networks for muscle development. *Curr Opin Genet Dev* **6**, 445-453 (1996).
- 106 Fan, C. M., Li, L., Rozo, M. E. & Lepper, C. Making Skeletal Muscle from Progenitor and Stem Cells: Development versus Regeneration. *Wiley Interdiscip Rev Dev Biol* **1**, 315-327 (2012).
- 107 Yin, H., Price, F. & Rudnicki, M. A. Satellite cells and the muscle stem cell niche. *Physiological reviews* **93**, 23-67 (2013).
- 108 Asakura, A., Komaki, M. & Rudnicki, M. Muscle satellite cells are multipotential stem cells that exhibit myogenic, osteogenic, and adipogenic differentiation. *Differentiation* **68**, 245-253 (2001).

- 109 Charge, S. B. & Rudnicki, M. A. Cellular and molecular regulation of muscle regeneration. *Physiological reviews* **84**, 209-238 (2004).
- 110 Chal, J. & Pourquié, O. Making muscle: skeletal myogenesis *in vivo* and *in vitro*. *Development* **144**, 2104-2122 (2017).
- 111 Baghdadi, M. B. & Tajbakhsh, S. Regulation and phylogeny of skeletal muscle regeneration. *Developmental biology* **433**, 200-209 (2018).
- 112 Buckingham, M. & Relaix, F. The Role of Pax Genes in the Development of Tissues and Organs: Pax3 and Pax7 Regulate Muscle Progenitor Cell Functions. *Annual Review of Cell and Developmental Biology* **23**, 645-673 (2007).
- 113 Chang, N. C., Chevalier, F. P. & Rudnicki, M. A. Satellite Cells in Muscular Dystrophy - Lost in Polarity. *Trends Mol Med* **22**, 479-496 (2016).
- 114 Le Grand, F., Jones, A. E., Seale, V., Scimè, A. & Rudnicki, M. A. Wnt7a activates the planar cell polarity pathway to drive the symmetric expansion of satellite stem cells. *Cell Stem Cell* **4**, 535-547 (2009).
- 115 Brack, A. S., Conboy, I. M., Conboy, M. J., Shen, J. & Rando, T. A. A temporal switch from notch to Wnt signaling in muscle stem cells is necessary for normal adult myogenesis. *Cell Stem Cell* **2**, 50-59 (2008).
- 116 Figliola, R., Busanello, A., Vaccarello, G. & Maione, R. Regulation of p57(KIP2) during muscle differentiation: role of Egr1, Sp1 and DNA hypomethylation. *Journal of Molecular Biology* **380**, 265-277 (2008).
- 117 Berkes, C. A. & Tapscott, S. J. MyoD and the transcriptional control of myogenesis. *Semin Cell Dev Biol* **16**, 585-595 (2005).
- 118 Skapek, S. X., Rhee, J., Spicer, D. B. & Lassar, A. B. Inhibition of myogenic differentiation in proliferating myoblasts by cyclin D1-dependent kinase. *Science* **267**, 1022-1024 (1995).
- 119 Massari, M. E. & Murre, C. Helix-loop-helix proteins: regulators of transcription in eucaryotic organisms. *Mol Cell Biol* **20**, 429-440 (2000).
- 120 Weintraub, H. The MyoD family and myogenesis: redundancy, networks, and thresholds. *Cell* **75**, 1241-1244 (1993).
- 121 Bentzinger, C. F., Wang, Y. X. & Rudnicki, M. A. Building muscle: molecular regulation of myogenesis. *Cold Spring Harbor perspectives in biology* **4** (2012).
- 122 Ott, M. O., Bober, E., Lyons, G., Arnold, H. & Buckingham, M. Early expression of the myogenic regulatory gene, myf-5, in precursor cells of skeletal muscle in the mouse embryo. *Development* **111**, 1097-1107 (1991).
- 123 Francetic, T. & Li, Q. Skeletal myogenesis and Myf5 activation. *Transcription* **2**, 109-114 (2011).
- 124 Braun, T., Bober, E., Rudnicki, M. A., Jaenisch, R. & Arnold, H. H. MyoD expression marks the onset of skeletal myogenesis in Myf-5 mutant mice. *Development* **120**, 3083-3092 (1994).
- 125 Nabeshima, Y. *et al.* Myogenin gene disruption results in perinatal lethality because of severe muscle defect. *Nature* **364**, 532-535 (1993).
- 126 Feige, P., Brun, C. E., Ritso, M. & Rudnicki, M. A. Orienting Muscle Stem Cells for Regeneration in Homeostasis, Aging, and Disease. *Cell Stem Cell* **23**, 653-664 (2018).

- 127 Andres, V. & Walsh, K. Myogenin expression, cell cycle withdrawal, and phenotypic differentiation are temporally separable events that precede cell fusion upon myogenesis. *J Cell Biol* **132**, 657-666 (1996).
- 128 Summerbell, D., Halai, C. & Rigby, P. W. J. Expression of the myogenic regulatory factor Mrf4 precedes or is contemporaneous with that of Myf5 in the somitic bud. *Mechanisms of Development* **117**, 331-335 (2002).
- 129 Hinterberger, T. J., Sassoon, D. A., Rhodes, S. J. & Konieczny, S. F. Expression of the muscle regulatory factor MRF4 during somite and skeletal myofiber development. *Developmental biology* **147**, 144-156 (1991).
- 130 Bober, E. *et al.* The muscle regulatory gene, Myf-6, has a biphasic pattern of expression during early mouse development. *J Cell Biol* **113**, 1255-1265 (1991).
- 131 Kassar-Duchossoy, L. *et al.* Mrf4 determines skeletal muscle identity in Myf5:Myod double-mutant mice. *Nature* **431**, 466-471 (2004).
- 132 Zhang, W., Behringer, R. R. & Olson, E. N. Inactivation of the myogenic bHLH gene MRF4 results in up-regulation of myogenin and rib anomalies. *Genes Dev* **9**, 1388-1399 (1995).
- 133 Pownall, M. E., Gustafsson, M. K. & Emerson, C. P., Jr. Myogenic regulatory factors and the specification of muscle progenitors in vertebrate embryos. *Annu Rev Cell Dev Biol* **18**, 747-783 (2002).
- 134 Tapscott, S. J. & Weintraub, H. MyoD and the regulation of myogenesis by helix-loop-helix proteins. *The Journal of clinical investigation* **87**, 1133-1138. (1991).
- 135 Wardle, F. C. Master control: transcriptional regulation of mammalian Myod. *Journal of Muscle Research and Cell Motility* **40**, 211-226 (2019).
- 136 Carvajal, J. J. & Rigby, P. W. Regulation of gene expression in vertebrate skeletal muscle. *Exp Cell Res* **316**, 3014-3018 (2010).
- 137 Faralli, H. & Dilworth, F. J. Turning on myogenin in muscle: a paradigm for understanding mechanisms of tissue-specific gene expression. *Comp Funct Genomics* **2012**, 836374 (2012).
- 138 Carvajal, J. J., Cox, D., Summerbell, D. & Rigby, P. W. A BAC transgenic analysis of the Mrf4/Myf5 locus reveals interdigitated elements that control activation and maintenance of gene expression during muscle development. *Development* **128**, 1857-1868 (2001).
- 139 Fomin, M., Nomokonova, N. & Arnold, H.-H. Identification of a critical control element directing expression of the muscle-specific transcription factor MRF4 in the mouse embryo. *Developmental biology* **272**, 498-509 (2004).
- 140 Hadchouel, J. *et al.* Modular long-range regulation of Myf5 reveals unexpected heterogeneity between skeletal muscles in the mouse embryo. *Development* **127**, 4455-4467 (2000).
- 141 Hadchouel, J. *et al.* Modular long-range regulation of Myf5 reveals unexpected heterogeneity between skeletal muscles in the mouse embryo. *Development* **127**, 4455-4467 (2000).
- 142 Thayer, M. J. *et al.* Positive autoregulation of the myogenic determination gene MyoD1. *Cell* **58**, 241-248 (1989).
- 143 Carvajal, J. J., Keith, A. & Rigby, P. W. Global transcriptional regulation of the locus encoding the skeletal muscle determination genes Mrf4 and Myf5. *Genes Dev* **22**, 265-276 (2008).

- 144 Mignone, F., Gissi, C., Liuni, S. & Pesole, G. Untranslated regions of mRNAs. *Genome biology* **3**, Reviews0004 (2002).
- 145 López-Lastra, M., Rivas, A. & Barría, M. I. Protein synthesis in eukaryotes: the growing biological relevance of cap-independent translation initiation. *Biol Res* **38**, 121-146 (2005).
- 146 Lee, J. E., Lee, J. Y., Wilusz, J., Tian, B. & Wilusz, C. J. Systematic analysis of cis-elements in unstable mRNAs demonstrates that CUGBP1 is a key regulator of mRNA decay in muscle cells. *PLoS One* **5**, e11201 (2010).
- 147 Keene, J. D. Minireview: global regulation and dynamics of ribonucleic Acid. *Endocrinology* **151**, 1391-1397 (2010).
- 148 Shaw, G. & Kamen, R. A conserved AU sequence from the 3' untranslated region of GM-CSF mRNA mediates selective mRNA degradation. *Cell* **46**, 659-667 (1986).
- 149 Jankowsky, E. & Harris, M. E. Mapping specificity landscapes of RNA-protein interactions by high throughput sequencing. *Methods* **118-119**, 111-118 (2017).
- 150 Chen, C. Y. & Shyu, A. B. AU-rich elements: characterization and importance in mRNA degradation. *Trends Biochem Sci* **20**, 465-470 (1995).
- 151 Otsuka, H., Fukao, A., Funakami, Y., Duncan, K. E. & Fujiwara, T. Emerging Evidence of Translational Control by AU-Rich Element-Binding Proteins. *Front Genet* **10**, 332 (2019).
- 152 Halees, A. S. *et al.* Global assessment of GU-rich regulatory content and function in the human transcriptome. *RNA biology* **8**, 681-691 (2011).
- 153 Vlasova, I. A. & Bohjanen, P. R. Posttranscriptional regulation of gene networks by GU-rich elements and CELF proteins. *RNA biology* **5**, 201-207 (2008).
- 154 Takeda, J. I., Masuda, A. & Ohno, K. Six GU-rich (6GU(R)) FUS-binding motifs detected by normalization of CLIP-seq by Nascent-seq. *Gene* **618**, 57-64 (2017).
- 155 Tollervey, J. R. *et al.* Characterizing the RNA targets and position-dependent splicing regulation by TDP-43. *Nat Neurosci* **14**, 452-458 (2011).
- 156 Good, P. J. The role of elav-like genes, a conserved family encoding RNA-binding proteins, in growth and development. *Seminars in Cell & Developmental Biology* **8**, 577-584 (1997).
- 157 Ford, L. P., Watson, J., Keene, J. D. & Wilusz, J. ELAV proteins stabilize deadenylated intermediates in a novel in vitro mRNA deadenylation/degradation system. *Genes Dev* **13**, 188-201 (1999).
- 158 Chen, C. Y. *et al.* AU binding proteins recruit the exosome to degrade ARE-containing mRNAs. *Cell* **107**, 451-464 (2001).
- 159 Gherzi, R. *et al.* A KH domain RNA binding protein, KSRP, promotes ARE-directed mRNA turnover by recruiting the degradation machinery. *Mol Cell* **14**, 571-583 (2004).
- 160 Chen, C. Y. *et al.* Nucleolin and YB-1 are required for JNK-mediated interleukin-2 mRNA stabilization during T-cell activation. *Genes Dev* **14**, 1236-1248 (2000).
- 161 Takahashi, N., Sasagawa, N., Suzuki, K. & Ishiura, S. The CUG-binding protein binds specifically to UG dinucleotide repeats in a yeast three-hybrid system. *Biochem Biophys Res Commun* **277**, 518-523 (2000).

- 162 Dembowski, J. A. & Grabowski, P. J. The CUGBP2 splicing factor regulates an ensemble of branchpoints from perimeter binding sites with implications for autoregulation. *PLoS Genet* **5**, e1000595 (2009).
- 163 Mori, D., Sasagawa, N., Kino, Y. & Ishiura, S. Quantitative analysis of CUG-BP1 binding to RNA repeats. *J Biochem* **143**, 377-383 (2008).
- 164 Marquis, J. *et al.* CUG-BP1/CELF1 requires UGU-rich sequences for high-affinity binding. *Biochem J* **400**, 291-301 (2006).
- 165 Vlasova-St Louis, I., Dickson, A. M., Bohjanen, P. R. & Wilusz, C. J. CELF1 ways to modulate mRNA decay. *Biochim Biophys Acta* **1829**, 695-707 (2013).
- 166 Tebo, J. *et al.* Heterogeneity in control of mRNA stability by AU-rich elements. *The Journal of biological chemistry* **278**, 12085-12093 (2003).
- 167 Barreau, C., Paillard, L. & Osborne, H. B. AU-rich elements and associated factors: are there unifying principles? *Nucleic acids research* **33**, 7138-7150 (2005).
- 168 Fialcowitz-White, E. J. *et al.* Specific protein domains mediate cooperative assembly of HuR oligomers on AU-rich mRNA-destabilizing sequences. *The Journal of biological chemistry* **282**, 20948-20959 (2007).
- 169 Vasudevan, S. & Steitz, J. A. AU-rich-element-mediated upregulation of translation by FXR1 and Argonaute 2. *Cell* **128**, 1105-1118 (2007).
- 170 von Roretz, C., Di Marco, S., Mazroui, R. & Gallouzi, I. E. Turnover of AU-rich-containing mRNAs during stress: a matter of survival. *Wiley interdisciplinary reviews. RNA* **2**, 336-347 (2011).
- 171 Kim, V. N., Han, J. & Siomi, M. C. Biogenesis of small RNAs in animals. *Nature Reviews Molecular Cell Biology* **10**, 126-139 (2009).
- 172 Chekulaeva, M. & Filipowicz, W. Mechanisms of miRNA-mediated post-transcriptional regulation in animal cells. *Curr Opin Cell Biol* **21**, 452-460 (2009).
- 173 Leitão A.L., C. M. C., Enguita F.J. . *A Guide for miRNA Target Prediction and Analysis Using Web-Based Applications.*, Vol. 1182 (Humana Press, 2014).
- 174 Millar, A. A. The Function of miRNAs in Plants. *Plants (Basel)* **9** (2020).
- 175 He, L. & Hannon, G. J. MicroRNAs: small RNAs with a big role in gene regulation. *Nat Rev Genet* **5**, 522-531 (2004).
- 176 Lee, R. C. & Ambros, V. An extensive class of small RNAs in *Caenorhabditis elegans*. *Science* **294**, 862-864 (2001).
- 177 Díaz-Muñoz, M. D. & Turner, M. Uncovering the Role of RNA-Binding Proteins in Gene Expression in the Immune System. *Front Immunol* **9**, 1094 (2018).
- 178 Lu, Y. C. *et al.* ELAVL1 modulates transcriptome-wide miRNA binding in murine macrophages. *Cell reports* **9**, 2330-2343 (2014).
- 179 Kundu, P., Fabian, M. R., Sonenberg, N., Bhattacharyya, S. N. & Filipowicz, W. HuR protein attenuates miRNA-mediated repression by promoting miRISC dissociation from the target RNA. *Nucleic Acids Res* **40**, 5088-5100 (2012).
- 180 Liu, N. *et al.* An intragenic MEF2-dependent enhancer directs muscle-specific expression of microRNAs 1 and 133. *Proc Natl Acad Sci U S A* **104**, 20844-20849 (2007).

- 181 Zhao, Y., Samal, E. & Srivastava, D. Serum response factor regulates a muscle-specific microRNA that targets Hand2 during cardiogenesis. *Nature* **436**, 214-220 (2005).
- 182 Rao, P. K., Kumar, R. M., Farkhondeh, M., Baskerville, S. & Lodish, H. F. Myogenic factors that regulate expression of muscle-specific microRNAs. *Proc Natl Acad Sci U S A* **103**, 8721-8726 (2006).
- 183 Wang, Z., Qin, G. & Zhao, T. C. HDAC4: mechanism of regulation and biological functions. *Epigenomics* **6**, 139-150 (2014).
- 184 Liu, N. *et al.* microRNA-133a regulates cardiomyocyte proliferation and suppresses smooth muscle gene expression in the heart. *Genes Dev* **22**, 3242-3254 (2008).
- 185 Yuasa, K. *et al.* MicroRNA-206 is highly expressed in newly formed muscle fibers: implications regarding potential for muscle regeneration and maturation in muscular dystrophy. *Cell Struct Funct* **33**, 163-169 (2008).
- 186 Pelt, D. W. V., Hettinger, Z. R. & Vanderklish, P. W. RNA-binding proteins: The next step in translating skeletal muscle adaptations? *J Appl Physiol* **127**, 654-660 (2019).
- 187 Lukong, K. E., Chang, K. W., Khandjian, E. W. & Richard, S. RNA-binding proteins in human genetic disease. *Trends Genet* **24**, 416-425 (2008).
- 188 Lunde, B. M., Moore, C. & Varani, G. RNA-binding proteins: modular design for efficient function. *Nat Rev Mol Cell Biol* **8**, 479-490 (2007).
- 189 Kadlec, J., Izaurralde, E. & Cusack, S. The structural basis for the interaction between nonsense-mediated mRNA decay factors UPF2 and UPF3. *Nat Struct Mol Biol* **11**, 330-337 (2004).
- 190 Fribourg, S., Gatfield, D., Izaurralde, E. & Conti, E. A novel mode of RBD-protein recognition in the Y14-Mago complex. *Nat Struct Biol* **10**, 433-439 (2003).
- 191 Apponi, L. H., Corbett, A. H. & Pavlath, G. K. RNA-binding proteins and gene regulation in myogenesis. *Trends Pharmacol Sci* **32**, 652-658 (2011).
- 192 Okamura, M., Inose, H. & Masuda, S. RNA Export through the NPC in Eukaryotes. *Genes (Basel)* **6**, 124-149 (2015).
- 193 Natalizio, B. J. & Wente, S. R. Postage for the messenger: designating routes for nuclear mRNA export. *Trends Cell Biol* **23**, 365-373 (2013).
- 194 Cautain, B., Hill, R., de Pedro, N. & Link, W. Components and regulation of nuclear transport processes. *FEBS J* **282**, 445-462 (2015).
- 195 O'Reilly, A. J., Dacks, J. B. & Field, M. C. Evolution of the karyopherin- β family of nucleocytoplasmic transport factors; ancient origins and continued specialization. *PLoS One* **6**, e19308 (2011).
- 196 Gallouzi, I. E., Brennan, C. M. & Steitz, J. A. Protein ligands mediate the CRM1-dependent export of HuR in response to heat shock. *RNA* **7**, 1348-1361. (2001).
- 197 van der Giessen, K. & Gallouzi, I. E. Involvement of transportin 2-mediated HuR import in muscle cell differentiation. *Molecular biology of the cell* **18**, 2619-2629 (2007).
- 198 Trotta, C. R., Lund, E., Kahan, L., Johnson, A. W. & Dahlberg, J. E. Coordinated nuclear export of 60S ribosomal subunits and NMD3 in vertebrates. *Embo j* **22**, 2841-2851 (2003).
- 199 Brennan, C. M., Gallouzi, I. E. & Steitz, J. A. Protein ligands to HuR modulate its interaction with target mRNAs in vivo. *J Cell Biol* **151**, 1-14 (2000).

- 200 Corral-Debrinski, M. mRNA specific subcellular localization represents a crucial step for fine-tuning of gene expression in mammalian cells. *Biochimica et Biophysica Acta (BBA) - Molecular Cell Research* **1773**, 473-475 (2007).
- 201 Gavis, E. R. & Lehmann, R. Localization of nanos RNA controls embryonic polarity. *Cell* **71**, 301-313 (1992).
- 202 Sylvestre, J., Vialette, S., Corral Debrinski, M. & Jacq, C. Long mRNAs coding for yeast mitochondrial proteins of prokaryotic origin preferentially localize to the vicinity of mitochondria. *Genome biology* **4**, R44 (2003).
- 203 Sinnamon, J. R. & Czaplinski, K. mRNA trafficking and local translation: the Yin and Yang of regulating mRNA localization in neurons. *Acta Biochimica et Biophysica Sinica* **43**, 663-670 (2011).
- 204 Kim, H. H., Lee, S. J., Gardiner, A. S., Perrone-Bizzozero, N. I. & Yoo, S. Different motif requirements for the localization zipcode element of β -actin mRNA binding by HuD and ZBP1. *Nucleic Acids Research* **43**, 7432-7446 (2015).
- 205 Jansen, R.-P. mRNA localization: message on the move. *Nature Reviews Molecular Cell Biology* **2**, 247-256 (2001).
- 206 Hüttelmaier, S. *et al.* Spatial regulation of beta-actin translation by Src-dependent phosphorylation of ZBP1. *Nature* **438**, 512-515 (2005).
- 207 Gama-Carvalho, M. & Carmo-Fonseca, M. The rules and roles of nucleocytoplasmic shuttling proteins. *FEBS letters* **498**, 157-163 (2001).
- 208 Kim, H. H. & Gorospe, M. Phosphorylated HuR shuttles in cycles. *Cell cycle* **7**, 3124-3126 (2008).
- 209 Doller, A., Schulz, S., Pfeilschifter, J. & Eberhardt, W. RNA-dependent association with myosin IIA promotes F-actin-guided trafficking of the ELAV-like protein HuR to polysomes. *Nucleic Acids Res* **41**, 9152-9167 (2013).
- 210 Cheng, Y. C. *et al.* MPT0B098, a novel microtubule inhibitor that destabilizes the hypoxia-inducible factor-1 α mRNA through decreasing nuclear-cytoplasmic translocation of RNA-binding protein HuR. *Mol Cancer Ther* **12**, 1202-1212 (2013).
- 211 Fujiwara, Y. *et al.* Microtubule association of a neuronal RNA-binding protein HuD through its binding to the light chain of MAP1B. *Biochimie* **93**, 817-822 (2011).
- 212 Gebauer, F. & Hentze, M. W. Molecular mechanisms of translational control. *Nat Rev Mol Cell Biol* **5**, 827-835 (2004).
- 213 Richter, J. D. & Sonenberg, N. Regulation of cap-dependent translation by eIF4E inhibitory proteins. *Nature* **433**, 477-480 (2005).
- 214 Gingras, A. C., Raught, B. & Sonenberg, N. Regulation of translation initiation by FRAP/mTOR. *Genes Dev* **15**, 807-826 (2001).
- 215 Pelletier, J. & Sonenberg, N. The involvement of mRNA secondary structure in protein synthesis. *Biochemistry and Cell Biology* **65**, 576-581 (1987).
- 216 Eley, H. L., Russell, S. T., Baxter, J. H., Mukerji, P. & Tisdale, M. J. Signaling pathways initiated by beta-hydroxy-beta-methylbutyrate to attenuate the depression of protein synthesis in skeletal muscle in response to cachectic stimuli. *Am J Physiol Endocrinol Metab* **293**, E923-931 (2007).

- 217 Tsai, S. *et al.* Muscle-specific 4E-BP1 signaling activation improves metabolic parameters during aging and obesity. *J Clin Invest* **125**, 2952-2964 (2015).
- 218 Fitzgerald, K. D. & Semler, B. L. Bridging IRES elements in mRNAs to the eukaryotic translation apparatus. *Biochim Biophys Acta* **1789**, 518-528 (2009).
- 219 Meng, Z. *et al.* The ELAV RNA-stability factor HuR binds the 5'-untranslated region of the human IGF-IR transcript and differentially represses cap-dependent and IRES-mediated translation. *Nucleic Acids Res* **33**, 2962-2979 (2005).
- 220 Jo, O. D. *et al.* Heterogeneous nuclear ribonucleoprotein A1 regulates cyclin D1 and c-myc internal ribosome entry site function through Akt signaling. *The Journal of biological chemistry* **283**, 23274-23287 (2008).
- 221 Bushell, M. *et al.* Polypyrimidine tract binding protein regulates IRES-mediated gene expression during apoptosis. *Mol Cell* **23**, 401-412 (2006).
- 222 Henis-Korenblit, S. *et al.* The caspase-cleaved DAP5 protein supports internal ribosome entry site-mediated translation of death proteins. *Proc Natl Acad Sci U S A* **99**, 5400-5405 (2002).
- 223 Newbury, S. F. Control of mRNA stability in eukaryotes. *Biochem Soc Trans* **34**, 30-34 (2006).
- 224 Stowell, J. A. W. *et al.* Reconstitution of Targeted Deadenylation by the Ccr4-Not Complex and the YTH Domain Protein Mmi1. *Cell reports* **17**, 1978-1989 (2016).
- 225 Niedzwiecka, A., Lekka, M., Nilsson, P. & Virtanen, A. Global architecture of human poly(A)-specific ribonuclease by atomic force microscopy in liquid and dynamic light scattering. *Biophysical Chemistry* **158**, 141-149 (2011).
- 226 Ramanathan, A., Robb, G. B. & Chan, S. H. mRNA capping: biological functions and applications. *Nucleic Acids Res* **44**, 7511-7526 (2016).
- 227 Heck, A. M. & Wilusz, J. The Interplay between the RNA Decay and Translation Machinery in Eukaryotes. *Cold Spring Harb Perspect Biol* **10** (2018).
- 228 Zinder, J. C. & Lima, C. D. Targeting RNA for processing or destruction by the eukaryotic RNA exosome and its cofactors. *Genes Dev* **31**, 88-100 (2017).
- 229 Jones, C. I., Zabolotskaya, M. V. & Newbury, S. F. The 5' → 3' exoribonuclease XRN1/Pacman and its functions in cellular processes and development. *Wiley Interdiscip Rev RNA* **3**, 455-468 (2012).
- 230 Lai, R. Y., Ljubicic, V., D'Souza, D. & Hood, D. A. Effect of chronic contractile activity on mRNA stability in skeletal muscle. *Am J Physiol Cell Physiol* **299**, C155-163 (2010).
- 231 Connor, M. K., Takahashi, M. & Hood, D. A. Tissue-specific stability of nuclear- and mitochondrially encoded mRNAs. *Arch Biochem Biophys* **333**, 103-108 (1996).
- 232 D'Souza, D., Lai, R. Y., Shuen, M. & Hood, D. A. mRNA stability as a function of striated muscle oxidative capacity. *Am J Physiol Regul Integr Comp Physiol* **303**, R408-417 (2012).
- 233 Chakkalakal, J. V., Miura, P., Bélanger, G., Michel, R. N. & Jasmin, B. J. Modulation of utrophin A mRNA stability in fast versus slow muscles via an AU-rich element and calcineurin signaling. *Nucleic Acids Res* **36**, 826-838 (2008).
- 234 Gramolini, A. O., Bélanger, G., Thompson, J. M., Chakkalakal, J. V. & Jasmin, B. J. Increased expression of utrophin in a slow vs. a fast muscle involves posttranscriptional events. *American Journal of Physiology-Cell Physiology* **281**, C1300-C1309 (2001).

- 235 Beauchamp, P. *et al.* The cleavage of HuR interferes with its transportin-2-mediated nuclear import and promotes muscle fiber formation. *Cell Death Differ* **17**, 1588-1599 (2010).
- 236 Di Marco, S. *et al.* NF-(kappa)B-mediated MyoD decay during muscle wasting requires nitric oxide synthase mRNA stabilization, HuR protein, and nitric oxide release. *Molecular and cellular biology* **25**, 6533-6545 (2005).
- 237 Briata, P. *et al.* p38-dependent phosphorylation of the mRNA decay-promoting factor KSRP controls the stability of select myogenic transcripts. *Mol Cell* **20**, 891-903 (2005).
- 238 Janice Sanchez, B. *et al.* Depletion of HuR in murine skeletal muscle enhances exercise endurance and prevents cancer-induced muscle atrophy. *Nat Commun* **10**, 4171 (2019).
- 239 Mubaid, S. *et al.* HuR counteracts miR-330 to promote STAT3 translation during inflammation-induced muscle wasting. *Proc Natl Acad Sci U S A* **116**, 17261-17270 (2019).
- 240 Phillips, B. L. *et al.* Post-transcriptional regulation of Pabpn1 by the RNA binding protein HuR. *Nucleic Acids Res* (2018).
- 241 Cammas, A. *et al.* Destabilization of nucleophosmin mRNA by the HuR/KSRP complex is required for muscle fibre formation. *Nat Commun* **5**, 4190 (2014).
- 242 Dormoy-Raclet, V. *et al.* HuR and miR-1192 regulate myogenesis by modulating the translation of HMGB1 mRNA. *Nat Commun* **4**, 2388 (2013).
- 243 Ohashi, S., Moue, M., Tanaka, T. & Kobayashi, S. Translational level of acetylcholine receptor alpha mRNA in mouse skeletal muscle is regulated by YB-1 in response to neural activity. *Biochem Biophys Res Commun* **414**, 647-652 (2011).
- 244 Ward, A. J., Rimer, M., Killian, J. M., Dowling, J. J. & Cooper, T. A. CUGBP1 overexpression in mouse skeletal muscle reproduces features of myotonic dystrophy type 1. *Hum Mol Genet* **19**, 3614-3622.
- 245 Timchenko, N. A., Iakova, P., Cai, Z. J., Smith, J. R. & Timchenko, L. T. Molecular basis for impaired muscle differentiation in myotonic dystrophy. *Mol Cell Biol* **21**, 6927-6938 (2001).
- 246 Timchenko, N. A. *et al.* Overexpression of CUG triplet repeat-binding protein, CUGBP1, in mice inhibits myogenesis. *The Journal of biological chemistry* **279**, 13129-13139 (2004).
- 247 Mahadevan, M. S. *et al.* Reversible model of RNA toxicity and cardiac conduction defects in myotonic dystrophy. *Nat Genet* **38**, 1066-1070 (2006).
- 248 Moore, A. E., Chenette, D. M., Larkin, L. C. & Schneider, R. J. Physiological networks and disease functions of RNA-binding protein AUF1. *WIREs RNA* **5**, 549-564 (2014).
- 249 Wagner, B. J., DeMaria, C. T., Sun, Y., Wilson, G. M. & Brewer, G. Structure and genomic organization of the human AUF1 gene: alternative pre-mRNA splicing generates four protein isoforms. *Genomics* **48**, 195-202 (1998).
- 250 Abbadi, D., Yang, M., Chenette, D. M., Andrews, J. J. & Schneider, R. J. Muscle development and regeneration controlled by AUF1-mediated stage-specific degradation of fate-determining checkpoint mRNAs. *Proc Natl Acad Sci U S A* **116**, 11285-11290 (2019).
- 251 Chenette, D. M. *et al.* Targeted mRNA Decay by RNA Binding Protein AUF1 Regulates Adult Muscle Stem Cell Fate, Promoting Skeletal Muscle Integrity. *Cell reports* **16**, 1379-1390 (2016).

- 252 Didier, D. K., Schiffenbauer, J., Woulfe, S. L., Zacheis, M. & Schwartz, B. D. Characterization of the cDNA encoding a protein binding to the major histocompatibility complex class II Y box. *Proc Natl Acad Sci U S A* **85**, 7322-7326 (1988).
- 253 Zasedateleva, O. A. *et al.* Specificity of mammalian Y-box binding protein p50 in interaction with ss and ds DNA analyzed with generic oligonucleotide microchip. *J Mol Biol* **324**, 73-87 (2002).
- 254 Eliseeva, I. A., Kim, E. R., Guryanov, S. G., Ovchinnikov, L. P. & Lyabin, D. N. Y-box-binding protein 1 (YB-1) and its functions. *Biochemistry. Biokhimiia* **76**, 1402-1433 (2011).
- 255 Dong, J. *et al.* RNA-binding specificity of Y-box protein 1. *RNA biology* **6**, 59-64 (2009).
- 256 Lyabin, D. N., Eliseeva, I. A. & Ovchinnikov, L. P. YB-1 protein: functions and regulation. *Wiley Interdiscip Rev RNA* **5**, 95-110 (2014).
- 257 Kohno, K., Izumi, H., Uchiumi, T., Ashizuka, M. & Kuwano, M. The pleiotropic functions of the Y-box-binding protein, YB-1. *BioEssays : news and reviews in molecular, cellular and developmental biology* **25**, 691-698 (2003).
- 258 Zhang, Y. F. *et al.* Nuclear localization of Y-box factor YB1 requires wild-type p53. *Oncogene* **22**, 2782-2794 (2003).
- 259 Song, Y. J. & Lee, H. YB1/p32, a nuclear Y-box binding protein 1, is a novel regulator of myoblast differentiation that interacts with Msx1 homeoprotein. *Exp Cell Res* **316**, 517-529 (2010).
- 260 Kobayashi, S., Tanaka, T., Moue, M., Ohashi, S. & Nishikawa, T. YB-1 gene expression is kept constant during myocyte differentiation through replacement of different transcription factors and then falls gradually under the control of neural activity. *The international journal of biochemistry & cell biology* **68**, 1-8 (2015).
- 261 Gherzi, R., Chen, C.-Y., Ramos, A. & Briata, P. KSRP Controls Pleiotropic Cellular Functions. *Seminars in Cell & Developmental Biology* **34**, 2-8 (2014).
- 262 Briata, P. *et al.* p38-Dependent Phosphorylation of the mRNA Decay-Promoting Factor KSRP Controls the Stability of Select Myogenic Transcripts. *Molecular cell* **20**, 891-903 (2005).
- 263 García-Mayoral, M. F., Díaz-Moreno, I., Hollingworth, D. & Ramos, A. The sequence selectivity of KSRP explains its flexibility in the recognition of the RNA targets. *Nucleic Acids Res* **36**, 5290-5296 (2008).
- 264 Robinow, S. & White, K. Characterization and spatial distribution of the ELAV protein during *Drosophila melanogaster* development. *J Neurobiol* **22**, 443-461 (1991).
- 265 Mazroui, R. *et al.* Caspase-mediated cleavage of HuR in the cytoplasm contributes to pp32/PHAP-I regulation of apoptosis. *The Journal of cell biology* **180**, 113-127 (2008).
- 266 Gallouzi, I. E. & Steitz, J. A. Delineation of mRNA export pathways by the use of cell-permeable peptides. *Science* **294**, 1895-1901. (2001).
- 267 von Roretz, C., Beauchamp, P., Di Marco, S. & Gallouzi, I.-E. HuR and myogenesis: Being in the right place at the right time. *Biochimica et Biophysica Acta (BBA) - Molecular Cell Research* **1813**, 1663-1667 (2011).
- 268 Abdelmohsen, K., Kuwano, Y., Kim, H. H. & Gorospe, M. Posttranscriptional gene regulation by RNA-binding proteins during oxidative stress: implications for cellular senescence. *Biol Chem* **389**, 243-255 (2008).

- 269 Simone, L. E. & Keene, J. D. Mechanisms coordinating ELAV/Hu mRNA regulons. *Curr Opin Genet Dev* **23**, 35-43 (2013).
- 270 von Roretz, C. & Gallouzi, I. E. Decoding ARE-mediated decay: is microRNA part of the equation? *The Journal of cell biology* **181**, 189-194 (2008).
- 271 Ripin, N. *et al.* Molecular basis for AU-rich element recognition and dimerization by the HuR C-terminal RRM. *Proc Natl Acad Sci U S A* **116**, 2935-2944 (2019).
- 272 Wang, H. *et al.* The structure of the ARE-binding domains of Hu antigen R (HuR) undergoes conformational changes during RNA binding. *Acta Crystallographica Section D* **69**, 373-380 (2013).
- 273 Doller, A., Schlepckow, K., Schwalbe, H., Pfeilschifter, J. & Eberhardt, W. Tandem phosphorylation of serines 221 and 318 by protein kinase Cdelta coordinates mRNA binding and nucleocytoplasmic shuttling of HuR. *Mol Cell Biol* **30**, 1397-1410 (2010).
- 274 Cho, S. J., Zhang, J. & Chen, X. RNPC1 modulates the RNA-binding activity of, and cooperates with, HuR to regulate p21 mRNA stability. *Nucleic Acids Res* **38**, 2256-2267 (2010).
- 275 Hinman, M. N. & Lou, H. Diverse molecular functions of Hu proteins. *Cell Mol Life Sci* **65**, 3168-3181 (2008).
- 276 von Roretz, C., Macri, A. M. & Gallouzi, I. E. Transportin 2 regulates apoptosis through the RNA-binding protein HuR. *The Journal of biological chemistry* **286**, 25983-25991 (2011).
- 277 Ma, J. F. *et al.* STAT3 promotes IFNgamma/TNFalpha-induced muscle wasting in an NF-kappaB-dependent and IL-6-independent manner. *EMBO molecular medicine* (2017).
- 278 Bentzinger, C. F., Wang, Y. X., von Maltzahn, J. & Rudnicki, M. A. The emerging biology of muscle stem cells: Implications for cell-based therapies. *BioEssays : news and reviews in molecular, cellular and developmental biology* (2012).
- 279 Hall, D. T., Ma, J. F., Marco, S. D. & Gallouzi, I. E. Inducible nitric oxide synthase (iNOS) in muscle wasting syndrome, sarcopenia, and cachexia. *Aging* **3**, 702-715 (2011).
- 280 Tisdale, M. J. Catabolic mediators of cancer cachexia. *Current opinion in supportive and palliative care* **2**, 256-261 (2008).
- 281 Tisdale, M. J. Mechanisms of cancer cachexia. *Physiological reviews* **89**, 381-410 (2009).
- 282 Tisdale, M. J. Cancer cachexia. *Curr Opin Gastroenterol* **26**, 146-151 (2010).
- 283 Guller, I. & Russell, A. P. MicroRNAs in skeletal muscle: their role and regulation in development, disease and function. *The Journal of physiology* **588**, 4075-4087 (2010).
- 284 Gomes, M. D., Lecker, S. H., Jagoe, R. T., Navon, A. & Goldberg, A. L. Atrogin-1, a muscle-specific F-box protein highly expressed during muscle atrophy. *Proceedings of the National Academy of Sciences of the United States of America* **98**, 14440-14445 (2001).
- 285 Gramolini, A. O. & Jasmin, B. J. Duchenne muscular dystrophy and the neuromuscular junction: the utrophin link. *Bioessays* **19**, 747-750 (1997).
- 286 Gramolini, A. O. *et al.* Induction of utrophin gene expression by heregulin in skeletal muscle cells: role of the N-box motif and GA binding protein. *Proceedings of the National Academy of Sciences of the United States of America* **96**, 3223-3227 (1999).
- 287 Huh, M. S., Smid, J. K. & Rudnicki, M. A. Muscle function and dysfunction in health and disease. *Birth Defects Res C Embryo Today* **75**, 180-192 (2005).

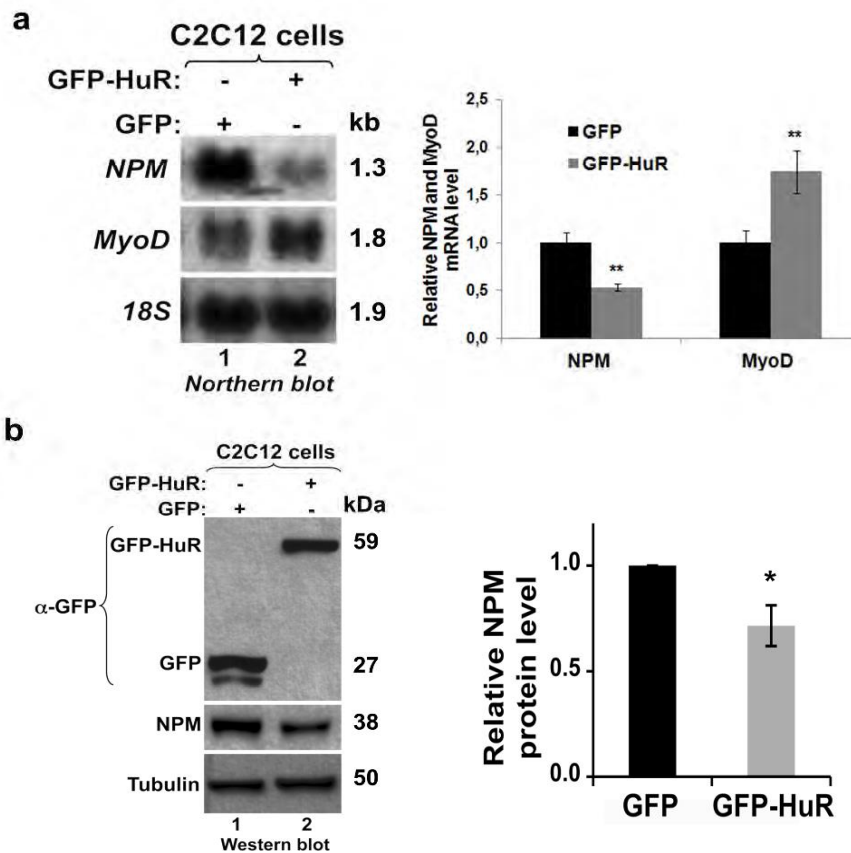
- 288 Lynch, G. S., Schertzer, J. D. & Ryall, J. G. Therapeutic approaches for muscle wasting disorders. *Pharmacology & therapeutics* **113**, 461-487 (2007).
- 289 Kim, H. H. *et al.* HuR recruits let-7/RISC to repress c-Myc expression. *Genes & development* (2009).
- 290 Lal, A. *et al.* p16(INK4a) translation suppressed by miR-24. *PLoS one* **3**, e1864 (2008).
- 291 Amirouche, A. *et al.* Activation of p38 signaling increases utrophin A expression in skeletal muscle via the RNA-binding protein KSRP and inhibition of AU-rich element-mediated mRNA decay: implications for novel DMD therapeutics. *Hum Mol Genet* **22**, 3093-3111 (2013).
- 292 Katsanou, V. *et al.* The RNA-binding protein Elavl1/HuR is essential for placental branching morphogenesis and embryonic development. *Molecular and cellular biology* (2009).
- 293 Cammas, A. *et al.* Destabilization of nucleophosmin mRNA by the HuR/KSRP complex is required for muscle fibre formation. *Nat Commun* **5**, 4190 (2014).
- 294 Gallouzi, I. E. *et al.* HuR binding to cytoplasmic mRNA is perturbed by heat shock. *Proc Natl Acad Sci U S A* **97**, 3073-3078 (2000).
- 295 Meinen, S., Barzaghi, P., Lin, S., Lochmuller, H. & Rugg, M. A. Linker molecules between laminins and dystroglycan ameliorate laminin-alpha2-deficient muscular dystrophy at all disease stages. *J Cell Biol* **176**, 979-993 (2007).
- 296 Grammatikakis, I., Abdelmohsen, K. & Gorospe, M. Posttranslational control of HuR function. *Wiley Interdiscip Rev RNA* **8** (2017).
- 297 Abdelmohsen, K. *et al.* Phosphorylation of HuR by Chk2 regulates SIRT1 expression. *Mol Cell* **25**, 543-557 (2007).
- 298 Kim, H. H. *et al.* Nuclear HuR accumulation through phosphorylation by Cdk1. *Genes & development* **22**, 1804-1815 (2008).
- 299 Li, H. *et al.* Lipopolysaccharide-induced methylation of HuR, an mRNA-stabilizing protein, by CARM1. Coactivator-associated arginine methyltransferase. *The Journal of biological chemistry* **277**, 44623-44630 (2002).
- 300 Schreiber, V., Dantzer, F., Ame, J. C. & de Murcia, G. Poly(ADP-ribose): novel functions for an old molecule. *Nat Rev Mol Cell Biol* **7**, 517-528 (2006).
- 301 Hottiger, M. O., Hassa, P. O., Luscher, B., Schuler, H. & Koch-Nolte, F. Toward a unified nomenclature for mammalian ADP-ribosyltransferases. *Trends Biochem Sci* **35**, 208-219 (2010).
- 302 Katsanou, V. *et al.* The RNA-binding protein Elavl1/HuR is essential for placental branching morphogenesis and embryonic development. *Mol Cell Biol* **29**, 2762-2776 (2009).
- 303 Chen, J. C., Mortimer, J., Marley, J. & Goldhamer, D. J. MyoD-cre transgenic mice: a model for conditional mutagenesis and lineage tracing of skeletal muscle. *Genesis* **41**, 116-121 (2005).
- 304 Rudnicki, M. A. *et al.* MyoD or Myf-5 is required for the formation of skeletal muscle. *Cell* **75**, 1351-1359 (1993).
- 305 Pant, M., Bal, N. C. & Periasamy, M. Sarcolipin: A Key Thermogenic and Metabolic Regulator in Skeletal Muscle. *Trends Endocrinol Metab* **27**, 881-892 (2016).
- 306 Zhang, C. *et al.* Tumor suppressor p53 negatively regulates glycolysis stimulated by hypoxia through its target RRAD. *Oncotarget* **5**, 5535-5546 (2014).

- 307 Derave, W., Everaert, I., Beeckman, S. & Baguet, A. Muscle carnosine metabolism and beta-alanine supplementation in relation to exercise and training. *Sports Med* **40**, 247-263 (2010).
- 308 Grote, C. W., Morris, J. K., Ryals, J. M., Geiger, P. C. & Wright, D. E. Insulin receptor substrate 2 expression and involvement in neuronal insulin resistance in diabetic neuropathy. *Exp Diabetes Res* **2011**, 212571 (2011).
- 309 Mynatt, R. L. *et al.* The RNA binding protein HuR influences skeletal muscle metabolic flexibility in rodents and humans. *Metabolism* **97**, 40-49 (2019).
- 310 Wilson, J. M. *et al.* The effects of endurance, strength, and power training on muscle fiber type shifting. *Journal of strength and conditioning research* **26**, 1724-1729 (2012).
- 311 Selsby, J. T., Morine, K. J., Pendrak, K., Barton, E. R. & Sweeney, H. L. Rescue of dystrophic skeletal muscle by PGC-1alpha involves a fast to slow fiber type shift in the mdx mouse. *PLoS One* **7**, e30063 (2012).
- 312 Wu, X. *et al.* Identification and validation of novel small molecule disruptors of HuR-mRNA interaction. *ACS chemical biology* **10**, 1476-1484 (2015).
- 313 D'Agostino, V. G. *et al.* Dihydratanthone-I interferes with the RNA-binding activity of HuR affecting its post-transcriptional function. *Scientific Reports* **5**, 16478 (2015).
- 314 Meisner, N. C. *et al.* Identification and mechanistic characterization of low-molecular-weight inhibitors for HuR. *Nat Chem Biol* **3**, 508-515 (2007).
- 315 Si, Y. *et al.* Posttranslational Modification Control of Inflammatory Signaling. *Adv Exp Med Biol* **1024**, 37-61 (2017).

13. Annexes

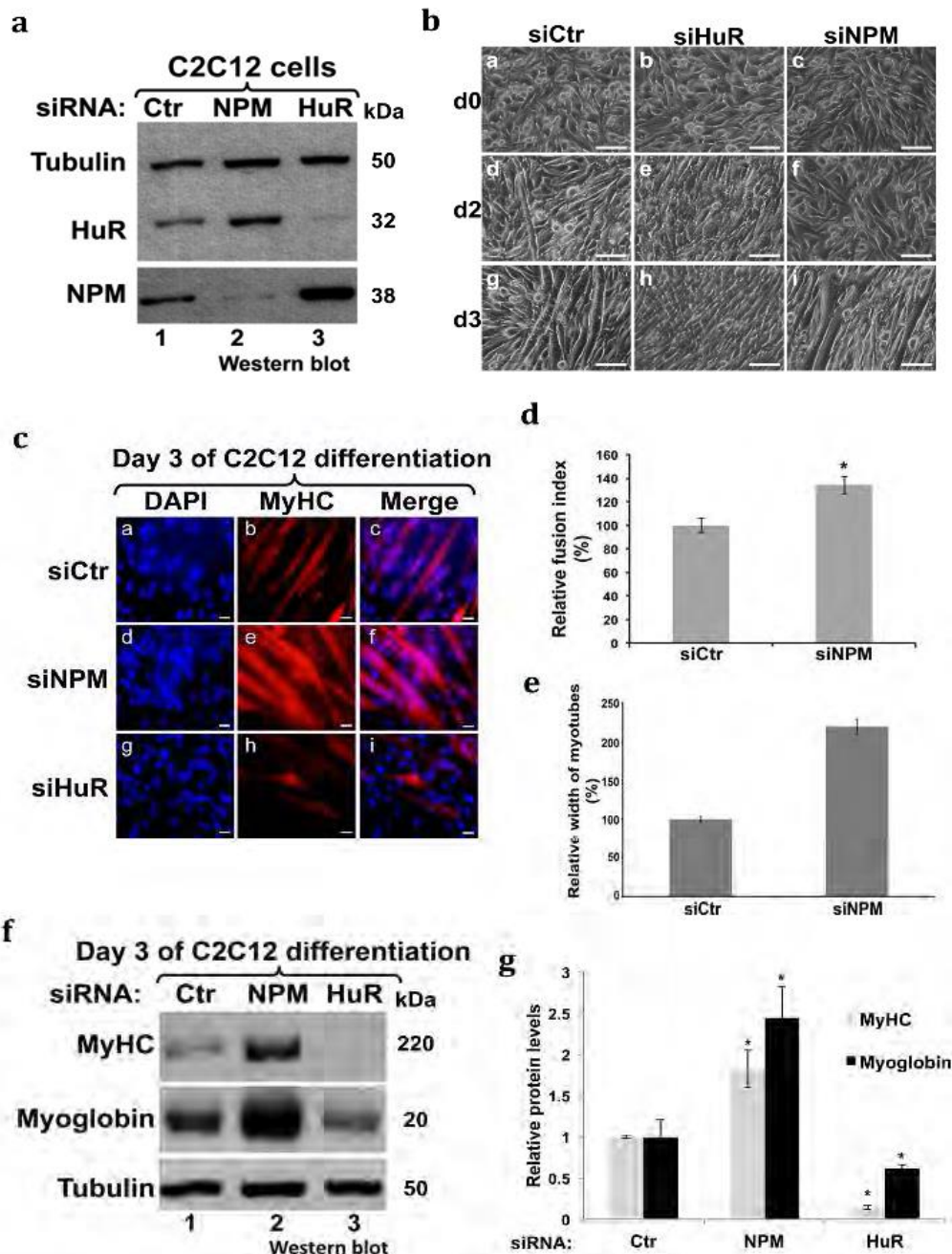
13.1. Annex 1. Supplemental material for CHAPTER I

Annex 1. Supplementary Figure 1. The overexpression of HuR negatively regulates NPM expression in myoblasts. Exponentially growing C2C12 myoblasts were transfected with GFP or GFP-HuR plasmids. **(a)** RNA extracts or total cell extracts from these cells were prepared 24 hrs posttransfection. **(a)** Northern blotting was performed using radiolabeled probes against *NPM*, *MyoD* mRNAs and *18S* (loading control). The band intensities of *NPM*, *MyoD* mRNAs and *18S* were determined using ImageQuant Software and the *NPM* and *MyoD* mRNA levels were normalized to *18S* levels. **(b)** Western blotting was performed using antibodies against NPM, GFP and α -tubulin (loading control). ImageQuant Software was used to determine the NPM levels that were normalized to α -tubulin levels. For all histograms, average values of the GFP-HuR condition was plotted relatively to the GFP condition +/- the standard error of the mean (S.E.M.) of three independent experiments * $P < 0.01$, ** $P < 0.001$ (t test).

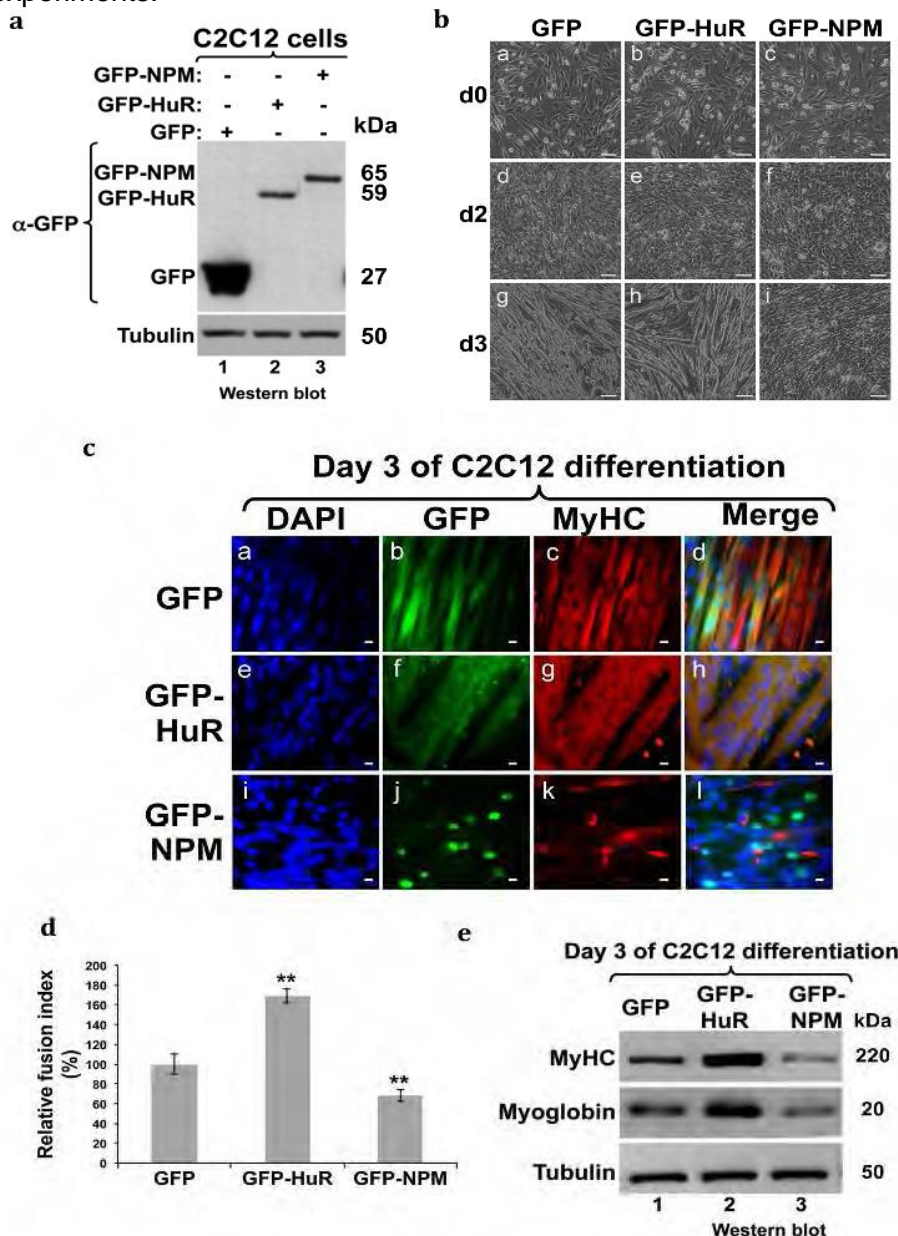


Annex 1. Supplementary Figure 2. Muscle fiber formation is promoted by NPM down regulation. The knockdown of HuR or NPM was performed in C2C12 cells and differentiation was induced 48 hours posttransfection of siHuR or siNPM. **(a)** Total cell lysates were prepared 48 hours posttransfection of siRNAs and HuR and NPM protein levels were analyzed by Western blotting using antibodies against NPM, HuR and α - tubulin (loading control). **(b)** Phase contrast

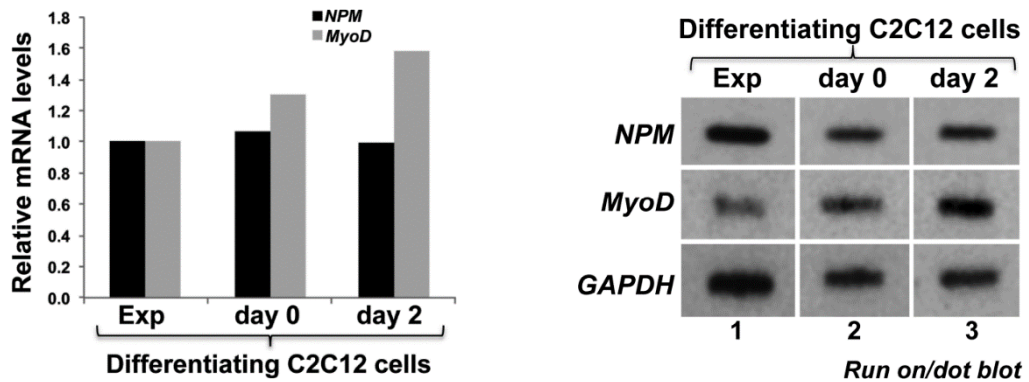
images of C2C12 cells depleted or not of HuR or NPM. Bars, 50µm. C2C12 cells depleted or not of HuR or NPM were fixed on d3 and used for an immunofluorescence (IF) experiments using the anti-My-HC antibody as well as DAPI staining. Images of a single representative field were shown. Bars, 10µm. **(d)** The fusion index and **(e)** width of fibers +/- S.E.M. (from 3 independent experiments) seen in siNPM-treated cells was determined and represented on the graph as a percentage relative to siCtr-treated myofibers +/- S.E.M. * $P < 0.01$ (t test). **(f)** Western blot analysis of My-HC, myoglobin and α -tubulin (loading control) protein levels. **(g)** Quantification of My-HC and myoglobin protein levels relative to α -tubulin. The protein levels for each protein under each siRNA treatment was plotted relative to the siRNA control condition +/- the S.E.M, * $P < 0.01$ (t test). lots shown in **(a)** and **(f)** and images shown in **(b)** and **(c)** are representative of three independent experiments.



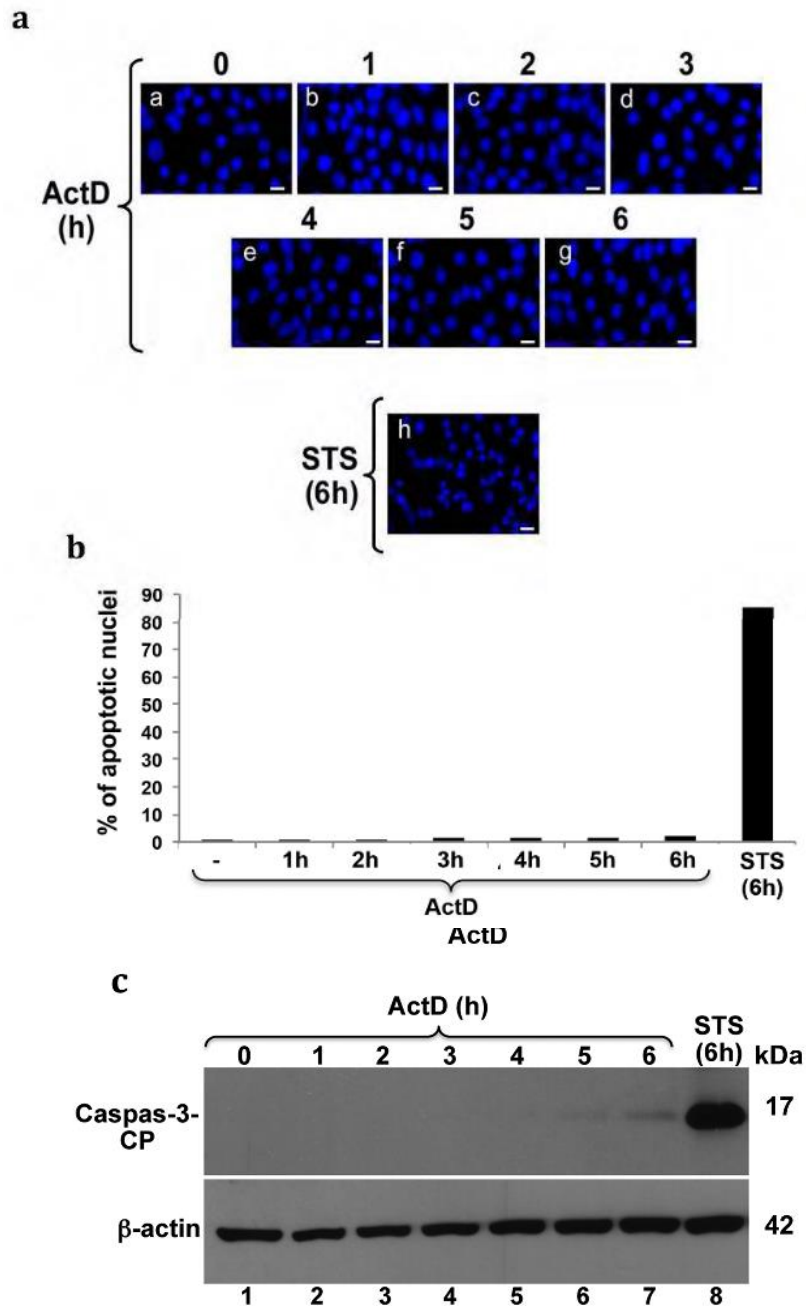
Annex 1. Supplementary Figure 3. Overexpression of NPM inhibits the formation of muscle fibers. (a) Stable C2C12 cell lines expressing GFP, GFP-HuR or GFP-NPM were generated as described in Material and Methods. The expression level of these proteins was determined by western blotting using antibodies against GFP and α -tubulin (loading control). (b-e) C2C12 cells stably expressing GFP, GFP-HuR or GFP-NPM were induced for differentiation for three days. (b) Phase contrast pictures showing the differentiation status at d0, d2 and d3. Bars, 50 μ m. (c) IF experiments were performed using the anti-My-HC antibody as well as GFP and DAPI staining. Images of a single representative field were shown. Bars, 10 μ m. (d) The fusion index \pm S.E.M. of three independent experiments was determined as described in Methods, $**P < 0.001$ (t test). (e) Total cell extracts were prepared from these cells and used for Western blotting analysis using antibodies against My-HC, myoglobin and α -tubulin (loading control). Blots shown in (a) and (e) and images shown in (b) and (c) are representative of three independent experiments.



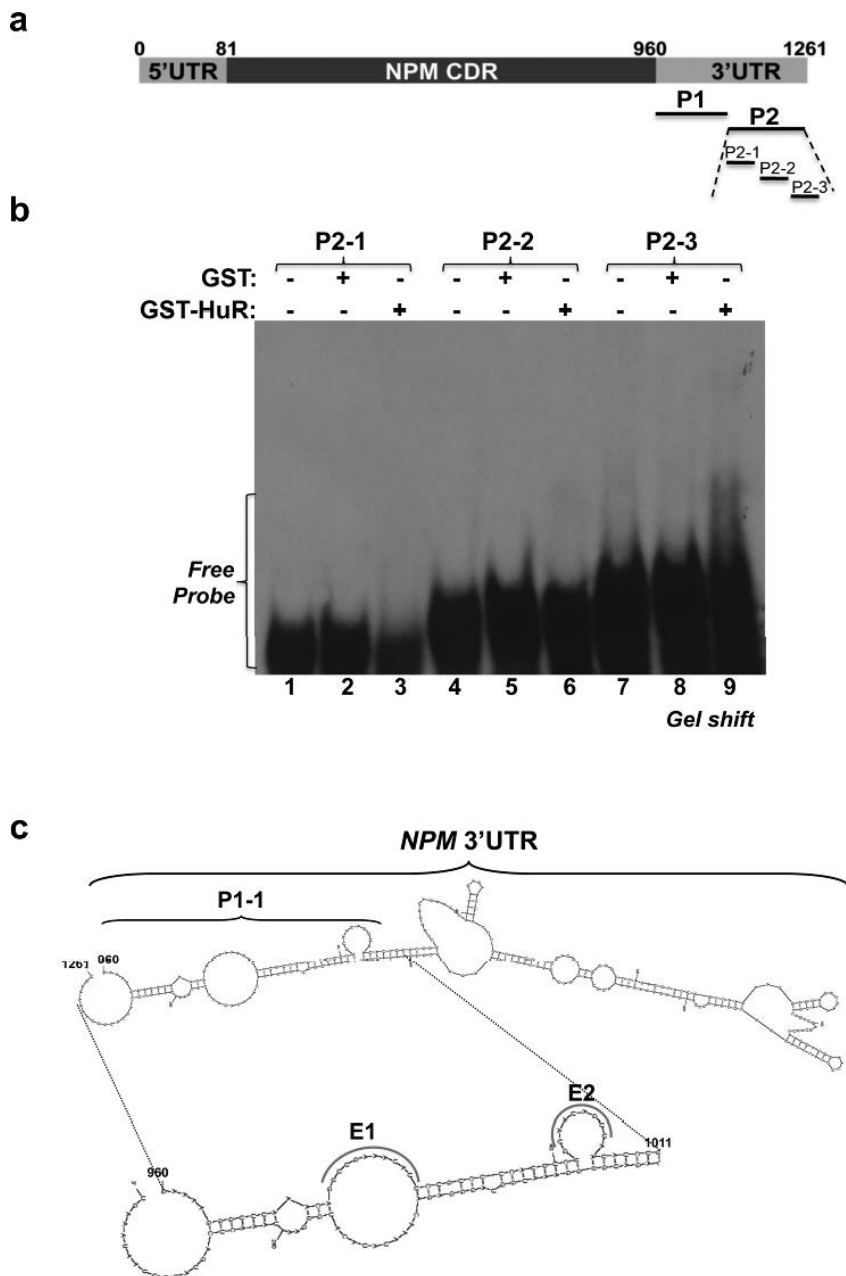
Annex 1. Supplementary Figure 4: Unlike *MyoD*, *NPM* transcription does not change during the myogenic process. Exponentially growing C2C12 cells (Exp) as well as cells on day 0 and day 2 of the differentiation process were collected and used for nuclear run-on analysis. Nuclei were isolated from these cells and nascent RNA transcripts were radiolabeled and hybridized with nitrocellulose filters onto which *NPM*, *MyoD* and *GAPDH* PCR products had been slotted. The band intensities of *NPM*, *MyoD* and *GAPDH* mRNAs were determined using ImageQuant Software and the *NPM* and *MyoD* mRNA levels were normalized over *GAPDH*.



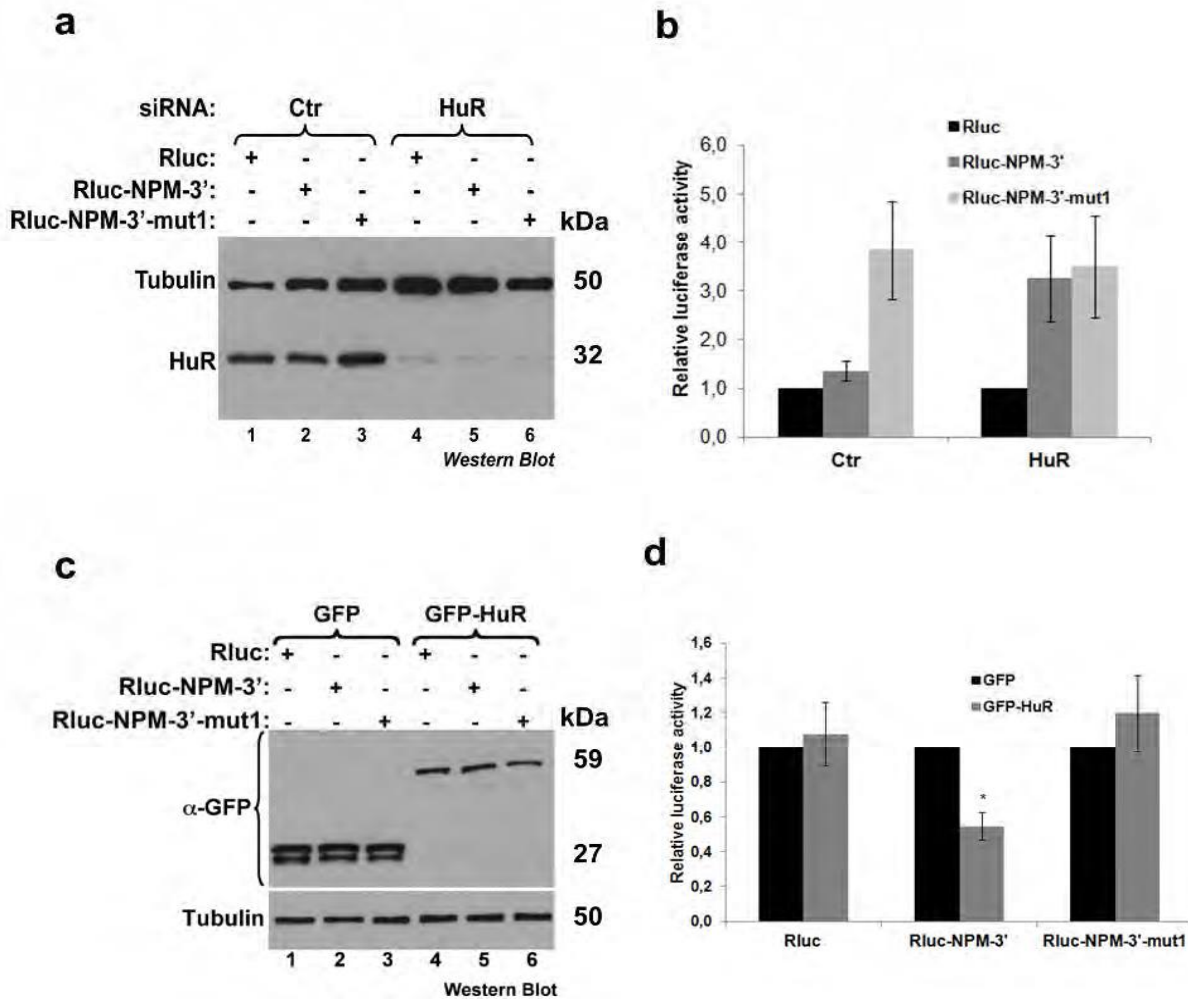
Annex 1. Supplementary Figure 5: Actinomycin D treatment does not induce apoptosis in C2C12 muscle cells. C2C12 cells were treated with ActD for the indicated period of time or with Staurosporine (STS) for 6h (included as a positive control for apoptosis). **(a)** The cells were fixed and stained with DAPI to detect apoptotic nuclei. Images of a single representative field are shown. Bars, 10 μ m. **(b)** Graph illustrating the percentage of cells with apoptotic nuclei in (a) from n=1 experiment. **(c)** The cleavage of caspase 3 (indicative of apoptosis) was assessed by western blot analysis with an antibody specific for the cleavage product of caspase-3. β -actin protein levels were included as a loading control.



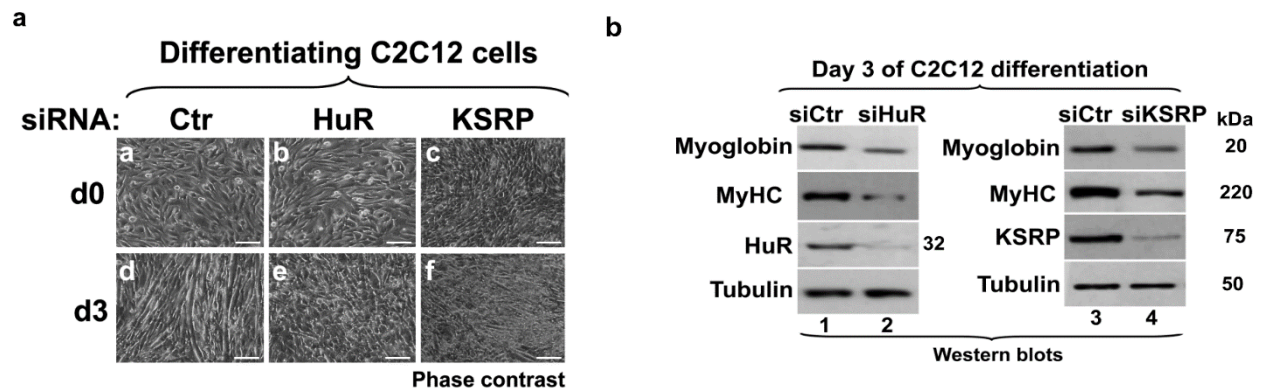
Annex 1. Supplementary Figure 6: Characterization of HuR binding site in the *NPM* 3'UTR. (a) Schematic representation of the probes covering the *NPM* 3'UTR (P1, P2, P2-1 to P2-3) used to generate radiolabeled RNA probes for RNA electromobility shift assays are indicated (black). (b) Gel-shift binding assay was performed by incubating 500 ng of purified GST or GST-HuR protein with the radiolabeled cRNA P2-1, P2-2 and P2-3 probes. This gel is representative of three independent experiments. (c) The structure of *NPM* 3'UTR was predicted with mfold software. The sequences highlighted as E1 and E2 were identified to be single-strand AU-rich sequences.



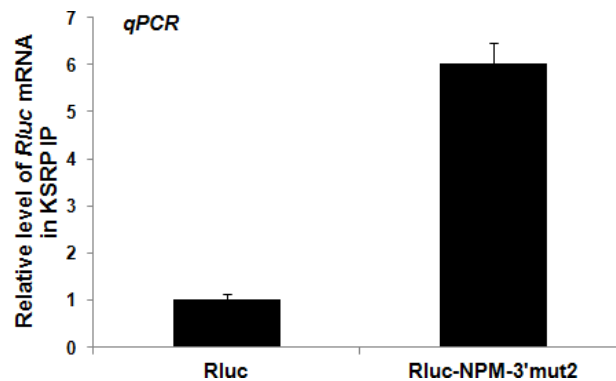
Annex 1. Supplementary Figure 7: Modulating the expression of HuR affects the luciferase activity of the Rluc-NPM-3'UTR reporter transfected in C2C12 cells. (a-b) Total cell extracts from C2C12 cells expressing Renilla luciferase reporters as described in Figure 5d and depleted or not of HuR were prepared and used for **(a)** western blotting analysis with anti-HuR or α -tubulin (loading control) antibodies or **(b)** luciferase activity measurement. **(c)** C2C12 cells expressing the Renilla luciferase reporters as described in Figures 5e and overexpressing GFP or GFP-HuR were used for **(c)** western blotting analysis with anti-GFP or α -tubulin (loading control) antibodies or **(d)** luciferase activity measurement. The histograms shown in b and d are representative of three independent experiments \pm S.E.M. * $P < 0.01$ (t test).



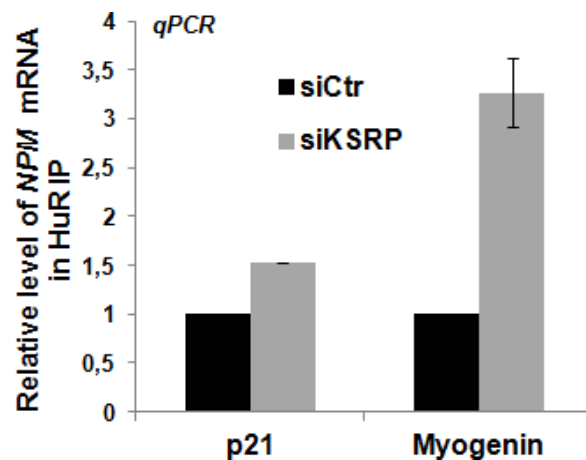
Annex 1. Supplementary Figure 8: The depletion of KSRP or HuR prevents myogenesis. The differentiation of C2C12 myoblasts was induced 48 hours after the transfection with a control (ctr), HuR or KSRP siRNA. **(a)** Phase contrast pictures of muscle cells treated as described above at day 0 (d0) (panels a-c) or day 3 (d3) (panels d-f) of the differentiation process. Bars, 50µm. **(b)** Total cell extracts were prepared on d3 of differentiation. Western blotting was performed using antibodies against My-HC, myoglobin, HuR, KSRP and α - tubulin (loading control). Blots and images are representative of three independent experiments.



Annex 1. Supplementary Figure 9: The R-Luc-NPM-3'mut2 transcript interacts with KSRP in C2C12 cells. IP experiments were performed on C2C12 cells expressing renilla luciferase reporters (Rluc and Rluc-NPM-3'- mut2) using the KSRP antibody or IgG antibodies. KSRP association with the reporter RNAs were determined as described in Figure 5c and is shown in the graph +/- S.E.M of two independent experiments.

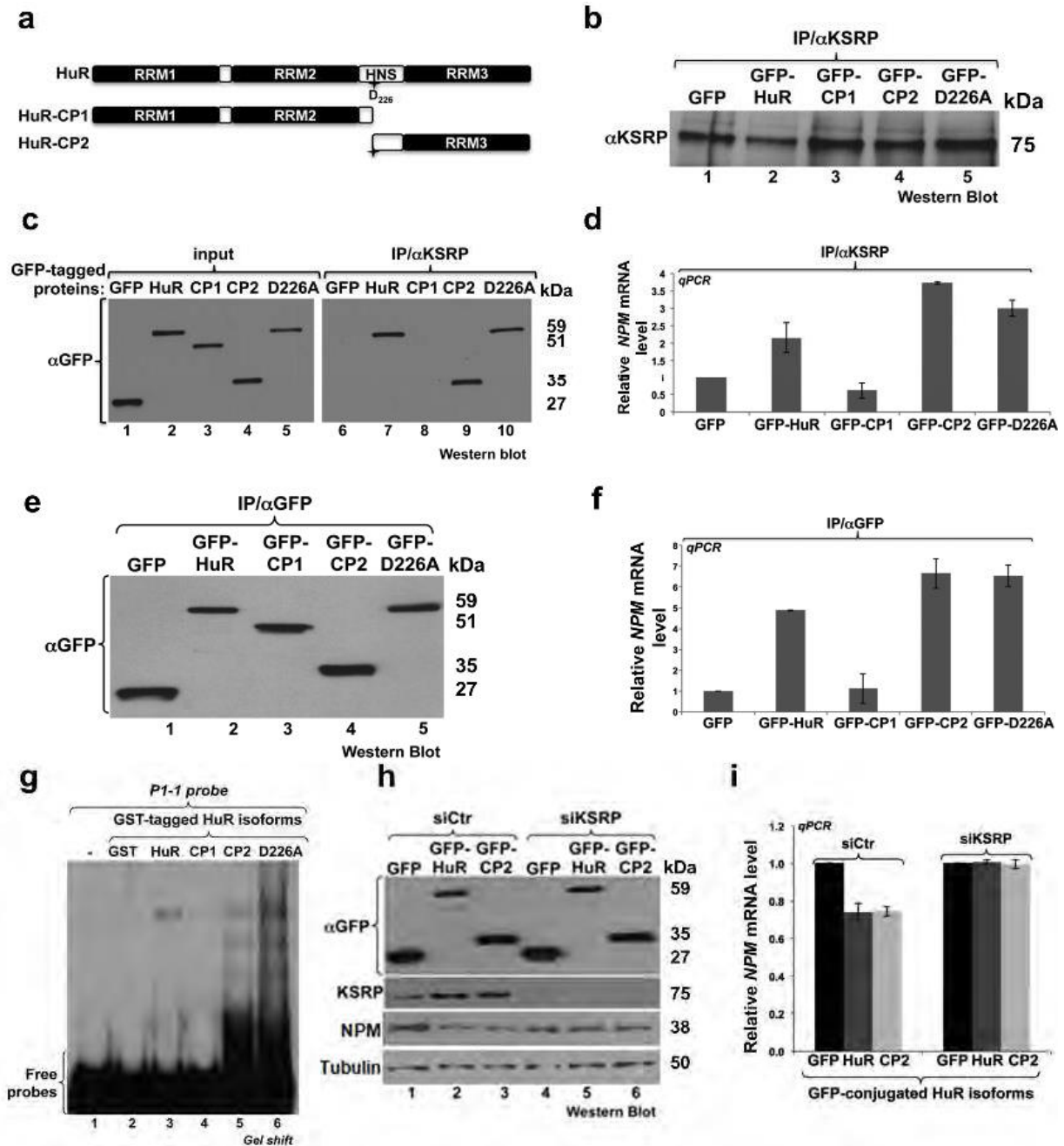


Annex 1. Supplementary Figure 10: The association of HuR with the *p21* or *Myog* mRNAs is increased in KSRP depleted muscle cells. IP experiments were performed using the HuR (3A2) antibody on total extract (TE) from C2C12 cells treated with siCtr or siKSRP. RNA was isolated from the immunoprecipitate, and RT-qPCR analysis was performed using specific primers for *NPM* and *RPL32* mRNAs as described in Figure 2.7j are shown in the graph +/- S.E.M of two independent experiments.

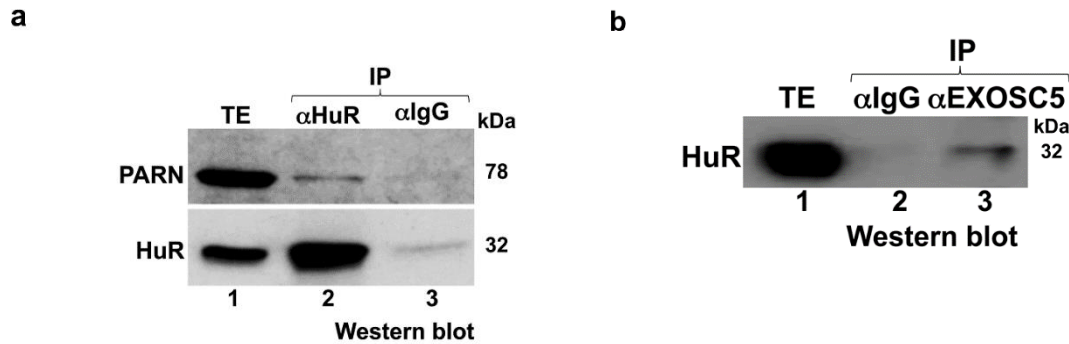


Annex 1. Supplementary Figure 11: HuR-CP2 is sufficient and required for the HuR/KSRP-mediated destabilization of the *NPM* mRNA. **(a)** Schematic diagram of HuR and the two cleavage products HuR-CP1 and HuR-CP2. **(b-f)** Total extracts prepared from C2C12 cells expressing GFP, GFP-HuR, GFP-CP1, GFP-CP2 or the non-cleavable isoform, GFP- D226A, were used for IP experiments with anti-KSRP (b-d) or -GFP (e-f) antibodies. (b-c) Western blot analysis was performed with anti-KSRP (to show KSRP immunoprecipitation) (b) or anti-GFP (to assess the KSRP/HuR isoforms association) (c). The input in (c) represent 10% of the total extract. (e) Western blot with anti-GFP antibody was performed to show the IP of HuR isoforms. (d, f) RNA was isolated from the KSRP- (d) or the GFP- (f) IP and *NPM* mRNA levels was assessed by RT-qPCR. For the histograms shown all the conditions were plotted relatively to the GFP Ctr condition +/- the S.E.M. of three independent experiments. **(g)** Gel-shift binding assay was performed using 500 ng of purified GST, GST-CP1, -CP2 or -D226A proteins with the radiolabeled cRNA P1-1 probe. This blot is representative of two independent experiments. **(h-i)** C2C12 cells expressing GFP, GFP-HuR or GFP-CP2 were depleted (siKSRP) or not (siCtr) of KSRP. (h) Total cell extracts from these cells was used for western blotting analysis with antibodies against KSRP, GFP, *NPM* or α -tubulin. (i) RT-qPCR analysis was performed to assess

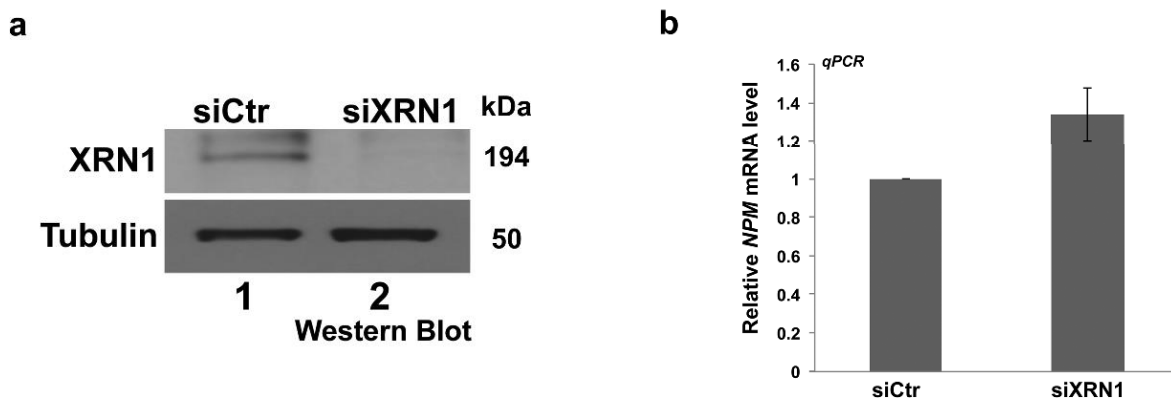
NPM mRNA levels that were standardized against *GAPDH* mRNA and plotted relatively to the siRNA Ctr-treated and GFP-transfected cells +/- the S.E.M. of three independent experiments.



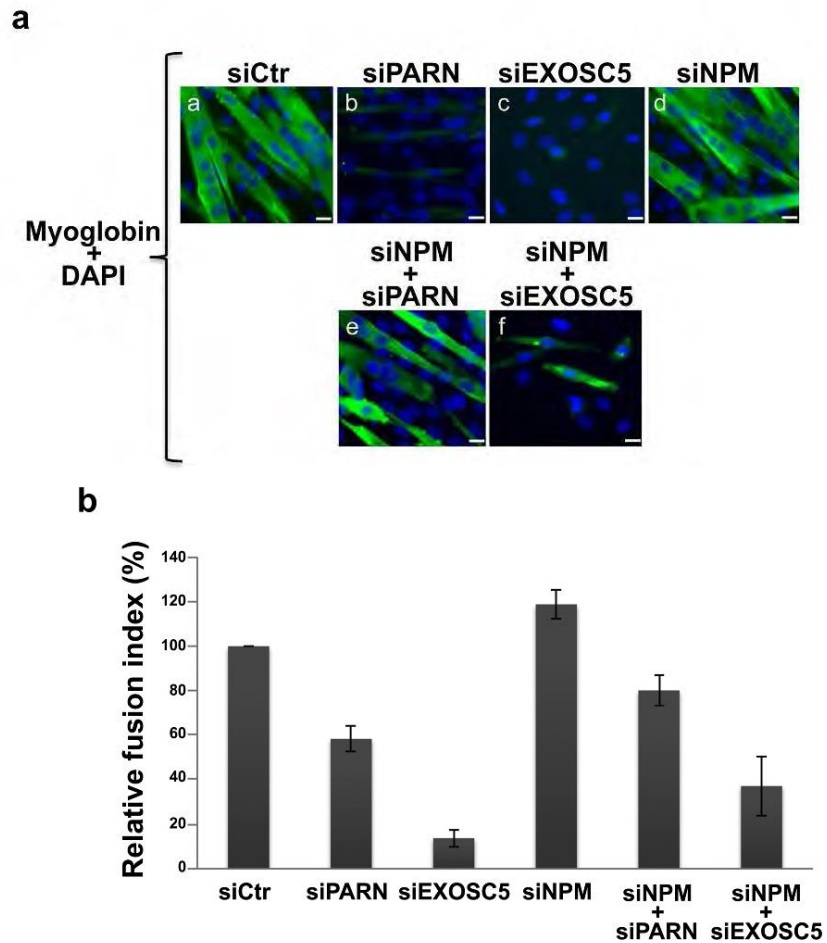
Annex 1. Supplementary Figure 12: PARN and EXOSC5 associate with HuR. **(a-b)** Proliferating C2C12 cells were harvested and used to prepare total cell extracts. These extracts were then subjected to an IP experiment with an anti-HuR (a) or EXOSC5 (b) antibody. The precipitates were then analysed by western blot using respectively either an anti-PARN (a) or an anti-HuR antibody (b). The gels shown are representative of two independent experiments.



Annex 1. Supplementary Figure 13: XRN1 depletion doesn't affect NPM levels. Exponentially growing C2C12 cells were treated with siRNA Ctr or siRNA against XRN1. **(a)** Total cell or **(b)** RNA extracts from these cells were prepared 48 hours after transfection. Western blotting analysis was performed using antibodies to detect XRN1 and α -tubulin (loading control). RT-qPCR analysis was performed using specific primers for *NPM* and *GAPDH* mRNAs. *NPM* mRNA levels were standardized against *GAPDH* mRNA. Relative *NPM* mRNA levels are shown +/- the S.E.M. of two independent experiments.



Annex 1. Supplementary Figure 14: PARN and EXOSC5 promote muscle differentiation by downregulating the expression of the *NPM* mRNA. The knockdown of PARN, EXOSC5 or NPM was performed in C2C12 cells and differentiation was induced 48 hours posttransfection of siPARN, siEXOSC5 or siNPM. C2C12 cells were fixed at day 3 of the differentiation process. **(a)** Immunofluorescence (IF) experiment using the anti-Myoglobin antibody as well as DAPI staining. Images of a single representative field are shown. Bars, 10 μ m. **(b)** The fusion index indicating the efficiency of C2C12 differentiation was determined as described in Material and Methods (section 9.1.5) and shown +/- the S.E.M. of two independent experiments.



Annex 1. Supplementary Table 1: mRNAs upregulated or downregulated in HuR-depleted myoblasts. Exponentially growing C2C12 myoblasts were transfected with HuR or Control (Ctr) siRNAs. RNA was prepared 48h after transfection. A cDNA array analysis was performed as described in the Material and Methods (section 9.1.5). A default external background setting was used in conjunction with a gene-based background signal threshold to determine gene signal significance. The mRNAs listed in this table represent the downregulated and upregulated mRNAs with z ratios (siRNA HuR/siRNA Ctr) below -2 or over 2, respectively, in two independent experiments.

	zratio Exp siRNA HuR vs siRNA Ctr	Gene Symbol	Gene Name
Upregulated mRNAs	1	4,40	Acta2 Mus musculus actin, alpha 2, smooth muscle, aorta (Acta2), mRNA
	2	3,88	Ftl1 ferritin light chain 1
	3	3,87	Anxa3 annexin A3
	4	3,72	Ftl1 ferritin light chain 1
	5	3,29	Npm1 nucleophosmin 1
	6	2,93	Rpl12 ribosomal protein L12
	7	2,88	Tnfrsf19 tumor necrosis factor receptor superfamily, member 19
	8	2,80	Ube3a ubiquitin protein ligase E3A
	9	2,76	Rps15 ribosomal protein S15
	10	2,65	Cycc cytochrome c, somatic
	11	2,24	Cdh1 cadherin 1
	12	2,06	Tm4sf9-pending transmembrane 4 superfamily member 9
Downregulated mRNAs	13	-2,05	Rpa2 replication protein A2
	14	-2,09	H3f3b H3 histone, family 3B
	15	-2,45	Grcc8 gene rich cluster, C8 gene
	16	-2,55	Calm1 calmodulin 1
	17	-2,72	Ctsl cathepsin L
	18	-2,86	Slc16a2 solute carrier family 16 (monocarboxylic acid transporters), member 2
	19	-2,90	Hsd3b1 hydroxysteroid dehydrogenase-1, delta<5>-3-beta
	20	-2,96	Ptpn21 protein tyrosine phosphatase, non-receptor type 21
	21	-3,13	Ctsl cathepsin L
	22	-3,31	Selel selectin, endothelial cell, ligand
	23	-3,46	Map3k7 mitogen activated protein kinase kinase kinase 7
	24	-3,76	no value Mus musculus GOBLIN mRNA for Golgi-associated band 4.1-like protein, complete cds
	25	-3,78	Hnrpa2b1 heterogeneous nuclear ribonucleoprotein A2/B1
	26	-3,78	Snta1 syntrophin, acidic 1
	27	-4,13	Pscd2 pleckstrin homology, Sec7 and coiled/coil domains 2
	28	-4,33	no value Mus musculus oasl7 gene for 2',5'-oligoadenylate synthetase-like 7, complete cds
	29	-5,35	Hmgn2 high mobility group nucleosomal binding domain 2
	30	-6,19	Xpo4-pending exportin 4

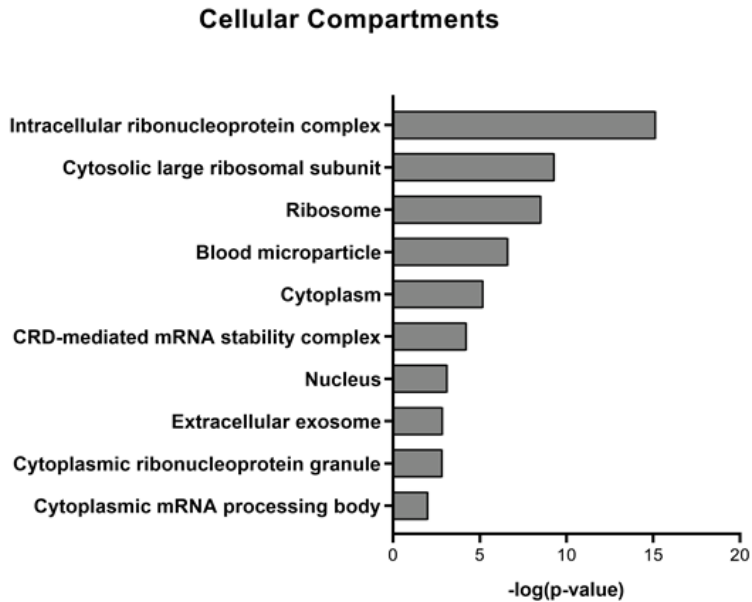
Annex 1. Supplementary Table 2: Primers used for the RT- PCR and –qPCR experiments.

Experiment	Gene / Probes	Sequence
Northern Blot	NPM	<u>Forward:</u> 5'-AAA AAG CGC CAG TGA AGA AA-3' <u>Reverse:</u> 5'-CTT CCT CCA CTG CCA GAG A-3'
PCR and qPCR	NPM	<u>Forward:</u> 5'-CCG AGA TCA AAG GGT CAA GA-3' <u>Reverse:</u> 5'-TCT TGA ATA GCC TCC TGG TCA-3'
	RPL32	<u>Forward:</u> 5'-TTC TTC CTC GGC GCT GCC TAC GA -3' <u>Reverse:</u> 5'-AAC CTT CTC CGC ACC CTG TTG TCA-3'
	MyoD	<u>Forward:</u> 5'-CGA CAC CGC CTA CTA CAG TG-3' <u>Reverse:</u> 5'-TTC TGT GTC GCT TAG GGA TG-3'
	GAPDH	<u>Forward:</u> 5'-AAG GTC ATC CCA GAG CTG AA-3' <u>Reverse:</u> 5'-AGG AGA CAA CCT GGT CCT CA-3'
	P21	<u>Forward:</u> 5'-GTA CTT CCT CTG CCC TGC TG -3' <u>Reverse:</u> 5'-TTC AGG GTT TTC TCT TGC AG-3'
	Myogenin	<u>Forward:</u> 5'- CGA CAC CGC CTA CTA CAG TC -3' <u>Reverse:</u> 5'- TTC TGT GTC GCT TAG GGA TG -3'
	Rluc	<u>Forward:</u> 5'-TTG AAT CAT GGG ATG AAT GG-3' <u>Reverse:</u> 5'-TGT TGG ACG ACG AAC TTC AC-3'
Run-on assay	NPM	<u>Forward:</u> 5'- GGC GCA CGC GCA AAA GC-3' <u>Reverse:</u> 5'- TCC AGA CAT GCC TAA GAG TT-3'
	MyoD	<u>Forward:</u> 5'- AGG GGC CAG GAC GCC C -3' <u>Reverse:</u> 5'- TTG CGC TTG CAC GCC TTG-3'
	GAPDH	<u>Forward:</u> 5'- AGA GAC GGC CGC ATC TTC-3' <u>Reverse:</u> 5'- CAG GAT GCA TTG CTG ACA A-3'
Gel-Shifft	3'UTR	<u>Forward:</u> 5'-TAA TAC GAC TCA CTA TAG GGA AGG GTT TAA ACA GTT TGA AAT A-3' <u>Reverse:</u> 5'-ACT TTA TTA AAA TAC TGA GTT TAT T-3'
	5'UTR	<u>Forward:</u> 5'-GAA TTG TAA TAC GAC TCA CTA TAG GG-3' <u>Reverse:</u> 5'-GAG GTG GAG GCG CGC ACT TC-3'
	P1	<u>Forward:</u> 5'-TAA TAC GAC TCA CTA TAG GGA AGG GTT TAA ACA GTT TGA AAT A-3' <u>Reverse:</u> 5'-CAT TTT AGA CAA CAC ATT CTT G 3'
	P2	<u>Forward:</u> 5'-TAA TAC GAC TCA CTA TAG GGC CTG TTT AGT TTT CAA GGA TG-3' <u>Reverse:</u> 5'-ACT TTA TTA AAA TAC TGA GTT TAT T-3'
	P1-1	<u>Forward:</u> 5'-TAA TAC GAC TCA CTA TAG GGG AAA AGG GTT TAA ACA GTT TGA AAT ATT CTG TCT TCA TTT CTG TAA TAG TTA-3' <u>Reverse:</u> 5'-TAA CTA TTA CAG AAA TGA AGA CAG AAT ATT TCA AAC TGT TTA AAC CCT TTT CCC CTA TAG TGA GTC GTA TTA-3'

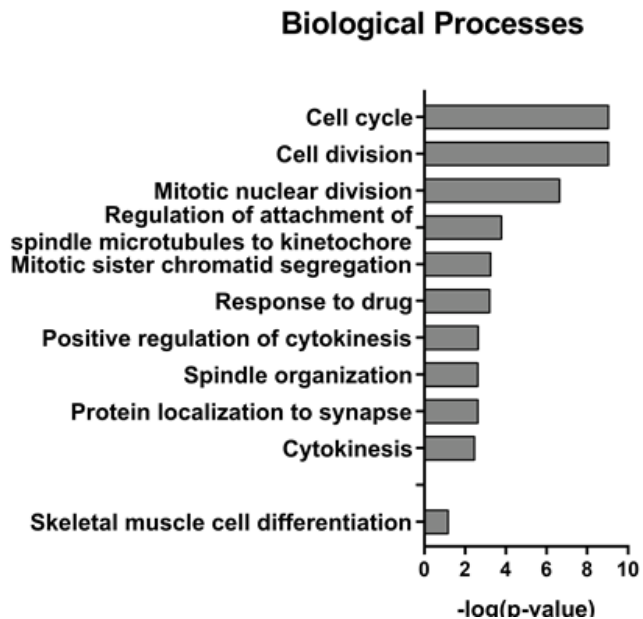
Gel-Shifft	P1-2	<u>Forward:</u> 5'-TAA TAC GAC TCA CTA TAG GGA TAT CTG GCT GTC CTT TTT ATA ATG CAA AGT GAG AAC TTT CCC TAC-3' <u>Reverse:</u> 5'-GTA GGG AAA GTT CTC ACT TTG CAT TAT AAA AAG GAC AGC CAG ATA TCC CTA TAG TGA GTC GTA TTA-3'
	P1-3	<u>Forward:</u> 5'-TAA TAC GAC TCA CTA TAG GGT ACT GTG TTT GAT AAA TGT TGT CCA GGT TCA CTT GCC AAG AAT GTG TTG TCT AAA ATG-3' <u>Reverse:</u> 5'-CAT TTT AGA CAA CAC ATT CTT GGC AAG TGA ACC TGG ACA ACA TTT ATC AAA CAC AGT ACC CTA TAG TGA GTC GTA TTA-3'
	P2-1	<u>Forward:</u> 5'- TAA TAC GAC TCA CTA TAG GGC CTG TTT AGT TTT CAA GGA TGG AAC TCC ACC CTT TAC TTG GTT TTA AGT-3' <u>Reverse:</u> 5'- ACT TAA AAC CAA GTA AAG GGT GGA GTT CCA TCC TTG AAA ACT AAA CAG GCC CTA TAG TGA GTC GTA TTA -3'
	P2-2	<u>Forward:</u> 5'- TAA TAC GAC TCA CTA TAG GGA GTA TGT ATG GAA TGT TAT GAT AGG ACA TAG TAA TAG TGG TCA GAT GTG GAA A -3' <u>Reverse:</u> 5'- TTT CCA CAT CTG ACC ACT ATT ACT ATG TCC TAT CAT AAC ATT CCA TAC ATA CTC CCT ATA GTG AGT CGT ATT A - 3'
	P2-3	<u>Forward:</u> 5'- TAA TAC GAC TCA CTA TAG GGA AAT GGT AGG GAG ACA AAT ATA CAT GTG AAA TAA ACT CAG TAT TTT AAT AAA GT- 3' <u>Reverse:</u> 5'- ACT TTA TTA AAA TAC TGA GTT TAT TTC ACA TGT ATA TTT GTC TCC CTA CCA TTT CCC TAT AGT GAG TCG TAT TA-3'

13.2. Annex 2. Supplemental material for CHAPTER II

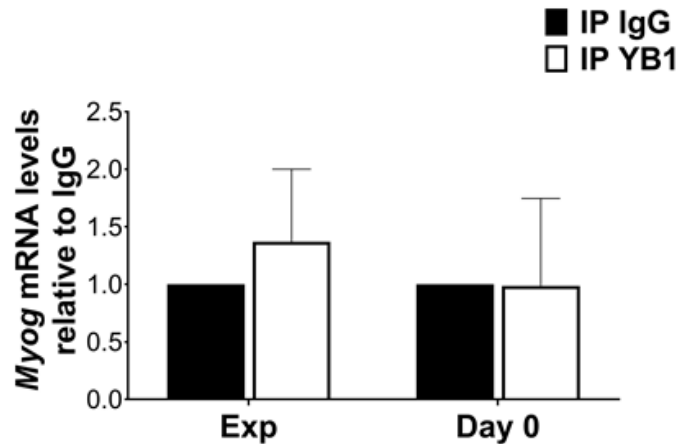
Annex 2. Supplementary Figure 1. Gene Ontology (GO) analysis was conducted using DAVID v6.8® to classify HuR putative protein partners based on Cellular Compartments. A total of 41 candidates were analyzed.



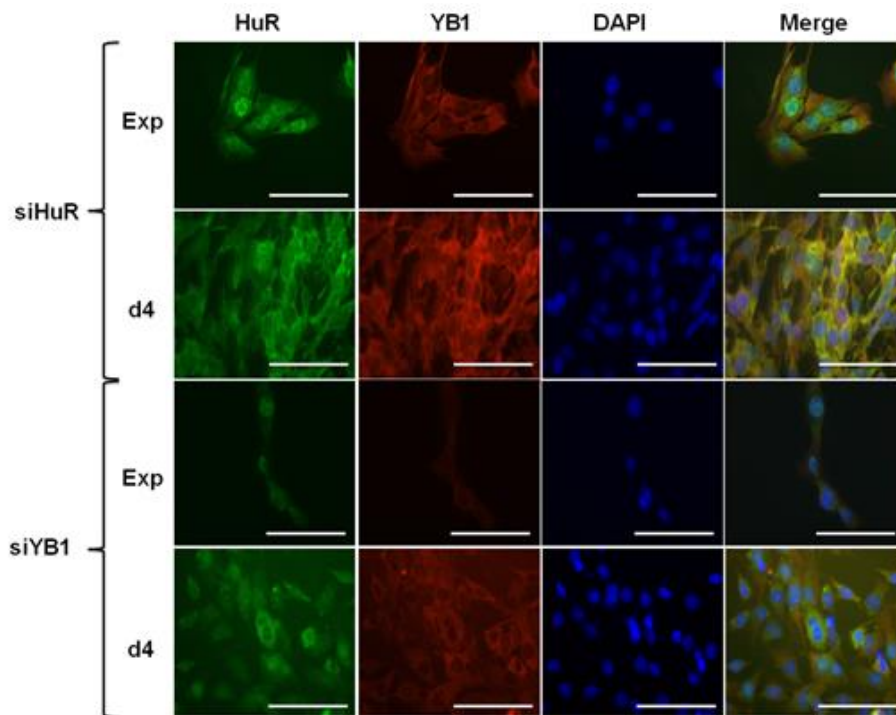
Annex 2. Supplementary Figure 2. Gene Ontology (GO) analysis was conducted using DAVID v6.8® to classify putative mRNA common targets of HuR and YB1 based on Biological Processes. A total of 409 candidates were analyzed.



Annex 2. Supplementary Figure 3. RNA was isolated from the IP of YB1 (IgG was used as a negative control) and RT-qPCR was performed using primers specific for *Myog* and *GAPDH* mRNAs. *Myog* mRNA levels were standardized against *GAPDH* mRNA levels. The normalized *Myog* mRNA levels were then plotted relatively to the IgG IP condition +/- s.e.m. of 3 independent experiments.



Annex 2. Supplementary Figure 4. IF experiments were performed on C2C12 cell treated with siRNAs against HuR (siHuR) or YB1 (siYB1) using a HuR or YB1 antibody as well as DAPI. Images of a single representative field are shown. Bars 100µm.



O70133	DHX9	DEAH (Asp-Glu-Ala-His) box polypeptide 9(Dhx9)
Q6A0A9	FAM120A	Family with sequence similarity 120, member A(Fam120a)
Q8C3F2	FAM120C	Family with sequence similarity 120, member C(Fam120c)
E9PV24	FGA	Fibrinogen alpha chain (Fga)
Q8K0E8	FGB	Fibrinogen beta chain (Fgb)
Q61584	FXR1	Fragile X mental retardation gene 1, autosomal homolog (Fxr1)
P70333	HNRNPH2	Heterogeneous nuclear ribonucleoprotein H2(Hnrnph2)
Q8VHM5	HNRNPR	Heterogeneous nuclear ribonucleoprotein R(Hnrnpr)
P51660	HSD17B4	Hydroxysteroid (17-beta) dehydrogenase 4(Hsd17b4)
Q9CPN8	IGF2BP3	Insulin-like growth factor 2 mRNA binding protein 3(Igf2bp3)
P01786	Ighvhs107.a3.106	Ig heavy chain V region VHS107.a3.106(Ighvhs107.a3.106)
A0A140LIF8	Irgm2	Immunity-related gtpase family M member 2(Irgm2)
P01843	LOC433053	Ig lambda1 chain c region (LOC433053)
Q5SUF2	LUC7L3	LUC7-like 3 (S. Cerevisiae) (Luc7l3)
Q8K310	MATR3	Matrin 3(Mat3)
P23249	MOV10	Moloney leukemia virus 10(Mov10)
Q5SX39	MYH4	Myosin, heavy polypeptide 4, skeletal muscle (Myh4)
P09405	NCL	Nucleolin(Ncl)
Q61838	PZP	Pregnancy zone protein(Pzp)
O09167	RPL21	Ribosomal protein L21(Rpl21)
P62751	RPL23A	Ribosomal protein L23A(Rpl23a)
Q8BP67	RPL24	Ribosomal protein L24(Rpl24)
P61358	RPL27	Ribosomal protein L27(Rpl27)
P14115	RPL27A	Ribosomal protein L27A(Rpl27a)
P41105	RPL28	Ribosomal protein L28(Rpl28)
P83882	RPL36A	Ribosomal protein L36A(Rpl36a)
Q9D8E6	RPL4	Ribosomal protein L4(Rpl4)
P62267	Rps23	Ribosomal protein S23(Rps23)
Q99LF4	RTCB	RNA 2',3'-cyclic phosphate and 5'-OH ligase (Rtcb)
Q8BTI8	SRRM2	Serine/arginine repetitive matrix 2(Srrm2)
P84104	SRSF3	Serine/arginine-rich splicing factor 3(Srsf3)
Q8BL97	SRSF7	Serine/arginine-rich splicing factor 7(Srsf7)
Q7TMK9	SYNCRIP	Synaptotagmin binding, cytoplasmic RNA interacting protein (Syncrip)
Q9EPU0	UPF1	UPF1 regulator of nonsense transcripts homolog (yeast)(Upf1)
P29788	VTN	Vitronectin (Vtn)
P62960	YBX1	Y box protein 1(Ybx1)

Annex 2. Supplementary Table 2. List of proteins used in the geneMANIA analysis to investigate the HuR protein-protein interaction network (PPI) in muscle cells.

Protein	Gene	Description	ACC
AGO2	Ago2	Argonaute RISC catalytic subunit 2	MGI:2446632
DHX9	Dhx9	DEAH (Asp-Glu-Ala-His) box polypeptide 9	MGI:108177
FAM120A	Fam120a	Family with sequence similarity 120, member C	MGI:2446163
FXR1	Fxr1	Fragile X mental retardation gene 1, autosomal homolog	MGI:104860
HNRNPH2	Hnrnph2	Heterogeneous nuclear ribonucleoprotein H2	MGI:1201779
HuR	Elavl1	ELAV-like protein 1, Human antigen R	MGI:1100851
IGF2BP3	Igf2bp3	Insulin-like growth factor 2 mRNA binding protein 3	MGI:1890359
MATR3	Matr3	Matrin 3	MGI:1298379
MOV10	Mov10	Moloney leukemia virus 10	MGI:97054
NCL	Ncl	Nucleolin	MGI:97286
RPL23A	Rpl23a	Ribosomal protein L23A	MGI:3040672
SRSF3	Srsf3	Serine/arginine-rich splicing factor 3	MGI:98285
SRSF7	Srsf7	Serine/arginine-rich splicing factor 7	MGI:1926232
SYNCRIP	Syncrip	Synaptotagmin binding, cytoplasmic RNA interacting protein	MGI:1891690
UPF1	Upf1	UPF1 regulator of nonsense transcripts homolog	MGI:107995
YBOX1	Ybx1	Y box protein 1	MGI:99146
AGO1	Ago1	Argonaute RISC catalytic subunit 1	MGI:2446630
ARPC4	Arpc4	Actin related protein 2/3 complex, subunit 4	MGI:1915339
DDX28	Ddx28	DEAD box helicase 28	MGI:1919236
DDX4	Ddx4	DEAD box helicase 4	MGI:102670
EIF4E	Eif4e	Eukaryotic translation initiation factor 4E	MGI:95305
HNRNPA0	Hnrnpa0	Heterogeneous nuclear ribonucleoprotein A0	MGI:1924384
HNRNPA3	Hnrnpa3	Heterogeneous nuclear ribonucleoprotein A3	MGI:1917171
Hnrnpdl	hnrnpd1	Heterogeneous nuclear ribonucleoprotein D-like	MGI:1355299
HNRNPF	Hnrnpf	Heterogeneous nuclear ribonucleoprotein F	MGI:2138741
Ilf3	Ilf3	Interleukin enhancer binding factor 3	MGI: 1339973
MRPL23	Mrpl23	Mitochondrial ribosomal protein L23	MGI:1196612
Nhp211	nhp211	NHP2 non-histone chromosome protein 2-like 1 (S. Cerevisiae)	MGI:893586
NUP43	Nup43	Nucleoporin 43	MGI:1917162
OGFOD1	Ogfod1	2-oxoglutarate and iron-dependent oxygenase domain containing 1	MGI:2442978
PDIA5	Pdia5	Protein disulfide isomerase associated 5	MGI:1919849
Rpl11	rol11	Ribosomal protein L11	MGI:1914275

SMG1	Smg1	SMG1 homolog, phosphatidylinositol 3-kinase-related kinase	MGI:1919742
SPG11	Spg11	SPG11, spatacsin vesicle trafficking associated	MGI:2444989
TRA2B	Tra2b	Transformer 2 beta	MGI:106016
YARS2	Yars2	Tyrosyl-trna synthetase 2 (mitochondrial)	MGI:1917370

Annex 2. Supplementary Table 3. List of YB1 and HuR common mRNA targets in C2C12 cells identified by performing IP experiments using anti-HuR and anti-YB1 antibodies followed by RNA-seq analysis. Proteins that showed a 2-fold enrichment in the anti-HuR and anti-YB1 with respect to the anti-IgG controls were considered for analysis. mRNAs are placed in alphabetical order.

42433	A330009N23Rik	C920009B18Rik	Cdkn1a	D030025P21Rik
42618	AA414768	Cacna1b	Cdkn3	Dclk1
1110006O24Rik	Actb	Cage1	Cenpi	Dctd
1110059M19Rik	Agmat	Calr	Cenpl	Defb41
1700008I05Rik	Al467606	Calr4	Cenpw	Depdc1a
1700012B09Rik	Aif1l	Camk2n2	Cep128	Depdc1b
1700013G24Rik	Aim1l	Capn12	Cep164	Dhcr7
1700019L03Rik	Aim2	Car13	Cfl1	Dlg4
1700034F02Rik	Akr1b3	Car5b	Chaf1b	Dlgap1
1700055N04Rik	Apol9b	Casp8	Chn1	Dlgap2
1700086L19Rik	Arhgef39	Ccdc116	Chn2	Dlgap5
1700088E04Rik	Arl14epl	Ccdc24	Chrna1	Dlx2
1810041L15Rik	Asf1b	Ccdc73	Chst11	Dlx3
1810055G02Rik	Atp1a3	Ccdc83	Chsy1	Dmbx1
2210409D07Rik	Atp6v0e	Ccdc92	Ckap2l	Dnaic1
2310008H04Rik	AU018091	Ccl17	Cks1b	Dnase1l3
2310034O05Rik	Aurkb	Ccl2	Cldn2	Dynap
2410018L13Rik	Bard1	Ccnb1	Cmtm3	Dynll1
2610034B18Rik	Bcl3	Ccne1	Cnn3	Dynlrb1
2610318N02Rik	Bean1	Cd27	Cnr1	Dzip1
2810408A11Rik	Bend6	Cd44	Cntd1	E2f1
2810433D01Rik	Best1	Cd63	Cntrob	E2f8
4833427G06Rik	Bgn	Cd80	Cpa4	Ect2
4930427A07Rik	Birc5	Cdc25b	Cpne2	Eme1
4930500J02Rik	Bsn	Cdca3	Creb3l1	Eno2
4930592A05Rik	Btbd11	Cdca7l	Cxcl13	Epb4.1l3
4933412E12Rik	C1ql1	Cdca8	Cxcl5	Evl
5031414D18Rik	C1qtnf3	Cdh1	Cxcr4	Ezr

F2rl2
Fads2
Faim
Fam110c
Fam129c
Fam189a1
Fam194a
Fam211b
Fam71b
Fam71f1
Fam83d
Fancd2
Fanci
Fbxl13
Fgfbp1
Foxc2
Foxq1
Frk
Fstl3
Fzd2
Gata4
Gatm
Gja3
Gjd2
Gjd4
Glipr2
Glis3
Gm10471
Gm10494
Gm10653
Gm12191
Gm13139
Gm14005
Gm14635
Gm15706
Gm16197
Gm17455
Gm2694
Gm4371
Gm4636
Gm6634

Gm773
Gm8234
Gm8615
Gm9776
Gp1bb
Gp5
Gpr126
Gpr3
Gpr37
Gpr63
Gprc5a
H2afy2
Hebp2
Heph11
Hmga2-ps1
Hmox1
Hmx2
Hoxc13
Hs1bp3
Hsd11b2
Htr1d
Hyi
Igf2
Igf2bp2
Igsf11
Il12a
Il12rb1
Il13ra2
Il18
Il1rn
Isx
Katnal2
Kctd13
Kctd7
Kif14
Kif20a
Kif23
Kif24
Kifc5b
Klk1b22
Knstrn

Kremen2
Krt7
Lef1
Letmd1
Lif
Limk1
Lpar1
Lpar2
Lpcat4
Lrp11
Lrp8
Lrrc73
M1ap
Mab21l3
Macc1
Mad1l1
Mad2l1
Map3k19
Marcks11
Mcpt8
Meis2
Mfap3l
Mgam
Mgarp
Mis18bp1
Mmd
Mmp10
Mmp12
Morn4
Mov10l1
Msh5
Mt1
Mustn1
Mxd1
Myc
Mycl1
Myh3
Myl12b
Myo1h
Myo7b
Myod1

Myog
Nanos3
Nap1l2
Nefl
Nek2
Ngfrap1
Nhlrc4
Nme5
Nmnat2
Npas3
Nppb
Nptx1
Nsdhl
Nudt17
Nxf3
Olfml2b
Onecut2
Orai2
Ormdl2
Otx1
P4ha3
Pabpc1l
Palb2
Parppb
Pcdhb21
Pced1b
Pcgf2
Pclo
Pcyox1l
Pcyt1b
Pdk3
Pdpn
Peg10
Peg12
Pet2
Phex
Phlda1
Pigf
Pnma1
Polr3g
Pqlc3

Prc1
Prim2
Prr11
Psat1
Ptchd1
Ptgds
Qrfp
Rab31
Rad51ap1
Rad54b
Rad54l
Ranbp1
Rapgef11
Rgs10
Rhov
Rhox10
Rnase1
Rpl27
Rps15a-ps6
Runx3
S100a11
S100a3
Sc4mol
Scml4
Scn10a
Scrn1
Sdc1
Sdsl
Sema4b
Serpib1a
Serpib9b
Sesn2
Sfxn3
Sgol1
Sh2d7
Shcbp1
Sla
Sla2
Slc23a3
Slc25a14
Slc44a4

Slc6a17	Spock1	Syt8	Tnfrsf22	Ubal2
Slc6a19	Spp1	Tcf7	Tnfrsf25	Ube2c
Slc7a5	St3gal4	Tes	Tnnt2	Ube2l6
Slurp1	St8sia1	Tgfb1i1	Tor1a	Ucp2
Smim6	St8sia2	Tgif1	Tpgs2	Uhrf1
Soat1	Stac2	Tigd3	Tpx2	Unc5c
Spag5	Stambpl1	Tmem121	Tram11	Upp1
Spc25	Stil	Tmem151a	Try5	Usp29
Specc1	Sult2b1	Tmem158	Tspan31	Vash2
Speer4a	Susd3	Tmem184a	Tspan6	Zfp239
Spg21	Syn1	Tmem194b	Ttll1	Zfp41
Spink4	Synpr	Tmem200a	Tuba1a	Zic1
Spn	Syt13	Tmprs2	Tyms	

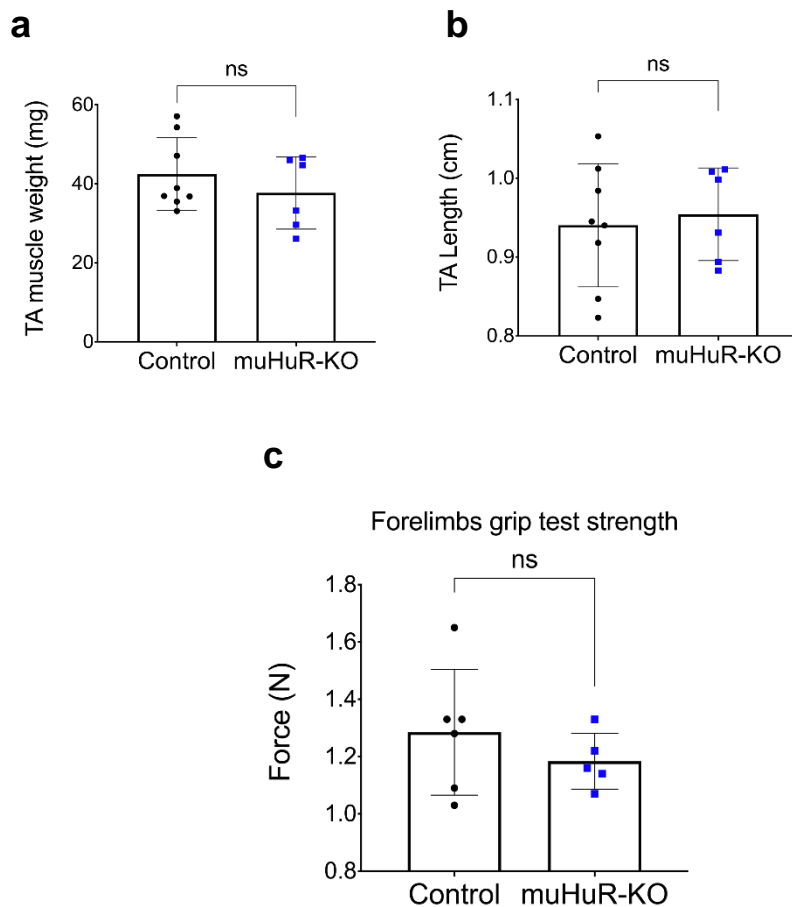
Annex 2. Supplementary Table 4. Primer sequence used for plasmid construction as well as gel shift and qPCR experiments.

Experiment	Gene / Probe	Sequence
Plasmid	GST-YB1	Forward 5'-CGC GGA TCC ATG AGC AGC GAG GCC GAG ACC-3' Reverse 5'-CCG CTC GAG TTA CTC AGC CCC GCC CTG CTC -3'.
	GST-HuR	Forward 5'-GGC AGA TCT AAT GGT TAT GAA GAC CAC A-3' Reverse 5'-GGC GAA TTC TTA TTT GTG GGA CTT GTT GGT T-3'.
	GFP-HuR	Forward 5'-TTC TTC CTC GGC GCT GCC TAC GA -3' Reverse 5'-AAC CTT CTC CGC ACC CTG TTG TCA-3'
qPCR	<i>Myog</i>	Forward: 5'-CCG AGA TCA AAG GGT CAA GA-3', Reverse: 5'-TCT TGA ATA GCC TCC TGG TCA-3'
	<i>GAPDH</i>	Forward: 5'-AAG GTC ATC CCA GAG CTC AA -3', Reverse: 5'-AGG AGA CAA CCT GGT CCT CA -3'
	<i>Luciferase</i>	Forward: 5'-TTG AAT CAT GGG ATG AAT GG-3', Reverse: 5'-TGT TGG ACG ACG AAC TTC AC -3'
	<i>RPL32</i>	Forward 5'-TTC TTC CTC GGC GCT GCC TAC GA -3' Reverse 5'-AAC CTT CTC CGC ACC CTG TGG TCA -3'
Gel-Shift	G/URE-1	Sense: 5'- CAAACTCAGGAGCTTCTTTTTTGTATCATAAT-3' Anti-sense: 5'- ATTATGATAAACAAAAAAGAAGCTCCTGAGTTTG -3'
	G/URE-2	Sense: 5'- TGTGTATTGTTTATTGTTTTGTGTGTTGTTTGTA AAA -3' Anti-sense: 5'- TGTGTATTGTTTATTGTTTTGTGTGTTGTTTGTA AAA -3'
	G/URE-3	Forward: 5'- GGG TGA CTT CTT TTG TTA AC -3' Reverse: 5'- TTA CAA AAG AAA AAA AAT TG -3'

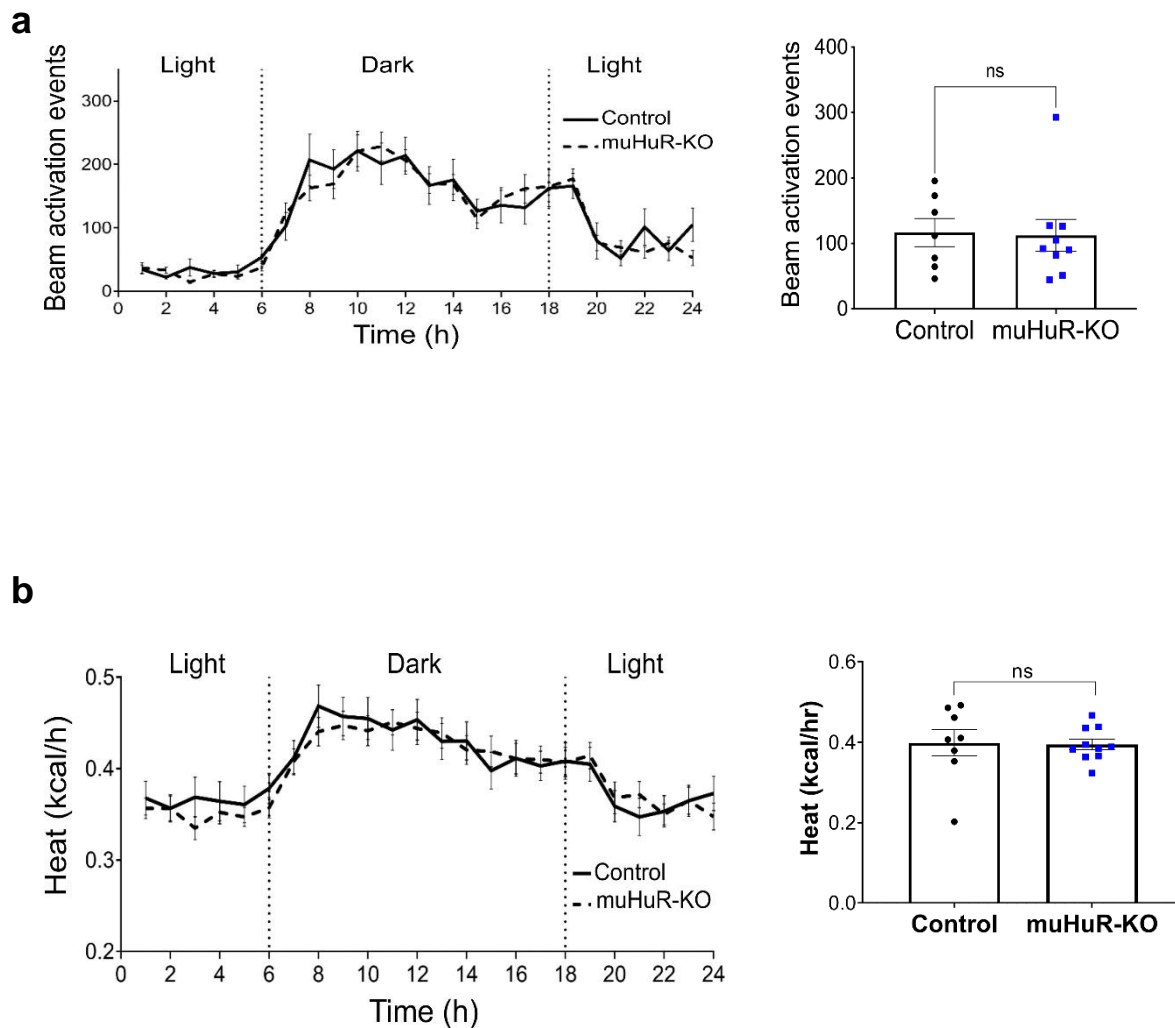
13.3. Annex 3. Supplemental material for CHAPTER III

Annex 3. Supplementary Figure 1. HuR muscle specific KO mice exhibit a decrease in muscle contraction strength. **a** Fatigability in Fig. 2a was normalized to TA muscle weight (**Left panel**) and length (**Right panel**). **b** Grip strength was evaluated on age-matched control and muHuR- KO mice using a digital force gauge. Peak force (N) was measured from forelimbs in 2 sessions. Each session consisted of triplicate measurements taken during 3 consecutive days. 4 days of resting were allowed in between sessions. The results are presented as mean \pm S.E.M, unpaired t-test. (**a**, control n=8 and muHuR-KO n=6), (**b**, control n=6 and muHuR-KO n=5).

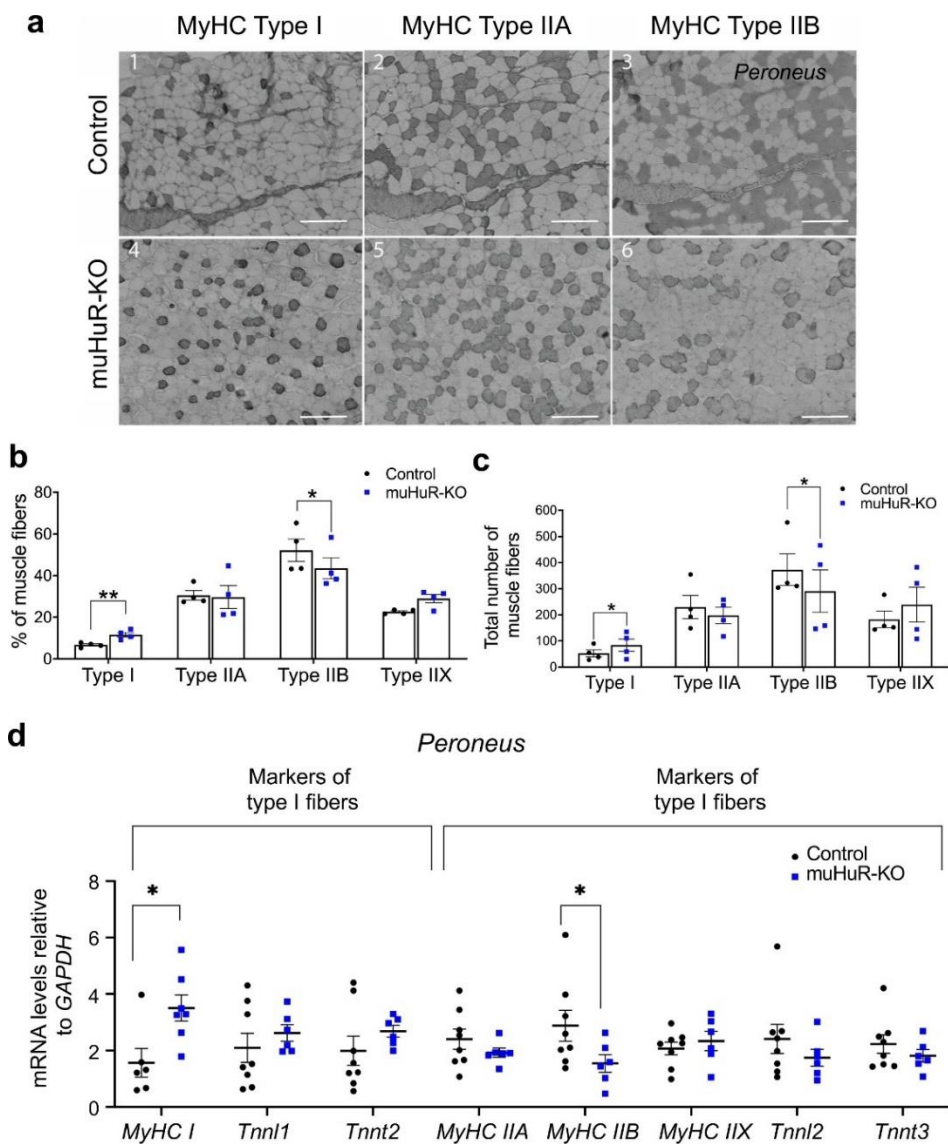
Muscle contraction force experiment



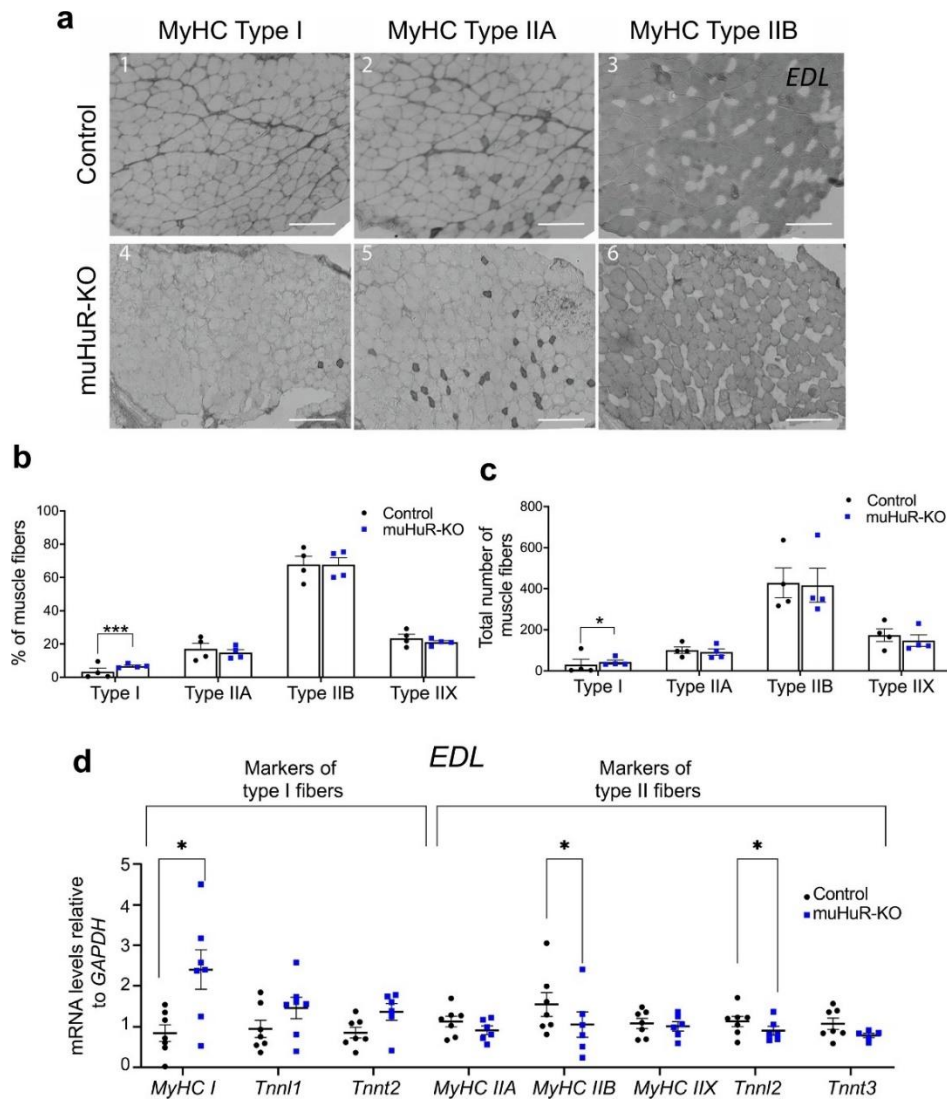
Annex 3. Supplementary Figure 2 muHuR-KO mice display no significant difference in heat production (Energy expenditure) or ambulatory activity when compared to control littermates. **a-b** A Comprehensive Animal Monitoring System (CLAMS; Columbus Instruments, Columbus, OH) was used for a 3-day indirect calorimetry study in age-matched mice under a 12h light–12h dark cycle. **(b)** Heat production was calculated using the following equation: $((3.82 + 1.23 \times \text{RER}) \times \text{VO}_2)$. **(a)** **(Left panel)** Ambulatory activity was estimated by the number of infrared beam breaks along the x-axis of the metabolic cage. **(Right panel)** Mean values of beam activation events during 72h in control and muHuR-KO mice. **(b)** **(Left panel)** Graph depicting the average values at each time point. **(Right panel)** Mean values of heat production during 72h in control and muHuR-KO mice. Data was analyzed using CLAMS examination tool (CLAX; Columbus Instruments) version 2.1.0 (**a** and **b** right panels, Control: n=7, muHuR-KO: n=9). The results are presented as mean \pm S.E.M, *p < 0.05 unpaired t-test.



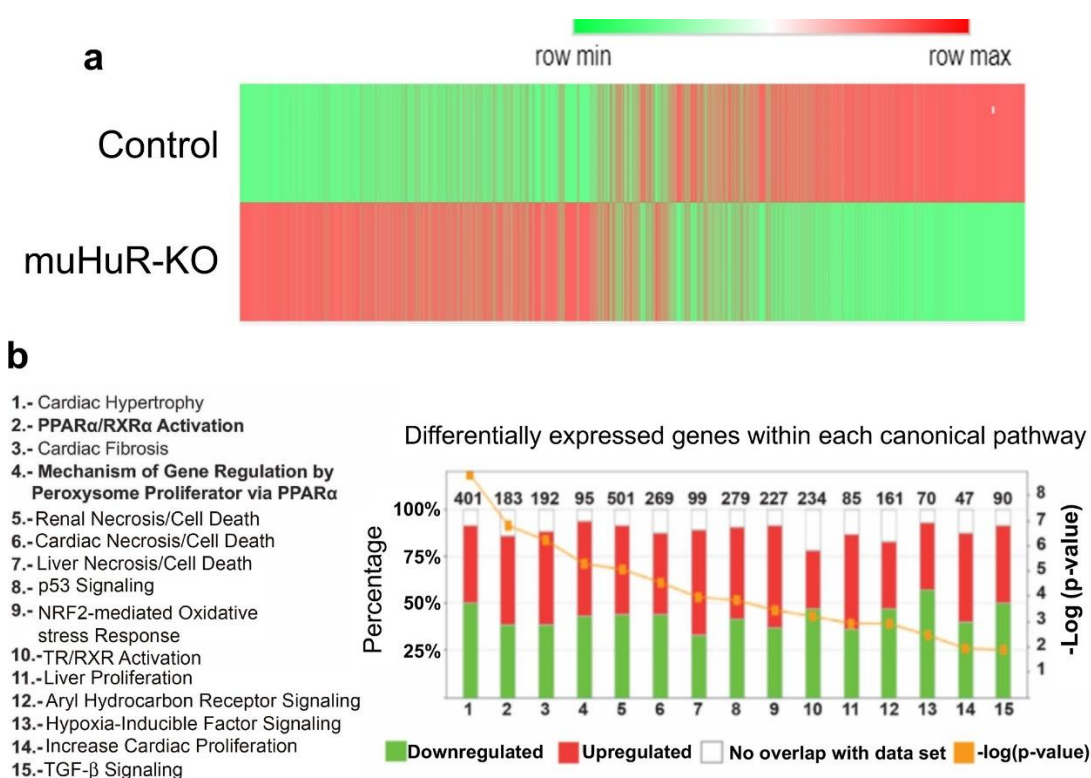
Annex 3. Supplementary Figure 3 Depletion of HuR in skeletal muscle increases the proportion of type I fibers in *peroneus* muscle. **a** Representative photomicrograph of serial sections of *peroneus* muscle from control and muHuR-KO mice taken after immunostaining with anti-Myosin Heavy Chain (MyHC) antibodies type I, type IIA and type IIB. scale bars: 100 μ m. **b-c** Quantification of muscle fibers type I, type IIA, and type IIB, was ascertained manually. Fibers type IIX were calculated by counting the unstained fibers. Results are graphed as the percentage (%) of the total number of fibers per muscle (**b**) and absolute total number of fibers per muscle (**c**) (n=4 mice). **d** mRNA expression of known markers of fiber type specificity (*Tnn1*, *Tnn2*, *Tnnt2*, *Tnnt3*, *MyHC I*, *MyHC IIA*, *MyHC IIB*, *MyHC IIX*) was assessed by RT-qPCR. mRNA levels were standardized against *GAPDH* and plotted relative to the expression in control mice (muHuR-KO n=6 except for *MyHC I* where n=7), (Control n=8, except for *MyHC I* where n=6).



Annex 3. Supplementary Figure 4 Depletion of HuR in skeletal muscle increases the proportion of type I fibers in EDL muscle. **a** Representative photomicrograph of serial sections from of EDL muscle from control and muHuR-KO mice taken after immunostaining with anti-Myosin Heavy Chain (MyHC) antibodies type I, type IIA and type IIB. Scale bars: 100 μ m. **b-c** Quantification of muscle fibers type I, type IIA, and type IIB, was ascertained manually. Fibers type IIX were calculated by counting the unstained fibers. Results are graphed as percentage (%) of the total number of fibers per muscle (**b**) and total number of fibers per muscle (**c**) (n=4 mice). **d** mRNA expression of known markers of fiber type specificity (*Tnn1*, *Tnnl2*, *Tnnt1*, *Tnnt3*, *MyHC I*, *MyHC IIA*, *MyHC IIB*, *MyHC IIX*) was assessed by RT-qPCR. mRNA levels were standardized against *GAPDH* and plotted relative to the expression in control mice. (muHuR-KO n=6 except for *MyHC I* n=5, *Tnn1* and *Tnnt2* n=7), (Control n=7, except for *MyHC I* where n=8).

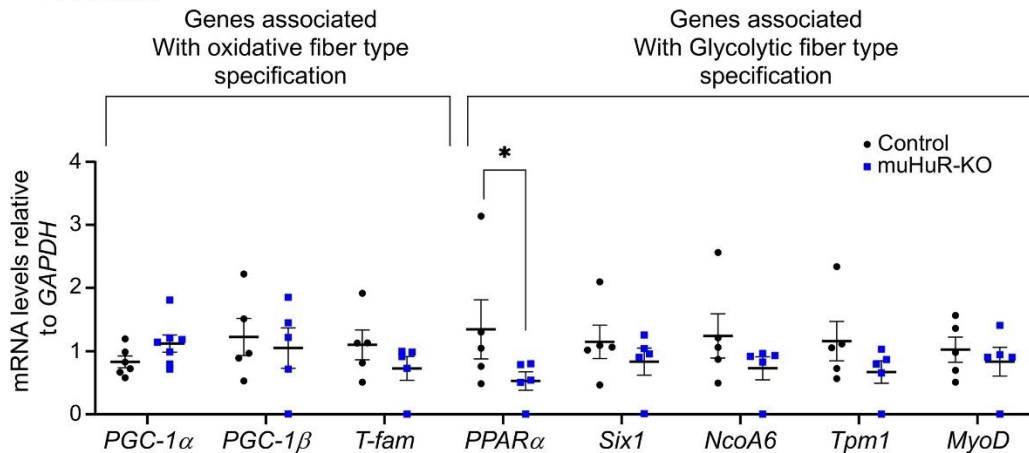


Annex 3. Supplementary Figure 5 Heat Map and IPA analysis of RNAseq data. **a** Heat map analysis of RNA-seq data depicting the changes of gene expression in muHuR-KO mice *soleus* muscles. All transcripts with normalized read counts >0 across all samples were selected for *in silico* analysis and used as input into the website Morpheus to generate a heat map according to the instruction. **b** Differential expression in signaling pathways as analyzed by IPA®. Percentage of genes down-regulated (green), up-regulated (red) or not represented in our data set (white) are shown in the left Y-axis. The total number of genes found within each pathway are shown above each bar graph. The right Y-axis, represented by the orange points, shows the $-\log p$ value for each pathway. Raw data for RNAseq are provided in Annex 3. Supplementary Table 2.

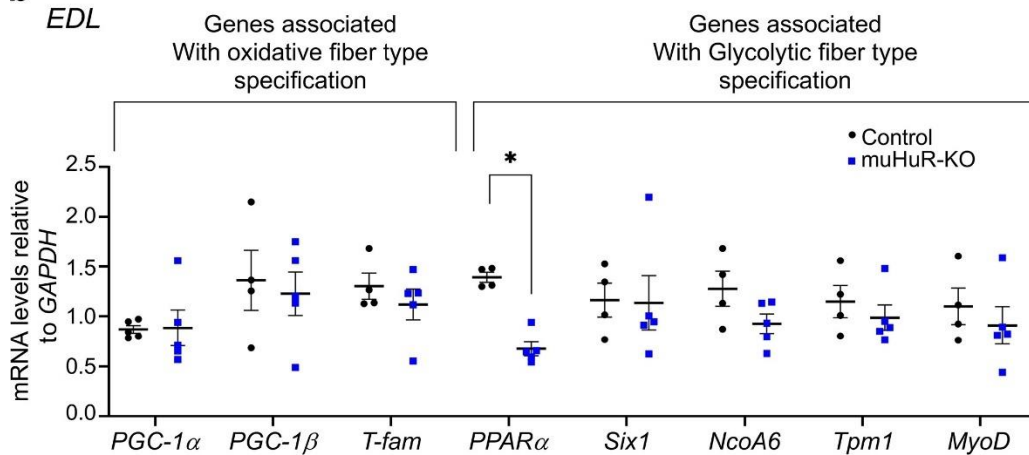


Annex 3. Supplementary Figure 6. HuR differentially affects the expression of mRNAs associated to metabolism in peroneus and EDL muscles. **a-b** Total RNA was isolated from *peroneus* (**a**) or EDL muscles (**b**) of control and muHuR-KO mice and relative expression level of genes associated to PPAR signaling and/or fiber type specification (*PGC-1 α* , *PGC-1 β* , *Tfam*, *PPAR α* , *Six1*, *Tpm1*, *NCOA6*, *MyoD*) was assessed by RT-qPCR. Relative mRNA levels were standardized against *GAPDH* and plotted relatively to the expression in control mice (muHuR-KO n=6, (Control n=4, except for *PGC-1 α* where n=5). The results are presented as mean \pm S.E.M, * $p < 0.05$, ** $p < 0.005$ unpaired t-test.

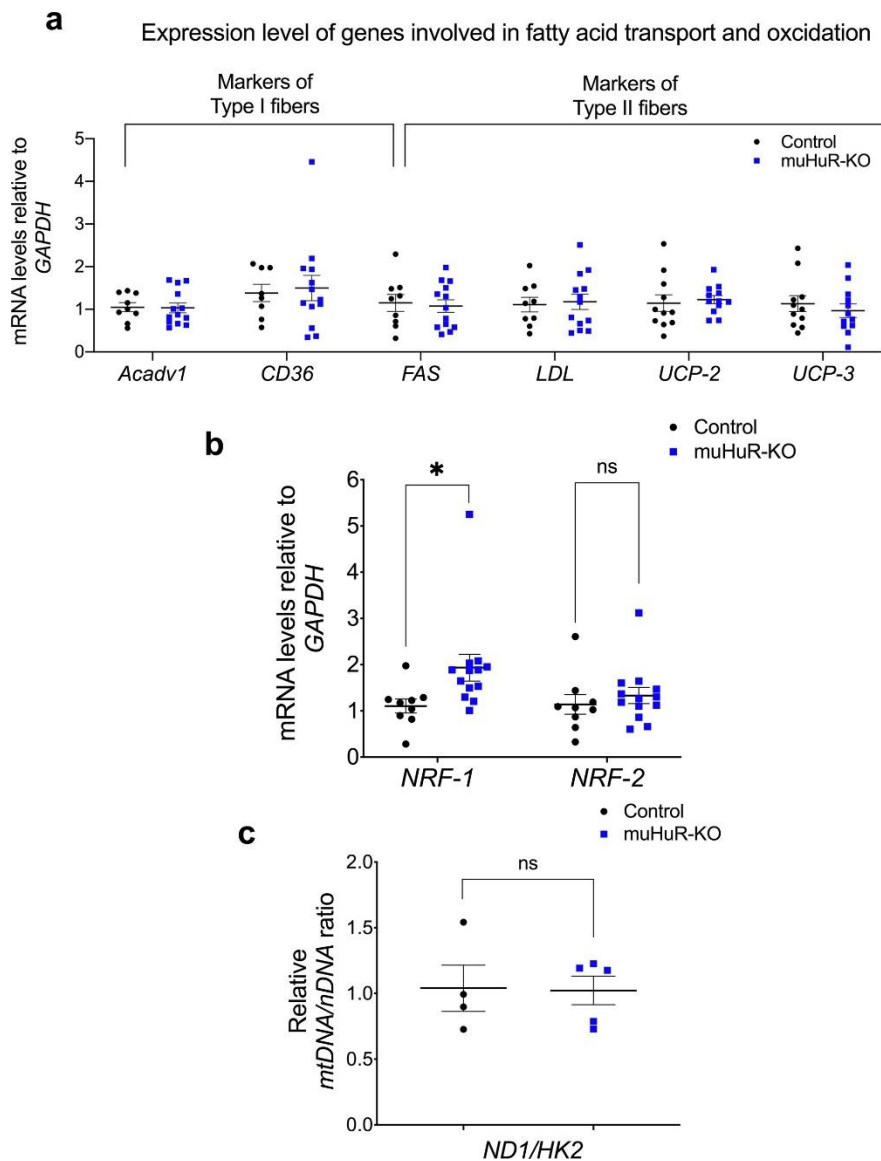
a *Peroneus*



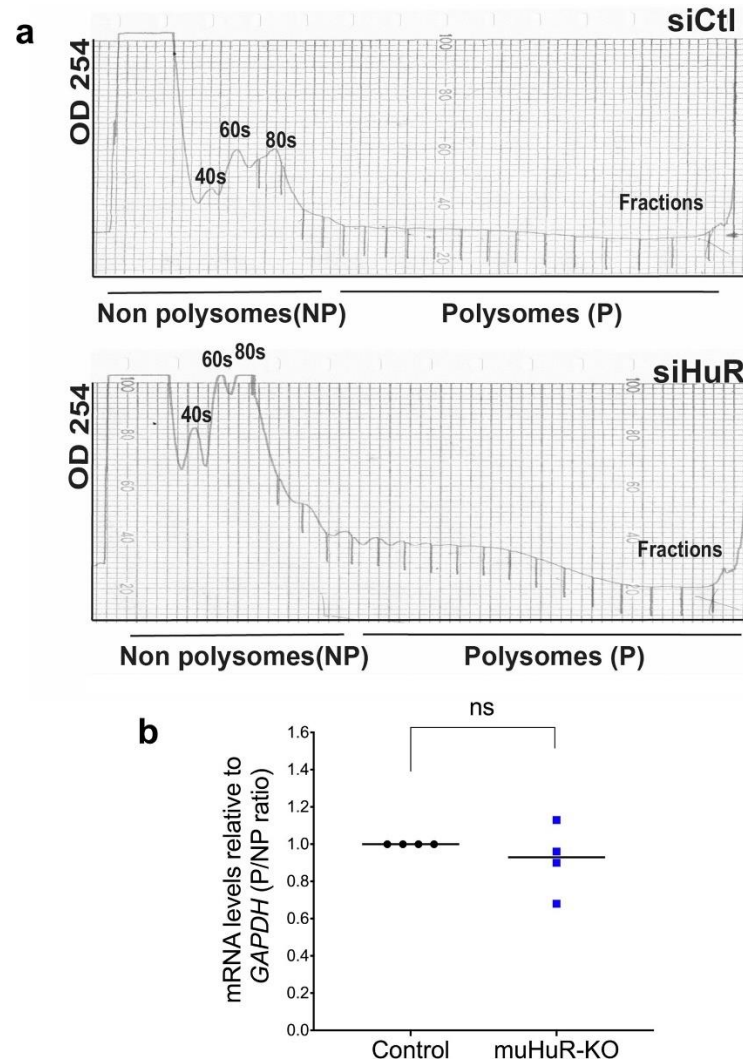
b



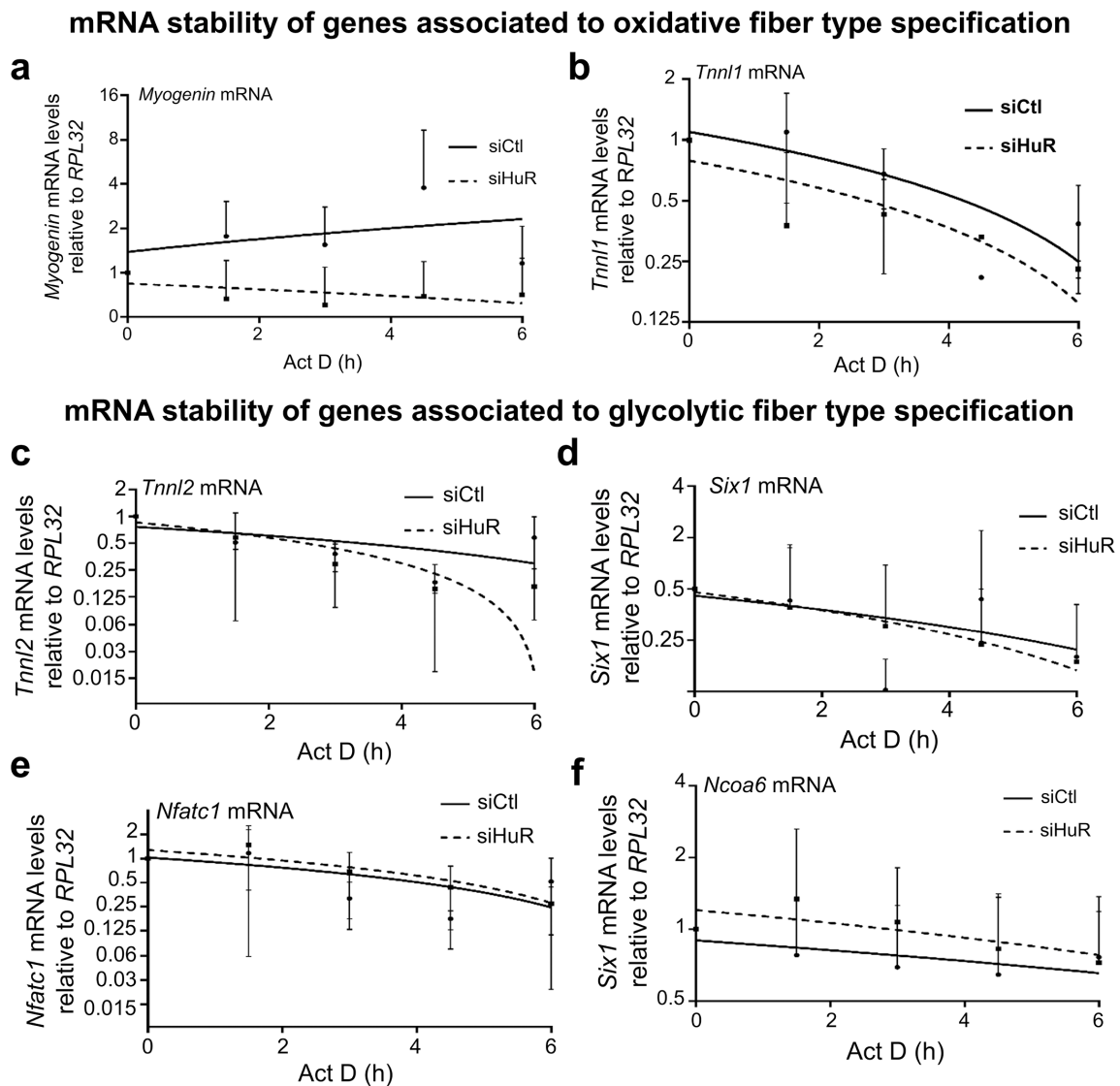
Annex 3. Supplementary Figure 7 Effect of HuR depletion in lipid metabolism and oxidative phosphorylation. **a-b** Total RNA was isolated from *soleus* muscles from control and muHuR- KO mice and relative expression of genes involved in **(a)** fatty acid transporters and oxidation [*Acadv1* (control n=9, muHuR-KO n=12), *CD36* (control n=8, muHuR-KO n=13), *FAS* (control n=9, muHuR-KO n=13), *LDL* (control n=9, muHuR-KO n=12), *UCP-2* and *UCP-3* (control n=11, muHuR-KO n=13) and **(b)** mitochondrial biogenesis [*NRF-1*, *NRF-2* (control n=9, muHuR-KO n=13)] was assessed by RT-qPCR in *soleus* muscles of Ctl and muHuR-KO mice. mRNA levels were standardized against *GAPDH* and plotted relatively to control animals. **c** DNA extracted from *gastrocnemius* muscle was used to determine the mtDNA/nDNA ratio. Expression levels were standardized against Hexokinase 2 (HK2) and plotted relatively to control animals (control n=4, muHuR-KO n=5). The results are presented as mean \pm S.E.M, *p < 0.05 unpaired t-test.



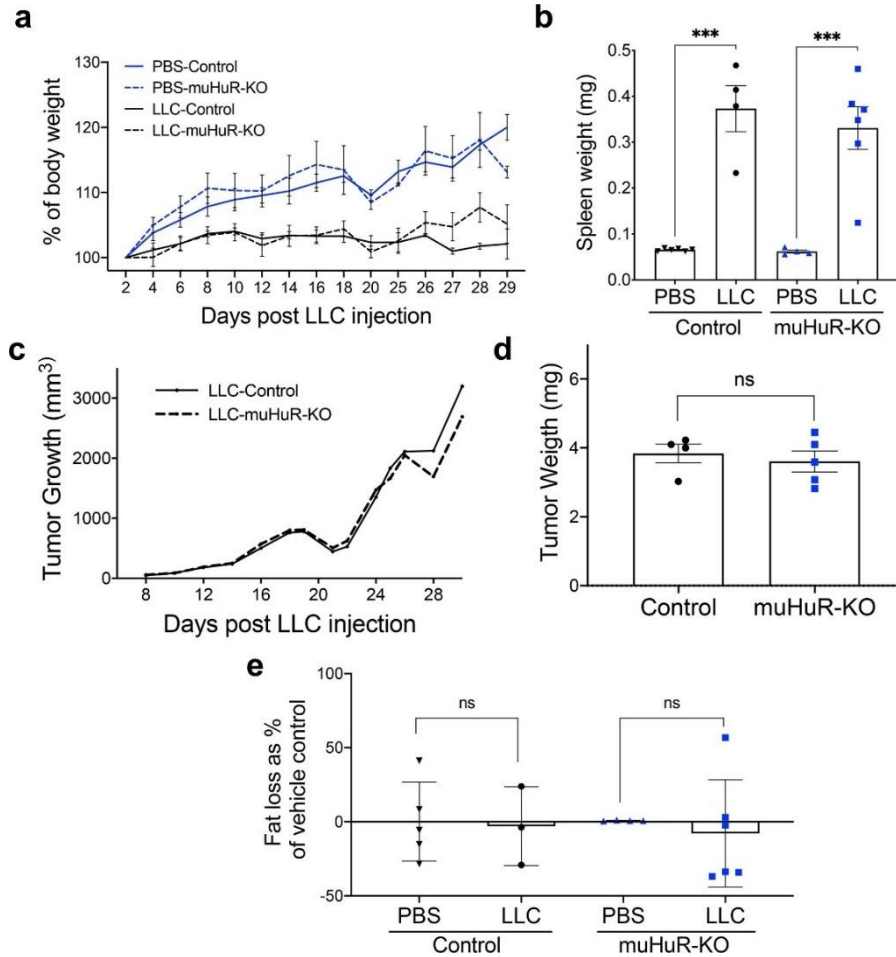
Annex 3. Supplementary Figure 8 HuR does not regulate the translation of *PGC-1 α* mRNA. Cytoplasmic extracts obtained from C2C12 myoblasts treated with or without siHuR were prepared and fractionated on sucrose gradients (15–50% w/v). **a** Fractions were divided into two groups: non-polysome (NP, fractions 1–6) and polysome (P, fractions 7–20). **b** The level of *PGC-1 α* and *GAPDH* mRNAs in the Polysome and Non-Polysome were quantified by RT–qPCR using the $\Delta\Delta C_t$ method and plotted as a Polysome to Non-Polysome ratio (n=4). The results are presented as mean \pm S.E.M, *p < 0.05 unpaired t-test.



Annex 3. Supplementary Figure 9 HuR differentially affects the stability of mRNAs associated to fiber type specification. **a-f** C2C12 myoblasts treated with or without siHuR were used to assess the stability of *Myogenin* (**a**), *Tnn1* (**b**), *Tnn2* (**c**), *Six1* (**d**), *NFATc1* (**e**) and *NCOA6* (**f**) mRNAs. Cells were treated with actinomycin D (ActD) for 0, 1.5, 3, 4.5 or 6 hours and mRNA from the different time points was processed by RT-qPCR. mRNA levels of the genes of interest were standardized against *RPL32* mRNA levels and plotted as a percent of the abundance of mRNA at time 0 of ActD treatment, which is considered as 1 (n=3, except for *Tnn1* where n=2). The line of best fit was determined by linear regression using the data points for siCtl and siHuR. Error bars represent \pm S.E.M.



Annex 3. Supplementary Figure 10 Validation of the LLC model in control and muHuR-KO mice. **a-e** Control and muHuR-KO mice were inoculated subcutaneously in their right flank with LLC cells or PBS and evaluated 29 days after inoculation by measuring (a) total body weight gain (LLC- Control n=4, LLC-muHuR-KO n=5). (n=5 LLC-Control n=4), (b) sign of inflammation (spleen weight) (LLC-Control and PBS-muHuR n=4, PBS-Control and PBS-Control and LLC-muHuR- KO n=6), (c) tumor growth progression (n=5 except for LLC-Control where n=4), (d) tumor burden (LLC-Control n=4, and LLC-muHuR-KO n=5), (e) hindlimb fat pad loss (LLC-Control and PBS-muHuR n=4, PBS-Control n=5 and LLC-muHuR-KO n=6). (**a-e**). The results are presented as mean \pm S.E.M.



Annex 3. Supplementary Table 1 Effect of HuR ablation on fiber type composition in soleus (SOL), EDL and peroneus (PER) muscles.

	Total number of fibers counted				
	Muscle	MyHC Type I	MyHC Type IIA	MyHC Type IIB	MyHC Type IIX
Control	EDL	1.53 ±0.50	22.66 ±2.26	75.81 ±2.60	22.97 ±1.95
	PER	5.84 ±0.51	33.31 ±1.87	60.85 ±2.30	23.42 ±1.79
	SOL	43.12 ±1.43	52.81 ±1.65	0.46 ±0.20	8.22 ±2.18
muHuR-OK	EDL	7.31 ±0.95***	17.81 ±1.67	74.88 ±2.38	21.01 ±1.22
	PER	12.76 ±1.99**	39.14 ±4.08	48.10 ±4.76*	26.65 ±3.29
	SOL	60.23 ±2.04***	36.75 ±1.59***	0.00 ±0.00*	15.08 ±1.62

Abbreviations: EDL (Extensor digitorum longus), PER (Peroneus), SOL (Soleus). Results are shown as mean ± S.E.M. *p < 0.05, **p < 0.005, ***p < 0.001

Annex 3. Supplementary Table 2. Sequence of primers and siRNAs use in this study

Experiment	Gene	Sequence
PCR	LoxP	Forward 5'-TGG TTA TGA AGA CCA CAT GGC GGA AGA-3' Reverse 5'-AGC TTA GCA GGT ACC GTC TCC-3'.
	Cre	Forward 5'-CAT TTG GGC CAG CTA AAC AT-3' Reverse 5'-CGG ATC ATC AGC TAC ACC AG-3'
	HuR exon 2	Forward 5'-ATA TCA TGT TCC CAA CTC CC-3' Reverse 5'-TGG CAC TCA CTG AAC TGG AA-3'.
siRNA	HuR	Sense: 5'-CAAACCTCAGGAGCTTCTTTTTGTTTATCATAAT-3' Anti-sense: 5'- ATTATGATAAACAAAAAGAAGCTCCTGAGTTTG -3'
	CTL	Sense: 5'- TGTGTATTGTTTATTGTTTTGTGTGTTGTTTGTAAT -3' Anti-sense: 5'-TGTGTATTGTTTATTGTTTTGTGTGTTGTTTGTAAT -3'
	KSRP	Sense: 5'- CAAACCTCAGGAGCTTCTTTTTGTTTATCATAAT-3' Anti-sense: 5'- ATTATGATAAACAAAAAGAAGCTCCTGAGTTTG -3'
	Tnnl1	Forward 5'-GAA CAC GAG GAG CGA GAG G-3'

	Reverse 5'-CCT TCA GCT TCA GGT CCT TG-3'.
Tnnl2	Forward 5'-GGA GGG TGC GTA TGT CTG C-3'
	Reverse 5'-GGG AAG TGG GCA GTT AGG AC-3'.
Tnnt1	Forward 5'-GCC CAG GAG CTG TCA GAA T-3'
	Reverse 5'-CTC CAC ACA GCA GGT CAT GT-3'.
Tnnt3	Forward 5'-TGA TAT CAC CAC CCT CAG GA-3'
	Reverse 5'-TCC TGA GTT CCC AAA GAT GC-3'.
MyHC I	Forward 5'-CTC AAG CTG CTC AGC AAT CTA TTT-3'
	Reverse 5'-GGA GCG CAA GTTTGT CAT AAG T -3'.
MyHC IIA	Forward 5'-AGG CGG CTG AGG AGC ACG TA-3'
	Reverse 5'-GCG GCA CAA GCA GCG TTG G-3'.
MyHC IIX	Forward 5'-GAG GGA CAG TTC ATC GAT AGC AA-3'
	Reverse 5'-GGG CCA ACT TGT CAT CTC TCA T -3'.
MyHC IIB	Forward 5'-CAC CTG GAC GAT GCT CTC AGA-3'
	Reverse 5'-GCT CTT GCT CGG CCA CTC T-3'.
Tfam	Forward 5'-CCA AAA AGA CCT CGT TCA GC-3'
	Reverse 5'-CCA TCT GCT CTT CCC AAG AC-3'
PGC-1 α	Forward 5'-CAG GAA CAG CAG CAG AGA CA-3'
	Reverse 5'-GTT AGG CCT GCA GTT CCA GA-3'.
PGC-1 β	Forward 5'-GCC AGA AGC ACG GTT TTA TC-3'
	Reverse 5'-ATC CAT GGC TTC GTA CTT GC-3'.
Six 1	Forward 5'-AGG GAG AAA CGG GAG CTG-3'
	Reverse 5'-GGG GGT GAG AAC TCC TCT TC-3'.
NCOA6	Forward 5'-CCA TAG CCT CTG GAC AAA GC-3'
	Reverse 5'-TGG ATT TTC GCT TGG AT-3'.
NFATc1	Forward 5'-TGG AGA AGC AGA GCA CAG AC-3'
	Reverse 5'-GCG GAA AGG TGG TAT CTC AA-3'.
Murf1	Forward 5'-GAG CAA GGC TTT GAG AAC ATG GAC T-3'
	Reverse 5'-GCG TCC AGA GCG TGT CTC ACT-3'.
TPM1	Forward 5'-TGC TTT TCT CCA ATT TGG TT-3'.
	Reverse 5'-GGG CTG AGC TCT CAG AAG G-3'
RPL32	Forward 5'-TTC TTC CTC GGC GCT GCC TAC GA-3'
	Reverse 5'-AAC CTT CTC CGC ACC CTG TTG TCA-3'.
GAPDH	Forward 5'-AAG GTC ATC CCA GAG CTG AA-3'
	Reverse 5'-AGG AGA CAA CCT GGT CCT CA-3'.
NRF-1	Forward 5'-CAGCACCTTTGGAGAATGTG-3'
	Reverse 5'-CCTGGGTCATTTTGTCCACA-3'.
NRF-2	Forward 5'-GATCCGCCAGCTACTCCCAGGTTG-3'
	Reverse 5'-CAGGGCAAGCGACTCATGGTCATC-3'.
MyoD	Forward 5'-CGACACCGCCTACTACAGTG-3'

qPCR

	Reverse 5'-TTCTGTGTCGCTTAGGGATG-3'
Myogenin	Forward 5'-CTACAGGCCTTGCTCAGCTC-3' Reverse 5'-AGATTGTGGGCGTCTGTAGG-3'
UCP-2	Forward 5'-TCTACAATGGGCTGGTCGC-3' Reverse 5'-CAAGCGGAGAAAGGAAGGC-3'.
UCP-3	Forward 5'-CCTACAGAACCATCGCCAGG-3' Reverse 5'-ACCGGGGAGGCCACCACTGT-3'.
Acadv1	Forward 5'-GGAGGACGACACTTTGCAGG-3' Reverse 5'-AGCGAGCATACTGGGTATTAGA-3'.
CD36	Forward 5'-GATGACGTGGCAAAGAAGCAG-3' Reverse 5'-TCCTCGGGGTCCTGAGTTAT-3'.
FAS	Forward 5'-AGAGATCCCGAGACGCTTCT-3' Reverse 5'-GCCTGGTAGGCATTCTGTAGT-3'.
LDL	Forward 5'-TGTGAATTTGGTGGCTGAAAAC-3' Reverse 5'-AATAGGGAAGAAGATGGACAGGAAC-3'.
ND1	Forward 5'-CTAGCAGAAACAAACGGGGC-3' Reverse 5'-CCGGCTGCGTATTCTACGTT-3'.
HK2	Forward 5'-GCCAGCCTCTCCTGATTTTAGTGT-3' Reverse 5'-GGGAACACAAAAGACCTCTTCTGG-3'.
PPAR α	Forward 5'-GCGTACGGCAATGGCTTTAT-3' Reverse 5'-ACAGAACGGCTTCCTCAGGTT-3'.

Annex 3. Supplementary Data 1 Differentially expressed genes as analyzed by RNA-Seq in the *soleus* muscle from muHuR-KO and control mice (\log_2 FC > 0.5 or < -0.5, $p=0.05$). Data can be access at <https://www.ncbi.nlm.nih.gov/pmc/articles/PMC6744452/> under ID number 41467_2019_12186_MOESM2_ESM.xlsx GUID: 4779B0CA-A71C-4D1F-AA2E-53D0860FF4F2. The raw RNASeq data have been deposited into NCBI Gene Expression Omnibus (GEO) database under accession number GSE134241.